17

PNL-6800 Pt. 1
UC-408

Pacific Northwest Laboratory Annual Report for 1988 to the DOE Office of Energy Research

Part 1: Biomedical Sciences
June 1989

Prepared for the U.S. Department of Energy
under Contract DE-AC06-76RLO 1830

Pacific Northwest Laboratory
Operated for the U.S. Department of Energy
by Battelle Memorial Institute

Battelle

DISCLAIMER

This program was prepared as an account of work sponsored by an agency of the United States Government. Neither the United States Government nor any agency thereof, nor Battelle Memorial Institute, nor any of their employees, makes **any warranty, express or implied, or assumes any legal liability or responsibility for the accuracy, completeness, or usefulness of any information, apparatus, product, or process disclosed, or represents that its use would not infringe privately owned rights.** Reference herein to any specific commerical product, process, or service by trade name, trademark, manufacturer, or otherwise, does not necessarily constitute or imply its endorsement, recommendation, or favoring by the United States Government or any agency thereof, or Battelle Memorial Institute. The views and opinions of authors expressed herein do not necessarily state or reflect those of the United States Government or any agency thereof.

PACIFIC NORTHWEST LABORATORY
operated by
BATTELLE MEMORIAL INSTITUTE
for the
UNITED STATES DEPARTMENT OF ENERGY
under Contract DE-AC06-76RLO 1830

Printed in the United States of America
Available from
National Technical Information Service
United States Department of Commerce
5285 Port Royal Road
Springfield, Virginia 22161

NTIS Price Codes
Microfiche A01

Printed Copy

Pages	Price Codes
001-025	A02
026-050	A03
051-075	A04
076-100	A05
101-125	A06
126-150	A07
151-175	A08
176-200	A09
201-225	A10
226-250	A11
251-275	A12
276-300	A13

3 3679 00056 4130

PNL-6800 Pt. 1
UC-408

Pacific Northwest Laboratory Annual Report for 1988 to the DOE Office of Energy Research

Part 1: Biomedical Sciences

J. F. Park and Staff

June 1989

Prepared for
the U.S. Department of Energy
under Contract DE-AC06-76RLO 1830

Pacific Northwest Laboratory
Richland, Washington 99352

PREFACE

This 1988 Annual Report from Pacific Northwest Laboratory (PNL) to the U.S. Department of Energy (DOE) describes research in environment, safety and health conducted during fiscal year 1988. The report again consists of five parts, each in a separate volume.

The five parts of the report are oriented to particular segments of the PNL program. Parts 1 to 4 report on research performed for the DOE Office of Health and Environmental Research in the Office of Energy Research. Part 5 reports progress on all research performed for the Assistant Secretary for Environment, Safety and Health. In some instances, the volumes report on research funded by other DOE components or by other governmental entities under interagency agreements. Each part consists of project reports authored by scientists from several PNL research departments, reflecting the multidisciplinary nature of the research effort.

The parts of the 1988 Annual Report are:

Part 1: Biomedical Sciences		
Program Manager: J. F. Park		D. L. Felton, Report Coordinator and Editor
Part 2: Environmental Sciences		
Program Manager: R. E. Wildung		S. G. Weiss, Report Coordinator and Editor G. P. O'Connor, Editor
Part 3: Atmospheric Sciences		
Program Manager: C. E. Elderkin		C. E. Elderkin, Report Coordinator E. L. Owczarski, Editor
Part 4: Physical Sciences		
Program Manager: L. H. Toburen		L. H. Toburen, Report Coordinator K. A. Parnell, Editor
Part 5: Environment, Safety, Health, and Quality Assurance		
Program Managers:	L. G. Faust W. T. Pennell J. M. Selby	L. G. Faust and W. T. Pennell, Report Coordinators S. K. Ennor, Editor

Activities of the scientists whose work is described in this annual report are broader in scope than the articles indicate. PNL staff have responded to numerous requests from DOE during the year for planning, for service on various task groups, and for special assistance.

Credit for this Annual Report goes to the many scientists who performed the research and wrote the individual project reports, to the program managers who directed the research and coordinated the technical progress reports, to the editors who edited the individual project reports and assembled the five parts, and to Ray Baalman, editor in chief, who directed the total effort.

Members of the Scientific Advisory Committee, established in 1985, are:

Dr. Franklin I. Badgley	University of Washington
Dr. Leo K. Bustad	Washington State University
Dr. Franklin Hutchinson	Yale University
Dr. Albert W. Johnson	San Diego State University
Dr. J. Newell Stannard	University of Rochester; University of California, San Diego

W. J. Bair
T. S. Tenforde
Environment, Health and Safety
Research Program

Previous reports in this series:

Annual Report for:

1951	HW-25021, HW-25709
1952	HW-27814, HW-28636
1953	HW-30437, HW-30464
1954	HW-30306, HW-33128, HW-35905, HW-35917
1955	HW-39558, HW-41315, HW-41500
1956	HW-47500
1957	HW-53500
1958	HW-59500
1959	HW-63824, HW-65500
1960	HW-69500, HW-70050
1961	HW-72500, HW-73337
1962	HW-76000, HW-77609
1963	HW-80500, HW-81746
1964	BNWL-122
1965	BNWL-280, BNWL 235, Vol. 1-4; BNWL-361
1966	BNWL-480, Vol. 1; BNWL-481, Vol. 2, Pt. 1-4
1967	BNWL-714, Vol. 1; BNWL-715, Vol. 2, Pt. 1-4
1968	BNWL-1050, Vol. 1;, Pt. 1-2; BNWL-1051, Vol. 2, Pt. 1-3
1969	BNWL-1306, Vol. 1;, Pt. 1-2; BNWL-1307, Vol. 2, Pt. 1-3
1970	BNWL-1550, Vol. 1;, Pt. 1-2; BNWL-1551, Vol. 2, Pt. 1-2
1971	BNWL-1650, Vol. 1;, Pt. 1-2; BNWL-1651, Vol. 2, Pt. 1-2
1972	BNWL-1750, Vol. 1;, Pt. 1-2; BNWL-1751, Vol. 2, Pt. 1-2
1973	BNWL-1850, Pt. 1-4
1974	BNWL-1950, Pt. 1-4
1975	BNWL-2000, Pt. 1-4
1976	BNWL-2100, Pt. 1-5
1977	PNL-2500, Pt. 1-5
1978	PNL-2850, Pt. 1-5
1979	PNL-3300, Pt. 1-5
1980	PNL-3700, Pt. 1-5
1981	PNL-4100, Pt. 1-5
1982	PNL-4600, Pt. 1-5
1983	PNL-5000, Pt. 1-5
1984	PNL-5500, Pt. 1-5
1985	PNL-5750, Pt. 1-5
1986	PNL-6100, Pt. 1-5
1987	PNL-6500, Pt. 1-5

FOREWORD

This report summarizes progress on OHER biomedical and health-effects research conducted at PNL in FY 1988. The research develops the knowledge and scientific principles necessary to identify, understand, and anticipate the long-term health consequences of energy-related radiation and chemicals. Our continuing emphasis is to decrease the uncertainty of health-effects risk estimates from existing and/or developing energy-related technologies through an increased understanding of how radiation and chemicals cause health effects.

The report is arranged to reflect PNL research relative to OHER programmatic structure. The first section, on human health effects, concerns statistical and epidemiological studies for assessing health risks. The next section, which contains reports of health-effects research in biological systems, includes research with radiation and chemicals.

Human Health Effects

The section on human health and risk assessments reports the status of epidemiologic studies, including occupational studies of radiation workers and a study of biological markers related to cancer in Japanese atomic-bomb survivors. It also reports on a data-base design effort with a long-term end point of standardizing laboratory animal and human information for use in inferring human health effects from exposure to radiation.

An update on analyses of causes of mortality in the Hanford worker population was published, as was a paper on methods for analysis of occupational exposure to low levels of radiation. Prevalence and case control studies of congenital malformations were published. Lung-cancer data from the case-cohort study were analyzed, and a paper was submitted for publication. For these and other research efforts related to health of workers at Hanford, an article describing monitoring programs and results was distributed to all Hanford Site workers. A program has begun to evaluate effects of errors in dosimetry on results of analyses. This includes general documentation of historical dosimetry practices and a detailed evaluation of selected data, including data on workers that died of multiple myeloma or leukemia.

Data from worker studies at several DOE facilities were combined and analyzed, and papers reporting results and methodology are being prepared. Use of combined data gives more precise risk estimates than any individual study and allows evaluation of exposure standards established based on higher-level data. A protocol for international pooling of data from occupational studies of low-level radiation is also being prepared, with PNL serving as the coordinating organization for the United States.

In Japanese atomic-bomb survivors, stomach cancer cases had significantly lower precancer diagnosis levels of serum ferritin and higher transferrin than controls. Another study of total serum protein showed that cigarette smokers have lower levels than nonsmokers.

A data base was designed to allow investigators to combine experimentally derived dose-effect data for evaluating potential effects in humans from exposure to radiation. The data base currently includes data on dosimetry and histopathology from five OHER laboratories conducting lifespan health effects studies in beagle dogs. The terminology for pathology and dosimetry at the five laboratories was standardized, so that reporting is consistent. Data on other species, including humans, can eventually be included in the data base.

Health Effects Research in Biological Systems

The section on health effects research in biological systems reports results from experimental animal inhalation dose-effect relationship studies with inhaled radionuclides. Lifespan studies in dogs that inhaled $^{239}PuO_2$, $^{238}PuO_2$, or $^{239}PuO(NO_3)_4$ are summarized to 16, 14, and 11 years after exposure, respectively. The primary plutonium-exposure-related causes of death are lung cancer for inhaled $^{239}PuO_2$, and lung and bone cancer for inhaled $^{238}PuO_2$ and $^{239}PuO(NO_3)_4$. Dose-effect relationship studies on inhaled $^{239}PuO_2$ in rats are in progress to obtain lung-tumor-incidence data at lifetime doses of 5 to 1500 rad.

Thus far, the lung cancer dose-response curve is best fitted by a quadratic function and a "practical" threshold of >100 rad; maximum lung cancer incidence was at 800 rad. Bronchiolar alpha-star distribution, determined by quantitative scanning electron microscopy and autoradiography, indicated lung carcinoma formation was preceded by proliferative dysplastic lesions associated with plutonium aggregates. Studies are also in progress in rats that inhaled radon daughters to determine the influence of dose, dose rate and cigarette smoke on lung-cancer incidence. Analyses of rat histopathological data for 10-, 100-, and 1000-working-level exposure rates confirm a previously noted trend of higher lifetime lung cancer risks for lower exposure rates. Also noted was the tapering-off of the exposure-rate effect at occupational and, possibly, at environmental rates of radon exposure.

Mechanistic studies of radon injury are using an *in vitro* radon cell-exposure system. Radon-induced mutations at the HGPRT locus in Chinese hamster ovary cells showed a linear induction response with induced frequency of 0.9×10^{-6} mutations/viable cell/centigray dose to the culture medium. Chromosome aberrations and sister chromatid exchange (SCE) in human peripheral blood lymphocytes were induced in a linear fashion, with a frequency of 0.009 aberrations/metaphase/centigray dose to the medium and 0.031 SCE/metaphase/centigray dose to the medium. We are investigating the microdosimetry of cells exposed to radon and daughters in tissue culture medium. Preliminary data show a preferential association of radon and daughters with the cell and, therefore, a higher dose to cells than to medium. Dosimetry models for the respiratory tract indicate that with exposures of 8.45 working level months, 70 to 90% of the basal and secretory cell nuclei were missed; most of the remainder were hit only once. While the main, lobar, and segmented bronchi had the highest fraction of these cell nuclei irradiated, more were irradiated in generations 14 to 16. However, they represented a smaller fraction of the cells present in these generations.

Studies to examine the role of oncogenes, growth factors, and their receptors in radiation-induced lung cancer are utilizing tumor tissue from the animal studies described above. Using immunocytochemical assays for detecting epidermal growth factor receptors (EGF-R) in formalin-fixed paraffin-embedded lung tissue, we have demonstrated abnormally high EGF-R associated with plutonium-induced epidermal lung carcinoma in dogs and radon-daughter-induced epidermal lung carcinoma in rats. We have detected activated *ras* oncogenes in these radiation-induced cancers and are determining whether radiation causes specific mutations in these genes. Methods were developed for extracting DNA from formalin-fixed paraffin-embedded tissues and amplifying it, using the polymerase chain reaction method, to detect the presence of mutated *ras* sequences. We want to determine whether alpha radiation causes patterns of genetic change that can be distinguished from those caused by chemicals.

Studies to understand the mechanisms of tumor initiation for chemicals are determining the influence of bulky adducts on chromatin structure at the nucleosome level of organization, using the pXP-14 plasmid, which contains the 5S rRNA gene and the SP-6 promoter. The location of the adducts relative to the gene and the promoter and their influence on nucleosome positioning will be determined.

In our developmental studies, inhalation of ^{85}Kr by pregnant sheep showed that blood concentrations rapidly reached a steady state and that kinetics in fetal and maternal compartments were similar. The data were used to predict the fetal dosimetry of radon during inhalation exposures. These predictions were tested by an experiment which detected neither embryofetal toxicity nor teratogenicity after 13-day exposures of rats to radon. Cumulative radon-daughter exposures to the dams were about four orders of magnitude higher than typical annual levels associated with indoor radon exposures. In studies to elucidate the molecular mechanism regulating lung maturation and differentiation, EGF-R and transforming growth factor alpha were altered, in both intensity and temporal sequence, in the hypoplastic lungs of rat fetuses when hypoplasia was induced by treating the dams with coal-derived complex mixtures or triamcinalone, a synthetic glucocorticoid. In other studies we are determining whether agents that alter cytochrome P-450 expression change the animal's susceptibility to tumor development, as indicated by DNA adduct concentration. Initial results indicate that neonatal exposure to diethylstilbestrol increased hepatic cytochrome P-450 concentration for female rats and decreased the binding of aflatoxin B1 to hepatic DNA for males.

In our mutation research a new genetic construct that allows analysis of mutations in small synthetic DNA targets of desired sequence in bacteria has been tested experimentally. Deletion mutations occurred

with high frequency in a target containing two 6-base pair stretches of alternating guanine and cytosine when the host cells were exposed to chemical mutagens. A target containing only one of the stretches was much less mutable. These results demonstrate that mutation is dependent on the target sequence and that the system will be useful for investigation of the relationship between DNA sequence and mutation rate.

Research related to OHER's human genome research is developing a computer-based information system containing archived information, research results, and computational capability to make information readily available and useful to researchers. Computer graphics interfaces with this information data base are being developed to provide pictorial representation of chromosomes, genetic and physical maps, and DNA sequences.

This health-effects research is an interdisciplinary effort requiring scientific contributions from many research departments at PNL. The personnel in the Biology and Chemistry Department and in the Computational Sciences Department are the principal contributors to this report.

Requests for reprints from the list of publications for 1988 will be honored while supplies last.

CONTENTS

Human
Health Effects
Research

Statistical Health Effects Study

Principal Investigator: E. S. Gilbert

Other Investigators: J. S. Buchanan, J. J. Fix, and N. A. Holter

The purpose of this project is to develop statistical and epidemiological methods for assessing health risks from low-level exposures. These methods are then applied to data on relevant human populations, thus providing a direct assessment of risk from these exposures. Chronic exposure to radiation, such as that received occupationally, is of special concern, and an important component of this project is the analysis of mortality data on workers at the Hanford Site. Efforts in the past year have focused on improving understanding of the dosimetry data that has been used in the Hanford mortality study and on pooling data from several occupational studies. The latter efforts included combined analyses of data from three DOE facilities, and contributing to efforts to combine data internationally.

Updated analyses of the Hanford mortality data, including deaths through 1981, were accepted for publication in *Health Physics*. These analyses included comparison of death rates with those of the general U.S. population, comparisons of death rates by level of radiation exposure, calculation of risk estimates and confidence limits, analyses of workers with internal depositions of plutonium, and analyses of female workers. A paper describing several statistical techniques that are useful in analyzing health effects of occupational exposure to low levels of radiation was accepted by *Statistics in Medicine*. This paper reviewed application of the Cox model for testing the association of radiation exposure and several diseases, described the method used to obtain risk estimates and confidence limits, discussed the problem of confounding related to the healthy-worker effect, illustrated the use of computer simulation for obtaining confidence limits, and described an approach for taking account of factors such as age at exposure and time since exposure.

In cooperation with the PNL Public Relations Department and researchers from the Hanford Environmental Health Foundation (HEHF), a non-technical article was prepared and published in the PNL publication *Profile*. Reprints of this article were distributed to all Hanford Site workers. The article described the Hanford mortality study, the lung-cancer case-cohort study, two congenital malformations studies (published in the February 1988 issue of the *American Journal of Epidemiology*), and HEHF's health surveillance system. Several presentations on these studies were made to local groups with an interest in health effects studies and the Hanford Site.

Additional analyses of data from the lung-cancer case-cohort study were conducted. First, uranium bioassay data were examined and used to analyze the possible association of lung-cancer risks with potential exposure to uranium. No evidence of such an association was found, but statistical power was limited. Second, special statistical procedures were developed and implemented to take account of correlations introduced by the case-cohort design. Rigorous statistical treatment of the case-cohort design is a relatively recent development, and this study is one of the first to implement appropriate analyses of data collected under this study design.

Although exposure to ionizing radiation is probably measured more accurately than exposures to other substances, virtually every epidemiological study of health effects and radiation exposure involves some level of dose measurement error. In occupational studies such as that of Hanford workers, exposure to external radiation is measured through the use of personnel dosimeters. The types of dosimeters used and the frequency of monitoring, as well as other practices, have changed over the years as technology improved. Understanding these practices and evaluating bias and uncertainty in annual dose estimates are important for appropriate interpretation of analyses relating health effects to dose.

To develop a better understanding of historical dosimetry practices at the Hanford Site, a technical report documenting these practices is being prepared. This report will describe the major characteristics of dosimeters and dosimetry practices that have been in use at Hanford from 1944 to the present. Many reports that provide information on various aspects of past dosimetry practices have been reviewed, and several past studies of dosimeter performance have been

evaluated; these reports and studies will provide important input to the report under preparation.

In addition, the detailed dosimetry source records for about 120 selected workers are being evaluated. The objectives of this investigation are: (1) to assess the extent to which dose estimates used in mortality analyses agree with information in original source records, and (2) to gain a better understanding of dosimetry practices. This investigation includes workers that died of either leukemia or multiple myeloma, matched controls for the leukemia and multiple myeloma deaths, selected cancer deaths with relatively high doses of radiation, a sample of workers in selected occupations of special interest, and a sample of workers known to have a high potential for neutron exposure. The records being examined include results of each dosimeter for each type of radiation measured. The data from the dosimetry records have been entered into a database system and will be checked for both internal consistency and for agreement with data included in mortality analysis files.

Analyses of combined data from the Hanford Site, Oak Ridge National Laboratory, and Rocky Flats Nuclear Weapons Plant are being conducted; workers at all three facilities have been exposed occupationally to external radiation. These analyses are part of a general cooperative effort to evaluate combined data from several epidemiological studies of workers at DOE facilities. These analyses include calculation of summary statistics describing the exposure and age distributions, assessment of the relationship of mortality and variables such as follow-up period and length of employment, and assessment of the relationship of mortality and cumulative radiation exposure. All analyses are being conducted for each of the studies individually, using comparable methods for both analysis and presentation. In addition, tests for trend and risk estimates and confidence limits are being obtained for pooled data from all studies. The objectives of these analyses are to better understand differences and similarities in the studies, and to provide tighter confidence limits for estimated risks.

A paper describing methodology for combining data from several studies is near completion. This paper, which will use data from the three studies described above for illustration, is a cooperative effort among researchers from Oak Ridge Associated Universities, Los Alamos National Laboratory, HEHF and PNL.

The possibility of international pooling of data from occupational studies of low-level radiation is under consideration. A meeting on cancer risk among workers in the nuclear industry was held at the International Agency for Cancer Research (IARC) in June 1988. This meeting, attended by principal investigators of major epidemiological studies in the United States (including the Hanford study), United Kingdom, and Canada, was aimed at discussing the feasibility and methodology for conducting statistical analyses of combined data from several studies on an international scale. All investigators attending were interested in conducting such analyses. Although no formal commitment has yet been made, it was tentatively agreed that IARC would serve as the coordinating agency but analyses would be planned and results interpreted by the cooperating investigators.

Iron Stores and Risk of Cancer

Principal Investigator: R. G. Stevens

Other Investigators: S. Akiba, M. Kabuto, and K. Neriishi, Radiation Effects Research Foundation, Hiroshima, Japan; W. Blot and C. Land, National Cancer Institute, Bethesda, Maryland

A case-control study of Japanese atomic bomb survivors showed that stomach cancer cases had significantly lower serum ferritin and higher transferrin before diagnosis than suitably chosen controls. Another study showed that cigarette smokers had significantly lower total serum protein than nonsmokers.

Research based on data and stored biological samples from Japanese atomic bomb survivors is helping to advance the understanding of factors that modify the risk of cancer, particularly radiation-induced cancer. Although nutritional antioxidants, such as tocopherol and selenium, have received a great deal of attention in this regard, the "oxidant" iron has received very little. Iron status is important for all people, and variations in iron stores may modify cancer risk after exposure to radiation.

The Japanese atomic bomb survivor population has been followed by the Radiation Effects Research Foundation (RERF) in Hiroshima and Nagasaki for nearly 40 yr. A wealth of information and stored biological materials from the survivors is available for analysis and is being used to understand the relationship of modifying factors (particularly iron status) to the risk of cancer. We are also studying how these modifying factors interact with known cancer risk factors, such as radiation exposure and cigarette-smoking, in determining cancer risk.

Ferritin, Transferrin, and Stomach Cancer

Serum ferritin and transferrin were determined in samples stored since 1970-72 for 233 individuals who subsequently developed stomach cancer and 84 who developed lung cancer. These serum proteins were also determined for 385 controls selected from the same cohort of Japanese atomic bomb survivors in Hiroshima and Nagasaki. The mean ferritin level in the stomach cancer cases was significantly lower and the transferrin level was significantly higher than in the controls (Table 1). This result was not anticipated; however, in retrospect it is consistent with findings in previous studies in Taiwan (Stevens et al., *J. Natl. Cancer Inst. 76*:605, 1986) and in the United States (Stevens et al., *N. Engl. J. Med. 319*:1047, 1988). In these studies, the original hypothesis was that evidence of large iron stores is associated with increased cancer risk, a relationship seen in two previous studies for overall cancer risk.

TABLE 1. Mean (Standard Error of the Mean) Serum Ferritin and Transferrin Levels in Cases of Stomach Cancer, Lung Cancer, and in Control Subjects. (Serum was stored from 1970-72.)

	Stomach Cancer	Lung Cancer	Controls
Number of Subjects	137	49	231
Log Ferritin (ng/ml)	1.69 (0.032)	1.83 (0.056)	1.84 (0.02)
Transferrin (mg/dl)	277 (3.4)	264 (5.0)	269 (2.5)

Unexpectedly, in the atomic bomb survivors we have found evidence that low iron stores are associated with stomach cancer risk. A possible explanation for the finding is that achlorhydria (or low stomach acidity) leads to gastric membrane atrophy, atrophic gastritis, and stomach cancer. Furthermore, at this higher pH, bioavailable iron is not as well absorbed. However, low iron stores observed in Japanese bomb survivors may result from some unknown condition that also greatly increases risk of stomach cancer.

In the lung cancer cases, serum ferritin levels and transferrin were not significantly different from those of controls.

Cigarette-Smoking and Serum Proteins

Smoking increases cancer risk and can also affect serum protein levels. For this project, we designed a study to examine effects of smoking on serum proteins for two reasons: (1) An effect on a serum protein may elucidate mechanisms by which smoking causes disease. (2) Biochemical epidemiological studies of serum markers and cancer risk often lack information on patients' smoking histories, thereby seriously confounding apparent effects and vitiating interpretation of the findings.

Levels of serum protein and protein fractions were compared according to smoking history in a population of 7753 members of the Adult Health Study component of the Japanese atomic bomb survivors in Hiroshima. Levels of total protein and its constituents (albumin, alpha 1 globulin, alpha 2 globulin, beta globulin, and gamma globulin) were measured for the period 1980-82. Smoking information on the same individuals was obtained from a survey taken in 1978-80. Additional data from a survey conducted in 1964-66 were used to estimate smoking duration.

Total protein, beta globulin, and gamma globulin were significantly lower in current smokers than in "never-smokers" (Table 2); alpha 1 and alpha 2 globulin were significantly higher in smokers. Serum albumin was lower in smokers, although not statistically significant. Serum protein levels in ex-smokers were not different from those of never-smokers. All analyses were adjusted for age, sex, and body mass index. Atomic bomb radiation exposure was considered an additional covariate whose effect was significant in some comparisons, however, it was much smaller than the smoking effect.

TABLE 2. Effect of Smoking on Serum Protein Levels. Values, obtained from regression analysis, are differences (standard error of difference) in g/L between smokers and non-smokers, and between ex-smokers and non-smokers.

	Smokers	Ex-Smokers
Total Protein	-1.04 (0.2)	0.0 (0.2)
Albumin	-0.22 (0.13)	-0.01 (0.19)
Alpha 1 Globulin	0.15 (0.02)	-0.01 (0.03)
Alpha 2 Globulin	0.25 (0.04)	0.06 (0.06)
Beta Globulin	-0.21 (0.04)	0.04 (0.06)
Gamma Globulin	-0.97 (0.12)	-0.06 (0.17)

Future Studies

Serum albumin was significantly lower long before diagnosis in individuals who subsequently developed cancer than in those who did not (Stevens et al., 1988). Smoking did not account for this result, which may be related to iron metabolism and bioavailability. We have begun analyses in the Japanese bomb survivors of the relation between serum albumin and subsequent cancer risk. In particular, the possible interaction with radiation exposure is being examined.

We are designing a study of the relationship of serum ferritin and transferrin and subsequent risk of colon cancer. Risk of colon cancer is higher in Japanese exposed to radiation from the atomic bomb than in those who were not exposed. Colon cancer was also strongly related to iron status in the National Health and Nutrition Examination Survey (NHANES) population from the United States (Stevens et al., 1988). The study will test the hypothesis that high iron status increases the effect of radiation in induction of colon cancer.

Interlaboratory Toxicology Knowledge Base

Principal Investigator: C. R. Watson

Technical Assistance: F. Carr, Jr., J. D. Kaschmitter, and J.R. Williams

The goal of this project is to provide a data base which will allow investigators to assess experimentally derived dose-effect data from many laboratories for evaluating potential radiotoxic insults to human health. Initial efforts, reported here, concentrate on beagle dog lifespan health effects studies supported by DOE at five laboratories. Significant steps toward this goal include standardization of the medical observation glossary, development of an independent off-site data archive, and design of a registry of common-format dosimetric estimates and histopathologic observations for each major tissue in the more than 8000 dogs under study. In FY89, this project will be incorporated in a larger effort to archive physical specimens and detailed records and summarize tissue information.

Our goal is to provide investigators with the capability to combine experimentally derived dose-effect data from many laboratories for evaluating potential insults to human health from exposure to radionuclides. A manageable subset of this large problem is to integrate information from the five DOE-supported laboratories that conduct lifespan studies of beagle dogs exposed to various radiotoxic insults. These laboratories, shown in Table 1 with their study protocols, are Pacific Northwest Laboratory; Inhalation Toxicology Research Institute; University of California, Davis; University of Utah; and Argonne National Laboratory. This program, consisting of studies designed to complement one another, was initiated over 20 years ago and is nearing completion.

This project focuses on three steps leading toward eventual synthesis of results:

- integration of diverse medical terminology glossaries into SNODOG
- development of procedures for archiving information from each institution
- design of a summary data base that includes dosimetric and histopathologic observations of each major tissue for all study animals.

Each of these steps is detailed below.

SNODOG. A major product of DOE's long-term studies in beagle dogs is pathologists' observations regarding tumor identification and classification and clinicians' findings on morbidity and tumor development. Eventually, it will be useful to analyze these observations by combining results of the various studies conducted at the five laboratories. To this end, each institution has made a commitment to encode their observations using the American Medical Association's hierarchical coding scheme: the Systematized Nomenclature of Medicine (SNOMED), as augmented by the American Veterinary Medical Association in the Systematized Nomenclature of Veterinary Medicine (SNOVET).

TABLE 1. Summary of Lifespan Experiments in Beagle Dogs Exposed to Radiotoxic Insults at DOE-Supported Laboratories.

Laboratory[a]	Exposure Route	Agent	Number of Dogs
PNL	Inhalation	$^{238}PuO_2$, $^{239}PuO_2$, $^{239}Pu(NO_3)_4$	479
ITRI	Inhalation	Alpha Emitters	599
	Inhalation	Beta Emitters	916
Davis	Injection	^{90}Sr, ^{226}Ra	379
	Ingestion	^{90}Sr	479
	External	X ray	360
Utah	Injection	Alpha Emitters	1148
	Injection	^{90}Sr	100
ANL	External	X or Gamma Rays	710
	Injection	Beta Emitters	268
Total			5438

(a) PNL = Pacific Northwest Laboratory; ITRI = Inhalation Toxicology Research Institute; Davis = University of California, Davis; Utah = University of Utah; ANL = Argonne National Laboratory.

We have created a canine-specific "superset" of the SNOVET glossary that contains well over 5000 items. This has been installed on computers at each laboratory and is used daily; data entry software for SNODOG-coded observations has

also been distributed. We act as the clearing house for terminology additions and clarifications, so that SNODOG is dynamic. The revised glossary is distributed on a semiannual basis.

Archiving Information. We have coordinated transfer of computer-tape copies of the beagle-related information at each institution to storage at DOE Headquarters. Off-site storage of tapes and documentation provides additional security for this valuable information. Each laboratory has developed techniques for translating information from its proprietary data management system to machine-independent, American Standard Code Information Interchange (ASCII) format flat files. Extensive documentation of the beagle information management system and a tape back-up process at each laboratory are now available.

Tissue Registry. The tissue registry data base will contain dose information and histopathology observations for each significant tissue from dogs under long-term study. Information for these lifespan observation animals is supplemented by data from ancillary, shorter-duration studies. For example, initial estimation of dose distribution patterns was obtained by serial sacrifice of animals exposed to the same agent as the lifespan dogs. These ancillary animals will be included in the tissue archive; therefore, the total number of animals in the data base will be approximately 8000. Meetings have been conducted at each laboratory to refine this concept. A five-level hierarchy (Table 2), which will probably be maintained on a microcomputer, is envisioned for the registry.

TABLE 2. Hierarchy for Tissue Registry Data Base.

Level	One Record Per	Number of Records	Source of Information
1	Laboratory	5	Annual Reports
2	Study	48	Annual Reports
3	Group	357	Annual Reports
4	Dog	8,000	Colony Master File in Each Laboratory
5	Tissue	80,000	SNODOG File and/or Manual Entry in Each Laboratory
Total		88,410	

A workshop, attended by the information management specialist from each laboratory, produced detailed specifications for the fields in this data base. A prototype of the tissue registry data base is being developed on a microcomputer, using ORACLE. This will draw heavily on the experience of our colleagues at Argonne, who use ORACLE with their beagle information.

Health Effects Research
In Biological Systems

Inhaled Plutonium Oxide in Dogs

Principal Investigator: J. F. Park

Other Investigators: R. L. Buschbom, G. E. Dagle, K. M. Gideon, E. S. Gilbert, G. J. Powers, H. A. Ragan, C. O. Romsos, R. E. Weller, E. L. Wierman, and J. R. Williams

Technical Assistance: K. H. Debban, R. F. Flores, B. B. Kimsey, B. G. Moore, R. P. Schumacher, M. J. Steele, and N. B. Valentine

This project is concerned with long-term experiments to determine the lifespan dose-effect relationships of inhaled $^{239}PuO_2$ or $^{238}PuO_2$ in beagles. The data will be used to estimate the health effects of inhaled transuranics. Beagle dogs given a single exposure to $^{239}PuO_2$ or $^{238}PuO_2$ aerosols to obtain graded levels of initial lung burdens (ILB) are being observed for lifespan dose-effect relationships. Mortality due to radiation pneumonitis and lung tumor increased in the four highest dose-level groups exposed to $^{239}PuO_2$ during the 16-year postexposure period. All of the dogs exposed to $^{239}PuO_2$ are dead. During the 14 years after exposure to $^{238}PuO_2$, mortality due to lung and/or bone tumors increased in the three highest dose-level groups. Chronic lymphopenia, occurring 0.5 to 2 years after exposure, was the earliest observed effect after inhalation of either $^{239}PuO_2$ or $^{238}PuO_2$ in the four highest dose-level groups that had ILB of ≥80 nCi. Other plutonium-exposure-related effects include sclerosis of the tracheobronchial lymph nodes, focal radiation pneumonitis, adenomatous hyperplasia of the liver, and dystrophic osteolytic lesions in the skeleton.

To determine the lifespan dose-effect relationships of inhaled plutonium, 18-month-old beagle dogs were exposed to aerosols of $^{239}PuO_2$ (mean AMAD, 2.3 μm; mean GSD, 1.9), prepared by calcining the oxalate at 750°C for 2 hours; or to $^{238}PuO_2$ (mean AMAD, 1.8 μm; mean GSD, 1.9), prepared by calcining the oxalate at 700°C and subjecting the product to $H_2{}^{16}O$ steam in argon exchange at 800°C for 96 hours. This material, referred to as pure plutonium oxide, is used as fuel in space-nuclear-power systems.

One hundred thirty dogs exposed to $^{239}PuO_2$ in 1970 and 1971 were selected for long-term studies; 14 were sacrificed to obtain plutonium distribution and pathology data; 116 were assigned to lifespan dose-effect studies (Table 1). One hundred sixteen dogs exposed to $^{238}PuO_2$ in 1973 and 1974 were selected for lifespan dose-effect studies (Table 2). Twenty-one additional dogs were exposed for periodic sacrifice. The Appendix (following the entire Annual Report) shows the status of the dogs on these experiments.

Table 3 summarizes, by dose-level group, the mortality and lesions associated with deaths through 16 years after exposure to $^{239}PuO_2$. All of the dogs exposed to $^{239}PuO_2$ are dead. Mean survival time was decreased in the three highest dose-level groups compared to that in the other groups. Fourteen dogs were sacrificed for comparison of plutonium tissue distribution. Table 4 shows the primary cause of death and the distribution of ^{239}Pu in the tissues of these animals as percent of final body burden. Figure 1 shows the plutonium tissue distribution as percent of initial lung burden (ILB).

TABLE 1. Lifespan Dose-Effect Studies with Inhaled $^{239}PuO_2$ in Beagles.[a]

Dose Level Group	Number of Dogs		Initial Lung Deposition[b]	
	Male	Female	nCi[c]	nCi/g Lung[c]
Control	10	10	0	0
1	12	12	3.5 ± 1.3	0.029 ± 0.011
2	10	11	22 ± 4	0.18 ± 0.04
3	10	10	79 ± 14	0.66 ± 0.13
4	11	11	300 ± 62	2.4 ± 0.4
5	10	11	1100 ± 170	9.3 ± 1.4
6	3	5	5800 ± 3300	50 ± 22
	66	70		

(a) Exposed in 1970 and 1971.
(b) Estimated from external thorax counts at 14 and 30 days after exposure and estimated lung weights (0.011 x body weight).
(c) Mean ± 95% confidence intervals around the means.

Table 4 indicates that, as survival time increased, the fraction of plutonium in the lung decreased to 16% of the final body burden by 15 to 16 years after exposure. During the first year after

exposure, plutonium was translocated primarily to the thoracic lymph nodes; little plutonium was translocated to other tissues. Plutonium content of the thoracic lymph nodes increased to 71% of the final body burden at 15 to 16 years after exposure; the abdominal lymph nodes, principally the hepatic nodes, contained ~3%. The fraction of plutonium in liver increased, accounting for 25% of the final body burden in the higher- (≥75 nCi final body burden) dose-level groups. The organ distribution of plutonium in the periodically sacrificed dogs was generally similar to that of the higher-dose-level dogs euthanized when death was imminent during the first 2 years after exposure. The lower-dose-level (≤75 nCi final body burden) dogs sacrificed or euthanized during the 4th to 16th postexposure years generally had a much smaller fraction of the final body burden in the liver, with a larger fraction retained in the lungs and/or thoracic lymph nodes. The fraction of plutonium in the livers of these dogs was ~7% of the final body burden 15 to 16 years after exposure; about 1% was in the skeleton.

TABLE 2. Lifespan Dose-Effect Studies with Inhaled $^{238}PuO_2$ in Beagles.[a]

Dose Level Group	Number of Dogs		Initial Lung Deposition[b]	
	Male	Female	nCi[c]	nCi/g Lung[c]
Control	10	10	0	0
1	10	10	2.3 ± 0.8	0.016 ± 0.007
2	11	10	18 ± 3	0.15 ± 0.03
3	12	10	77 ± 11	0.56 ± 0.07
4	10	10	350 ± 81	2.6 ± 0.5
5	10	10	1300 ± 270	10 ± 1.9
6	7	6	5200 ± 1400	43 ± 12
	70	66		

(a) Exposed in 1973 and 1974.
(b) Estimated from external thorax counts at 14 and 30 days after exposure and estimated lung weights (0.011 x body weight).
(c) Mean ± 95% confidance intervals around the means.

TABLE 3. Summary of Lesions in Dogs Euthanized During the 16-yr Period After Inhalation of $^{239}PuO_2$

	Dose Group						
	6	5	4	3	2	1	Control
Number of Dogs/Group	8	21	22	20	21	24	20
Number of Dead Dogs/Group	8	21	22	20	21	24	20
Mean Survival Postexposure, yr	2	6	10	13	13	12	13
Condition[a]							
Radiation Pneumonitis	7	1					
Radiation Pneumonitis and Lung Tumor	1						
Lung Tumor		19	13	6	2		4
Lung Tumor and Bile Duct Carcinoma			1				
Urinary Bladder Tumor, Lung Tumor		1					
Leiomyosarcoma, Lung Tumor			1		1		
Adrenal Cortical Carcinoma, Lung Tumor				1			
Kidney Tumor, Lung Tumor				1			
Nephropathy and Lung Tumor			1	1	1		
Malignant Lymphoma and Lung Tumor				1			
Pneumonia, Lung Tumor						1	
Bone Tumor					1	2	
Malignant Lymphoma				1		4	2
Malignant Lymphoma and Bile Duct Carcinoma							1
Lymphocytic Leukemia						1	
Hemangiosarcoma (Heart, Spleen, Liver)						3	2
Pituitary Tumor, Cushing's			1			1	
Cushing's Intestinal Carcinoma							1
Thyroid Carcinoma				1			
Reticulum Cell Sarcoma			1				
Ovarian Tumor					1		
Oral Tumor							1
Round Cell Sarcoma and Bile Duct Adenoma						1	
Hemangioma (Spleen)					1		
Malignant Melanoma					2		1
Pheochromocytoma					1		1

[a]Number of dogs with lesion associated with death.

TABLE 3. Continued

	Dose Group						
	6	5	4	3	2	1	Control
Number of Dogs/Group	8	21	22	20	21	24	20
Number of Dead Dogs/Group	8	21	22	20	21	24	20
Mean Survival Postexposure, yr	2	6	10	13	13	12	13
Condition[a]							
Urinary Bladder Tumor				1	2		
Neurofibrosarcoma				1			
Meningioma						1	
Pneumonia			2	2	4	4	
Epilepsy					1	1	1
Thromboembolism				1			1
Pyometra			1	1			
Unknown					1	1	
Liver Cirrhosis			1				
Septicemia						1	
Cardiac Insufficiency				1	1		
Peritonitis					1		
Adrenalitis							1
Kidney Failure						1	
Nephrosclerosis							1
Chronic Nephropathy				1	1	1	2
Glomerulosclerosis						1	
Luxated Vertebral Disc							1

[a]Number of dogs with lesion associated with death.

TABLE 4. Tissue Distribution of Plutonium in Beagles After Inhalation of $^{239}PuO_2$.

Dog Number	Time After Exposure, mo	Final Body Burden, μCi	Percent of Final Body Burden					Cause of Death
			Lungs	Thoracic Lymph Nodes[a]	Abdominal Lymph Nodes[b]	Liver	Skeleton	
478M	0.25	0.293	98	0.15	0.02	0.24	0.18	Sacrifice
435F	0.25	3.841	99	0.11	0.01	0.00	0.03	Sacrifice
816M	0.50	0.399	99	0.12	0.01	0.00	0.03	Sacrifice
918M	1	0.074	99	0.82	0.02	0.11	0.08	Sacrifice
920F	1	0.011	94	0.47	0.03	0.08	0.61	Sacrifice
913M	1	4.849	98	1.1	0.00	0.03	0.05	Sacrifice
702F	5	1.682	94	5.7	0.00	0.01	0.09	Sacrifice
709M	5	1.726	97	2.2	0.00	0.00	0.05	Sacrifice
734M	5	0.914	96	3.4	0.00	0.01	0.05	Sacrifice
739F	5	1.511	95	4.7	0.03	0.00	0.00	Sacrifice
910M	11	12.229	84	15	0.01	0.06	0.05	Radiation Pneumonitis
747F	12	5.434	71	29	0.03	0.07	0.07	Radiation Pneumonitis
906F	12	6.154	88	12	0.00	0.03	0.05	Radiation Pneumonitis
849F	13	0.0007	80	15	0.20	0.04	1.6	Sacrifice
896F	15	4.115	81	15	0.92	0.23	0.12	Radiation Pneumonitis
817M	21	3.794	64	34	0.13	1.4	0.19	Radiation Pneumonitis
815M	25	0.074	64	32	---	0.08	0.10	Sacrifice
829M	26	3.198	75	19	0.79	4.2	0.45	Radiation Pneumonitis

[a]Includes tracheobronchial, mediastinal and sternal lymph nodes.
[b]Includes hepatic, splenic and mesenteric lymph nodes.

TABLE 4. Continued

Dog Number	Time After Exposure, mo	Final Body Burden, µCi	Percent of Final Body Burden					Cause of Death
			Lungs	Thoracic Lymph Nodes[a]	Abdominal Lymph Nodes[b]	Liver	Skeleton	
760M	31	0.978	71	23	0.57	3.7	0.28	Radiation Pneumonitis
890F	31	2.012	55	28	2.2	13	0.26	Radiation Pneumonitis
804M	37	1.101	62	29	0.19	7.9	0.36	Radiation Pneumonitis, Lung Tumor
798F	43	0.0056	55	44	0.02	0.17	0.43	Sacrifice
772M	53	1.821	42	22	0.88	29	0.69	Lung Tumor
759M	53	0.707	43	27	12	15	0.65	Lung Tumor
796F	55	0.671	40	31	4.1	21	1.0	Lung Tumor
783M	59	1.377	59	11	1.8	26	0.67	Lung Tumor
873M	62	1.746	45	27	6.4	16	0.76	Lung Tumor
753F	69	1.171	35	31	0.09	24	0.64	Lung Tumor
761M	69	1.064	36	37	6.3	19	0.53	Lung Tumor
727M	72	0.585	39	24	12	23	0.78	Lung Tumor
762M	72	0.0017	51	42	0.34	0.71	0.66	Sacrifice
837M	72	1.034	42	38	0.70	14	0.46	Lung Tumor
863F	76	0.617	33	12	1.3	47	1.4	Lung Tumor
852F	77	1.067	33	35	0.88	26	0.94	Lung Tumor
803M	79	0.415	20	46	11	20	1.4	Interstitial Pneumonitis
875M	83	0.0026	24	66	0.34	0.64	6.3	Malignant Lymphoma, Kidney
754M	84	0.0046	29	66	0.23	0.39	1.2	Status Epilepticus
835F	86	0.099	27	65	0.95	3.1	1.7	Reticulum Cell Sarcoma
880F	86	0.468	19	31	13	34	0.37	Lung Tumor
769F	90	0.019	36	57	0.32	1.7	1.8	Ovarian Tumor
888M	93	0.179	32	40	10	12	2.1	Lung Tumor
856F	94	0.306	40	45	0.78	9.0	3.9	Lung Tumor
889F	94	0.613	14	27	6.9	41	8.1	Lung Tumor
787M	95	0.473	24	19	12	39	2.7	Lung Tumor
820F	96	0.387	14	40	7.6	29	1.4	Lung Tumor
834F	97	0.025	30	46	17	3.5	0.91	Pyometra
752M	98	0.055	24	62	1.2	7.7	0.98	Lung Tumor
864F	100	0.616	18	22	2.9	50	2.9	Lung Tumor
908F	101	0.0073	14	72	0.049	0.56	0.93	Unknown
778M	102	0.065	11	85	1.3	1.0	0.52	Pulmonary Thromboembolism
812M	103	0.288	15	36	29	16	2.2	Lung Tumor
814F	104	0.054	49	33	4.1	10	1.6	Lung Tumor
840F	107	0.389	17	35	5.8	37	2.0	Lung Tumor
777M	109	0.392	11	52	7.8	24	1.7	Lung Tumor
857M	109	0.333	20	39	9.4	27	2.4	Lung Tumor
898F	111	0.333	10	34	28	21	3.4	Urinary Bladder Tumor, Lung Tumor
899F	113	0.0066	7.5	87	0.14	0.27	1.6	Hemangiosarcoma, Heart
697M	114	0.141	15	64	8.1	9.9	1.4	Cardiac Insufficiency
909M	115	0.444	16	46	11	25	1.2	Lung Tumor
824F	116	0.178	21	75	0.50	2.3	0.70	Pneumonia
891M	116	0.0023	11	84	0.064	0.48	1.5	Septicemia
836M	117	0.333	12	63	15	7.4	0.97	Lung Tumor
892M	120	0.348	10	47	18	20	3.7	Lung Tumor
794M	120	0.397	13	33	14	31	3.5	Pituitary Tumor, Cushing's
781F	122	0.034	37	59	0.25	1.1	0.72	Kidney Tumor, Lung Tumor
809F	123	0.120	12	36	18	28	3.3	Liver Cirrhosis, Thyroid Tumor, Addison's
854M	124	0.435	12	66	15	3.8	1.3	Lung Tumor
807F	125	0.0021	10	71	0.55	1.2	1.3	Pituitary Tumor, Cushing's
810F	126	0.219	5.9	43	20	22	1.8	Lung Tumor

[a]Includes tracheobronchial, mediastinal and sternal lymph nodes.
[b]Includes hepatic, splenic and mesenteric lymph nodes.

TABLE 4. Continued

Dog Number	Time After Exposure, mo	Final Body Burden, µCi	Percent of Final Body Burden					Cause of Death
			Lungs	Thoracic Lymph Nodes[a]	Abdominal Lymph Nodes[b]	Liver	Skeleton	
900M	126	0.0016	13	60	2.3	9.0	2.9	Round Cell Sarcoma and Bile Duct Adenoma
748F	127	0.0015	10	50	0.87	0.33	1.2	Unknown
860M	133	0.335	8.2	68	8.0	11	2.5	Lung Tumor
805F	134	0.169	5.8	55	8.9	21	2.8	Esophageal Leiomyoma, Lung Tumor
780F	135	0.0074	28	69	0.37	0.02	0.79	Pheochromocytoma
905F	135	0.080	13	50	10	19	1.7	Malignant Lymphoma
825F	137	0.0020	9.5	85	0.74	0.54	2.7	Hemangiosarcoma, Spleen
764F	139	0.081	15	75	3.9	4.9	0.73	Lung Tumor
808F	139	0.206	11	30	1.8	53	3.0	Lung Tumor
806F	140	0.010	11	78	1.8	5.1	2.3	Malignant Melanoma, Palate
850F	140	0.00062	12	82	0.61	0.11	2.0	Bone Tumor
833F	143	0.157	3.1	40	22	31	1.1	Metritis, Adrenal and Thyroid Carcinoma
862M	145	0.0026	21	56	0.85	4.4	6.9	Peritonitis
904F	145	0.0013	8.9	87	0.30	0.88	1.0	Chondrosarcoma
756M	147	0.0016	15	75	1.0	1.6	4.1	Epilepsy
782M	148	0.043	12	72	4.9	9.0	0.86	Neurofibrosarcoma
886F	149	0.00085	13	51	15	3.6	13	Meningioma
795F	152	0.030	24	26	8.3	38	1.5	Lung Tumor
771F	153	0.019	20	71	1.0	5.8	1.1	Lung Tumor
813F	153	0.036	22	44	4.7	27	1.1	Multilobar Sarcoma, Skull
826F	153	0.0034	8.0	88	0.38	0.92	1.2	Hemangioma, Spleen
859M	154	0.048	19	31	29	7.3	0.79	Urinary Bladder Tumor
870F	154	0.00062	8.2	70	4.9	9.6	4.8	Pneumonia
879M	154	0.00093	19	75	0.52	0.81	1.6	Hemangiosarcoma
884M	155	0.077	13	45	9.4	30	1.6	Lung Tumor
831F	155	0.0087	24	71	0.65	3.3	1.0	Pneumonia
866M	156	0.145	15	41	9.3	34	0.20	Lung Tumor
823M	157	0.072	7.3	83	1.8	6.0	1.5	Urinary Bladder Tumor
838M	157	0.044	18.0	73	0.77	5.4	1.4	Malignant Lymphoma, Lung Tumor
788M	158	0.0022	22	70	2.0	1.8	0.11	Chronic Nephropathy
845F	158	0.012	28	69	0.25	1.5	0.63	Urinary Bladder Tumor
853M	158	0.0081	13	77	2.2	5.4	0.54	Bronchopneumonia
750M	161	0.071	20	51	13.0	9.5	2.4	Lung Tumor, Malignant Lymphoma
847M	163	0.00061	22	75	0.15	0.60	1.2	Kidney Failure
776M	163	0.0020	29	67	0.11	1.2	1.1	Bronchopneumonia
802M	164	0.019	13	45	33	6.7	1.3	Pneumonia
827F	164	0.075	4.5	49	17	27	1.5	Acute Pneumonia
874M	165	0.0048	5.6	90	0.54	1.4	0.56	Chronic Nephropathy
842M	166	0.0054	4.7	90	0.76	3.2	0.75	Lung Tumor, Chronic Nephropathy
770F	166	0.0023	17	80	0.15	0.69	0.52	Glomerulosclerosis
844F	170	0.097	19	50	8.9	19	1.3	Nephropathy, Lung Tumor
819F	170	0.085	18	42	4.2	30	3.0	Nephropathy, Lung Tumor
907F	174	0.00097	7.4	89	1.2	0.78	0.61	Pneumonia
876F	175	0.0080	10	80	1.8	6.1	0.88	Nephropathy, Lung Tumor
877F	175	0.011	13	79	2.2	3.8	0.70	Lung Tumor
867M	175	0.0027	23	52	5.8	16	1.6	Malignant Lymphoma
893M	177	0.0021	10	87	0.19	0.63	1.0	Pneumonia
839F	177	0.105	6.4	53	11	27	2.0	Lung Tumor, Bile Duct Carcinoma
841F	178	0.0028	6.8	89	0.13	2.1	0.84	Malignant Lymphoma
832F	178	0.0020	8.3	87	0.17	1.5	0.88	Malignant Lymphoma
767M	180	0.0088	33	64	0.22	1.1	0.96	Valvular Endocardiopathy
848F	180	0.047	9.8	80	4.9	3.7	0.80	Acute Pneumonia
871M	181	0.0028	10	86	0.59	1.6	1.0	Malignant Melanoma, Oral
851F	182	0.025	15	77	1.7	4.8	1.2	Thyroid Carcinoma, Hypothyroidism

[a]Includes tracheobronchial, mediastinal and sternal lymph nodes.
[b]Includes hepatic, splenic and mesenteric lymph nodes.

TABLE 4. Continued

Dog Number	Time After Exposure, mo	Final Body Burden, µCi	Percent of Final Body Burden					Cause of Death
			Lungs	Thoracic Lymph Nodes[a]	Abdominal Lymph Nodes[b]	Liver	Skeleton	
865F	182	0.00062	7.0	89	0.23	0.92	1.5	Acute Pneumonia, Lung Tumor
797F	182	0.056	11	43	11	31	1.7	Lung Tumor
881F	182	0.0066	13	85	0.27	0.33	0.75	Acute Pneumonia
786M	183	0.047	11	60	6.5	10	1.4	Adrenocortical Carcinoma, Lung Tumor
858M	183	0.00042	5.4	88	2.2	1.6	0.60	Lymphocytic Leukemia
757M	191	0.018	58	30	2.8	6.4	1.6	Leiomyosarcoma, Kidney and Lung Tumor
883M	196	0.036	11	76	3.2	6.0	2.0	Chronic Nephropathy

[a]Includes tracheobronchial, mediastinal and sternal lymph nodes.
[b]Includes hepatic, splenic and mesenteric lymph nodes.

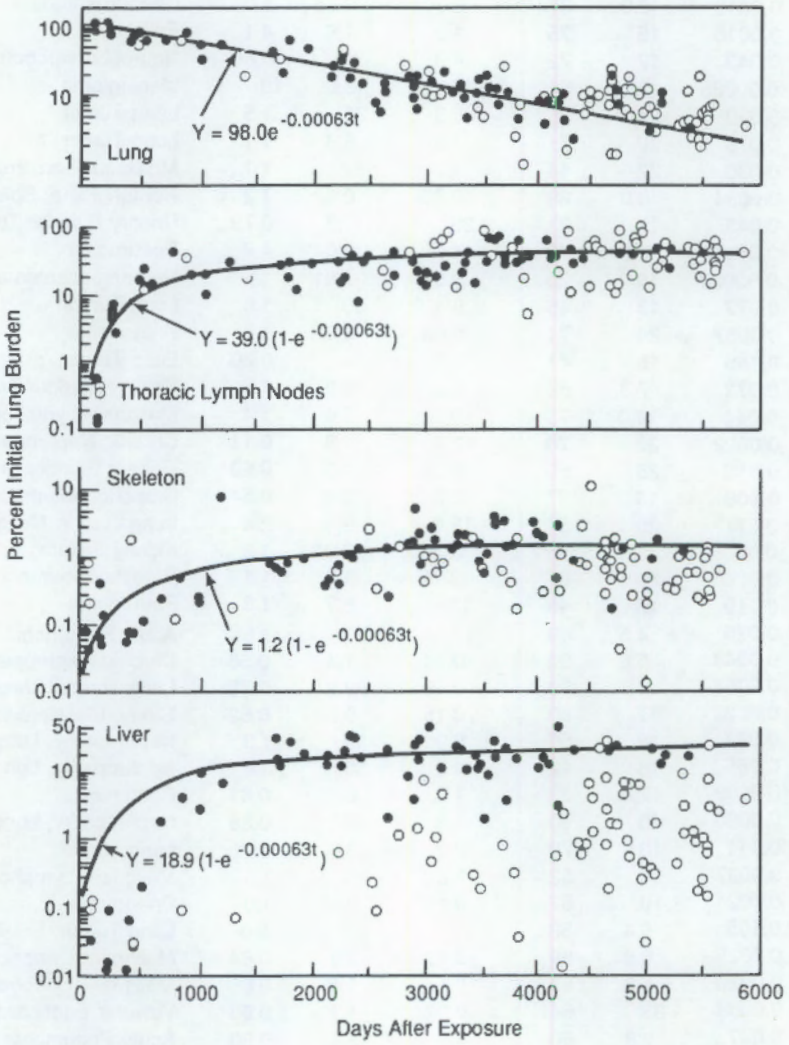

FIGURE 1. Plutonium in Tissues of Dogs After Inhalation of $^{239}PuO_2$. Points represent data from individual dogs (• = ≥ 75 nCi, O = ≤ 75 nCi final body burden). The uptake and retention curves and function were based on dogs in which initial lung burdens were estimated from external thorax counts at 14 and 30 days after exposure. The curves for liver were based on dogs with final body burdens ≥ 75 nCi.

Figure 1 shows the ^{239}Pu tissue distribution as percent of the ILB for all dogs for which tissue radiochemical analyses are complete. The ILB for those dogs for which radiochemical analysis of excreta were not complete were estimated from external thorax counts at 14 and 30 days after exposure. For dogs whose analyses were complete, ILB were estimated from the summation of the tissue burdens of plutonium, plus the plutonium excreted, minus plutonium excreted in the feces during the first 3 days after exposure. The latter was assumed to be deposited in the upper respiratory tract. Uptake and retention functions were fitted to the organ burden data. Based on the premise that the organ burdens were interrelated, the uptake and retention function for all organs was fitted simultaneously instead of fitting isolated functions for each organ. The organs were treated as compartments of a single system, with transfer rates specifying the total amount, leaving a compartment per unit time and the fractional distribution of that amount among the other compartments. The transfer rates assumed that plutonium moved through the body in a single pass. The material initially deposited in the lung was either excreted or moved to some other organ, from which it was excreted. It was assumed that there were no feedback loops in the system. Organ systems included lung, thoracic lymph nodes, liver, skeleton, and all other tissues. The functions were estimated using weighted, nonlinear least squares. The weights were estimated by bi-weighting procedures that give the more extreme data values very little weight. The curves for liver were based on dogs with final body burdens $\leq$75 nCi; dogs with $\leq$75 nCi had less plutonium translocated to the liver.

The nine dogs euthanized because of radiation pneumonitis during the 3-year postexposure period had increased respiration rates, and hypercapnia and hypoxemia associated with lesions in the lungs. Intermittent anorexia and body weight loss accompanied the respiratory insufficiency. Histopathologic examination of the lungs showed radiation pneumonitis, characterized by focal interstitial and subpleural fibrosis, increased numbers of alveolar macrophages, alveolar epithelial hyperplasia, and foci of squamous metaplasia. Autoradiographs showed activity primarily composed of large stars, more numerous in areas of interstitial and subpleural fibrosis. Dog 804M also had a pulmonary tumor, classified as a bronchiolar-alveolar carcinoma.

Fifty-two of the 116 exposed dogs euthanized 3 to 16 years after exposure had lung tumors. Radiographic evidence of pulmonary neoplasia frequently preceded development of respiratory insufficiency. In dogs with neoplasia in the lung, respiratory insufficiency, when it was observed, was usually a late clinical finding that occurred shortly before euthanasia. Eleven of the dogs with lung tumors were euthanized due to other causes. Two dogs in Dose Level 1 were euthanized 11.7 and 12.1 years, respectively, after exposure: one had an osteosarcoma involving the nasal cavity and maxilla; the other had a chondrosarcoma involving the nasal cavity. One dog in Dose Level 2, euthanized 12.8 years after exposure, had a multilobular sarcoma of the skull. Four control dogs were euthanized because of lung tumors. Dogs 794M, 803M, 809M, 824F, 833F, and 835F (Dose Level 4), 697M, 778M, 782M, 823M, 827F, 834F, 848F, 851F, 883M, and 905F (Dose Level 3), 748F, 754M, 769F, 767M, 776M, 780F, 802M, 806F, 826F, 831F, 845F, 859M, 862M, 871M, 874M, and 881F (Dose Level 2), and 756M, 770F, 788M, 807F, 825F, 832F, 841F, 847M, 853M, 858M, 867M, 870M, 875M, 879M, 886F, 891M, 893M, 899F, 900M, 907F, and 908M (Dose Level 1) died during the 7- to 16-yr postexposure period of causes presently thought to be unrelated to plutonium exposure.

In 23 of the dogs, the lung tumors were classified as bronchiolar-alveolar carcinoma; in six dogs as adenosquamous carcinoma; in nine dogs, adenocarcinoma; in four dogs, epidermoid and adenocarcinoma; in four dogs, epidermoid carcinoma; in one dog, epidermoid and bronchiolar-alveolar carcinoma; in three dogs, adenocarcinoma and bronchiolar-alveolar carcinoma; in one dog, epidermoid carcinoma, adenocarcinoma, and bronchiolar-alveolar carcinoma; and in another dog, adenocarcinoma, adenosquamous carcinoma and bronchiolar-alveolar adenocarcinoma. The epidermoid carcinomas metastasized to the lungs, skeletons, brains, intestines and thoracic lymph nodes; the bronchiolar-alveolar carcinomas metastasized only to the thoracic lymph nodes in eight dogs, and to several organs (including mediastinum; kidney; thyroid; skeleton; heart; adrenal gland; aorta; and axillary, prescapular, cervical, splenic, thoracic, and hepatic lymph nodes) in four other dogs. Three of the adenosquamous carcinomas metastasized to thoracic lymph nodes, mediastinum and thoracic pleura, and one to the hepatic and tracheobronchial lymph nodes. The adenocarcinomas

metastasized to the lungs; tracheobronchial, hepatic, splenic, sternal and axillary lymph nodes; heart, kidney, and esophagus in five dogs.

The lung tumors in the control dogs were classified as bronchiolar-alveolar adenocarcinomas in two dogs with metastases to thoracic and abdominal lymph nodes, trachea, esophagus and mediastinum; adenocarcinoma with metastases to the diaphragm and abdominal lymph nodes in one dog; and combined epidermoid and adenocarcinoma with metastases to the thoracic lymph nodes, diaphragm, liver and kidney in another.

Three of the exposed dogs had lesions of secondary hypertrophic osteoarthropathy. Sclerosing lymphadenopathy was associated with the high concentration of plutonium in the thoracic and hepatic lymph nodes of dogs in Dose-Level Groups 2, 3, 4, 5 and 6. There was also a generalized lymphoid atrophy that may be related, in the dogs with respiratory insufficiency, to debilitation or to lymphopenia. Livers of the dogs in Dose-Level Groups 4 and 5, which were euthanized during the 4- to 13-year postexposure period, showed moderate, diffuse, centrilobular congestion. Liver cells in these areas contained fine, granular, yellow pigment resembling lipofuscin, and were frequently vacuolated. Focal aggregation of vacuolated, lipofuscin-containing cells in the sinusoids was associated with alpha stars on autoradiographs.

Bile-duct tumors have been reported by other laboratories in beagles exposed to plutonium. In our $^{239}PuO_2$ study, one Dose-Level 4 dog and one control dog had a bile-duct carcinoma as an incidental lesion not related to the death of the dog. One Dose-Level 1 dog had an incidental bile-duct adenoma. In the $^{238}PuO_2$ study, two Dose-Level 4 dogs also had a bile-duct carcinoma or adenoma as an incidental observation. These five are the total number of bile-duct tumors observed thus far in these studies. One control and two exposed dogs had hepatomas unrelated to their deaths.

Lymphopenia developed after inhalation of $^{239}PuO_2$ in dose-level groups with mean initial lung depositions of 79 nCi or more (Figure 2). Through 123 months after exposure, mean lymphocyte values were significantly lower ($P < 0.05$) for Dose-Level Groups 3 and 4 than for the control group. At 127 months after exposure, mean lymphocyte values for Dose-Level Groups 3 and 4 were not significantly different from those of the control groups. The reduction in lymphocytes was dose-related, both in time of appearance and magnitude. Over the course of this study, there has been a slight age-related decrease in mean lymphocyte values of control dogs. In addition, mean lymphocyte concentrations in Groups 3 and 4 have tended to increase, making the differences between control dogs and these groups less significant than previously. At mean lung depositions of 3.5 and 22 nCi, lymphocyte values were within ranges observed in control dogs. A reduction in total leukocytes was evident in the higher-dose groups, which were also lymphopenic. No effects have been observed on red-cell parameters following $^{239}PuO_2$ inhalation. By 14 years after exposure, too few dogs were alive for meaningful dose-group comparison.

Serum chemistry assays have been performed to detect organ-specific damage from plutonium that translocated from lung to extrapulmonary sites. No consistent, dose-related alterations have occurred in serum constituents (glutamic pyruvic transaminase [GPT], glutamic oxaloacetic transaminase, alkaline phosphatase [ALP], urea nitrogen, and serum protein fractions) of dogs exposed to $^{239}PuO_2$.

Table 5 summarizes, by dose-level group, mortality and lesions associated with death through 14 years after exposure to $^{238}PuO_2$. During this period, all of the dogs in the highest-level dose group and in Dose-Level Group 5, nineteen dogs in Group 4, sixteen dogs in Group 3, fourteen dogs in Group 2, and fourteen dogs in Dose-Level Group 1 were euthanized when death was imminent. Eleven control dogs were euthanized during the 14-year postexposure period. Mean survival time was decreased in the two highest dose-level groups compared to the other groups. Twenty-one dogs were sacrificed for comparison of plutonium tissue distribution. Table 6 shows the primary causes of death and the distribution of ^{238}Pu in the tissues of these animals as percent of final body burden. Figure 3 shows the plutonium tissue distribution as percent ILB.

At 13 to 14 years after exposure, the fraction of the final body burden in the lungs of the ^{238}Pu-exposed dogs was about 1%, compared to 16% in the ^{239}Pu-exposed dogs (Table 6). At that time, ~7% of the ^{238}Pu was in the thoracic lymph nodes, compared to 69% of the ^{239}Pu. Livers of the ^{238}Pu-exposed dogs contained 41% of the plutonium burden, compared to 7% in the livers of the ^{239}Pu-exposed dogs. About 46% of the final body burden was in the skeletons of the ^{238}Pu-exposed dogs, at that time, compared to

~1% in the ^{239}Pu-exposed dogs. Tissue distribution of ^{238}Pu in low-dose-level dogs did not differ from that in high-dose-level dogs. Figure 3 shows the ^{238}Pu tissue distribution as percent of ILB for all dogs for which tissue radiochemical analyses are complete. The ILB and uptake and retention curves were estimated as described previously for ^{239}Pu. The uptake and retention curves were based on dogs in which ILB were estimated from the final plutonium body burden, plus the plutonium excreted, minus that excreted in the feces during the first 3 days after exposure.

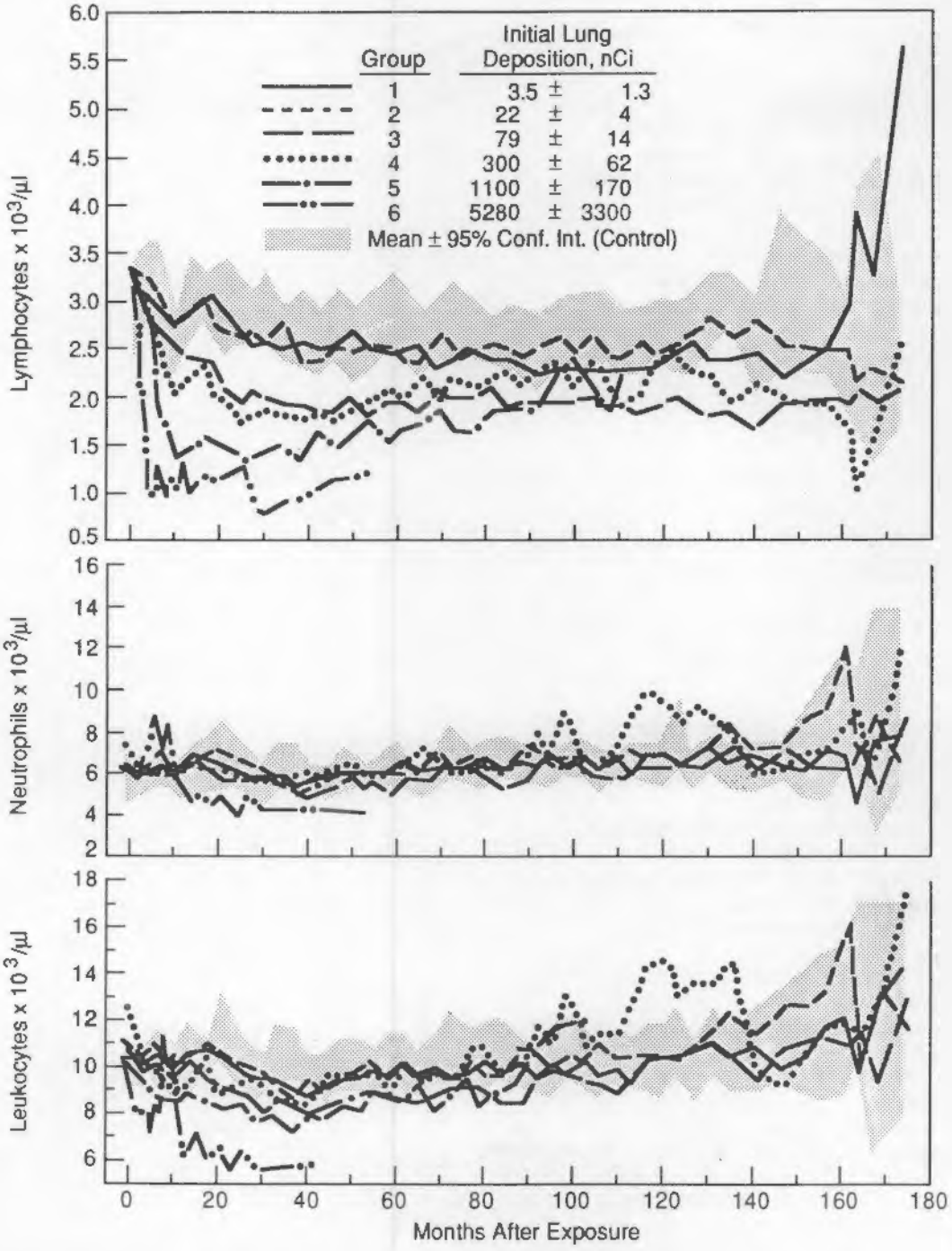

FIGURE 2. Mean Leukocyte, Neutrophil and Lymphocyte Values in Dogs After Inhalation of $^{239}PuO_2$.

TABLE 5. Summary of Lesions in Dogs Euthanized During the 14-yr Period After Inhalation of $^{238}PuO_2$.

	Dose Group						
	6	5	4	3	2	1	Control
Number of Dogs/Group	13	20	20	22	21	20	20
Number of Dead Dogs/Group	13	20	19	16	14	14	11
Mean Survival Postexposure, yr	5	7	12	12	12	12	12
Condition[a]							
Bone Tumor	2	11	4			1	
Lung Tumor	3		1	1	2	1	
Bone and Lung Tumor	6	4	2				
Bone Tumor and Bile Duct Carcinoma			1				
Bone Tumor and Addison's Disease	1						
Bone and Lung Tumor, Addison's Disease		1					
Nasal Sarcoma and Lung Tumor					1		
Pneumonia, Lung Tumor			1				
Addison's Disease	1	2					
Malignant Lymphoma, Lung Tumor					1		
Malignant Mesothelioma					1		
Malignant Lymphoma			1	3	1	3	4
Malignant Lymphoma, Addison's Disease			1				
Hemangioma; Spleen			1				
Hemangiosarcoma; Heart, Spleen, Liver			1	1	1	1	1
Fibrosarcoma, Spleen						1	
Pituitary Tumor							1
Pitutary Tumor, Cushing's			1	1			1
Urinary Bladder Tumor			1				2
Brain and Heart Tumor						1	
Brain Tumor					1		
Parathyroid Adenoma				1			
Adrenal Carcinoma						1	
Round Cell Sarcoma; Kidney					1		
Adrenal and Pituitary Tumor			1				
Lung Tumor, Metastatic					1		
Thyroid Carcinoma			1				
Pneumonia and Thyroid Carcinoma				2			
Pneumonia		1	1	2	2		
Allergic Bronchitis				1			
Radiation Pneumonitis				1			
Renal Amyloidosis, Splenic Hemangioma							1
Chronic Nephropathy				1			
Chronic Nephropathy, Bile Duct Adenoma			1				
Immune Hemolytic Anemia						1	
Spinal Cord Degeneration					1		
Posterior Paralysis				1			
Herniated Vertebral Disk		1					
Pyometra							1
Liver Abscess						1	
Hepatic Dysplasia				1			
Heart Failure					1	1	
Anesthesia						1	

[a]Number of dogs with lesion associated with death.

TABLE 6. Tissue Distribution of Plutonium in Beagles After Inhalation of $^{238}PuO_2$.

Dog Number	Time After Exposure, mo	Final Body Burden, µCi	Percent of Final Body Burden					Cause of Death
			Lungs	Thoracic Lymph Nodes[a]	Abdominal Lymph Nodes[b]	Liver	Skeleton	
1032M	0.25	0.150	97	0.34	0.20	1.7	0.16	Sacrifice
921F	1	0.0044	93	0.65	0.04	0.38	2.1	Sacrifice
930F	1	0.052	99	0.63	0.01	0.07	0.35	Sacrifice
931F	1	0.347	96	1.9	0.01	0.05	0.36	Sacrifice
929F	2	0.017	91	7.5	0.002	0.26	0.58	Sacrifice
932F	2	0.382	96	2.5	0.01	0.18	0.39	Sacrifice
923F	2	0.0023	88	9.4	0.03	0.09	0.44	Sacrifice
925M	3	0.0064	91	4.1	0.04	0.04	1.2	Sacrifice
926M	3	0.078	87	11	0.23	0.65	1.1	Sacrifice
934M	3	0.902	92	4.8	1.7	0.45	0.95	Sacrifice
1318M	12	0.030	45	27	0.08	10	15	Sacrifice
1319M	12	0.077	41	26	0.03	11	20	Sacrifice
1214M	13	0.014	52	9.2	0.32	6.2	16	Sacrifice
1310M	25	0.026	19	36	0.08	15	28	Sacrifice
1317M	25	0.041	20	33	0.16	17	26	Sacrifice
1315M	25	0.047	22	31	0.04	17	28	Sacrifice
1191F	35	0.658	26	32	0.13	18	22	Pneumonia
1215M	36	0.011	21	43	0.17	13	21	Sacrifice
1311M	37	0.036	13	31	0.22	21	32	Sacrifice
994F	42	5.024	17	45	0.50	18	18	Addison's Disease
970F	48	0.0022	20	34	0.36	16	24	Sacrifice
1312M	49	0.035	6.8	29	0.26	25	35	Sacrifice
1143M	49	6.331	11	43	2.0	15	22	Bone Tumor, Lung Tumor
1025M	50	10.033	16	27	7.1	24	23	Lung Tumor
1064M	51	8.427	13	48	1.9	15	20	Bone Tumor, Lung Tumor
1175F	52	3.641	14	31	0.08	25	26	Lung Tumor
1079M	56	2.182	9.8	40	4.3	13	25	Addison's Disease
1096F	59	1.204	4.3	22	2.7	36	24	Addison's Disease
1189M	60	0.044	8.9	25	0.16	37	25	Sacrifice
1115F	61	1.534	5.0	32	2.3	26	33	Bone Tumor
1162F	61	3.663	12	32	5.9	21	25	Bone Tumor, Addison's Disease
1009M	62	4.360	15	25	2.4	31	23	Lung Tumor
974F	64	1.465	5.1	24	5.9	33	29	Bone Tumor
1092M	65	1.515	2.1	26	9.1	29	30	Bone Tumor
975F	66	3.749	11	30	2.1	28	25	Bone Tumor, Lung Tumor
1042F	69	1.494	4.7	25	2.9	32	33	Bone Tumor, Lung Tumor
1037M	69	2.417	7.1	27	7.8	28	27	Bone Tumor
1027M	70	2.546	3.8	15	7.0	40	31	Bone Tumor, Lung Tumor
1006F	72	2.826	7.5	30	3.4	29	26	Bone Tumor, Lung Tumor
1057M	72	1.748	3.0	35	2.2	33	24	Bone Tumor
1082M	78	0.0083	2.4	20	0.31	40	34	Paralysis
1081M	80	0.361	4.6	15	0.48	47	29	Hemangiosarcoma, Heart
1058F	80	1.000	2.0	18	4.4	31	41	Bone Tumor, Adrenal Tumor
1002M	84	1.786	2.9	31	2.0	31	28	Bone Tumor, Lung Tumor
1109F	86	0.885	0.93	23	4.0	34	35	Bone Tumor, Addison's Disease, Lung Tumor
1218F	86	0.678	2.7	23	4.1	42	25	Bone Tumor
1071M	91	1.088	5.4	28	3.4	27	33	Bone Tumor, Lung Tumor
1063M	94	0.00060	3.4	15	1.3	22	43	Brain Tumor, Heart Tumor
1160F	95	0.956	1.6	21	0.91	43	30	Bone Tumor, Lung Tumor
960M	95	0.036	4.0	21	0.49	33	39	Malignant Lymphoma
1040M	96	0.059	3.0	17	0.96	40	35	Parathyroid Adenoma
1140M	97	0.504	3.8	18	7.7	37	30	Bone Tumor

[a] Includes tracheobronchial, mediastinal and sternal lymph nodes.
[b] Includes hepatic, splenic and mesenteric lymph nodes.

TABLE 6. Continued

Dog Number	Time After Exposure, mo	Final Body Burden, µCi	Percent of Final Body Burden					Cause of Death
			Lungs	Thoracic Lymph Nodes[a]	Abdominal Lymph Nodes[b]	Liver	Skeleton	
989F	99	0.0017	5.1	11	1.2	22	29	Bone Tumor (Fibrosarcoma)
1211M	99	0.895	1.3	29	4.7	39	23	Bone Tumor
1173M	99	0.462	2.0	33	7.5	21	33	Bone Tumor
1043F	103	0.037	3.5	16	0.57	33	42	Empyema, Pituitary Tumor, Cushing's
1192F	109	0.345	2.4	7.3	4.6	36	46	Bone Tumor
1178M	110	0.594	0.86	17	2.0	33	42	Bone Tumor, Lung Tumor
1047M	115	0.241	1.4	7.8	11	28	48	Herniated Vertebral Disc
1106F	117	0.0029	1.3	16	1.8	9.9	57	Adrenal Carcinoma
1103F	118	0.232	0.76	18	3.1	45	32	Bone Tumor, Lung Tumor
1188M	119	0.0089	0.71	2.5	0.94	68	24	Metastatic Lung Tumor
1066M	121	0.035	1.1	4.4	0.52	57	32	Malignant Lymphoma
1069F	121	0.0022	9.1	2.1	1.6	51	34	Malignant Lymphoma
1030F	122	0.160	1.5	15	1.1	22	56	Pneumonia
951M	122	0.0023	3.3	8.9	0.77	47	35	Anesthesia
1229M	123	0.0060	0.94	11	0.73	35	49	Pneumonia
1072M	124	0.079	0.65	4.1	1.6	57	34	Radiation Pneumonitis
1157M	124	0.294	0.55	3.5	3.7	41	44	Bone Tumor
971F	125	0.0095	1.7	5.5	0.44	49	41	Hemangiosarcoma, Spleen
1078F	125	0.025	0.98	9.6	0.60	46	41	Meningioma
952F	125	0.106	1.0	4.4	2.1	39	48	Bone Tumor
1059F	126	0.050	4.2	7.4	0.99	45	39	Malignant Lymphoma
991F	126	0.058	1.8	14	0.81	36	41	Urinary Bladder Tumor
1070M	126	0.011	1.9	9.5	0.70	51	34	Round Cell Sarcoma, Kidney
1166M	128	0.354	1.8	11	1.6	47	35	Malignant Lymphoma
983M	132	0.274	1.5	5.9	2.9	47	37	Adrenal Tumor, Pituitary Tumor
1035F	132	0.172	2.8	10	1.9	19	53	Bone Tumor, Cushing's
1031F	134	0.025	1.9	13	0.97	17	65	Pneumonia
1190F	134	0.033	0.84	4.4	1.2	49	41	Lung Tumor
1062M	135	0.270	0.63	2.6	3.9	46	44	Bone Tumor, Lung Tumor
1177M	136	0.142	0.77	5.0	0.89	36	53	Bone Tumor
959M	138	0.0025	3.4	14	0.62	33	48	Liver Abscess
992F	139	0.264	0.73	8.0	2.7	42	42	Bone Tumor
1194F	140	0.0014	0.67	10	9.0	20	56	Malignant Lymphoma
1105F	140	0.00074	0.62	5.6	0.70	44	45	Malignant Lymphoma
1193F	141	0.0037	0.58	9.2	1.0	37	48	Immune Hemolytic Anemia
973F	142	0.127	3.7	7.0	1.8	44	39	Bone Tumor
1060F	142	0.011	0.61	10	0.68	39	47	Pneumonia
1114M	143	0.272	0.51	7.4	2.9	39	47	Bone Tumor, Bile Duct Carcinoma
1222M	143	0.0051	8.5	4.0	0.82	36	47	Malignant Mesothelioma (Mediastinal)
1053F	143	0.061	1.9	5.0	0.83	45	41	Cushing's Disease
1176M	145	0.051	0.39	5.9	0.90	52	38	Hemangioma, Spleen
1309M	146	0.019	1.4	4.8	0.96	46	44	Hemangiosarcoma, Liver
1230M	150	0.0027	0.34	12	1.2	41	41	Hemangiosarcoma, Liver
1198M	151	0.156	0.52	2.4	4.5	59	30	Acute Pneumonia, Lung Tumor
1219F	152	0.020	0.76	8.4	0.97	34	50	Chronic Nephropathy
1220F	152	0.136	0.74	7.7	1.1	38	48	Malignant Lymphoma, Addison's
1165M	152	0.042	0.66	7.8	1.6	47	39	Acute Pneumonia
1008M	153	0.00049	1.4	13	0.57	34	47	Fibrosarcoma, Spleen
1033M	154	0.0042	0.93	5.3	0.84	19	70	Lung Tumor
1026M	154	0.072	0.99	4.2	0.46	51	40	Hepatic Dysplasia
1065F	154	0.0035	0.72	8.9	0.69	27	60	Malignant Lymphoma, Lung Tumor
1216M	156	0.0096	2.5	6.9	1.4	49	37	Malignant Lymphoma

[a]Includes tracheobronchial, mediastinal and sternal lymph nodes.
[b]Includes hepatic, splenic and mesenteric lymph nodes.

TABLE 6. Continued

Dog Number	Time After Exposure, mo	Final Body Burden, μCi	Percent of Final Body Burden					Cause of Death
			Lungs	Thoracic Lymph Nodes[a]	Abdominal Lymph Nodes[b]	Liver	Skeleton	
982M	157	0.067	1.5	4.2	0.79	52	37	Pneumonia, Thyroid Carcinoma
999F	157	0.0045	0.53	8.3	0.66	40	46	Nasal Sarcoma, Lung Tumor
972F	159	0.024	1.4	9.5	1.1	40	47	Allergic Bronchitis
998M	159	0.0010	1.4	13	0.56	46	35	Lung Tumor
1050F	159	0.0075	0.57	7.3	1.3	39	48	Lung Tumor
997M	160	0.112	5.7	8.9	0.85	42	40	Lung Tumor
1056M	160	0.060	0.58	2.1	1.5	37	56	Pneumonia, Thyroid, Carcinoma
1195M	161	0.099	0.57	2.1	1.0	52	43	Chronic Nephropathy, Bile Duct Adenoma
1091F	161	0.078	2.9	5.1	3.3	28	54	Thyroid Carcinoma
1039M	162	0.00079	0.71	5.8	0.50	54	36	Heart Failure
993F	162	0.0052	0.39	9.6	1.0	26	59	Malignant Lymphoma
1108F	164	0.027	0.85	6.2	0.78	37	50	Posterior Paralysis
1090F	167	0.0054	0.39	3.6	0.74	43	49	Heart Failure

[a]Includes tracheobronchial, mediastinal and sternal lymph nodes.
[b]Includes hepatic, splenic and mesenteric lymph nodes.

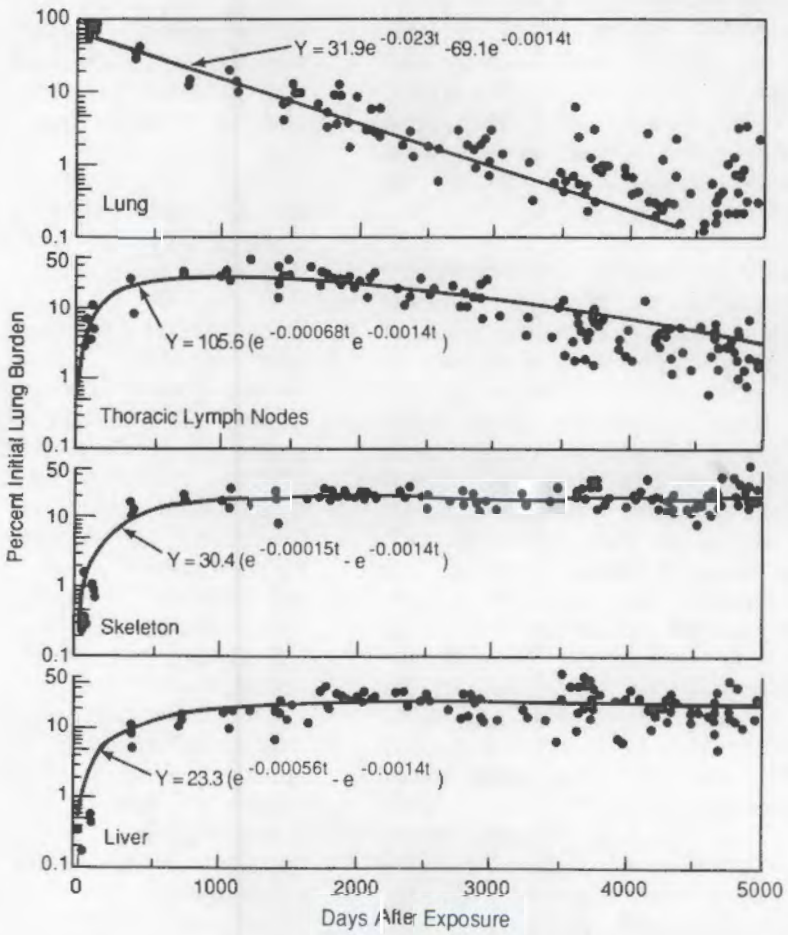

FIGURE 3. Plutonium in Tissues of Dogs After Inhalation of $^{238}PuO_2$. Points represent data from individual dogs. The uptake and retention curves and functions were based on dogs in which initial lung burdens were estimated from the final plutonium body burden, plus the plutonium excreted, minus that excreted in the feces during the first 3 days after exposure.

Of the 96 exposed dogs euthanized, 33 were killed because of bone tumors, 8 because of lung tumors, and 1 because of radiation pneumonitis. Thirteen of the dogs that had bone tumors also had lung tumors. Three dogs with lung tumors were euthanized for other causes. Thirty-one of the 33 dogs with bone tumors had osteosarcomas, one Dose-Level Group 1 dog (989F) had a fibrosarcoma in the ilium, and one Dose-Level Group 4 dog (1103F) had a fibrosarcoma in a vertebra. All of the exposed dogs with osteosarcomas and/or lung tumors were in Dose-Level Groups 2, 3, 4, 5, and 6. Lung tumors were observed in all dose-level groups. Thirteen of the 31 osteosarcomas were in vertebrae; two in femora; four in ribs; three in the scapulae; five in the pelvis; one in the tibia; one in the sternum; one in the sacrum; and one in the humerus. Dog 994F (Dose Level 6); dogs 1047M, 1079M, 1096M, and 1191F (Dose Level 5); 983M, 991F, 1030F, 1053F, 1081M, 1091F, 1166M, 1176M, and 1220F (Dose Level 4); 960M, 972F, 982M, 1026M, 1031F, 1040M, 1043M, 1056M, 1059F, 1108F, 1165M, 1066M, 1219F, and 1309M (Dose Level 3); 971F, 1060F, 1070M, 1078F, 1082M, 1090F, 1188M, 1216M, 1222M, and 1229M (Dose Level 2); and 951M, 959M, 993F, 1008M, 1039M, 1063M, 1069F, 1105F, 1106F, 1193F, 1194F, and 1230M (Dose Level 1) died during the 14-year postexposure period of causes presently thought to be unrelated to plutonium exposure.

The lung tumors were classified as bronchiolar-alveolar carcinomas in 14 dogs, bronchiolar-alveolar adenoma in one dog, adenocarcinoma in four dogs, adenosquamous carcinoma in three dogs and epidermoid carcinoma in one dog. In one dog, three lung-tumor types were observed: bronchiolar-alveolar, adenocarcinoma and fibrosarcoma. Metastases were observed in the lungs; thoracic, hepatic and splenic lymph nodes; trachea; esophagus; mediastinum; thyroid; diaphragm; and hearts of two dogs with pulmonary adenocarcinoma. One dog with adenosquamous carcinoma had metastases to the lung, thoracic lymph nodes and heart. The dog with epidermoid carcinoma had metastases to the lungs, thoracic lymph nodes, and diaphragm. Bone-tumor metastases were found in the lungs of six dogs; in three dogs, the bone tumor metastasized to lungs, thoracic lymph nodes, liver, spleen and heart; in one dog, the bone tumor metastasized to the iliac lymph nodes; and in one dog, the bone tumor metastasized to the lungs, pleura, diaphragm and heart. The six dogs with Addison's disease, which were in Dose-Level Groups 4, 5 and 6, had adrenal cortical atrophy.

In addition to the lesions associated with the cause of death, lesions in the lungs of the Dose-Level Groups 4, 5, and 6 dogs included focal alveolar histocytosis, alveolitis, alveolar epithelial cell hyperplasia, alveolar emphysema, pleural fibrosis, and interstitial fibrosis. Numerous alpha stars were observed, mainly in foci of fibrosis, and single alpha tracks were scattered throughout sections in foci of alveolar histocytosis and in alveolar septa. Sclerosing lymphadenopathy in the tracheobronchial and mediastinal lymph nodes was associated with high concentrations of plutonium observed as alpha stars in Dose-Level Groups 3, 4, 5 and 6. Similar but less severe lesions were seen in the hepatic lymph nodes. In Dose-Level Groups 5 and 6, there were extensive alterations in bone, including multiple areas of focal atrophy of bone; endosteal, trabecular and peritrabecular bone fibrosis; and osteolysis of cortical, endosteal and trabecular bone. One dog had lesions of secondary hypertrophic osteoarthropathy.

Radioactivity in the bone was present as single tracks, generally scattered throughout the bone, cartilage, and bone marrow. The liver contained foci of hepatocellular fatty change, where small clusters of single tracks were seen. There was also mild, focal, nodular hyperplasia of hepatocytes in Dose-Level Groups 3, 4, 5 and 6. Elevated serum GPT levels, suggestive of liver damage, were observed in Dose-Level Groups 3, 4, 5 and 6 dogs.

Dose-related lymphopenia was observed in groups with mean lung $^{238}PuO_2$ deposition of 77 nCi or more (Figure 4). The lymphocyte depression was more pronounced in magnitude and appeared earlier than in dogs exposed to similar doses of $^{239}PuO_2$. Through 126 months after exposure, mean lymphocyte values were significantly lower ($P < 0.05$) for Dose-Level Groups 4 and 5 than for the control group. However, lymphocyte values in the $^{238}PuO_2$-exposed dogs tended to increase sooner after reaching a minimum than in $^{239}PuO_2$-exposed dogs, and mean lymphocyte concentrations in Group 3 dogs were not significantly different from values of control dogs 86 to 94 months following exposure. As with ^{239}Pu, lymphocyte values in the two lowest exposure groups (2.3 and 18 nCi) were not different from control values. A dose-related reduction in total leukocytes was evident, primarily because of lymphopenia, except in Groups 5 and 6, in which neutropenia was also observed. Through 118 months after exposure, mean leukocyte and

neutrophil values were significantly lower ($P < 0.05$) for Dose-Level Group 5 than for the control group. No difference in monocyte values was seen in relation to dose levels. A significant and progressive reduction in eosinophils was evident only in Group 6 dogs following $^{238}PuO_2$ inhalation. No chronic effects have been observed in red-cell parameters. By 14 years after exposure too few dogs were alive for meaningful dose-group comparisons.

Lymphopenia, the earliest observed effect after inhalation of either $^{239}PuO_2$ or $^{238}PuO_2$, occurred after deposition of ~80 nCi plutonium in the lungs. On a concentration basis, the 80-nCi dose level is about 40 times the 16-nCi maximum permissible human lung deposition, based on 0.3 rem/week to the lung.

In serum chemistry assays of $^{238}PuO_2$ dogs, performed more than 120 months following exposure, ALP and GPT values were higher than those of the control group only in Dose-Level Groups 3, 4, and 5 dogs (Figure 5). Elevations in GPT are consistent with liver histopathologic findings and radiochemical analyses indicating ^{236}Pu translocation to the liver. Alkaline phosphatase elevations occurred in some of the dogs with primary bone tumors and in others in which the increase was attributable to the liver (by heat inactivation of ALP) as the source of the largest portion of the ALP.

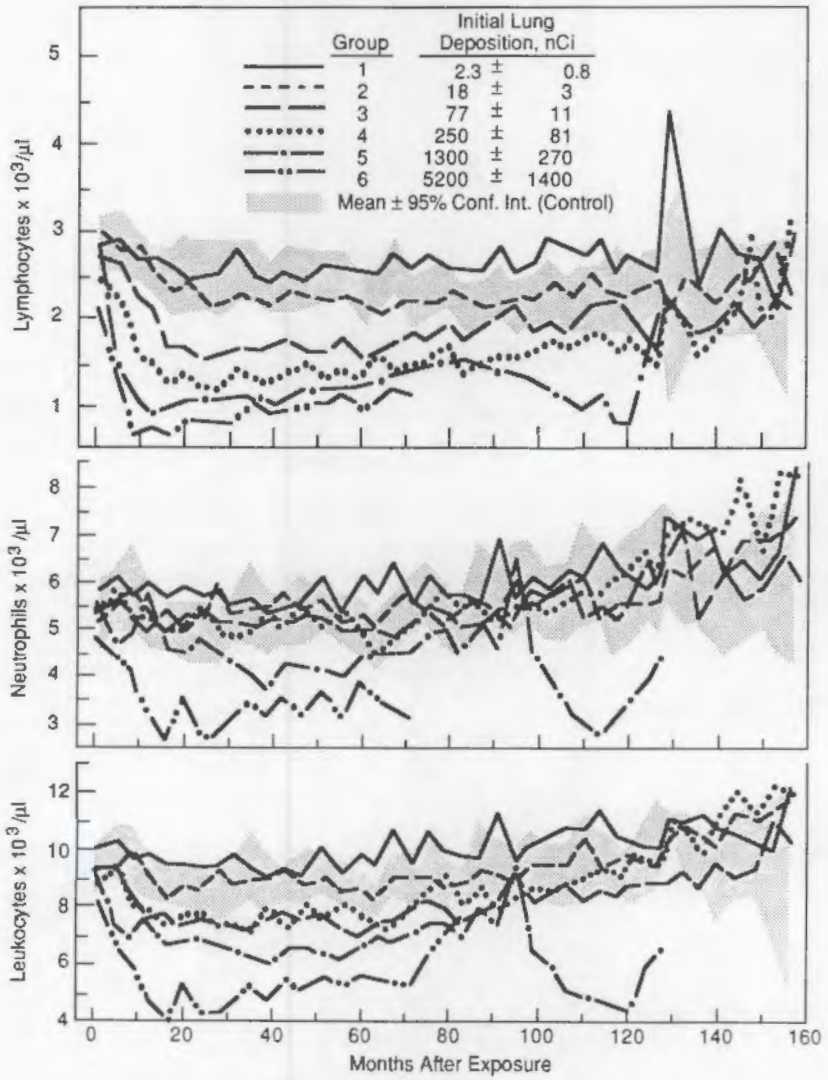

FIGURE 4. Mean Leukocyte, Neutrophil and Lymphocyte Values in Dogs After Inhalation of $^{238}PuO_2$.

Using the uptake and retention curves shown in Figures 1 and 3, cumulative radiation doses to death were estimated for the lungs of the ^{239}Pu dogs and the lungs and skeletons of the ^{238}Pu dogs (Table 7). For the dose calculations, mean plutonium concentration in the entire lung and skeleton was used.

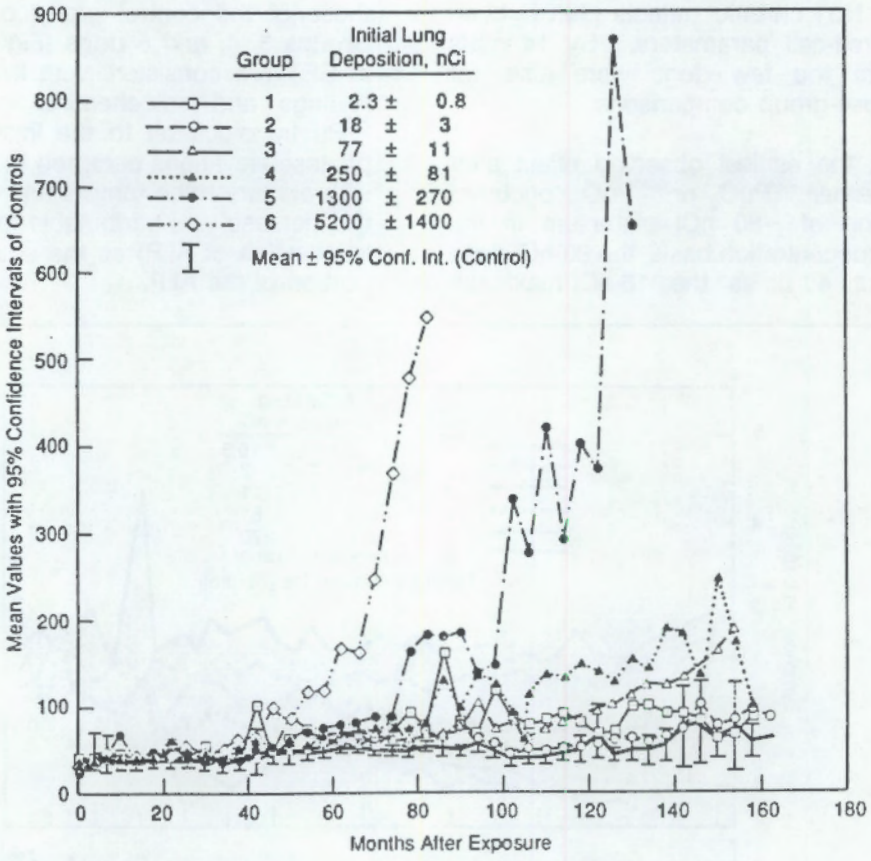

FIGURE 5. Serum Glutamic Pyruvate Transaminase Values in Dogs After Inhalation of $^{238}PuO_2$.

TABLE 7. Estimates of Cumulative Radiation Doses to Lungs (^{239}Pu-Exposed) or Lungs and Skeletons (^{238}Pu-Exposed) of Dogs with Lung and/or Bone Tumors After Inhalation Exposure.

	Dose Level Group	Number of Dogs with Tumors	Survival Time Postexposure, mo	Cumulative Dose to Organ, rad
$^{239}PuO_2$ - Lung Tumors	6	1	69	7400[a]
	5	20	37 - 115	1700 - 4000
	4	16	93 - 177	550 - 1500
	3	10	98 - 183	150 - 550
	2	4	166 - 191	30 - 120
	1	1	182	4
$^{238}PuO_2$ - Lung Tumors	6	9	49 - 84	2300 - 9800[a]
	5	5	70 - 110	1350 - 2900
	4	4	118 - 160	200 - 480
	3	1	134	100
	2	4	154 - 159	8 - 30
	1	1	159	2
$^{238}PuO_2$ - Bone Tumors	6	9	49 - 84	180 - 480[b]
	5	16	61 - 132	80 - 230
	4	7	118 - 143	50 - 100
	3	0	0	---
	2	0	0	---
	1	1	99	<1

[a]Dose to lungs.
[b]Dose to skeleton.

Inhaled Plutonium Nitrate in Dogs

Principal Investigator: G. E. Dagle

Other Investigators: R. R. Adee, R. L. Buschbom, K. M. Gideon, E. S. Gilbert, G. J. Powers, H. A. Ragan, C. O. Romsos, C. R. Watson, R. E. Weller, and E. L. Wierman

Technical Assistance: K. H. Debban, R. F. Flores, B. B. Kimsey, B. G. Moore, R. P. Schumacher, M. J. Steele, and N. B. Valentine

The major objective of this project is to determine dose-effect relationships of inhaled plutonium nitrate in dogs to aid in predicting health effects of accidental exposure in man. For lifespan dose-effect studies, beagle dogs were given a single inhalation exposure to $^{239}Pu(NO_3)_4$ in 1976 and 1977. The skeleton is generally considered the critical tissue with inhaled soluble plutonium that translocates to bone surfaces. Thus far, 11 years after exposure, 10 of 58 exposed dogs had bone tumors, 10 had lung tumors but no bone tumors, and 15 had both bone and lung tumors.

The skeleton is generally considered the critical tissue after inhalation of "soluble" plutonium (e.g., plutonium nitrate), on the assumption that the plutonium will be rapidly translocated from the respiratory system to skeleton. In several rodent studies, however, inhalation of "soluble" plutonium has resulted primarily in lung tumors. Skeletal tumors were seen less often, perhaps because they were not expressed within the short lifespan of the rodents. Therefore, beagle dogs were chosen for this study, to compare relative risks with those from intravenously injected radionuclides in beagles at the University of Utah, inhalation studies with beta-, gamma- and alpha-emitting radionuclides at the Inhalation Toxicology Research Institute (Lovelace), and external irradiation at the University of California (Davis) and Argonne National Laboratory. More specifically, this study can be compared with inhaled $^{239}PuO_2$ and $^{238}PuO_2$ studies in beagle dogs at PNL (see Park et al., this report).

Six dose groups (105 dogs) were exposed, in 1976 and 1977, to aerosols of $^{239}Pu(NO_3)_4$ for lifespan observations (Table 1). In addition, 20 dogs were exposed to nitric acid aerosols as vehicle controls, 25 dogs were exposed to aerosols of $^{239}Pu(NO_3)_4$ for periodic sacrifice to obtain plutonium distribution and pathogenesis data in developing lesions; 7 dogs were selected as controls for periodic sacrifice; and 20 dogs were selected as untreated controls for lifespan observations. The Appendix (following the entire Annual Report) shows the current status of each dog on these experiments.

The average amount of plutonium in the lung decreased to approximately 1% of the final body burden in dogs surviving 5 years or more (Table 2). Over 90% translocated to the liver and skeleton, in approximately equal proportions, with only about 1% translocated to thoracic and abdominal lymph nodes. This was in contrast to dogs that inhaled $^{239}PuO_2$, where ~50% of the final body burden was present in thoracic lymph nodes, but only about 2% in the skeleton at 10-11 years after exposure.

TABLE 1. Lifespan Dose-Effect Studies with Inhaled $^{239}Pu(NO_3)_4$ in Beagles.[a]

Dose Level Group	Number of Dogs		Initial Lung Deposition[b]	
	Male	Female	nCi[c]	nCi/g Lung[c]
Control	10	10	0	0
Vehicle	10	10	0	0
1	10	10	2 ± 2	0.02 ± 0.02
2	10	10	8 ± 4	0.06 ± 0.04
3	10	10	56 ± 17	0.5 ± 0.2
4	10	10	295 ± 67	2 ± 0.8
5	10	10	1709 ± 639	14 ± 6
6	3	2	5445 ± 1841	47 ± 17

(a) Exposed in 1976 and 1977.
(b) Estimated from external thoracic counts at 2 weeks postexposure and estimated lung weights (0.011 x body weight).
(c) Mean ± standard deviation.

TABLE 2. Tissue Distribution of Plutonium in Beagles After Inhalation of $^{239}Pu(NO_3)_4$.

Dog Number	Time After Exposure, mo[a]	Final Body Burden, µCi	Percent of Final Body Burden					Cause of Death
			Lungs	Thoracic Lymph Nodes[b]	Abdominal Lymph Nodes[c]	Liver	Skeleton	
1359M	0.1	0.080	90.50	0.15	0.06	2.46	3.20	Sacrifice
1375F	0.1	0.073	89.61	0.14	0.01	0.97	4.68	Sacrifice
1407F	0.1	0.092	51.87	0.41	0.13	10.99	18.70	Sacrifice
1389M	0.5	0.053	24.07	0.38	0.08	41.28	26.21	Sacrifice
1390M	0.5	0.051	24.62	0.32	0.11	20.05	44.45	Sacrifice
1445F	0.5	0.057	26.42	0.32	0.11	21.28	44.73	Sacrifice
1329F	1	0.485	70.05	0.16	0.04	8.28	18.79	Sacrifice
1346M	1	0.902	76.81	0.32	0.03	10.45	10.30	Sacrifice
1347F	1	0.699	71.71	0.36	0.08	9.33	14.09	Sacrifice
1336M	1	0.032	71.38	0.22	0.05	5.72	19.73	Sacrifice
1341F	1	0.022	64.43	0.29	0.10	12.92	18.63	Sacrifice
1344F	1	0.052	58.68	0.25	0.04	21.87	16.09	Sacrifice
1335M	1	0.003	19.52	0.07	0.06	6.68	25.04	Sacrifice
1339F	1	0.001	19.08	0.13	0.08	20.92	45.47	Sacrifice
1351M	1	0.002	40.68	1.22	0.09	17.09	28.89	Sacrifice
1522F	3	0.059	54.68	0.57	0.10	11.52	28.24	Sacrifice
1529F	3	0.049	51.68	0.40	0.07	18.48	23.74	Sacrifice
1539M	3	0.072	52.45	0.31	0.05	18.58	25.03	Sacrifice
1564F	12	0.037	18.00	1.27	0.11	33.53	42.63	Sacrifice
1571F	12	0.053	22.37	1.47	0.11	28.76	42.91	Sacrifice
1588M	12	0.053	13.14	0.40	0.12	35.85	46.18	Sacrifice
1424M	14	4.625	33.10	1.43	0.16	26.49	36.88	Radiation Pneumonitis
1517F	16	4.025	18.99	0.94	0.18	29.51	47.88	Radiation Pneumonitis
1510F	17	4.048	22.00	1.15	0.05	20.71	52.00	Radiation Pneumonitis
1420M	25	1.616	16.51	0.86	0.20	7.77	70.06	Radiation Pneumonitis
1471M	34	1.375	9.25	0.73	0.12	26.92	58.34	Radiation Pneumonitis
1518M	42	1.880	6.87	0.24	0.07	21.34	67.51	Radiation Pneumonitis, Lung Tumor
1512M	42	2.136	4.31	0.60	0.08	49.93	42.66	Bone Tumor
1508M	43	1.730	3.24	0.62	0.08	41.53	52.70	Bone Tumor
1459F	51	1.567	4.40	0.15	0.12	30.86	61.41	Radiation Pneumonitis, Lung Tumor
1492F	52	1.202	2.81	0.20	0.17	27.02	66.38	Bone Tumor
1485F	54	1.052	0.82	0.35	0.07	31.13	63.94	Bone Tumor
1502F	55	3.113	0.80	0.39	0.09	33.33	62.51	Bone Tumor, Lung Tumor
1387F	55	0.167	1.41	0.22	0.12	45.48	49.10	Bone Tumor
1429M	59	1.159	4.14	0.35	0.10	37.06	54.70	Bone Tumor, Lung Tumor
1598F	60	0.058	0.90	0.14	0.17	24.44	31.62	Sacrifice
1576M	60	0.065	1.54	0.36	0.13	46.23	39.15	Sacrifice
1605F	60	0.025	1.87	0.11	0.12	52.32	39.37	Sacrifice
1646F	60	0.806	0.72	0.20	0.40	46.92	48.42	Bone Tumor
1619F	62	1.361	0.55	0.59	0.13	37.87	58.63	Bone Tumor
1589F	63	0.029	0.68	0.04	0.13	46.43	50.32	Sacrifice
1636M	66	0.634	1.21	0.27	0.52	53.97	39.09	Bone Tumor
1652F	68	0.658	1.46	0.23	0.29	50.47	44.32	Bone Tumor, Lung Tumor
1498F	69	0.845	0.59	0.32	0.13	26.63	53.37	Bone Tumor, Lung Tumor
1659F	69	0.736	1.14	0.34	0.40	38.90	55.89	Bone Tumor
1640M	76	0.177	4.01	0.64	0.63	54.41	36.59	Lung Tumor
1419M	76	0.873	0.69	0.28	0.39	44.06	50.70	Bone Tumor, Lung Tumor
1660M	82	0.854	0.76	0.53	0.53	37.51	56.17	Bone Tumor, Lung Tumor
1621M	84	0.840	0.94	0.56	0.29	40.87	54.55	Bone Tumor, Lung Tumor
1655M	88	0.505	1.05	0.22	0.93	41.83	52.14	Lung Tumor, Bone Tumor
1501M	92	0.002	1.62	0.50	0.79	38.05	48.41	Thyroid Tumor
1648M	92	0.639	1.12	0.25	0.73	42.83	50.61	Bone Tumor, Lung Tumor
1641M	92	0.869	0.78	0	0.48	45.72	48.89	Lung Tumor
1408F	93	0.181	0.60	0.19	0.37	49.47	45.52	Bone Tumor

[a] Radioanalysis not completed in dogs that died more than 106 mo after exposure.
[b] Includes tracheobronchial, mediastinal and sternal lymph nodes.
[c] Includes hepatic, splenic and mesenteric lymph nodes.

TABLE 2. Continued

Dog Number	Time After Exposure, mo[a]	Final Body Burden, µCi	Percent of Final Body Burden					Cause of Death
			Lungs	Thoracic Lymph Nodes[b]	Abdominal Lymph Nodes[c]	Liver	Skeleton	
1404M	93	0.217	0.82	0.28	0.72	46.24	48.62	Pleuritis
1470F	95	0.001	1.11	0.48	0.34	43.21	50.23	Meningioma
1489F	98	0.002	1.23	0.73	0.70	41.36	48.52	Esophageal Tumor
1565F	101	0.001	0.77	1.55	0.87	43.62	44.09	Hemangiosarcoma
1385M	101	0.362	0.62	0.51	0.42	46.38	49.36	Bone Tumor, Lung Tumor
1364M	102	0.370	1.13	0.32	0.40	49.46	46.17	Lung Tumor
1503F	103	0.007	0.37	0.64	0.25	60.15	35.37	Thyroid Tumor
1645F	105	0.182	0.73	0.41	0.46	55.96	40.70	Lung Tumor
1587M	106	0.027	0.65	0.74	0.51	20.11	74.97	Hemangiosarcoma, Lung Tumor
1534M	106	0.201	0.96	0.43	0.49	50.78	43.95	Congestive Heart Failure
1521F	106	0.146	0.88	0.34	0.36	51.77	44.41	Bone Tumor, Lung Tumor

[a]Radioanalysis not completed in dogs that died more than 106 mo after exposure.
[b]Includes tracheobronchial, mediastinal and sternal lymph nodes.
[c]Includes hepatic, splenic and mesenteric lymph nodes.

The earliest observed biological effect was on the hematopoietic system: chronic lymphopenia occurred at the two highest dose levels at 4 weeks after exposure to $^{239}Pu(NO_3)_4$. Total leukocyte concentrations were reduced significantly in the two highest dose groups, i.e., Group 5 (mean initial alveolar deposition, ~1700 nCi), and Group 6 (~5500 nCi). The reduction in white cells in Groups 5 and 6 is due to an effect on most leukocyte types (neutrophils, lymphocytes, monocytes and eosinophils). This is in contrast to the effects of both $^{239}PuO_2$ and $^{238}PuO_2$, which significantly depressed lymphocyte concentrations by 21 months after exposure in groups with initial lung burdens of ~80 nCi or more. The lymphopenia at lower dose levels of plutonium oxides may be related to the more-extensive translocation of plutonium oxide to the tracheobronchial lymph nodes and subsequent higher dosage levels to lymphocytes circulating through those lymph nodes. The results of these continuing evaluations are shown in Figure 1.

Serum enzyme assays have been performed throughout the postexposure period in an attempt to identify specific damage to liver and/or bone by plutonium translocated from the lung. Currently (more than 11 years following exposure), glutamic pyruvic transaminase (GPT) and alkaline phosphatase (ALP) values in Dose-Level Groups 3 and 4 are significantly ($P < 0.05$) higher than those for the control group (Figures 2 and 3).

Table 3 summarizes, by dose-level group, the mortality and lesions associated with deaths through 11 years after exposure to $^{239}Pu(NO_3)_4$. All five dogs at the highest dose level (Group 6) died from radiation pneumonitis 14 to 41 months after exposure. Histopathologic examination of these dogs' lungs revealed interstitial fibrosis, alveolar epithelial hyperplasia, increased numbers of alveolar macrophages, occasional small emphysematous cavities and, at times, very small nodules of squamous metaplasia at the termini of respiratory bronchioles. One dog at the highest dose level had a small bronchioloalveolar carcinoma as well as radiation pneumonitis.

All the dogs in Dose-Level Group 5 died or were euthanized 34 to 92 months after plutonium exposures. The principal cause of death at this exposure level was osteosarcoma, which occurred in 17 of 20 dogs; several had more than one site. The sites of the osteosarcomas were lumbar vertebrae (four dogs), cervical vertebrae (three dogs), thoracic vertebrae (two dogs), humerus (five dogs), pelvis (two dogs), facial bones (two dogs), ribs (two dogs), and nasal turbinates (one dog). Metastases to distal sites occurred in six dogs; these dogs also had radiation osteosis, generally characterized by peritrabecular fibrosis.

Other deaths in Dose-Level Group 5 were caused by radiation pneumonitis (two dogs) and multiple lung tumors (one dog). The multiple lung tumors, in different lobes, were papillary adenocarcinomas, combined epidermoid and adenocarcinoma, and bronchioloalveolar carcinoma; metastases were present in the tracheobronchial lymph nodes.

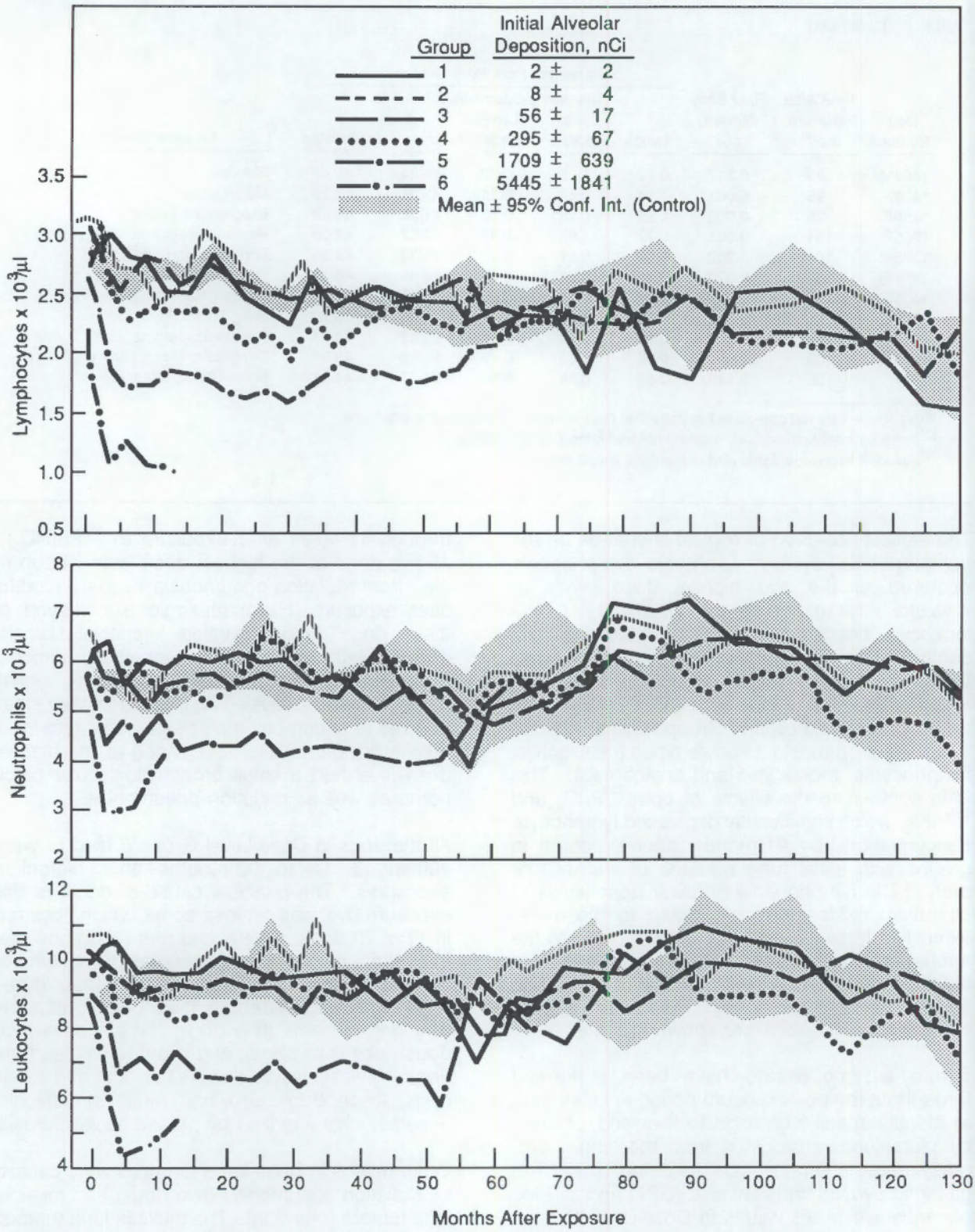

FIGURE 1. Mean Leukocyte, Neutrophil and Lymphocyte Values in Dogs After Inhalation of $^{239}Pu(NO_3)_4$.

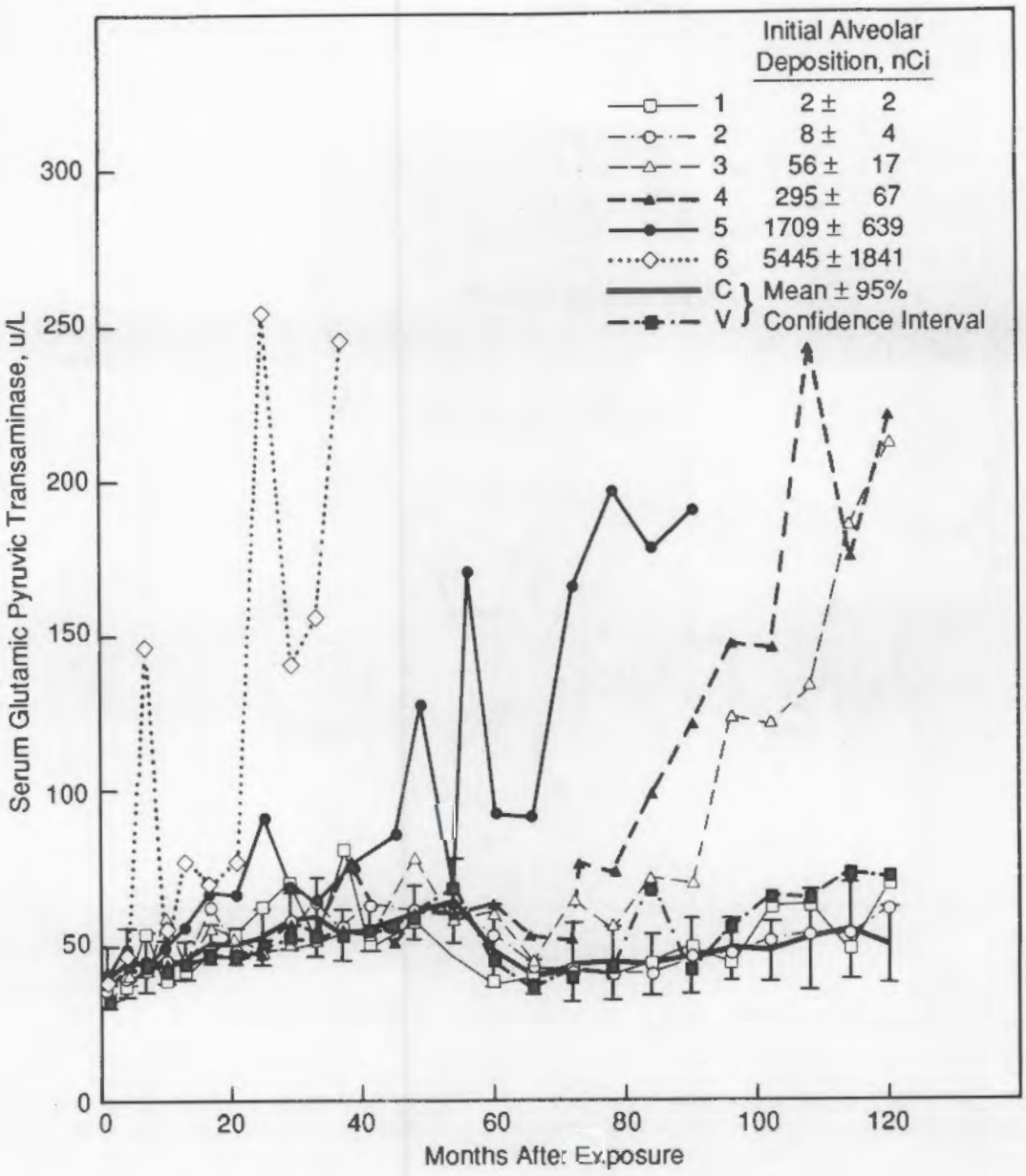

FIGURE 2. Serum Glutamic Pyruvic Transaminase (GPT) in Dogs After Inhalation of $^{239}Pu(NO_3)_4$.

Malignant but nonfatal lung tumors were also present in nine dogs from Dose-Level Group 5 that died from osteosarcomas and in one dog that died from radiation pneumonitis. Typically, these arose subpleurally, proximal to areas of interstitial fibrosis or small cavities communicating with bronchioles. They consisted of bronchioloalveolar carcinomas in four dogs; papillary adenocarcinomas in two dogs; both bronchioloalveolar carcinoma and papillary adenocarcinoma in one dog; both papillary and tubular adenocarcinomas in one dog; a combined epidermoid and adenocarcinoma in one dog; and a bronchioloalveolar carcinoma, papillary adenocarcinoma, and a mixed lung tumor in one dog. No metastases of these lung tumors were observed.

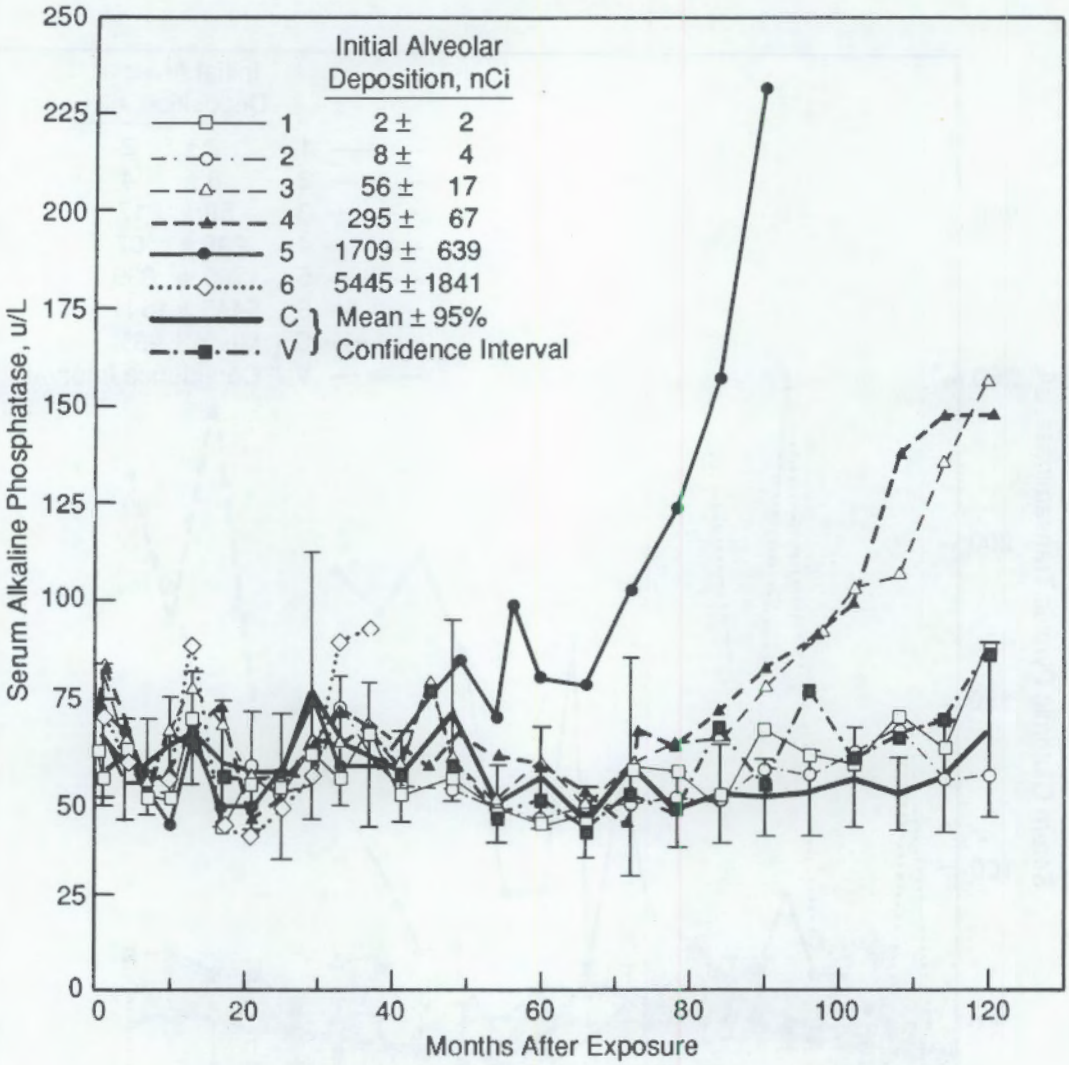

FIGURE 3. Serum Alkaline Phosphatase (ALP) in Dogs After Inhalation of $^{239}Pu(NO_3)_4$.

In Dose-Level Group 4, 13 dogs have now died, 54 to 126 months after plutonium exposure. The causes of death included bone tumors (seven dogs), lung tumors (three dogs), suppurative pleuritis (one dog), congestive heart failure (one dog), and pyometra (one dog). Five dogs that died as a result of bone tumors also had nonfatal lung tumors. Small solitary bile-duct tumors were present in the livers of two dogs that died from other causes.

In Dose-Level Group 3, two dogs have died from lung tumors. Each of three dogs that died due to a bone tumor, a thyroid tumor, and a hemangiosarcoma, respectively, also had a lung tumor. This is the lowest exposure level with a mortality rate or incidence of lesions that was different from that of control groups.

Although the skeleton is generally considered the critical tissue after inhalation of soluble plutonium, and 25 of 58 exposed dogs have died with bone tumors, by 11 years after exposure, it should be noted that 25 of these 58 exposed dogs also had lung tumors. We have calculated that lung-cancer risks for these dogs, based on estimated cumulative dose to the lung, are approximately 12 times higher for $^{239}Pu(NO_3)_4$ than for inhaled $^{239}PuO_2$, and 50 times higher than for inhaled $^{238}PuO_2$.

TABLE 3. Lesions in Beagle Dogs 11 Years After Inhalation of $^{239}Pu(NO_3)_4$.

	Dose Group							
	6	5	4	3	2	1	Vehicle	Control
Number of Dogs/Group	5	20	20	20	20	20	20	20
Number of Dead Dogs/Group	5	20	13	9	5	6	2	5
Condition[a]								
Radiation Pneumonitis	4	1						
Radiation Pneumonitis and Lung Tumor	1	1						
Bone Tumor		8	2					
Bone and Lung Tumor		9	4	1				
Bone, Lung, and Liver Tumor			1					
Lung Tumor		1	3	2				
Hemangiosarcoma and Lung Tumor				1				
Thyroid and Lung Tumor				1				
Pyometra and Liver Tumor			1					
Pneumonia or Pleuritis			1	2				1
Lymphoma				1			1	
Thyroid Tumor					1	1		1
Meningeal Tumor						1		
Status Epilepticus					1			1
Congestive Heart Failure			1					
Hemangiosarcoma				1		2		
Adrenal Tumor					1			
Esophageal/Stomach Tumor						2		
Intervertebral Disc Protrusion							1	1
Mammary Tumor					1			
Cerebral Hemorrhage								1
Prostate Tumor					1			

[a]Number of dogs with lesions associated with death.

Low-Level $^{239}PuO_2$ Studies

Principal Investigator: C. L. Sanders

Other Investigators: K. E. Lauhala, K. E. McDonald, J. D. Mahaffey, and M. E. Frazier

A total of 3192 female Wistar, 198 male Wistar, 192 female Long-Evans and 200 female Fischer-344 rats were either sham-exposed or given a single inhalation to $^{239}PuO_2$ and are being examined for tumor formation over their life spans. Histopathological analyses have been completed on 1707 of the 3192 rats in the initial lifespan study. The dose-response curve continued to be best fitted by a quadratic function and a "practical" threshold of >100 rad; maximum lung-tumor incidence was at 800 rad. Bronchiolar alpha-star distribution was determined by quantitative scanning electron microscopy autoradiography. The majority of the bronchiolar dose was delivered by plutonium particles retained for prolonged periods in peribronchiolar alveoli. A biphasic bronchiolar proliferation was observed coincident with early clearance of plutonium particles deposited on the airway surface and later plutonium aggregate formation adjacent to bronchioles. Carcinoma formation was preceded by proliferative dysplastic lesions associated with plutonium aggregates.

Lifespan Tumor Studies

Previous lifespan studies in rats exposed to ^{239}Pu aerosols indicated that lung-tumor incidence might be increased at radiation doses to the lung comparable to doses received by humans from a maximum permissible occupational lung deposition of 16 nCi ^{239}Pu. A total of 3192 young-adult, female, specific-pathogen-free, Wistar rats were used in the initial lifespan study: 2134 were exposed to $^{239}PuO_2$ at initial lung burdens (ILB) ranging from 0.25 nCi to about 180 nCi, and 1058 were sham-exposed controls. Histopathological analyses have been completed on 1707 of the 3192 rats, including 554 sham-exposed controls and 1153 exposed animals. Cell kinetic, autoradiographic and morphometric techniques are being used to evaluate the spatial-temporal dose-distribution patterns and the cellular events leadings up to lung-tumor formation in 140 serially sacrificed female Wistar rats given a single exposure to $^{239}PuO_2$. An additional 198 male Wistar rats, 192 female Long-Evans rats, and 200 female Fischer-344 rats were exposed to aerosols of $^{239}PuO_2$ in order to compare lung-tumor responses at lung doses of about 100 rad and 1000 rad in other strains and in male rats (Table 1).

TABLE 1. Status of Study Groups as of October 1, 1988.

Strain	Sex	Mean ILB, nCi	Number of Rats		No. with Completed Histopathology
			Alive	Dead	
Wistar	F	0	0	1058	554
Wistar	F	0.44 ± 0.09	0	919	363
Wistar	F	0.79 ± 0.20	0	610	247
Wistar	F	1.7 ± 0.33	0	163	136
Wistar	F	3.5 ± 0.90	0	112	97
Wistar	F	6.1 ± 1.2	0	105	92
Wistar	F	15 ± 3.1	0	36	34
Wistar	F	26 ± 5.7	0	68	66
Wistar	F	58 ± 20	0	46	44
Wistar	F	120 ± 37	0	75	74
Wistar	M	0	5	55	0
Wistar	M	6.8 + 2.8	12	66	0
Wistar	M	94 + 21	1	59	0
Long-Evans	F	0	21	39	0
Long-Evans	F	5.1 + 1.3	26	46	0
Long-Evans	F	77 + 16	3	57	0
Fischer-344	F	0	17	43	0
Fischer-344	F	5.6 + 1.1	27	53	0
Fischer-344	F	75 + 7.9	1	59	0
Wistar[a]	F	0	0	40	---
Wistar[a]	F	104 ± 32	0	99	---

[a]Serially killed at intervals up to 700 days after inhalation.

The percentages of all rats with lung tumors (mean dose level) were: 0.7% (sham-exposed controls), 0.3% (6 rad), 0% (11 rad), 0.7% (23 rad), 2.1% (47 rad), 0% (83 rad), 12% (190 rad), 17% (350 rad), 66% (740 rad), and 81% (1500 rad) (Table 2). Four primary lung tumors, including one adenocarcinoma, were seen in 554 sham-exposed controls. A total of 116 lung tumors were found in 1153 exposed rats, including 60 squamous cell carcinomas, 29 adenocarcinomas, 10 hemangiosarcomas, 8 adenomas, 3 adenosquamous carcinomas and 3 fibrosarcomas. To date, only 8 lung tumors have been found in 918 rats with lung doses >0 to <100 rad (malignant tumor incidence of 0.44%); 108 lung tumors have been found in 235 rats with lung doses >100 rad (malignant tumor incidence of 44%). This study continues to indicate the presence of a possible "practical" threshold dose of about 100 rad for lung-tumor formation from inhaled $^{239}PuO_2$. Below this threshold, a tumor is much less likely (Table 2).

The dose-response relationship appears to be well fitted by a pure quadratic function. A quadratic function also provides the best fit for both lung adenocarcinomas and squamous carcinomas. We continue to believe that the lower dose-range of the quadratic curve (<100 rad) represents primarily initiation (mutation) events, and that the much steeper, higher-dose portion of the curve (>100 rad) represents mostly promotion events due to plutonium particle aggregation, resulting in the progressive expression of carcinogenesis.

TABLE 2. Lung Tumors in Female Wistar Rats Following Inhalation of $^{239}PuO_2$ Particles.

Mean Dose to Lung, rad	Number of Rats	Lung Tumors (% of Rats with Lung Tumor)				
		Squamous Carcinoma	Adeno-carcinoma	Hemangio-sarcoma	Other	Total
0	554	0	0.18	0	0.54	0.73
6 ± 1.3	363	0	0.28	0	0	0.28
11 ± 2.1	247	0	0	0	0	0
23 ± 4.5	136	0.73	0	0	0	0.73
47 ± 9.6	97	0	0	0	2.1	2.1
83 ± 15	92	0	0	0	0	0
190 ± 38	34	8.8	2.9	0	0	11.7
350 ± 71	66	0	13.6	0	3.0	16.6
740 ± 140	44	41.0	13.7	9.1	2.3	66.1
1500 ± 360	74	51.4	16.2	8.1	5.4	81.1

Scanning Electron Microscopic Pathology, Quantitative Autoradiography and Cell Proliferation Kinetics

An SEM autoradiographic technique has been developed that gives a better three-dimensional view of a comparatively large lung tissue mass than is possible with light or transmission electron microscopy autoradiography (PNL Annual Report, 1987). Ninety-nine young-adult Wistar rats were exposed to an aerosol of high-fired, submicron-sized ^{169}Yb, $^{239}PuO_2$ particles (mean initial alveolar deposition, 104 nCi). These tissues, together with those from 40 sham-exposed rats, are being examined with the scanning electron microscope (SEM) at 20-yw time intervals from 1 day to 700 days after exposure.

Rats were given an intraperitoneal injection of 1.5 μCi tritiated thymidine/g body weight at 1 hr before sacrifice; plutonium contents in the apical lobe were determined by liquid scintillation counting. The cardiac lobe was prepared for SEM pathologic and SEM autoradiographic examination, and the left lobe for autoradiographic determination of cell nucleus labeling. All airways, sectioned at an oblique angle to expose a flat epithelial surface, were examined by SEM autoradiography. The total area of this flat surface was measured, and the number of alpha stars within were counted. Stars were differentiated according to whether they were on the epithelial surface or radiating through the mucosa from adjacent alveoli (Figures 1 and 2).

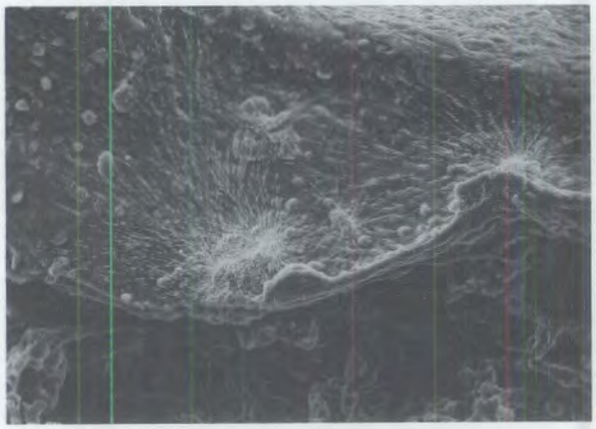

FIGURE 1. Plutonium Particles on the Surface of a Bronchiole (Scanning Electron Microscopic Autoradiograph). x 500

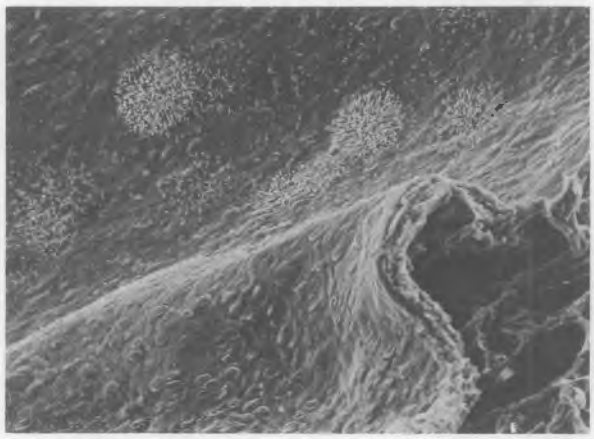

FIGURE 2. Plutonium Particles Irradiating the Bronchiolar Epithelium from Adjacent Peribronchiolar Alveoli (Scanning Electron Microscopic Autoradiograph). x 500

At all time periods, plutonium particle concentration on the surface of bronchioles was about 10 times greater than particle concentration on the surface of the trachea. Particles were rapidly cleared from the surface of bronchioles during the first few weeks after exposure. Thereafter, about five times more alpha-track exposure to the bronchiolar epithelium was delivered from plutonium particles found in peribronchiolar alveoli than from particles on the bronchiolar surface (Figure 3). Lung clearance of plutonium at an ILB of 3.9 kBq was considerably slower than clearance at an ILB of 0.4 kBq (Figure 4). The slower lung clearance at the higher ILB may have been due to a greater alveolar macrophage toxicity from plutonium particle concentration in macrophages during the early clearance phase and to the formation of particle aggregates during the later clearance phase. Large particle aggregates are rarely seen at an ILB of 0.4 kBq but are proportionately more common with increasing ILB (PNL Annual Report, 1987). Aggregated peribronchiolar particles appeared to be more tenaciously retained; most alveolar particles were more rapidly cleared from the lung. The prolonged peribronchiolar particle retention appears to play a prominent role in the development of lung carcinomas.

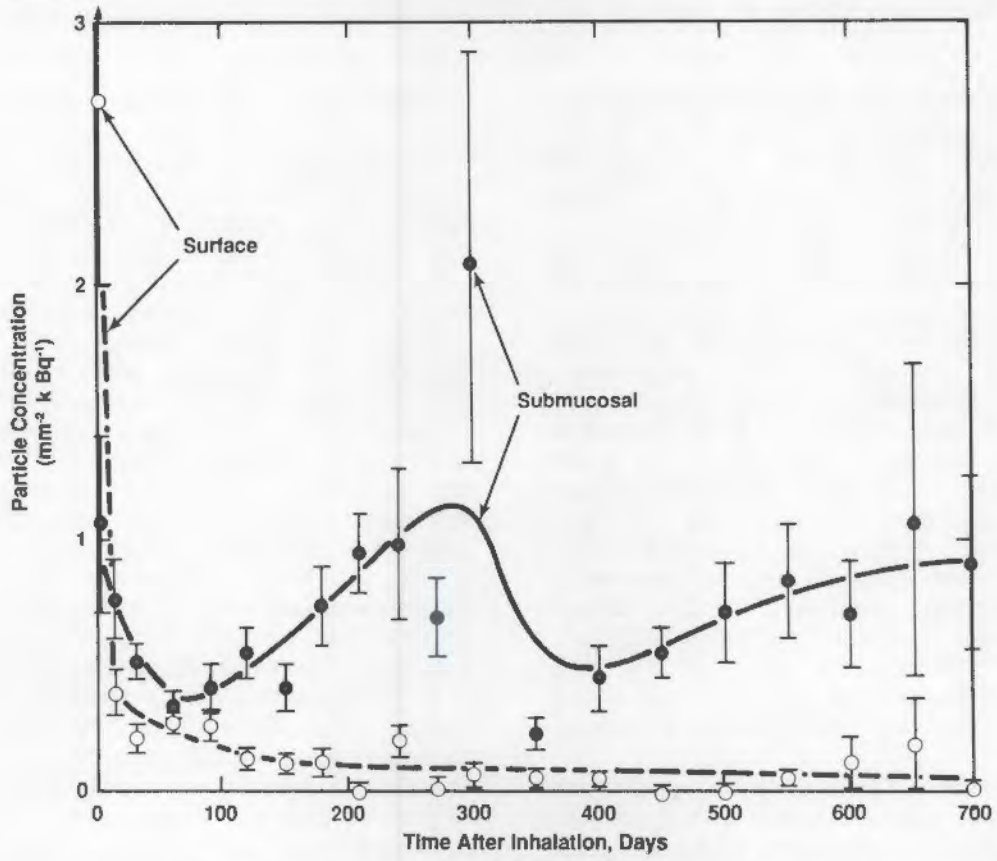

FIGURE 3. Concentration of Inhaled $^{239}PuO_2$ Particles on the Surface of Bronchioles and in Adjacent Submucosal Regions, as a Function of Time After Exposure. Points are means (n,5) with standard error bars.

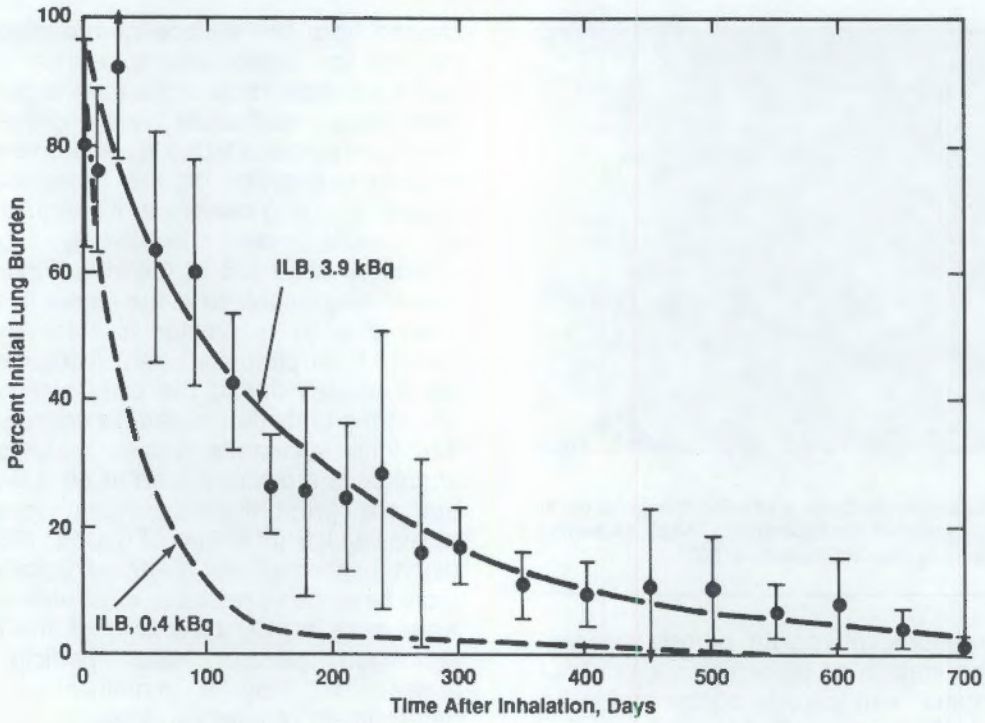

FIGURE 4. Clearance of Inhaled $^{239}PuO_2$ from the Lung as a Function of Initial Lung Burden (ILB). Values for the 3.9-kBq curve (with SE bars) are means of five rats; the 0.4-kBq curve is reproduced from a previous PNL Annual Report (1985).

Primary lung carcinoma formation is preceded by a cellular evolution of focal inflammation, fibrosis and epithelial hyperplasia and metaplasia associated with plutonium aggregates. Particle aggregation increased with time, resulting in well-defined, focal inflammatory lesions by 120 days and well-defined fibrotic lesions by 180 days after exposure. High alpha-radiation doses were delivered to bronchiolar epithelium adjacent to plutonium particle aggregates. Nonciliated, bronchiolar, epithelial hypertrophy and hyperplasia were first seen at 15 days after exposure; epithelium returned to normal a few months later. Alveolar bronchiolarization, composed of ciliated and nonciliated cells, was first seen at 120 days, increasing in severity and maximum incidence by 300 days after exposure. Bronchiolarization appeared to be always associated with plutonium particle aggregation. Adenocarcinoma was first seen at 600 days, squamous metaplasia at 270 days, squamous carcinoma at 450 days after exposure (Figure 5).

A maximal increase in proliferation of alveolar cells (primarily type 2 alveolar epithelium) was seen by 60 days after exposure, decreasing gradually to proliferation levels the same as those of controls by 400 days (Figure 6). Bronchiolar epithelial proliferation appeared in two phases; the first at 15 days after exposure, probably associated with initial deposition and clearance of particles deposited on bronchiolar surfaces. The second phase, which reached maximum proliferation at about 250 days, may have been associated with peribronchiolar plutonium aggregate formation (Figure 7). Only nonciliated bronchiolar epithelial cells were labeled. All epithelial dysplastic and neoplastic lesions in the lung exhibited labeling indices much greater than those of unexposed alveolar or bronchiolar epithelium. There was a temporal relationship in labeling of cells associated with alveolar bronchiolarization, with higher proliferative rates in early lesions. The proliferative rate of adenocarcinomas was similar to that of bronchiolarization lesions. Both squamous metaplastic lesions and squamous carcinomas had similarly high proliferative rates. Squamous metaplasia preceded the appearance of squamous carcinoma by about 100 days, and alveolar bronchiolarization preceded adenocarcinoma by about 500 days (Figures 5 and 8). These studies indicate an evolution of squamous metaplastic cells into squamous carcinoma. The association of cells involved with alveolar bronchiolarization and adenocarcinoma formation is less clear. Both type 2 alveolar epithelium and

nonciliated bronchiolar epithelium in terminal bronchioles may participate in alveolar bronchiolarization and adenocarcinoma formation.

Growth Factors, DNA Aneuploidy and Analysis of DNA recovered from Archived Tissues

Proto-oncogene activation is being examined in archived tissues from lifespan studies. The DNA was extracted from fresh and formalin-fixed normal and lung-tumor tissues and from paraffin-block-embedded sections. Less than 1 μg of DNA was required for amplification by the polymerase chain reaction method; it was then used to sequence DNA at the ki-*ras* and at other proto-oncogene loci. Formalin fixation and paraffin-embedding did not substantially interfere with the amplification step (see Frazier Annual Report, this volume). The role of growth factors and growth-factor receptors is also being examined in plutonium-induced lung tumors from archival paraffin-block sections. Flow cytometry analysis of DNA has been performed on nuclear suspensions recovered from formalin-fixed, paraffin-embedded tissue blocks of plutonium-induced rat lung tumors. Small hyperplastic and dysplastic lung lesions are being examined by microspectrophotometry of Feulgen-stained nuclei for cellular DNA content.

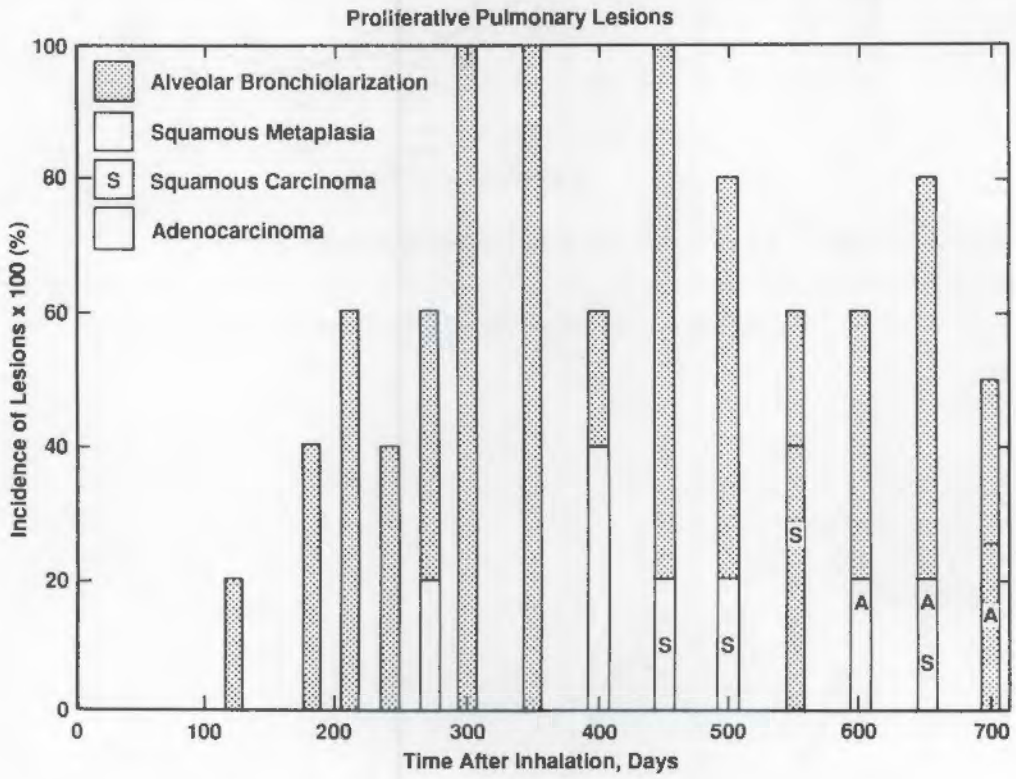

FIGURE 5. Incidence of Premalignant and Malignant Epithelial Lesions in the Lung, as a Function of Time Following Inhalation of $^{239}PuO_2$.

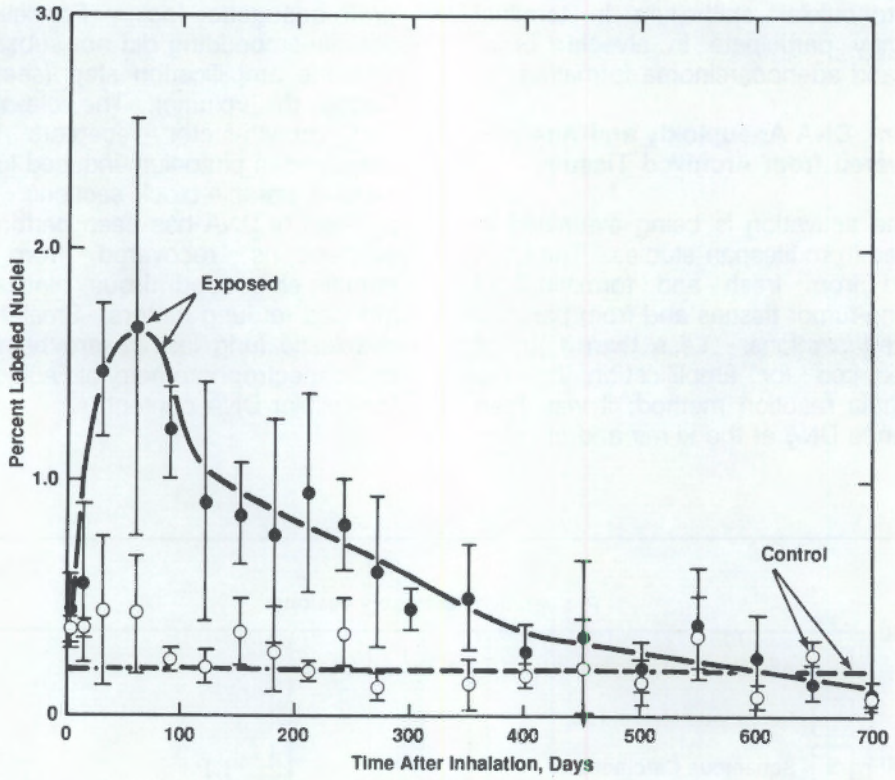

FIGURE 6. Proliferation of Alveolar Cells as a Function of Time Following Inhalation of $^{239}PuO_2$.

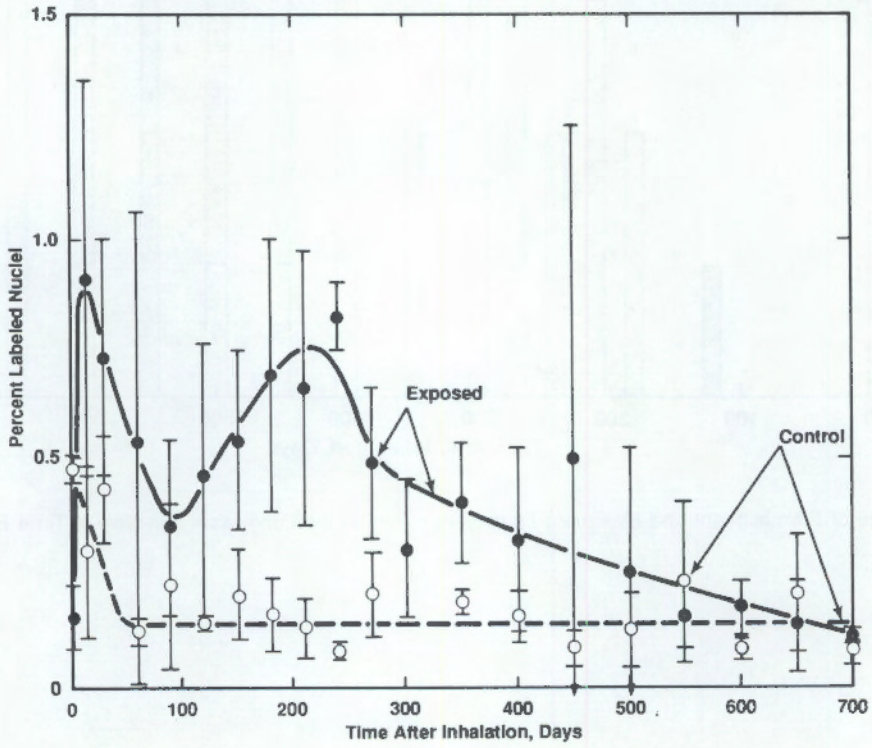

FIGURE 7. Proliferation of Nonciliated Bronchiolar Epithelium, as a Function of Time Following Inhalation of $^{239}PuO_2$.

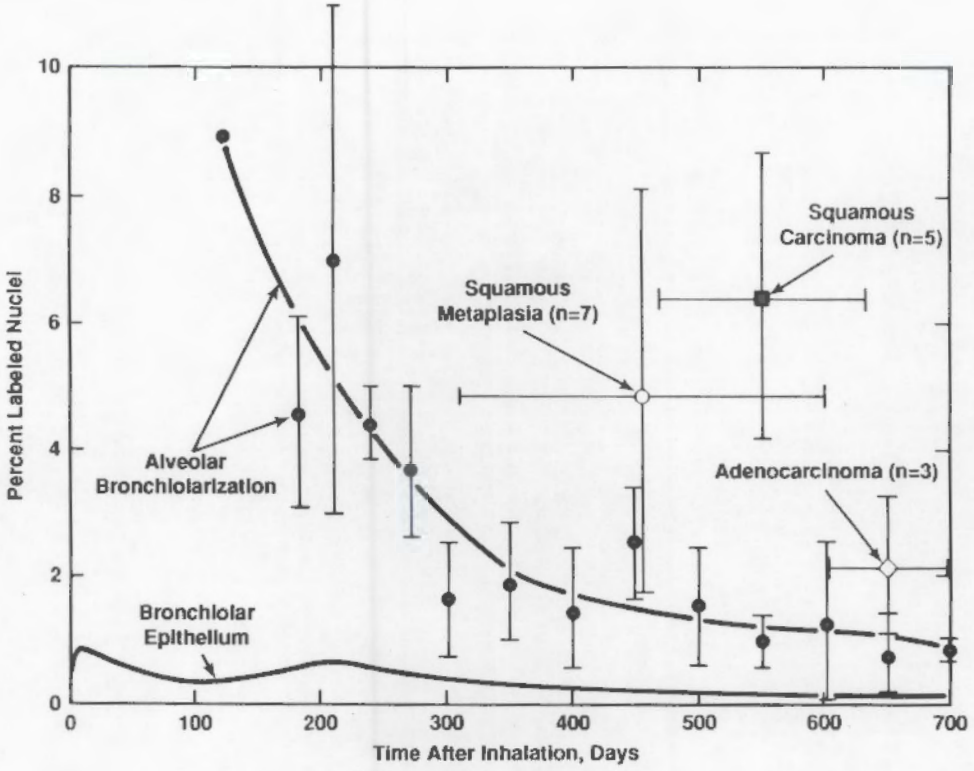

FIGURE 8. Proliferation of Dysplastic and Neoplastic Epithelial Lesions, as a Function of Time Following Inhalation of $^{239}PuO_2$.

Inhalation Hazards to Uranium Miners

Principal Investigator: F. T. Cross

Other Investigators: R. L. Buschbom, G. E. Dagle, K. M. Gideon, R. A. Gies, E. S. Gilbert, T. J. Mast, S. H. Moolgavkar,[a] R. L. Rommereim, and M. R. Sikov

Technical Assistance: R. M. Briones and C. R. Petty

Using both large and small experimental animals, we are investigating levels of air contaminants that produce respiratory system disease in radon-exposed populations. Lung-cancer incidence and deaths from degenerative lung disease are significantly elevated among uranium miners, but the cause-effect relationships for these diseases are based on inadequate epidemiological data. This project identifies agents or combinations of agents (both chemical and radiological), and their exposure levels, that produce respiratory tract lesions, including respiratory epithelial carcinoma, pneumoconiosis, and emphysema. Analyses of rat histopathologic data for 10-, 100-, and 1000-working-level (WL) exposure rates confirm the previously noted trend of higher lifetime lung-tumor risks for lower exposure rates, and the tapering-off of the exposure-rate effect at occupational and, possibly, environmental rates of radon exposure. A summary of primary tumors of the respiratory tract for 9000 Series (10-WL) animals is presented. Teratologic data indicate no apparent hazard to the rat fetus following cumulative radon-daughter exposures to the dam about four orders-of-magnitude higher than typical annual levels associated with indoor radon exposures.

Small-Animal Studies

Exposure Protocols. The 6000 Series (1000-working level; WL) and 7000 Series (100-WL) experiments (Table 1) are designed to develop the relationships between response and exposure to radon daughters (at two rates of exposure) and carnotite uranium ore dust. The 8000 Series (100-WL) experiments (Table 2) are designed to extend the exposure-response relationships to cumulative exposure levels comparable to current conditions in the mines and to lifetime environmental exposures. The 9000 Series experiments (Table 3) continue the "low-dose" studies at exposure rates comparable to former occupational working levels (10 WL). They will help to further evaluate the hypothesis that the tumor probability per working-level-month (WLM) exposure increases with decreasing exposure rate. In addition, concurrent exposure to varying levels of uranium ore dust tests the hypothesis that irritants (both specific and nonspecific) act synergistically with radiation exposures. The exposures of 6000, 7000 and 8000 Series animals are completed. Exposures of 9000 Series animals are temporarily discontinued, ceasing with the 80-WLM and 15-mg/m^3 ore dust exposures, pending analyses of existing data. Exposures of rats to uranium ore dust alone (10,000 Series experiments; Table 4) were completed. The ore-dust studies address recent experimental data in rats (as well as human epidemiological data) linking silica exposures to lung cancer. Because the silica content of the ore dust in the animal studies exceeds 60%, this potential link in the response to combined ore-dust and radon-daughter exposures needs to be clarified.

Respiratory Tract Pathology. A current summary of primary tumors of the respiratory tract for 9000 Series animals exposed to 320 WLM is shown in Table 5. The data show no significant differences in tumor probability with varying ore-dust concentrations. No tumors were found in six animals from each exposed group, sacrificed at 6 months after exposure; one adenocarcinoma was found in each exposed group at 12 months after exposure. Alveolar proteinosis, generally observed in quartz-dust exposures, was noted in the 15-mg/m^3 ore-dust-exposed group but was not observed at 3 mg/m^3 concentrations.

Histopathologic examinations are in progress on tissues from 8000, remainder of 9000, and 10,000 Series animals.

(a) Fred Hutchinson Cancer Research Center, Seattle, Washington.

TABLE 1. Exposure-Response Relationship Study for Radon-Daughter Carcinogenesis in Rats (6000 and 7000 Series Experiments).

Number of Animals[a]	Exposure Regimen[b,c]	Total Exposure WLM[d]
32	1000 WL Radon Daughters 15 mg/m^3 Uranium Ore Dust	10,240
32	1000 WL Radon Daughters 15 mg/m^3 Uranium Ore Dust	5120
32	1000 WL Radon Daughters 15 mg/m^3 Uranium Ore Dust	2560
32	1000 WL Radon Daughters 15 mg/m^3 Uranium Ore Dust	1280
64	1000 WL Radon Daughters 15 mg/m^3 Uranium Ore Dust	640
128	1000 WL Radon Daughters 15 mg/m^3 Uranium Ore Dust	320
64	Controls	

(a) Number of animals is sufficient to detect the predicted incidence of lung tumors at the 0.05 to 0.1 level of significance, assuming linearity of response between 0 and 9200 WLM (see footnote d), and 0.13% spontaneous incidence.
(b) Exposure rate, 90 hr/wk; planned periodic sacrifice.
(c) Study will be repeated @ 100 WL rate (without periodic sacrifice) to augment previous limited exposure-rate data (7000 series experiments).
(d) Working level (WL) is defined as any combination of the short-lived radon daughters in 1 liter of air that will result in the ultimate emission of 1.3 x 10^5 MeV of potential α-energy. Working level month (WLM) is an exposure equivalent to 170 hr at a 1-WL concentration. Previous exposure at 900 WL for 84 hr/wk to 9200 WLM produced an 80% incidence of carcinoma.

TABLE 2. Low-Exposure-Response Relationship Study for Radon-Daughter Carcinogenesis in Rats (8000 Series Experiments).

Number of Animals[a]	Exposure Regimen[b]	Total Exposure WLM[c]
64	100 WL Radon Daughters 15 mg/m^3 Uranium Ore Dust	640[d]
64	100 WL Radon Daughters 15 mg/m^3 Uranium Ore Dust	320[d]
160	100 WL Radon Daughters 15 mg/m^3 Uranium Ore Dust	160
352	100 WL Radon Daughters 15 mg/m^3 Uranium Ore Dust	80
448	100 WL Radon Daughters 15 mg/m^3 Uranium Ore Dust	40
512	100 WL Radon Daughters 15 mg/m^3 Uranium Ore Dust	20
192	Controls	

(a) Number of animals is sufficient to detect lung tumors at the 0.05 to 0.1 level of significance, assuming linearity of response between 0 and 640 WLM (see footnote c), and 0.13% spontaneous incidence.
(b) Exposure rate, 90 hr/wk; planned periodic sacrifice.
(c) Recent exposures indicate a tumor incidence of 16% at 640 WLM. Working level (WL) is defined as any combination of the short-lived radon daughters in 1 liter of air that will result in the ultimate emission of 1.3 x 10^5 MeV of potential α-energy. Working level month (WLM) is an exposure equivalent to 170 hr at a 1-WL concentration.
(d) Repeat exposure is for normalization with Table 1 data.

Lung-Tumor Risk. Tumor probabilities based on raw data in 6000, 7000, and 9000 Series rats versus radon-daughter exposure rate and level were shown in the FY1987 Annual Report. The data indicated an increase in lung tumors with decrease in exposure rate at all exposure levels that exceeded 320 WLM. Further analyses of these data by Suresh Moolgavkar of the Fred Hutchinson Cancer Research Center, Seattle, Washington, show that the probability of tumor is a complicated function of age, exposure rate and exposure level. Tumor probabilities are higher at early ages with high exposure rates than with low exposure rates but are lower at older ages, producing net results of higher lifetime risks of lung cancer (in rats) for low exposure rates. At 320-WLM exposures, the lifetime risk in rats is apparently independent of exposure rate.

TABLE 3. Ultralow Exposure-Rate Study for Radon-Daughter Carcinogenesis in Rats (9000 Series Experiments).

Number of Animals[a]	Exposure Regimen[b]	Total Exposure WLM[c]
64	10 WL Radon Daughters 15 mg/m^3 Uranium Ore Dust	320
64	10 WL Radon Daughters 3 mg/m^3 Uranium Ore Dust	320
352	10 WL Radon Daughters 15 mg/m^3 Uranium Ore Dust	80
352	10 WL Radon Daughters 3 mg/m^3 Uranium Ore Dust	80
512	10 WL Radon Daughters 15 mg/m^3 Uranium Ore Dust	20
512	10 WL Radon Daughters 3 mg/m^3 Uranium Ore Dust	20
192	Controls	

(a) Number of animals is sufficient to detect lung tumors at the 0.05 to 0.1 level of significance, assuming linearity of response between 0 and 640 WLM (tumor incidence is approximately 16% at 640 WLM), and 0.13% spontaneous incidence.
(b) Exposure rate, 90 hr/wk; planned periodic sacrifice.
(c) Working level (WL) is defined as any combination of the short-lived daughters in 1 liter of air that will result in the ultimate emission of 1.3 x 10^5 MeV of potential α-energy. Working level month (WLM) is an exposure equivalent to 170 hr at a 1-WL concentration.

TABLE 4. Control Study for Uranium Ore Dust Carcinogenesis in Rats (10,000 Series Experiments).

Number of Animals	Exposure Regimen[a]
96	15 mg/m^3 Uranium Ore Dust
64	Sham-Exposed Controls

(a) Exposures, 12-18 mo at 72 hr/wk; planned periodic sacrifice.

The full significance of these findings has not yet been established, but the data continue to support a tapering-off of the exposure-rate effect at occupational and, possibly, environmental rates of radon exposure. Lifetime lung-tumor risk coefficients for radon-daughter exposure in 6000, 7000, and 9000 Series rats are shown in Figure 1. The hazard-function analysis assumed that all tumors are incidental to the death of the animal. Lifetime lung-tumor risk coefficients are approximately one-half the values in Figure 1 when the tumors are considered fatal to the animal. Important features of this figure are the high risks for protracted exposure; a power-function response versus exposure rate, with no decrease in risk at high exposure levels; and a tapering-off of the exposure rate effect at low exposure levels.

TABLE 5. Current Summary of Primary Tumors of the Respiratory Tract (9000 Series Experiments).

Nominal Exposure, WLM	Nominal OreDust Conc., mg/m^3	Extrathoracic Tumors			Lung Tumors						
		Nasal	Oropharyngeal[a]	Laryngeal	No. Animals Examined	Adenoma	Adeno-Carcinoma	Epidermoid Carcinoma	Adeno-squamous Carcinoma	Sarcoma[b]	No. Animals with Lung Tumors
320	3	0/50[c]	1	0/36	51	0	6	1	0	1	8
320	15	0/50		0/41	52	1	4	4	1	0	10
Controls		0/31		0/22	32	0	0	0	0	0	0

(a) 1 squamous carcinoma, considered radon-daughter exposure-related; found in tissue not routinely sectioned for histopathology.
(b) 1 malignant mesothelioma in mediastinum, considered a primary tumor of the lung.
(c) No. tumors/no. examined

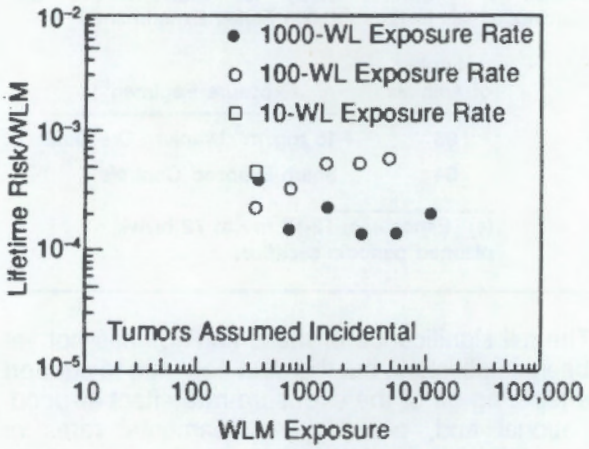

FIGURE 1. Lifetime Lung-Tumor Risk Coefficients for Radon-Daughter Exposure (Data Adjusted for Life-Shortening). WLM = working level month (see text).

Teratology Data. Pregnant SPF Sprague-Dawley rats were exposed to mean concentrations of 339.3 nCi/L radon, 5.1 mg/m^3 ore dust, and 1168 WL radon daughters. Cumulative radon-daughter exposures over 13 days of gestation (days 6 to 19) averaged 1607 WLM.

Teratologic data indicate no apparent hazard to the fetus. Cumulative radon-daughter exposures to the dams were about four orders-of-magnitude higher than typical annual levels associated with indoor radon exposures. (These data are discussed further in the Fetal and Juvenile Radiotoxicity report.) The dosimetry of these exposures is in progress.

Mechanisms of Radon Injury

Principal Investigator: F. T. Cross

Other Investigators: R. L. Buschbom, G. E. Dagle, H. S. DeFord, M. E. Frazier, R. A. Gies, R. F. Jostes, F. C. Leung, S. Marks, J. A. Reese, L. L. Scott, L. G. Smith, and G. L. Stiegler

Technical Assistance: R. M. Briones and C. R. Petty

In this project we conduct molecular, cellular and whole-animal research relevant to understanding the mechanisms of radon and radon-daughter injury to the respiratory tract. The work specifically addresses the exposure-rate effect in radon-daughter carcinogenesis; the induction-promotion relationships associated with exposure to radon and cigarette-smoke mixtures; the role of oncogenes in radon-induced cancers; the effects of radon on DNA as well as on DNA repair processes; and the involvement of growth factors and their receptors in radon-induced carcinogenesis. Preliminary experiments revealed that Kirsten *ras* proto-oncogenes are activated by radon exposures and that there is abnormal expression of epidermal growth factor and its receptor, as well as transforming growth factor-α, in radon-induced rat lung tumors. Exposures specific to oncogene and growth-factor studies were completed. The design of an *in vitro* radon cell-exposure system was improved, and cell-exposure studies, including collaborative studies with other laboratories, were initiated. Initiation-promotion-initiation exposures with radon and cigarette-smoke mixtures continued. Carcinogenesis modeling in experiments with radon and ore-dust mixtures was initiated, and a radon health-effects bibliography is being compiled.

Oncogene Studies

Preliminary experiments revealed that Kirsten (Ki)-*ras* proto-oncogenes were activated in radon-induced lung tumors. High-molecular-weight DNA from three radon-exposed rats caused transformation frequencies ten times more often than DNA from normal lung. The polymerase-chain-reaction method will be used to determine mutated DNA sequences in radon-induced rat lung-tumor tissues (fresh, frozen and paraffin-block-embedded).

Exposures of male SPF Wistar rats to mixtures of radon, uranium ore dust and cigarette smoke were completed for eventual determination of oncogene and growth factor/receptor involvement in tumorigenesis. Cumulative radon-daughter levels were 320 working level months (WLM); uranium ore-dust concentrations ranged from 4 to 6 mg/m^3. Cigarette smoke from Kentucky 1R4F cigarettes, in exposures of 1 hour/day, 5 days/week, for 17 weeks, contained total particulate mass concentrations of about 0.5 mg/L and carbon monoxide concentrations between 600 and 700 ppm. Mean plasma concentrations of nicotine and cotinine were about 260 and 125 ng/ml, respectively, in cigarette-smoke-exposed animals; carboxyhemoglobin levels were about 30%.

Growth Factor/Receptor Studies

We are using immunocytochemical assays to examine the involvement of growth factors (GF) and receptors in radon-induced and spontaneously occurring lung tumors that have been preserved in paraffin block sections. Many of the tumors that will be analyzed for GF/receptor involvement were produced in animals exposed to mixtures of radon and cigarette smoke.

Preliminary data show abnormal expression of epidermal growth factor (EGF) and its receptor (EGF-R) and transforming GF-α in tumors from animals exposed to radon and uranium-ore-dust mixtures (see Growth Factors in Radiation Carcinogenesis, elsewhere in this volume).

In Vitro Radon Cell-Exposure System and Cellular Studies

The design of PNL's *in vitro* radon cell-exposure system (described in the FY1987 Annual Report) was improved to incorporate simultaneous exposure of two cell cultures, thus ensuring identical dose-delivery capability. The system was extensively employed in PNL experiments as well as in several collaborative experiments with other laboratories.

Radon-induced mutations at the HGPRT locus in Chinese hamster ovary (CHO) cells showed a linear induction response with an induced frequency of 0.9×10^{-6} mutations/viable cell/centigray dose to the culture medium. For molecular analysis, using Southern blot techniques, we have isolated 15 radon-induced

HGPRT mutants and four spontaneous mutants from one experiment.

Preliminary investigations of radon-induced chromosomal aberrations and sister chromatid exchange (SCE) have been evaluated in human peripheral blood lymphocytes. Cycling lymphocytes were irradiated for aberration analysis and quiescent lymphocytes were treated, then stimulated for SCE analysis. Aberrations and SCE were induced in a linear fashion with a frequency of 0.009 aberrations/metaphase/centigray dose to the medium and 0.031 SCE/metaphase/centigray dose to the medium.

We are currently investigating the microdosimetry of cells exposed to radon and daughters in tissue culture medium. Preliminary data show a preferential association of radon and daughters with the cell and, therefore, a higher dose to cells than to the medium.

Initiation-Promotion-Initiation and Carcinogenesis Modeling Studies

Initiation-promotion-initiation (IPI) experiments continue in male SPF Wistar rats with radon and cigarette-smoke mixtures. Our objective is to determine: (1) the respective roles of radon and cigarette smoke in lung tumorigenesis, and (2) whether these lung tumors are consistent with the two-mutation recessive oncogenesis model (two-stage model of carcinogenesis) developed elsewhere in mouse-skin studies. The exposure protocols are shown in Table 1.

Initial exposures are at 100-WL concentrations with cumulative levels of 320 WLM; other exposure parameters are as described under Oncogene Studies above. Exposures of 64 animals each in Groups 1 to 6 were completed as well as sacrifice of 10 animals in each group at 25 weeks and 10 more animals in Groups 1 to 4 at 52 weeks.

While waiting for results from the IPI experiments, data from approximately 1800 rats previously exposed to radon, radon daughters, and uranium ore dust were analyzed by Suresh Moolgavkar of the Fred Hutchinson Cancer Research Center, Seattle, Washington, for parameters in the two-mutation recessive oncogenesis model. Preliminary main conclusions are that radon and its daughters strongly affect the first mutation rate, have a significant effect on the kinetics of intermediate cells (dust-exposure influence?), and have a lesser effect on the second mutation rate. Final conclusions and interpretations of these data are not yet developed.

Radon Health-Effects Bibliography

We are compiling a bibliography on the health effects of radon inhalation exposures. Topics currently included are experimental animal studies and human epidemiology studies. A final report, "Radon Inhalation Studies in Animals," and a draft report, "Radon Epidemiology: A Guide to the Literature," were submitted to DOE/OHER for publication in their Radon Literature Survey Series.

TABLE 1. Initiation-Promotion-Initiation Protocol for Radon (R), Dust (D), and Cigarette Smoke (S) Inhalation Exposure of Rats.[a]

	Duration of Exposure, wk					
Group	0	4	8	17	21	25
1	R + D----------→					
2	R + D----------→				R + D---------→	
3	R + D----------→	S----------→			R + D---------→	
4	R + D----------→	S----------→				
5	S----------→			R + D----------→		
6	D----------→	S----------→				

(a) Moderately low concentrations of uranium ore dust (D) accompany radon exposures as the carrier aerosol for the daughters; sham-exposed control animals (not shown) are included in each exposure group. Animals from each group are killed at 25, 52 and 78 weeks to evaluate developing lesions. Protocol may be repeated for different radon-daughter exposure rates and levels.

Microdosimetry of Radon Daughters

Principal Investigator: D. R. Fisher

Other Investigators: F. T. Cross, T. E. Hui,[a] A. C. James, and J. W. Poston[a]

The purpose of this project is to develop more precise methods for calculating the radiation dose to nuclei of secretory cells and basal cells within the tracheobronchiolar epithelium from inhalation of radon and radon-daughters. The nuclei of secretory cells and basal cells are considered important biological targets at risk for radiation-induced lung cancer in persons exposed to radon and radon daughters. Alpha-particle doses to small biological targets such as cell nuclei are highly variable because of the physical characteristics of the alpha-particle track and its interaction probabilities with such targets. This variability is described in terms of a probability density in specific energy. A microdosimetric approach to the dosimetry of alpha emitters also provides the mean dose to selected targets, the probability that targets are completely missed, and the hit-frequency distribution. This information is necessary for assessing the relationship between radiation dose and biological effects so that the risks may be better understood and predicted. It provides more precise dosimetry for mechanistic studies of biological effects.

The objective of this research is to provide radon-daughter dosimetry including site-specific probability densities in specific energy, for epithelial cell nuclei in each branching generation of the respiratory tract.

A number of investigators (ICRP, 1981; James, 1988; NCRP, 1984; NEA, 1983) have previously estimated the absorbed dose to cells and tissues of the respiratory tract at risk from the radiation effects of inhaled radon and its daughter products. However, none of the previous studies involved an effort to evaluate doses to small targets in terms of probability density in specific energy using principles of stochastic microdosimetry. Microdosimetry (International Commission on Radiation Units and Measurements, *Microdosimetry*, ICRU Pub. 36, 1983) involves calculation of the dose to each microscopic target and then to present the dosimetry result as a statistical probability function from which useful information may be drawn for interpreting the radiobiology of the radiation exposure.

Lung Model, Deposition, and Clearance Parameters

Published lung models were reviewed, and the 16-generation, dichotomous branching model adapted by James (1988) was chosen for this study to represent the morphometry of the respiratory tract. A nasal breathing rate of 15 L min^{-1} and a tidal volume of 1 L were assumed. Regional surface deposition probabilities for attached and unattached radon daughters were calculated using the preferred equations for diffusion, sedimentation, and inertial impaction. An average mucociliary clearance velocity (0.5 cm min^{-1}, NCRP, 1984) was assumed, and transfer of radon daughters to blood (40%), with partial trapping within bronchial and bronchiolar epithelium, was accounted for. The equilibrium alpha source distribution was then calculated for each airway generation.

We assumed a reference atmosphere containing 1 pCi L^{-1} radon and having a radon-daughter disequilibrium ratio of $^{222}Rn/^{218}Po/^{214}Pb/^{214}Bi$ of 1.0/0.9/0.6/0.4, an unattached fraction of 0.1/0.01 for $^{218}Po/^{214}Pb$, a diffusion coefficient for the unattached fraction of 0.054 cm^2 s^{-1}, and an activity median diameter of 0.15 μm (characteristic of indoor atmospheres). For this atmosphere, the surface equilibrium activities given in Table 1 were calculated for activity either in the mucus layer or deposited in bronchial epithelium.

Source-Target Geometries

A cross-sectional representation of bronchial epithelium, with basement membrane, basal cells, epithelial (secretory and ciliated) cells, and the mucus layer, is shown in Figure 1. The average depth of the mucus layer has been estimated to be about 15 μm. Basal cells were assumed to have a depth correlating with airway diameter such that

$$x = 80.8 - 73.8e^{-1.76d},$$

(a) Texas A&M University, College Station, Texas

where x is the median basal cell depth, distributed lognormally, and d is the diameter of the airway (cm). Secretory cell nuclei were assumed to be distributed uniformly in the epithelium.

TABLE 1. Equilibrium Activity of Alpha-Emitting Radon Daughters in Different Airway Generations for a Reference Atmosphere (Disintegrations min^{-1}).

	Mucas Layer		Bronchial Epithelium	
Generation	^{218}Po	^{214}Po	^{218}Po	^{214}Po
0[(a)]	0.277	0.365	0.552	4.226
1	0.232	0.235	0.441	3.114
2	0.168	0.120	0.331	2.047
3	0.131	0.075	0.282	1.593
4	0.080	0.064	0.213	1.282
5	0.111	0.098	0.291	1.805
6	0.138	0.134	0.357	2.278
7	0.188	0.215	0.458	3.109
8	0.241	0.332	0.541	4.002
9	0.287	0.472	0.558	4.666
10	0.335	0.680	0.515	5.305
11	0.400	1.030	0.408	6.198
12	0.488	1.483	0.255	7.292
13	0.623	2.090	0.149	9.226
14	0.841	2.918	0.135	12.493
15	1.204	3.918	0.183	9.185

(a) Trachea

A Monte-Carlo technique was used to determine the chord-length distributions for distances between the source of alpha-emitting activity and either the secretory cell nuclei or the basal cell nuclei. A simplified model of an airway is shown in Figure 2. For activity in the mucus layer, the distance between the source point and the center of a target cell nucleus is

$$L = \{x^2 + [(R+t)\sin\theta]^2 + [R+T+D - (R+t)\cos\theta]^2\}^{1/2},$$

where x is the distance along the airway,
R is the radius of the airway,
t is the depth of the source point below the surface of the mucus layer,
θ is the angle between the line joining the source point and the center of the airway and the line joining the center of the airway and the center of the target site,
T is the thickness of the mucus layer, and
D is the cell nucleus depth.

Microdosimetry Calculations

A developmental computer code based on principles of internal microdosimetry (Roesch, *Radiat. Res. 70*:494-510, 1977) was modified to calculate probability densities in specific energy for target cell nuclei irradiated by alpha particles from either ^{218}Po or ^{214}Po. The probability densities for irradiation by ^{218}Po and ^{214}Po were obtained separately, then combined by convolution.

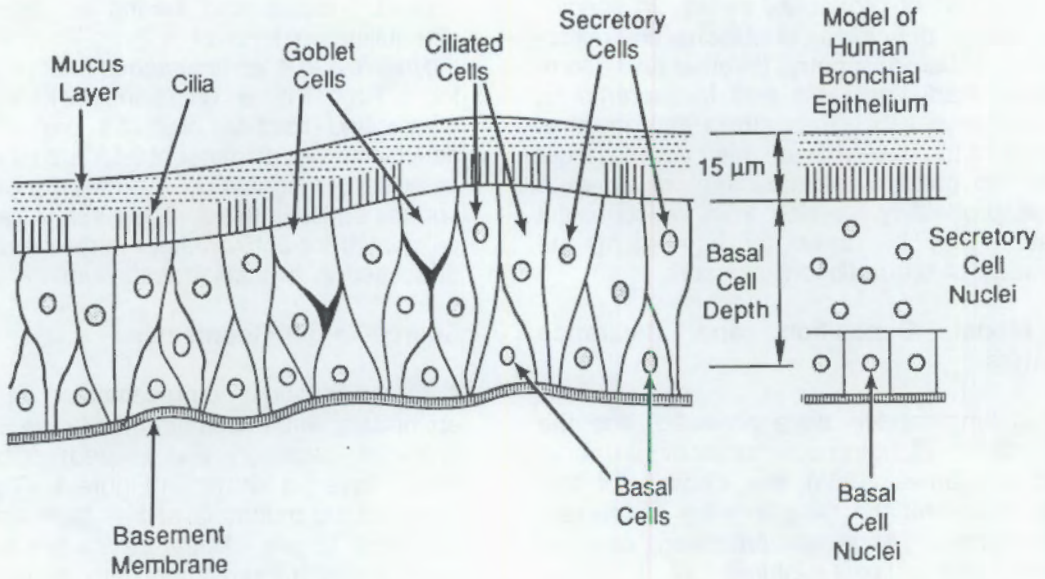

FIGURE 1. Typical Cross-Sectional View of a Portion of Bronchial Epithelium of a Human Lung Airway as a Model for Dosimetry.

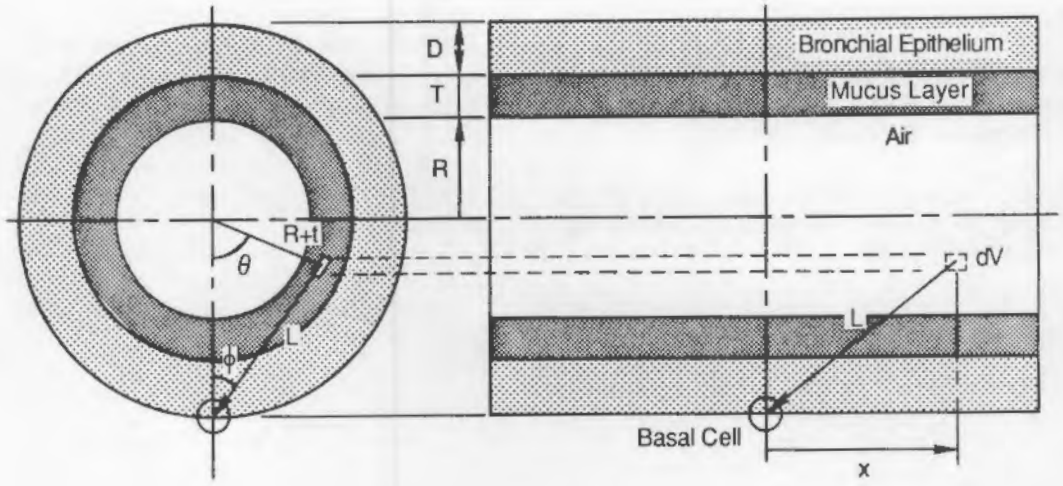

$$L = \sqrt{x^2 + [(R+t)\sin\theta]^2 + [R+T+D-(R+t)\cos\theta]^2}$$

FIGURE 2. Source-Target Geometry for Distances Between Radon-Daughter Activity and Basal Cell Nuclei.

Figure 3 shows the probability densities in specific energy for secretory cell nuclei and basal cell nuclei irradiated by alpha-emitting radon daughters in the whole tracheobronchiolar tree. The reference atmosphere (described above) was used to define the source term, and a cumulative exposure of 8.45 working level months (WLM) was assumed (corresponding to a 30-yr exposure at 1 pCi L^{-1}, or 0.28 WLM yr^{-1}).

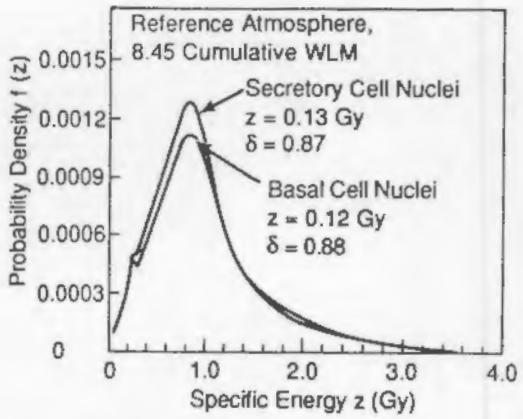

FIGURE 3. Probability Densities in Specific Energy for Secretory and Basal Cell Nuclei of the Tracheobronchial Tree from the Reference Atmosphere and a Cumulative Exposure of 8.45 Working Level Months (WLM).

Results of these calculations showed that most (70 to 90%) basal cell and secretory cell nuclei were missed by alpha-particle radiation from the reference atmosphere. Most of the remaining basal and secretory cell nuclei were hit only once. The main, lobar, and segmental bronchi (generations 1 to 4) had the highest fraction of cell nuclei irradiated; these are considered the epithelial tissues from which most bronchial tumor originate in humans exposed to radon atmospheres. While generations 1 to 4 had the highest fraction of their basal and secretory cells hit, more of these cells were hit in generations 14 to 16. However, they represented a smaller fraction of the cells present in these generations.

The average reference atmosphere doses to basal and secretory cell nuclei in the segmental bronchi were 0.12 Gy and 0.13 Gy (12 rad and 13 rad), respectively. These values correspond to 0.014 Gy WLM^{-1} and 0.015 Gy WLM^{-1}, respectively.

The ability to determine microdosimetric quantities makes it possible to evaluate fundamental dose-effect relationships needed to estimate risk from exposure to environmental levels of radon and daughters. It also provides dosimetry for mechanistic research at the cellular level. Future work will involve comparisons of different exposure conditions and analysis of the relationship between hit probability and risk estimates for lung cancer.

References

International Council on Radiation Protection and Measurements (ICRP), *Limits for Inhalation of Radon Daughters by Workers*, 1981.

James, A.C. Lung Dosimetry, pp. 259-309, In: *Radon and its Decay Products in Indoor Air*. Wiley, New York, 1988.

National Council on Radiation Protection and Measurements (NCRP), *Evaluation of Occupational and Environmental Exposures to Radon and Radon Daughters in the United States*, 1984.

Nuclear Energy Agency (NEA), *Dosimetry Aspects of Exposure to Radon and Thoron Daughter Products*, 1983.

Growth Factors in Radiation Carcinogenesis

Principal Investigator: F. C. Leung

Other Investigators: L. R. Bohn and J. R. Coleman

This research project examines the involvement of growth factors (GF) and their receptors (GF-R) in radiation-induced carcinogenesis of the lung in animals. We have developed a radioreceptor binding assay for examining epidermal growth factor receptor in lung tumors obtained from necropsy. We have also developed immunocytochemical assays for detecting GF and GF-R in archived, paraffin-block lung tumors from dogs and rats exposed to inhaled radionuclides, including $^{239}PuO_2$, $^{238}PuO_2$, $^{239}Pu(NO_3)_4$, and radon daughters. Our results showed abnormally high expression of epidermal growth factor receptor associated with epidermoid carcinoma of the lungs. These assays will enable us to obtain molecular and cellular information from tissues obtained from previous dose-effect-relationship studies with inhaled radionuclides.

The overall objective of this research is to examine the involvement of growth factors (GF) and their receptors in radiation-induced carcinogenesis of the lung. Recent studies have shown abnormally high levels of epidermal growth factor receptor (EGF-R) in human epidermoid carcinomas and of bombesin in small-cell carcinomas of the human lung. Using a gene transfer technique, NIH 3T3 mouse fibroblasts transfected with a human EGF-R gene are reported to have ligand-dependent transforming potential. This suggests that activation of overexpressed normal receptor is sufficient to transform NIH 3T3 cells *in vitro*. Our hypothesis is that radiation- and chemical-induced lung tumors, in both animals and humans, would have different, unique, and specific profiles of abnormally expressed GF and/or GF-R. We are using radioreceptor binding assays to examine EGF-R from lung tumors recently obtained at necropsy from radiation-exposed and control animals and immunocytochemical assays for examining archived, paraffin-block lung tumors obtained from previously exposed animals.

Radioreceptor Assay

We have examined a total of 8 lung tumors from six dogs recently necropsied; details of the radiation exposure and results of microscopic examination of tissues are shown in Table 1. Specific EGF-R binding of these tumors was compared with 13 normal lung-tissue samples. Seven of the tumors had significantly higher specific EGF-R binding than did normal lung tissue (Figure 1). The EGF-R binding of one tumor was not significantly different from that in the normal tissue. When EGF-R binding in four lung tumors was compared with "normal" lung tissue obtained from a different lung lobe in the same dog, the differences observed between tumor and normal lung tissues were the same as in the previous comparisons (Figure 2). Moreover, EGF-R binding in "normal" tissue immediately adjacent to tumor tissue was also "normal" (Figure 2).

TABLE 1. Radionuclide Exposure and Type of Tumor Resulting in Dogs Exposed by Inhalation.

Identification[a]	Sex	Radionuclide	Burden (nCi)	Tumor Type
A	F	$^{238}PuO_2$	22	Bronchioloalveola Carcinoma
B	F	$^{239}Pu(NO_3)_4$	72	Papillary Adenocarcinoma
C	F	$^{239}PuO_2$	140	Papillary Adenocarcinoma
D	M	$^{239}Pu(NO_3)_4$	54	Papillary Adenocarcinoma
E	M	$^{238}PuO_2$	17	Papillary Adenocarcinoma
F	M	Control	0	Papillary Adenocarcinoma

(a) Letters correspond to those shown in Figures 1 and 2.

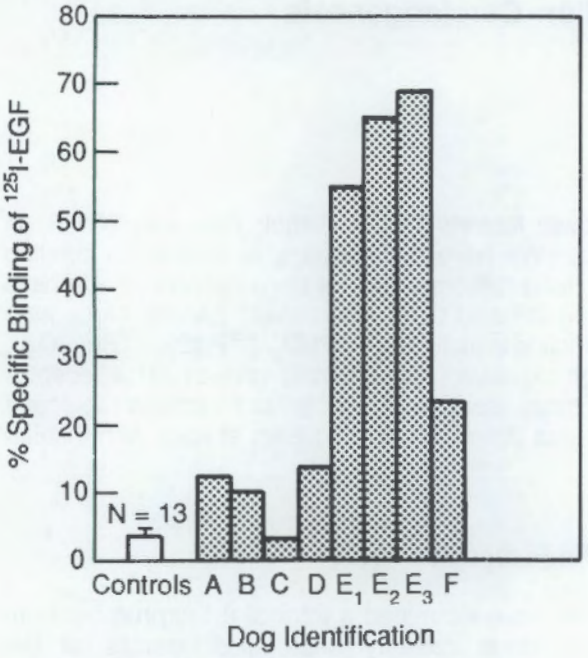

FIGURE 1. Specific Epidermal Growth Factor Receptor (EGF-R) Binding in Normal and Lung-Tumor Tissue. □ = mean EGF-R binding (±SE) in tissues from 13 normal lungs; ▨ = EGF-R binding from 8 lung-tumor tissue samples. Letters correspond to those in Table 1; subscript numbers represent different tumor samples obtained from the same dog.

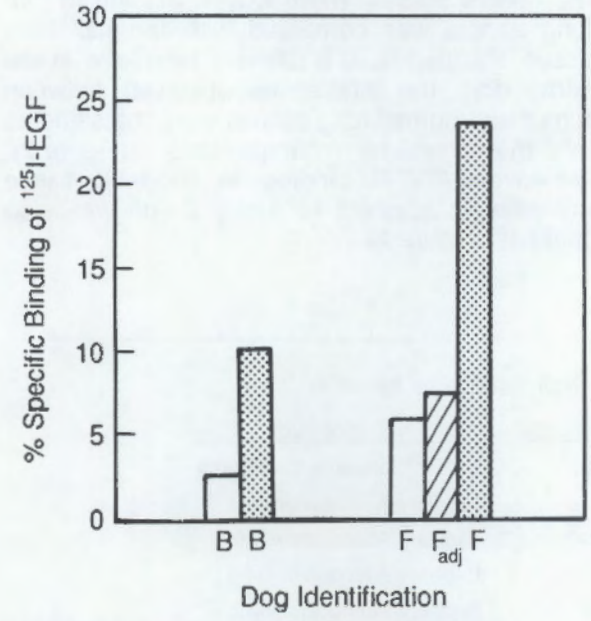

FIGURE 2. Comparison of Specific Epidermal Growth Factor Receptor (EGF-R) Binding in Tissues (□ = Normal, ▨ = Lung Tumor) Obtained from the Same Dog. F_a = (▨) Lung Tissue Immediately Adjacent to Tumor Tissue.

Scatchard analysis of tumors and normal tissues is shown in Figure 3; a summary of binding characteristics is given in Table 2. There were no significant differences in binding affinity between normal and tumor tissues, but binding capacities (receptor numbers) were at least 10-fold higher in tumor tissues compared to that in normal tissues.

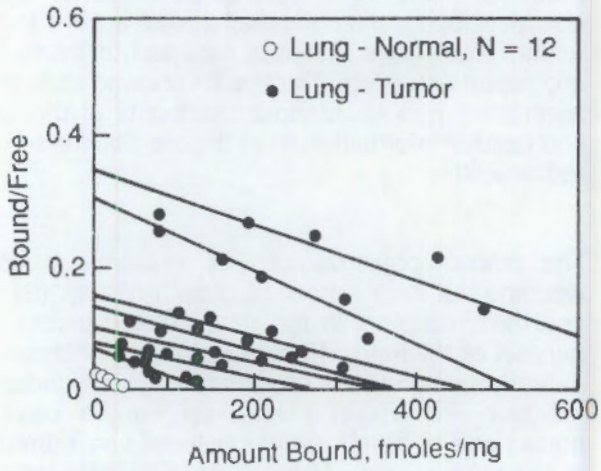

FIGURE 3. Scatchard Plot Analysis of ^{125}I-Epidermal Growth Factor Binding to Microsomal Preparations of Normal (●) and Tumor (○) Lung Tissue.

TABLE 2. Binding Characteristics of Epidermal Growth Factor Receptors in Normal and Tumorous Dog Lung-Tissue Preparations (Mean ± SE).

	kd (M)	Amount Bound (fmoles/mg)
Normal (N = 12)	$3.93 \pm 1.74 \times 10^{-8}$	53 ± 16
Tumor (N = 11)	$4.38 \pm 3.42 \times 10^{-8}$	619 ± 282

Immunocytochemical Assay

Using a monoclonal antibody against human EGF-R, and the Vesctastain ABC kit as the enzyme detection system, we have demonstrated that high levels of EGF-R binding were associated mainly with epidermoid carcinomas in dog lung tumors. A representative tumor, stained with EGF-R monoclonal antibody, is shown in Figure 4. The same monoclonal antibody also cross-reacted with rat EGF-R, using the immunocytochemical assay.

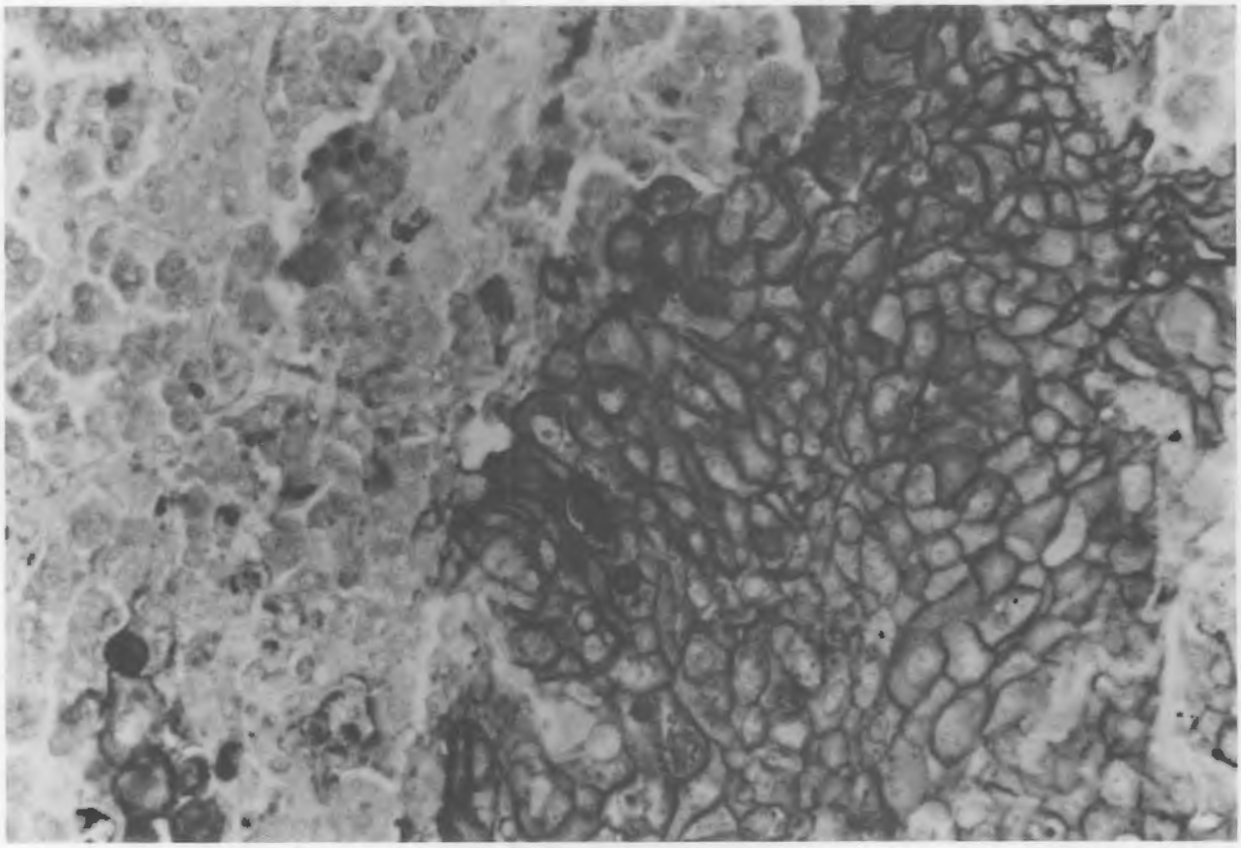

FIGURE 4. Epidermoid Carcinoma from Inhaled Plutonium-Induced Dog Lung Tumor, Stained with Monoclonal Antibody Against EGF-R, Demonstrating High Levels of EGF-R Binding.

We have also examined lung tumors from 32 rats exposed to 1000 working levels (WL)[a] of radon daughters and 15 mg/m^3 uranium ore dust, (total exposure of 5120 WLM), and 32 control rats for EGF-R expression (Table 3). Specific positive EGF-R staining was present in 12 of 14 epidermoid carcinomas observed. No other type of lung tumor was positive for EGF-R staining. There was no positive EGF-R staining in any lung tissue obtained from the 32 control rats.

We have demonstrated that EGF-R binding is significantly higher in plutonium-induced dog lung tumors, and that the increase in EGF-R binding is the result of increased receptor binding capacity rather than of affinity. We have also shown abnormally high expression of EGF-R in dogs with plutonium-induced epidermoid carcinoma of the lung. Our results also demonstrated that abnormally high expression of EGF-R was associated with epidermoid carcinoma induced by radon daughters in rats. Our data therefore suggest that EGF-R is involved in α-radiation-induced oncogenesis in the lung.

TABLE 3. Expression of Epidermal Growth Factor Receptor (EGF-R) in Primary Lung Tumors[a] and Radiation Pneumonitis Lesions in Rats Exposed to Radon Daughters (1000 Working Level [WL] 15 mg/m^3 Uranium Ore Dust, with a Total Exposure of 5120 WLM).

Tumor Type/Lesion	No. Positive for EGF-R/ No. Examined
Epidermoid Carcinoma	12/14
Adenocarcinoma	0/17
Adenoma	0/7
Adenosquamous Carcinoma	0/1
Sarcoma (Histiocytoma)[b]	0/1
Radiation Pneumonitis	0/32

(a) 25 animals with lung tumors out of 32 animals examined.
(b) One sarcoma (histiocytoma) in control group of 32 animals.

Oncogenes in Radiation Carcinogenesis

Principal Investigator: M. E. Frazier

Other Investigators: J. A. Reese, R. P. Schneider, T. M. Seed,[a] G. L. Stiegler, and L. L. Whiting

Technical Assistance: S. R. Peterson

We are using lung-tumor and leukemic cells obtained from studies of lifespan dose-effect relationships in experimental animals exposed either to plutonium or radon daughters by inhalation or to external, whole-body gamma radiation to examine the role of oncogenes in radiation-induced carcinogenesis. We have detected activated *ras* oncogenes in these radiation-induced malignancies and are determining whether radiation causes specific mutations in these genes. If so, we want to know whether alpha radiation causes patterns of genetic change which can be distinguished from the mutations caused by gamma radiation.

Previous studies in our laboratory provide evidence that dominant-acting oncogenes from the *ras* family are activated in canine radiation-induced malignancies. Tables 1 and 2 summarize these data. The results indicate that DNA from radiation-induced cancers (both lung tumors from inhaled plutonium and myelomonocytic leukemia from whole-body gamma radiation) can transform NIH 3T3 cells. Furthermore, the DNA from malignant cells display tumor-specific restriction fragment length polymorphisms (RFLP) in one or another of the known *ras*-related genes, and steady-state levels of *ras* gene transcripts are higher in radiation-induced cancer tissue than in normal cohort tissues. We also have evidence from examination of bone-marrow cells from animals with radiation-induced myelomonocytic leukemia that the leukemic cells show a number of cytogenic alterations which are consistent with gross chromosomal rearrangements: for example, a high incidence of first chromosomal changes. The most frequent observation is a translocation which results in the elongation of the q arm of the first chromosome. In addition, we have detected gene amplification in two of three dogs with myelomonocytic leukemia (Figure 1).

Dominant-acting transforming oncogenes have been detected in both plutonium-induced lung tumors and in gamma-radiation-induced leukemias. Furthermore, some of these animals have tumor-specific RFLP in *ras*-related DNA sequences, and Northern analyses show an increased expression of the *ras* gene.

(a) Argonne National Laboratory

TABLE 1. Oncogene Activation in Plutonium-Induced Lung Tumors.

Dominant-Acting Transforming Genes	
9 of 9 Plutonium-Induced Lung Tumors	
Tumor-Specific RFLP	
Ha-*ras*	3 of 6
Ki-*ras*	7 of 8
erb B	5 of 6
myc	1 of 8
src	1 of 4
Increased Transcription of	
ras	
erb B	
Gross Chromosomal Changes	
Gene Amplification	
Tumor-Specific RFLP	

According to a current hypothesis, proto-oncogenes are activated to become oncogenes (cancer-causing genes) by genetic alterations which result from point mutations, translocations, deletions, amplifications or other genetic mechanisms. This activation results in either an altered protein with a modified function, increased amounts of gene product, or some combination of these events, causing altered cellular activities and/or abnormal cell division. Evidence from our studies supports this hypothesis. The changes detected in oncogene sequences of tumor-cell DNA from a radiation-induced tumor often appear to be extensive, resulting in gross chromosomal rearrangements. This is supported by the presence of cytogenetic alterations, in the q arm of

the first chromosome, in a number of animals which either have or are developing radiation-induced chronic myeloproliferative disorders.

TABLE 2. Oncogene Activation in Radiation-Induced Myelomonocytic Leukemias.

Dominant-Acting Transforming Genes	
3 of 3 Leukemias	
Tumor-Spacific RFLP	
N-*ras*	3 of 3
Ki-*ras*	0 of 3
abl	2 of 3
myc	0 of 3
fms	3 of 3
Increased Transcription of	
ras	
myb	
fms	
abl	
Decreased Transcription of	
sis	
Gross Chromosomal Changes	
Gene Amplification	
Tumor-Specific RFLP	
Chromosomal Translocation	

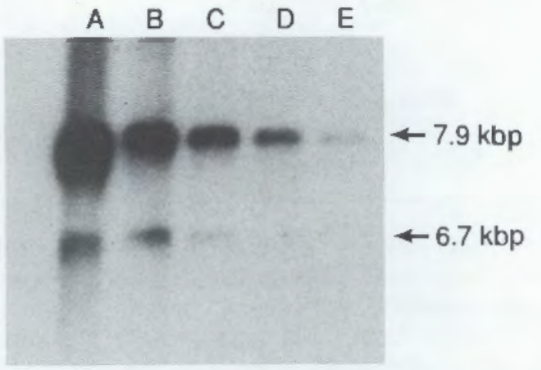

FIGURE 1. Detection of Amplified N-*ras* Sequences in DNA from a Dog with Whole-Body Gamma-Radiation-Induced Myelomonocytic Leukemia. Cellular DNA digested with *Eco* R1 was electrophoretically separated on 1% agarose, transferred to nitrocellulose, and hybridized to a ^{32}P-labeled fragment of c-N-*ras*. Ten micrograms of genomic DNA from a leukemic animal (spleen) were added to Lane A. Serial dilutions of DNA from the spleen were added to Lanes B through D. Lane B contained a 1:5 dilution; Lane C, a 1:15 dilution; and Lane D, a 1:45 dilution. Lane E contains 10 µg DNA extracted from a "normal" dog's spleen.

Studies in humans have shown a relationship between nonrandom chromosomal abnormalities and specific types of cancer. These abnormalities are usually adjacent to or within known proto-oncogenes. It is possible that proto-oncogene activation in radiation-exposed animals occurs as a result of similar gross chromosomal abnormalities.

It is also possible that single-base changes which have been observed in chemically induced or spontaneously occurring tumors may occur. Another mechanism by which normal cells may be converted to cancer cells involves mutations in genes (proto-oncogenes) which are important for normal growth and development. Such genes include growth factors, receptors for growth factors, transducers within the cell that can alter a signal by phosphorylation of proteins, and other molecules and nuclear effectors (regulatory genes) that cause the cells to respond to mitogenic signals. Evidence exists to support both mechanisms of oncogene activation. Also, considerable evidence is available to indicate that specific carcinogens cause characteristic activation mutations in *ras* genes. These mutations are usually observed in either the 12th or 59th to 61st codons (Table 3) of the *ras* gene.

TABLE 3. Insult-Specific Oncogene Activation.

Insult	Tumor	Activated Oncogene	Mutation
NMU[a]	Mammary Carcinoma	Ha-*ras*	G→A 12th Codon
DMBA[b]	Mammary Carcinoma	Ha-*ras*	?? 60th Codon
DMBA/TPA[c]	Skin Carcinoma	Ha-*ras*	A→T 60th Codon
NMU[d]	Thymoma	N-*ras*	?? Codon
X-rays[d]	Thymoma	Ki-*ras*	G→A 12th Codon
TNM[e]	Lung Tumor	Ki-*ras*	G→A 12th Codon

(a) Zarbl et al. 1985. *Nature* 315:382.
(b) Sukumar et al. 1983. *Nature* 306:658.
(c) Balmain et al. 1984. *Nature* 307:658.
(d) Guerrero et al. 1984. *Proc. Natl. Acad. Sci. USA* 81:202.
(e) Stowers et al. 1987. *Cancer Res.* 47:3213.

We are in the process of examining *ras* proto-oncogene sequences from animals with plutonium-induced lung tumors to determine whether they contain mutated sequences. The isolation and complete characterization of these changes by transfection analysis, cloning and sequencing previously required either fresh tissue or frozen samples. In addition, cloning restriction-mapping,

subcloning, and sequencing were slow and expensive, and required considerable amounts of DNA. Transfection assays use ~20 μg/assay to detect dominant-acting oncogenes; Southern analysis requires 5 μg/ oncogene (there are three *ras* genes) and three different restriction enzymes (a total of 45 μg) in order to detect a tumor-specific RFLP.

Although such studies can be carried out on most canine lung tumors, the numbers of cancer cells available in a bone marrow aspirate (from a leukemic dog), or from a rodent lung tumor, are usually not sufficient for complete analysis. For example, the total weight of a rat lung is 0.7 to 1.4 g, which converts to 280 to 560 μg total DNA. Often, the tumor tissue available for molecular studies is less than 0.2 g (~80 μg DNA). The polymerase chain-reaction (PCR) method that we have recently developed has provided an alternative method for making these analyses which is faster than cloning the gene. It requires considerably less material (usually 10 to 100 ng of DNA) in order to provide DNA sequence information for the target region.

Another objective of our studies this year was to devise a method for examining formalin-fixed, paraffin-embedded tissues for the presence of mutated *ras* sequences. We have extracted DNA from formalin-fixed, paraffin-embedded rat lung tissues by gently melting the tissue sample from the paraffin block while agitating it in the presence of xylene on a heated stir plate. After 30 minutes the tissue was removed, blotted on filter paper and placed in fresh xylene, and stirred for another 30 minutes. This was followed by sequential 30-minute washes in absolute alcohol (95% alcohol, 80% alcohol, and 70% alcohol, respectively). The tissue was then washed three times for 30 minutes in normal saline. The DNA was extracted using the standard method (T. Maniatis, E. F. Fritsch, and J. Sambrook, *Molecular Cloning, A Laboratory Manual*, Cold Springs Harbor Laboratory, New York, 1982), except that 5 mg/ml of proteinase K was used, and the sample was incubated with that enzyme for 6 hours at 60°C.

Figure 2 provides evidence that the DNA obtained from formalin-fixed, paraffin-embedded rat lung tissues (in lanes 4 and 5) is of sufficient size that genes in the 2- to 30-kbp size range should be represented. The *ras* genes are ~6 kbp in size, and the coding regions of interest are only ~100 bp in size. Based on the quantity and quality of the DNA obtained (Table 4), it appears that formalin-fixed, paraffin-embedded tissues may provide an important resource for studying oncogene activation. Several attempts to obtain DNA from tissues which had been fixed only in formalin were not successful (Figure 2 lane 3). The formalin remaining after several washes in normal saline was sufficient to inactivate the proteinase K and prevent complete digestion of the sample. A process similar to the sequential dehydration steps used in embedding the tissue is necessary to remove excess formalin from these tissues.

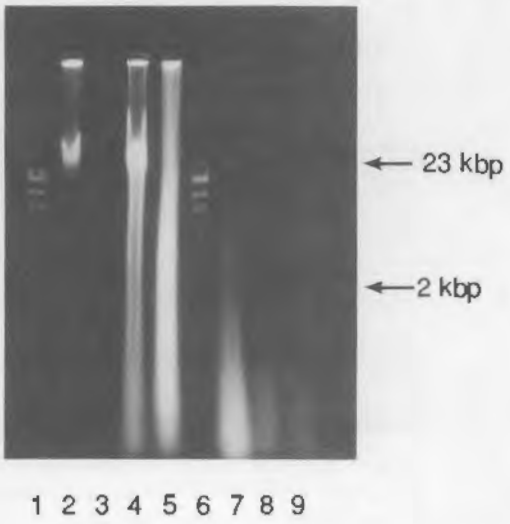

FIGURE 2. DNA Samples Were Examined by Electrophoresis on a 0.8% Agarose Gel. These samples included DNA from lambda bacteriophage, which served as a molecular size marker (Lane 1); isolated normal rat lung (rat), sample taken immediately after sacrifice (Lane 2); normal rat lung after formalin fixation for 3 weeks (Lane 3); normal rat lung after formalin fixation and paraffin-embedding (Lane 4); paraffin-embedded, normal rat lung stored for more than 6 yr (Lane 5); and an additional lane of lambda marker DNA (Lane 6).

TABLE 4. Isolation of DNA from Rat Lung.

	Weight g	DNA Yield, μg	DNA Quality
Fresh	0.3	108	+ + + +
Formalin-Fixed	0.3	~15	±
Formalin-Fixed, Embedded (3 wk)	0.15	56	+ + +
Formalin-Fixed, Embedded (yr)	0.13	43	+

Key: + + + + = High-Quality HMW DNA
+ + + = Considerable HMW DNA
+ = DNA sheared some HMW DNA
± = DNA badly sheared

The next important question was whether the DNA from embedded tissues would be amplified using

the PCR method. In order to evaluate this, we prepared primers to the first exon in the rat Ki-*ras* gene (Figure 3). The PCR method was then used to amplify the Ki-*ras* first exon in DNA extracted from fresh and paraffin-embedded, fixed tissues. It can be seen (Figure 4) that the paraffin-embedded tissues (lanes 9-11) are amplified as well as the DNA from fresh tissues (lanes 3-5, 7, and 8). Furthermore, it appears that the amplification was very specific, as only 1 or, at most, 2 bands are observed in each lane. The DNA produced was also homologous to the viral Ki-*ras* probe, as determined by Southern blot analysis (Figure 5).

We have also shown that the amplified DNA from the paraffin-embedded tissues was a faithful copy of the original DNA. In other words, the fixation or amplification processes did not produce "mutation/artifacts." In order to evaluate this, we purified the DNA produced by the PCR method using polyacrylamide gel electrophoresis (Figure 6). It is evident from this preparative gel that the tissue-produced DNA is similar to viral K-*ras* DNA: only the band which hybridized to the *ras* gene is observed. The DNA from these bands is currently being sequenced.

5' TGAAAATGACTGAATATAAACTTGTGGTAGTTGGAGCT**GGT**GGCGTAGGCAAGA
3' ACTTTTACTGACTTATATTTGAACACCATCAACCTCGA**CCA**CCGCATCCGTTCT

GTGCCTTGACGATACAGCTAATTCAGAATCATTTTGTGGACGAAT 3'
CACGGAACTGCTATGTCGATTAAGTCTTAGTAAAACACCTGCTTC 5'

First Primer 5' TGAAAATGACTGAATATAAACTTGTGGT 3'

Second Primer 5' CTTCGTCCACAAAATGATTCTGAATTA 3'

FIGURE 3. DNA Sequences of the First Exon of the Rat Ki-*ras* Gene and the Primers Used in the Synthesis of These Sequences by the Polymerase-Chain-Reaction Method.

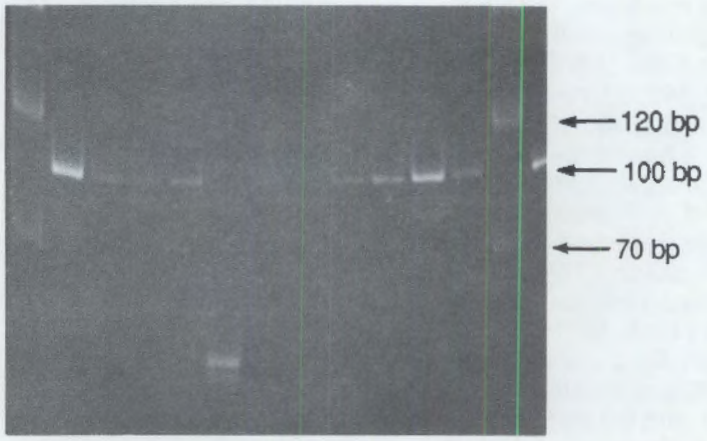

FIGURE 4. Analysis of DNA Produced by the Polymerase-Chain-Reaction (PCR) Method. Samples were examined by electrophoresis in a 6% polyacrylamide gel and stained with ethidium bromide. In Lane 1, OX174 DNA digest with Hae III as a size marker; Lane 2, DNA copy of the viral Kirsten *ras* gene; Lane 3, DNA from a fresh lung tumor of rat #93343, induced by radon; Lane 4, DNA from a radon-induced lung tumor in rat #93398; Lane 5, DNA from a radon-induced fresh lung tumor in rat #93175; Lane 6, DNA primers used in the PCR method, without added genomic DNA; Lane 7, DNA from a plutonium-induced lung tumor (fresh) in rat #5510; Lane 8, DNA from a plutonium-induced lung tumor (fresh) in rat #5519; Lane 9, DNA from a plutonium-induced lung tumor in rat #184-517-3 (paraffin-embedded sample stored for >6 yr); Lanes 10 and 11, DNA from the lungs of unexposed rats (samples were formalin-fixed and embedded in paraffin for ~1 month prior to DNA extraction); Lane 12, DNA from the lung of an unexposed rat, extracted immediately after sacrifice; Lane 13, OX174 DNA as a marker; Lane 14, viral Kirsten *ras* DNA.

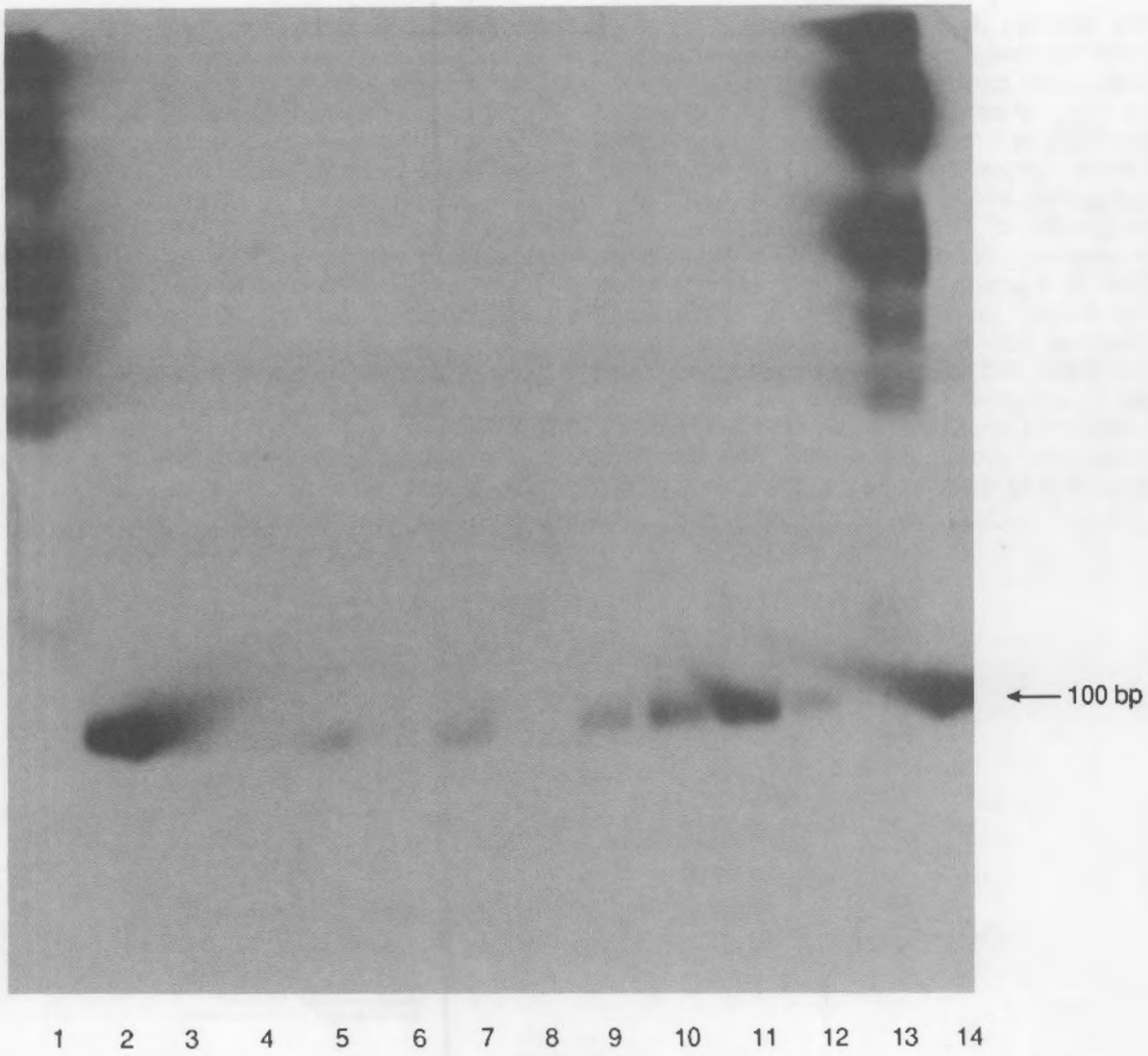

FIGURE 5. Southern Analysis of the Gel in Figure 4. Following the electrophoretic separation of the DNA on a 6% polyacrylamide gel, sample was transformed to nitrocellulose, and hybridized to a ^{32}P-labeled fragment of viral Kirsten *ras* gene. Five microliters of the polymerase-chain-reaction products were added to each lane.

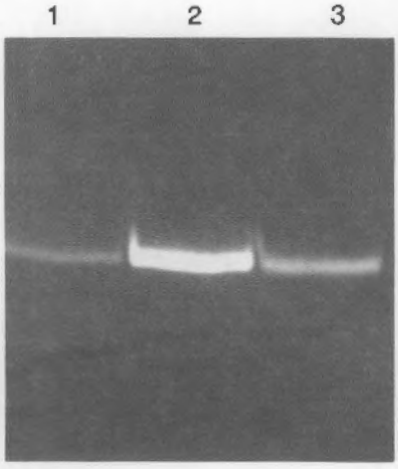

FIGURE 6. Products of Polymerase-Chain-Reaction (PCR) Experiments Were Electrophoretically Separated on a 6% Polyacrylamide Gel in Order to Purify Them for Direct DNA-Sequence Determination. Lane 1, DNA produced from approximately 10 ng of DNA which was isolated from normal rat lung which had been paraffin-embedded for >6 yr; Lane 2, DNA produced from approximately 10 ng of viral Kirsten *ras* DNA; Lane 3, DNA produced from approximately 10 ng of DNA which was obtained from a plutonium-induced rat lung tumor. The tissue had been embedded in paraffin for several years prior to extraction. Each lane contained a 90-μl sample of PCR products.

The methods described can be used for specimens from rats, mice, and humans. In order to analyze our canine tumors using these methods, we need to construct DNA probes and primers (for PCR), and compare the sequence of normal cellular genes to those of the "activated" oncogenes, and to do that, we need to know the sequences of dog cellular oncogenes (proto-oncogenes). We have generated a library of dog DNA in a phage cloning vector (lambda dash) that accepts up to 22-kbp fragments (Figure 7). Evidence from RFLP analysis by Southern blot techniques and transfection assays has implicated *ras* in tumorigenesis in plutonium-exposed dog lung tumors, and myelomonocytic leukemias; thus, these genes are our first priority. After screening about 1 x 10^6 plaques from our library by plaque hybridization techniques, we found two clones that contained *ras* sequences. Analysis of the DNA of these clones by Southern blot techniques shows that they contain *ras* sequences (Figure 8). We are now characterizing the cloned genes and will then ascertain their DNA sequence.

We have begun screening the library for the epidermal growth factor (EGF) gene. We are searching for this gene because the level of EGF is higher in tumor cells than in normal lung cells (see Leung's Annual Report this volume). We have evidence that this gene is amplified in at least one lung tumor. Once this gene is isolated, we will sequence it and prepare primers which will allow us to examine DNA from lung tumors for mutations in the EGF gene.

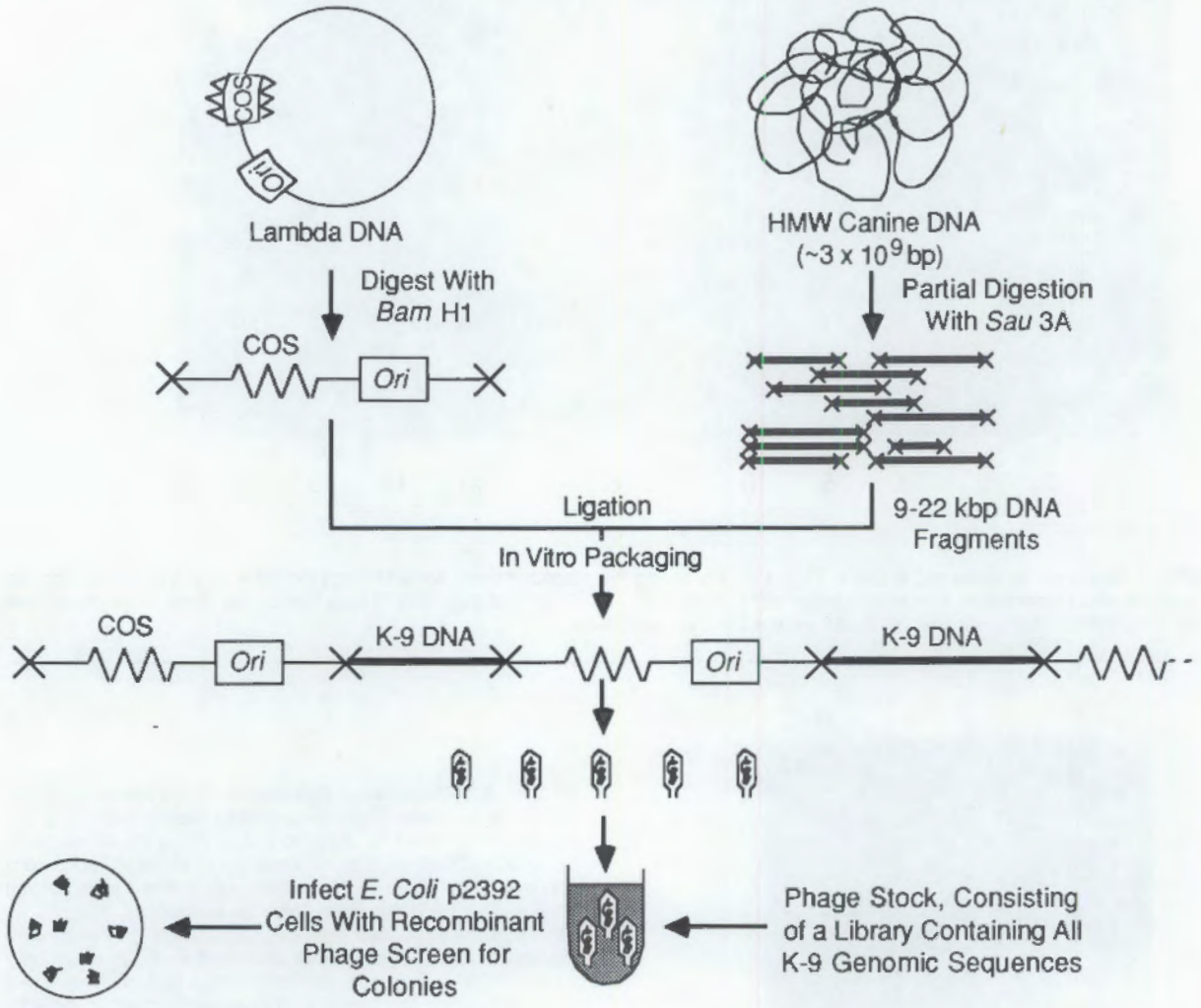

FIGURE 7. Schematic Representation of Canine DNA Fragment Library Construction. DNA from a normal dog was partially digested with the restriction enzyme *Sau* 3A, and the 9- to 22-kbp fragments which resulted were ligated into bacteriophage lambda DNA which had been digested with *Bam* HI. The resultant concatameric DNA was then packaged in individual bacteriophage particles, using a packaging mix obtained from Stratogene® (La Jolla, California).

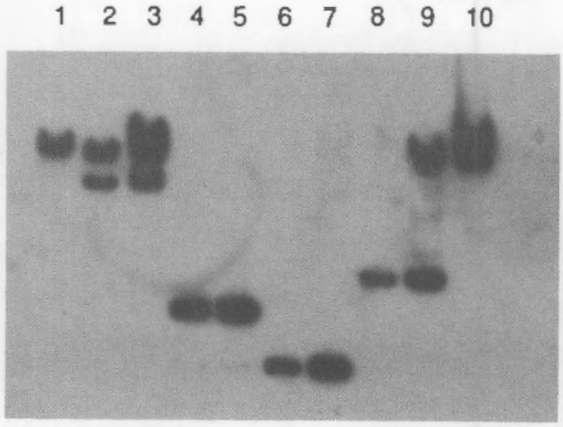

FIGURE 8. Autoradiograph of DNA from the Canine DNA Fragment Library. Two colonies were selected, and DNA from these isolates was hybridized with viral Ki-*ras*. The DNA extracted from each isolate was digested with restriction enzyme and electrophoresed on a 0.9% agarose gel. A Southern blot was prepared from the agarose gel and hybridized with the ^{32}P-labeled virus *ras* genes under conditions allowing for ~10% mismatch of sequences. Lane 1 contains uncut DNA from isolate RI; Lane 2, DNA from RI digested with *Sal* I; Lane 3, DNA from isolate RII digested with *Sal* I; Lane 4, RI digested with *Eco* RI; Lane 5, RII digested with *Eco* RI; Lane 6, RI digested with *Bam* HI; Lane 7, RII digested with *Bam* HI; Lane 8, RI digested with *Hind* III; Lane 9, RII digested with *Hind* III; Lane 10, uncut DNA from isolate RII.

Molecular Events During Tumor Initiation

Principal Investigator: D. L. Springer

Other Investigators: D. B. Mann and G. L. Stiegler

Although tumor development may involve addition of the carcinogen to DNA, the events that lead to the appearance of tumors probably involve loss of gene control at the chromatin level. For several genes it has been shown that activity or inactivity of the gene may be correlated with changes in chromatin, and it is possible that adducts may change gene expression by altering chromatin structure. Because of this, we have used simple *in vitro* systems to determine the influence of bulky adducts on chromatin structure at the nucleosome level of organization. The pXP-14 plasmid which contains the 5S rRNA gene and SP-6 promoter was adducted with anti-benzo[a]pyrene diolepoxide to give an average of 1 adduct per 500 bp. Digestion of the plasmid with restriction enzymes resulted in double-stranded DNA fragments that contained the 5S rRNA gene and SP-6 promoter regions. Adduct location on the gene and promoter fragments will be determined after ^{32}P-5′ end-labeling of the transcribed and nontranscribed strands, followed by incubation with T4 polymerase, which will digest the DNA in a 3′-5′ direction until a bulky adduct is reached. Results from this work will contribute to our understanding of the influence of bulky adducts on nucleosome positioning.

Previously, we demonstrated that the carcinogenic activity of benzo[a]pyrene (BaP) was inhibited by complex organic mixtures containing aromatic compounds and that binding of BaP to mouse-skin DNA in the presence of the mixtures was decreased to a greater extent than was predicted from the tumor initiation data. Since these data suggest that tumor initiation cannot be fully explained on the basis of BaP-DNA binding alone, it is possible that the mixtures influenced chromatin structure in a manner that enhanced the cancer process. In addition, the molecular changes associated with bulky adduct initiation of tumor development have not been extended over time to identify changes that involve loss of gene and cellular control associated with promulgation of initiated cells to tumors. For several genes it has been shown that activity or inactivity of the gene may be correlated with changes in chromatin, and it is possible that adducts may change gene expression by altering chromatin structure. For example, Chen (*Biochemistry* 24:6219-6227, 1985) demonstrated that anti-benzo[a]pyrene-diolepoxide (BPDE) adducts stabilized the DNA structure in the B-conformation in areas proximal to the adducts and destabilized distal base pairs so that the B to Z transition was more favorable. These adduct-induced changes in chromatin structure may be important because the Z-DNA conformation has been associated with actively transcribed genes.

Other studies have shown that the affinity of DNA for adducted core histones is less than that for the native states. These results suggest that it may be possible that an epigenetic mechanism plays a role in the progression from adduction to the appearance of tumors. This is supported by the fact that approximately one-half of the material adducted to chromatin is to the histones. Since core histones turn over at very low rates relative to other proteins, studies to identify these kinds of changes may help explain how histone adducts influence gene expression and, ultimately, progression of the cancer process.

Because of the need to identify the regulatory processes involved in tumor development, we are conducting studies to determine the influence of BPDE adducts with respect to nucleosome positioning and other structural changes in chromatin. For this we have chosen the 5S rRNA gene as our model system because the gene has been cloned into a plasmid and is readily available, as is sequence information. In addition, it has been shown that incubation of the gene with core histone particles isolated from chick erythrocytes resulted in the formation of a single nucleosome. The position of this nucleosome is known with respect to the DNA sequence, and the positioning is fixed with respect to location along the 5S rRNA gene. The model therefore allows manipulation of bulky adducts and lends itself to experimental designs that address questions on the influence of bulky adducts on nucleosome positioning.

For this work we obtained a sample of the pXP-14 plasmid (Wolffe et al. *Cell 50*:381-389, 1986) from Dr. Donald Brown at the Carnegie Institute. This

plasmid contained the *Xenopus borealis* 5S rRNA gene and the SP-6 promoter. A map of the pXP-14 plasmid, along with the restriction sites used for preparation of the 5S rRNA gene and SP-6 promoter region, are shown in Figure 1. The plasmid was grown in *Escherichia coli* strain JM83 in LB media containing ampicillin. Combined samples from 2.0-L incubations resulted in isolation of approximately 4 mg of purified plasmid DNA.

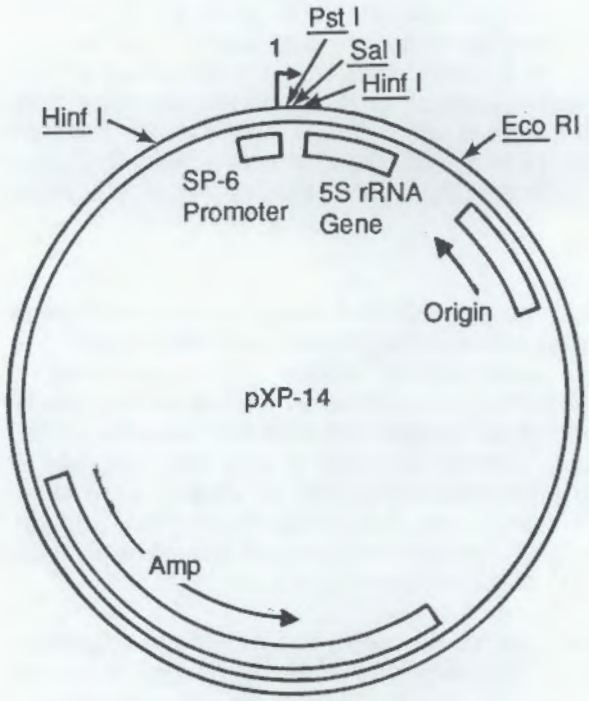

FIGURE 1. Diagram of pXP-14 Plasmid, Showing Location of the 5S rRNA Gene, Promoter Region, and Restriction Endonuclease Cut Sites.

When this plasmid was incubated with radiolabeled (±) r-7,t-8-dihydroxy-t-9,10-epoxy-7,8,9,10-tetrahydrobenzo[a]pyrene (anti-BPDE), we found that binding was linear with dose from 5 to 125 μM BPDE (Table 1). The highest BPDE concentration resulted in an average of 1 adduct per 500 bp (6 to 7 adducts per plasmid molecule). The plasmid was digested with the restriction enzyme *Hinf* I, which was expected to produce eight DNA fragments. Agarose gel electrophoresis of the restriction digestate confirmed the presence of several fragments with lengths of 65 to 1199 bp. Radioactivity measurements indicated that the adduction levels were approximately equal when they were calculated as picocuries per base pair. These data suggest that the adduction was random. Future studies will be designed to identify the location and adduction levels within the 5S rRNA gene and promoter regions, using the methods described below.

TABLE 1. Amount of Adduction Determined After Incubation of pXP-14 Plasmid with ^{3}H-Benzo[a]pyrene Diol Epoxide (BPDE).

μM BPDE	pmoles/mg DNA	Adducts/ Plasmid Molecule
5	108	0.2
25	586	1.2
125	3186	6.5

In preparation for BPDE adduct location studies within the SP-6 and 5S rRNA fragments, the adducted plasmid was treated as follows: Four equal samples of the adducted plasmid were prepared and treated with a number of digestion and processing steps which resulted in isolation of labeled transcribed and nontranscribed strands of the SP-6 and 5S rRNA fragments. Each sample was treated by the following procedure, using the appropriate restriction enzymes. For the first step, the plasmid was digested with *Hinf* I, which cleaves the plasmid as described above. The 176-bp fragment (Figure 2), which contained the SP-6 promoter, was purified by agarose gel electrophoresis. It was then removed from the agarose, and the 5′-end dephosphorylated, using alkaline phosphatase. The double-stranded DNA was 5′-^{32}P-end-labeled, using γ^{32}P ATP and T4 polynucleotide kinase. The DNA was treated with the restriction enzyme *Pst* I, which produces a double-strand cleavage near the 5′ end of the transcribed strand, leaving a 5′-end label only on the nontranscribed strand of the fragment containing the SP-6 promoter. Similar procedures resulted in 5′-^{32}P-end-labeling of the transcribed fragment containing the promoter region and of each strand of the 5S rRNA gene.

Currently, we are implementing methods to determine the location of BPDE adducts on the fragments described above. For this, we are using the T4 polymerase assay, which has 3′-5′ exonuclease activity and digests the DNA until it reaches a base with an attached bulky adduct. This method has the advantage of digesting nonadducted DNA fragments to nucleotides and very short 5′-end fragments. This limits the preparation to fragments with attached adducts, thereby enhancing electrophoretic analysis by eliminating interfering unadducted DNA. These preparations will be run on a polyacrylamide

sequencing gel together with a Maxam-Gilbert sequence of the fragment to give the location of the bulky adducts along the four strands of the SP-6 promoter and 5S rRNA gene fragments. Using this approach we will locate adduction sites on the 5S rRNA gene and the promoter region. (This work is being conducted in collaboration with Dr. Michael Smerdon at Washington State University.) Once adduction sites and frequencies of adduction are determined, we will be able to determine the influence of bulky adducts on nucleosome positioning.

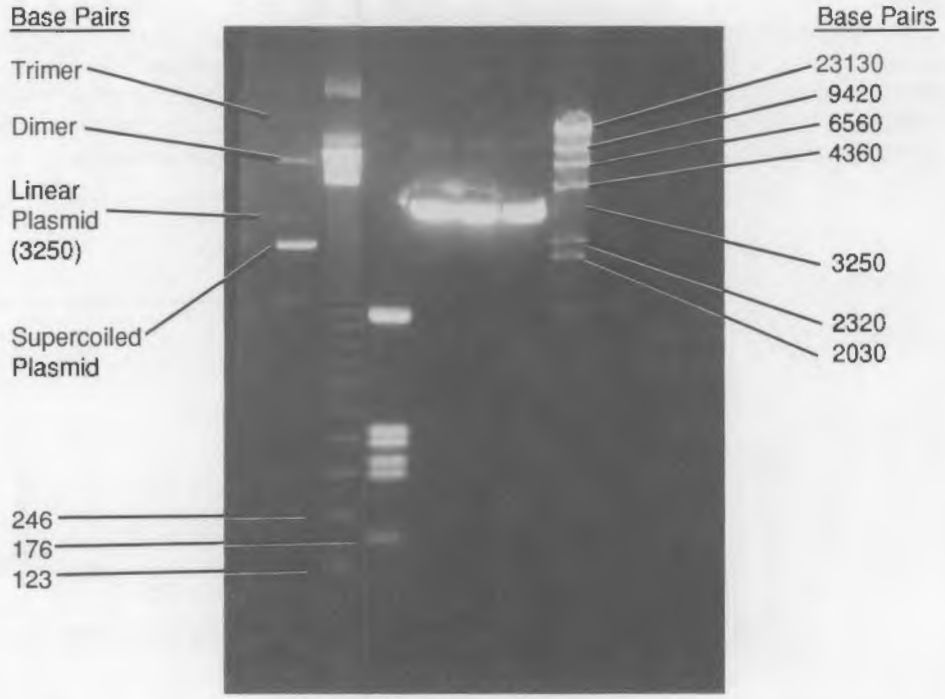

Restriction endonuclease digestion of pXP-14 plasmid and comparison to molecular weight standards.
Lane 1, uncut supercoiled plasmid, along with dimers and linked polymers of the plasmid.
Lane 2, a molecular weight marker, consisting of DNA fragments 123 bp in length (and multiples thereof).
Lane 3, a Hinf I digest of the pXP-14 plasmid. The 176-bp fragment contains SP-6 promoter and will be isolated for mapping the BPDE adduct locations in the nontranscribed strand.
Lane 4, a Sal I digest of the pXP-14 plasmid. The principal band in this lane is plasmid linearized by a single cut. This band will be isolated, ^{32}p-end-labeled, and cut a second time with Hinf I to isolate the transcribed strand of the SP-6 promoter.
Lane 5, a Sal I digest of the pXP-14 plasmid. This band, after end-labeling, will be cut with Eco RI to isolate the nontranscribed strand of the 5S rRNA gene.
Lane 6, a Eco RI digest of the pXP-14 plasmid. This band, after end-labeling, will be cut with Pst I to isolate the transcribed strand of the 5S rRNA gene.
Lane 7, a Hind III digest of lamda phage DNA, a molecular weight marker.

FIGURE 2. Agarose Gel, Showing Restriction Digests of the pXP-14 Plasmid Together with Molecular Weight Standards.

Current solvent extraction methods for isolation and purification of DNA are very time-consuming and expensive. Because of this we have been developing high-performance liquid chromatography (HPLC) procedures to purify DNA from cellular debris and radiolabeled metabolites produced during the adduction reactions. For this we are using a Waters model 600E HPLC equipped with a diode array ultraviolet (UV)/visible detector and controlled by an NEC computer with a 40-megabyte hard disk. The sample was applied to a Nucleogen-DEAE-4000-10 column equilibrated with a 20-mM potassium phosphate buffer (pH 6.8) containing 6 M urea (buffer A). The DNA

was separated from proteins and RNA by increasing the concentration of buffer B from 0 to 100% (buffer B consisted of buffer A with the addition 2 M KCl). This procedure resulted in highly purified pXP-14 DNA ($A_{260:280}$ ratios of 1.8-1.9) that eluted with a retention time of 34 min (Figure 3a). Agarose gel electrophoresis of the same sample indicated that the fragment was approximately 3250 bp in length. The HPLC separation of ^{3}H-BPDE-adducted plasmid DNA resulted in co-elution of radioactivity and DNA, demonstrating that the adduct was covalently bound to the DNA (Figure 3b). These results were confirmed by agarose gel electrophoresis. In another study, the *Hinf*-I-digested plasmid sample was separated by HPLC, and UV absorbance at 254 nm indicated that at least six fragments were obtained (Figure 4). Agarose gel electrophoresis of the sample confirmed that they were the six largest fragments of the *Hinf* I digest.

Upon completion of this phase of the proposed work we will have: (1) determined the location of BPDE adducts to the 5S rRNA gene and the SP-6 promoter, (2) determined whether these adducts influence the positioning of nucleosomes, and (3) contributed to understanding of the influence on bulky adducts gene structure.

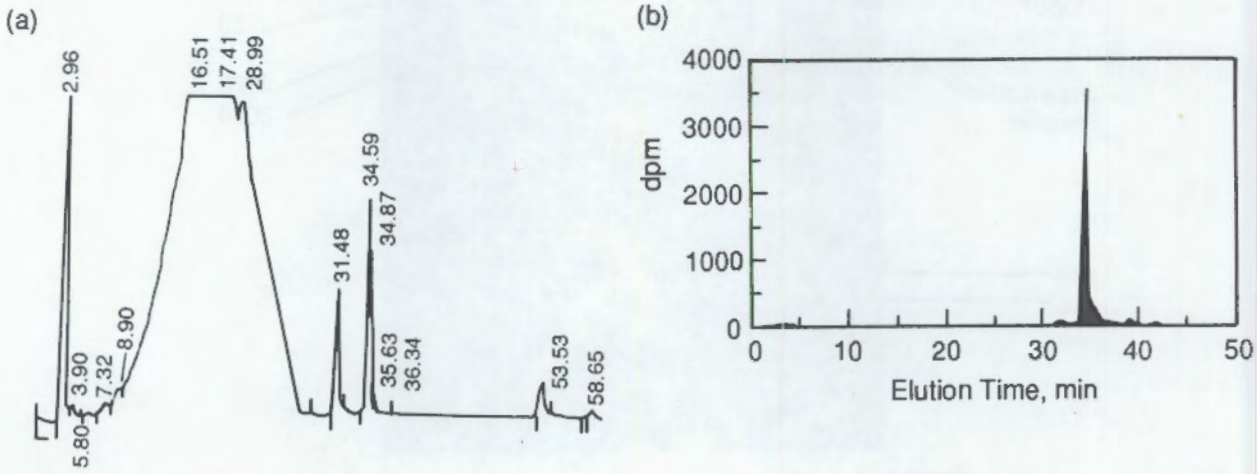

FIGURE 3. High-Performance Liquid Chromatography Separation of pXP-14 Plasmid: (a), Crude Preparation, Containing Plasmid and Other Cellular Components, Was Separated as Described Above. Results indicated separation of plasmid (retention time, 34.7 min) from RNA and proteins; (b), radiochromatogram for ^{3}H-benzo[a]pyrene diol epoxide-adducted plasmid, confirming that adduction was to the plasmid.

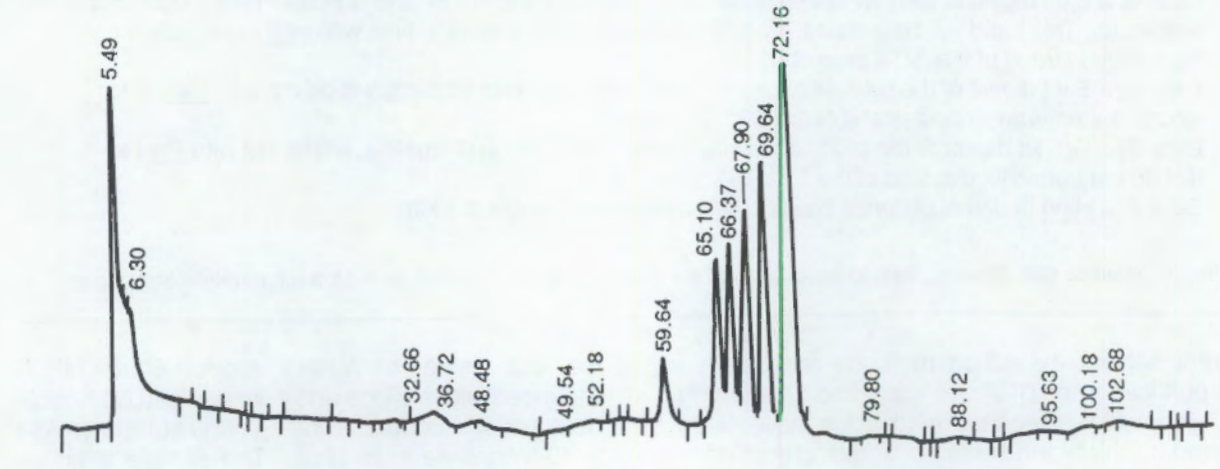

FIGURE 4. High-Performance Liquid Chromatography Chromatogram of Restriction Digest of Plasmid pXP-14 with *Hinf* I.

Aerosol Technology Development

Principal Investigators: W. C. Cannon and O. R. Moss

Other Investigators: J. K. Briant, J. R. Decker, B. J. Greenspan, C. L. Leach, and L. G. Smith

We have developed methods and apparatus for using aerosols to study the biological effects of energy-related pollutants in animals. We report here the advances we have made this year in electric field nebulization, technology transfer of the nose-only exposure system, production of lung and nose casts for use in dose-estimation experiments, and in the application of optical traps to particle and cell research.

Electric Field Nebulization Research

The aerosol tetrode, a device for generating liquid droplet aerosols by electric field nebulization (EFN), was redesigned. The device has four charged electrodes, a positively charged capillary which emits charged droplets, a negative corona source, and two grids. These grids create a region of low potential gradient, or a drift zone, to allow the positively charged droplets to interact with the negative ions from the corona and become neutralized. In the original tetrode the electrodes were inserted through the wall of a spherical glass flask by means of side arms or slots, making it difficult to subsequently alter the configuration or spacing of the electrodes.

Recognizing that it is important to control inter-electrode spacing as well as electrode potentials, we made a new design in which we can more easily adjust the spacing of electrodes and also install different kinds of electrodes. The electrodes are held in plastic brackets, which clamp to two vertical plastic rods (Figure 1). The apparatus rests on feet attached to the plastic base, allowing electrical leads to pass upward through the base to the electrodes. Because of the high voltages applied to the electrodes, these brackets and rods must act as electrical insulators.

Since many of the liquid droplet aerosols produced by the generator are flammable, the apparatus is operated in a fume hood to avoid fire or explosion hazards. So that air currents in the hood do not disrupt aerosol measurements, a glass enclosure, which resembles a bell jar and can easily be removed to make adjustments, covers the apparatus. Aerosol sampling is accomplished through two ports in the wall of the glass enclosure.

For special experiments to study the effects of electric field strength, capillary size, and material properties on particle size, the grids and corona source will be removed, and a special electrode for collecting particles directly on a scanning electron microscope (SEM) post will be installed (see Figure 2). The entire collection electrode will be operated at ground potential. A hole in the collector shutter will momentarily rotate to a position above the post to collect a short burst of particles for examination in the SEM. A series of such samples, taken under varying conditions, will be studied to determine the optimal conditions to achieve the desired particle size.

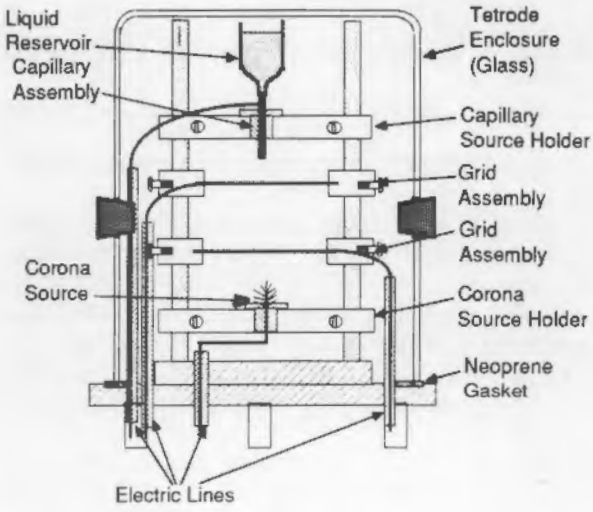

FIGURE 1. Aerosol Tetrode Mark II.

Nose-Only Exposure System Technology Transfer

Arrangements were initiated with Lab Products, Inc. (a bioMedic company) for the license and commercializing of a nose-only-inhalation exposure system for small animals developed as part of this project. This exposure system is superior to systems commercially available. Major advantages are its highly uniform nose-only aerosol

exposures and the flexibility it affords in blocking off unused ports so that aerosol is delivered only to animal-occupied ports. This allows accurate and efficient nose-only exposures of from 1 to 48 animals. We have received requests for access to this technology from laboratories in Europe and the United States. Commercialization will make the system readily available for inhalation toxicology research.

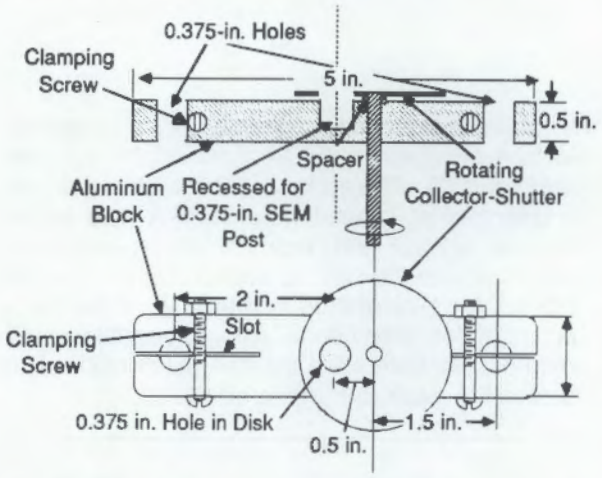

FIGURE 2. Scanning Electron Microscope (SEM) Particle Collector.

Dose Estimation from Lung and Nasal Casts

Solid casts of rat and quail respiratory systems were prepared for future studies to estimate aerosol deposition and dosimetry for inhalation research. Both lung and nasal cavity casts were prepared by infusion with Dow Corning 734 RTV diluted 2:5 (v/v) with toluene under positive pressure, followed by tissue digestion in 1N NaOH.

Details of rat lungs and nasal sinuses obtained with this procedure were good. Some fairly good casts were obtained of the avian respiratory system, although air sacs tended to fill unevenly when RTV was used. Liquid gelatin, beeswax, and egg whites were also tried. Liquid gelatin was used with gravity flow, followed by dissection of the refrigerated bird for anatomical studies of the avian respiratory tract. Pure beeswax was too fragile, and less-friable beeswax (diluted with tricaprylin) did not provide sufficient detail. In a series of experiments we used egg whites for making lung casts of small birds. Egg whites readily filled the sacs and lung cavities of the birds and solidified following 15 to 20 seconds of microwave cooking. Portions of air sacs could be separated from surrounding tissue following serial slicing.

Optical Trap Development

A prototype three-dimensional optical trap system attached to a standard light microscope was evaluated for trapping particles and 3T3 mouse fibroblast cells. We found that particles and cells floating in a hanging-drop preparation in the microscope's field of view could be trapped in the focal zone of the laser and thereafter moved at will by the operator. Previously, the laser beam often pushed the cell out of the field of view instead of holding and trapping it. However, by defocussing the microscope 5 μm above or below the cell or particle being trapped, a successful three-dimensional capture could be completed at least 80% of the time. At the lowest laser power where trapping was possible, there was no visible cell swelling in the 30 to 60 seconds of observation. By increasing the laser power, cells swelled up to 27 times their initial volume over a 30-second period. These observations open the possibility for injection of fluid into cells under controlled swelling conditions, a technique that may be useful in molecular biology research for control and modification of cultured cell lines.

Fetal and Juvenile Radiotoxicity

Principal Investigator: M. R. Sikov

Other Investigators: R. L. Buschbom, G. E. Dagle, D. R. Kalkwarf, T. J. Mast, D. D. Mahlum, H. K. Meznarich, and D. N. Rommereim

Technical Assistance: J. P. Bramson

This project obtains comparative information on the disposition, dosimetry, and toxicity of several radionuclides during the perinatal stages of life relative to that in more mature mammals. Emphasis is directed at investigating mechanisms, establishing patterns, and identifying phenomenologic interactions for developing meaningful radiological protection practices for rapidly growing infants and children and for pregnant women. Tritiated thymidine autoradiographs from suckling rats were studied to further our understanding of neonatal thyroid development and elevated perinatal sensitivity to radiogenic thyroid neoplasms. A study involving inhalation of ^{85}Kr by pregnant sheep showed that blood concentrations rapidly reached a steady state, and there were marked similarities between kinetics in fetal and maternal compartments. These data were used to predict the dosimetry and potential for embryofetal toxicity of radon during inhalation exposures. These predictions were tested by an experiment which detected neither embryofetal toxicity nor teratogenicity after 13-day exposures of rats to radon. Further efforts to understand the patterns of placental transfer and fetoplacental distribution of heavy metals showed a consistent association between the amount transferred to the fetus and deposited in placental structures. These are, perhaps, related to the chemical and biological factors that lead to enhanced binding by transferrin or a related transport protein.

Thyroid Proliferation

We speculated that susceptibility to radiogenic thyroid neoplasia in the perinatal period, which was elevated compared to that of adults, might be associated with amplification of induced changes by a higher proliferation rate. This led us to extend our study of thyroid development to include measurements of cell proliferation. Rats of several ages between birth and weaning were injected with tritiated thymidine and killed at sequential times. Autoradiographs of thyroid glands were prepared and evaluated.

The peak of follicular cell proliferation, as indicated by percent of labeled cells, occurred during the middle of the second postnatal week. This increase was primarily related to increased numbers of follicles containing proliferating cells, indicated as labeled follicles (Figure 1). The fraction of cells in labeled follicles, however, remained relatively constant and was greater in areas between follicles than in the follicles themselves. This was indicated by a ratio which remained unity until a rapid rise at about 17 days of age (Figure 2). The size of this population relative to the number of cells constituting follicles, and the fraction of cells that were labeled, also declined toward weaning. The identity of the cells incorporating thymidine could not be established definitively, but several lines of evidence indicated that only a small fraction (< 10 %) were perifollicular or C-cells.

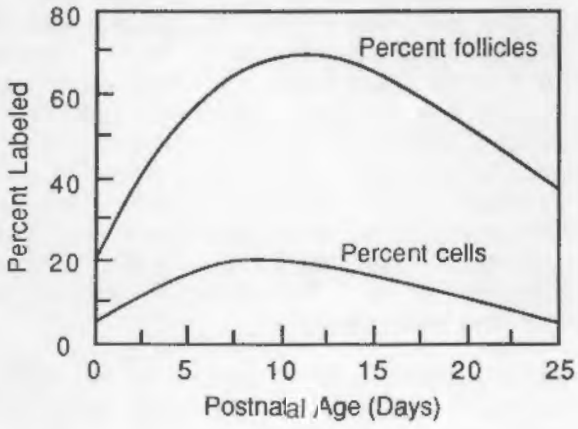

FIGURE 1. Percent of Follicles and of Follicular Cells that Display Labeling in Autoradiographs of Thyroid Glands After Tritiated Thymidine Injection in Suckling Rats.

These histologic observations, which are consistent with reports in the literature, provide further evidence that the interfollicular cell is progressively organized into definitive follicles, most likely through the secretion of thyroid-hormone-containing colloid into central volumes, which

become the lumina as they fill. These findings contribute to our understanding of thyroid development, although they provide only partial explanations for the age-related differences in sensitivity to radiogenic thyroid tumors on the basis of cell proliferation.

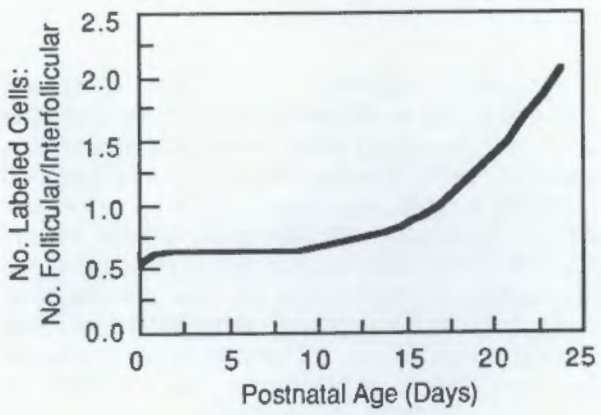

FIGURE 2. Age Dependence of the Ratio of Numbers of Labeled Follicular to Intrafollicular Cells in Autoradiographs of Thyroid Glands After Tritiated Thymidine Injection in Rats During the Suckling Period.

Gestational Exposures to Krypton

We previously performed studies to evaluate placental transfer and fetoplacental distribution of radiokrypton (^{85}Kr) in sheep and rats and embryofetal toxicity in the latter species (Annual Reports, 1977, 1978). Recent concerns about radon exposure of pregnant women and their fetuses led us to begin a series of calculations to estimate fetal dose from inhaled radon that used the ^{85}Kr data as a starting point, because both are noble gases with potentially similar biological behaviors. Data on blood concentrations from the sheep experiments were used for additional calculations, including kinetic analyses.

As described previously (Annual Report, 1977), pregnant ewes were obtained during mid- to late gestation, and indwelling catheters were inserted in an artery and a vein of each of 14 pregnant ewes and in an artery or vein of their fetuses. After a 1- to 2-day recuperation period, ewes were exposed, via a face mask, to an atmosphere of ^{85}Kr in air (1850 Bq/ml) for 1 1/2 to 2 hours. Periodic blood samples were collected from each cannula during the accumulation, equilibration, and postexposure clearance periods and were assayed by liquid scintillation counting. One or 2 days later, most ewes were again exposed again in the same manner but were euthanized after steady-state conditions were reached. Tissues from the ewes, fetuses, and placentas were removed, weighed, and assayed by liquid-scintillation counting, as reported previously (Annual Report, 1977).

Adequate numbers of samples for calculation and comparisons with blood samples collected from maternal catheters were obtained from patent fetal arterial catheters in four preparations at about 120 days of gestation and from fetal venous catheters in three animals at 90 days. Statistical comparisons were based on direct comparisons of rates, derived from the slope data from contemporaneous measurements from all catheters in individual animals, as contrasted with the incomplete mean blood concentrations reported previously. In general agreement with the previous conclusions, the rate of appearance of ^{85}Kr in blood was rapid during exposure and, as indicated by the K_a values shown in Figure 3, pairwise comparisons detected no difference between values in the maternal arteries and veins, but they were significantly higher than in either of the fetal vessels.

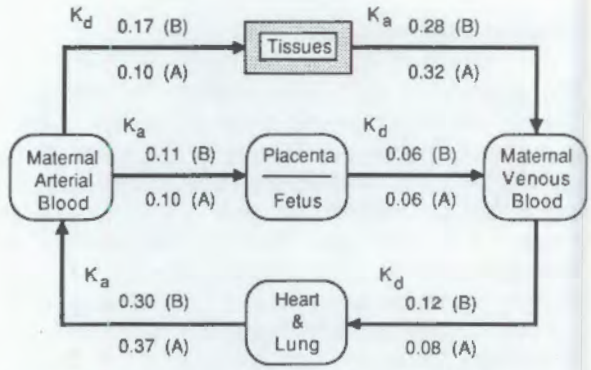

FIGURE 3. Calculated Values for Rate Constants (Fraction/Min) of ^{85}Kr Entry into (K_a) and Disappearance from (K) Various Blood Compartments of Pregnant Ewes and Their Fetuses at About 90 (A) and 120 (B) Days of Gestation.

During the steady-state period, the mean concentration in maternal venous blood was significantly higher than in maternal arterial blood. This is consistent with the observation that the venous concentrations tended to increase with time. It is explained by the fact that they are the net differences between the rate of entry into venous blood from tissue (rate constant, k_a = 0.28), which was higher than the rate constant (K = 0.12) for disappearance from venous blood via expiration from the lung. There was no significant difference between values for maternal arterial blood and fetal blood from either site, indicating that fetal

blood had reached equilibrium with the maternal. After cessation of exposure, ^{85}Kr disappeared rapidly from maternal arterial blood; half-times were roughly similar: 10 and 5 min in ewes at 90 and 120 dg, respectively. There were no significant differences between the K values for artery and vein. The K values for both fetal vessels were significantly less than for the maternal arteries, but there were no apparent differences between the two gestational ages.

Teratologic Studies with Radon

There are few data concerning placental transfer, fetoplacental distribution, or prenatal effects of inhaled radon. We therefore used the foregoing kinetic data and previously reported results on maternal and fetoplacental tissue concentrations in sheep (Annual Report, 1978) and rats (Sikov et al., *Health Phys. 47*:417-427, 1984) with krypton to begin a series of calculations for radon.

As first-order approximations, we made the following assumptions: the biological behaviors of radon and krypton were similar; radon freely crosses the placenta in both directions during continuous exposure; and radon itself—rather than its daughters—provides the primary contribution to dose. In the absence of measured values, the partition coefficients of radon and krypton in tissues were considered to be the same. Our calculations suggested that the average tissue concentrations in the fetoplacental unit from radon exposure concentrations of 130 working level months (WLM)[a] per day (~350 nCi/L) would approximate those in soft tissues (other than fat) of the dam. It was estimated that these exposures would result in radiation absorbed doses throughout the fetoplacental unit of about 0.25 cGy/day, an amount that was not expected to produce developmental toxicity.

To test this hypothesis, an experiment was initiated using the system employed at PNL for prolonged inhalation exposures of rats. Beginning at 6 dg, a group of 42 pregnant rats was exposed for 18 hours/day, for 13 days, to 124 WLM/day of radon, with daughters, adsorbed onto ore dust. As controls, a group of 26 pregnant rats from the same shipment were exposed to a filtered-air atmosphere in identical chambers and conditions. For the portion of the experiment in which effects were evaluated, the rats were removed from the chambers and killed at 20 dg. Fetuses were examined for the presence of toxic effects, using the standard teratologic protocols employed at PNL. Two rats removed from the radon chambers on the last day of exposure provided samples for radioanalysis to obtain distribution and dosimetry.

Further analyses and calculations are required to complete our results, but tentative conclusions can be derived from the limited measurements now available. In our previous experiments with krypton in rats, the concentrations were the same in the fetus and the placenta. In contrast to these results, the average fetoplacental concentrations of radon on the last day of exposure (20 dg) were not homogeneous. It appears that the placenta received about 0.1 cGy and the fetus 0.03 cGy during that day; these doses were less than those received by soft tissues of their dams and less than expected from our previous calculations. As shown by the synoptic data in Table 1, it is clear that these exposures produced neither developmental nor reproductive toxicity and were not teratogenic.

TABLE 1. Comparison of Representative Measures of Reproductive and Developmental Integrity in Rats Exposed to Filtered Air or Radon Atmospheres During the Period from 6 Through 20 Days of Gestation.

	Filtered Air	Radon
Percent Pregnant	89.7	92.9
Extragestational Weight Gain, g	41.6 ± 12.3	31.0 ± 11.8
Number Implants/Dam	14.2 ± 2.2	14.6 ± 3.2
Percent Resorptions/Litter	2.8 ± 4.3	4.2 ± 6.6
Fetal Weight, g	3.3 ± 0.23	3.3 ± 0.24
Percent Fetuses with Malformations	0.6	0
Percent Litters with Malformed Fetuses	7.7	0
Percent Fetuses with Variations or Reduced Ossification	13.4	22.0
Percent Litters with Variations or Reduced Ossification	61.5	89.7

Patterns and Mechanisms in Placental Transfer

In last year's annual report, we illustrated the patterns and operational models that had evolved from our comparisons of placental transfer and fetoplacental distribution of the heavy metals, as developed from data of our studies and those of

(a) Working level (WL) is defined as any combination of the short-lived radon daughters in 1 liter of air that will result in the ultimate emission of 1.3×10^5 MeV of potential α-energy. Working level month (WLM) is an exposure equivalent to 170 hr at a 1-WL concentration.

others. Comparisons with the chemical and physical characteristics of these materials indicated consistent associations between the patterns of transfer to the fetus, deposition in placental structures, and a variety of chemical and physical characteristics of the elements (Figure 4). These trends were primarily reflections of the radionuclide's position in the periodic table, however our tentative inference is that these results may derive from factors that lead to enhanced binding by transferrin or a related transport protein, thus providing a hypothesis for experimental testing.

These efforts also provide a basis from which to make further interpretations and extrapolations from current knowledge, to identify empirical measurements that are required, and to design definitive experiments that can test the mechanistic hypotheses that evolve.

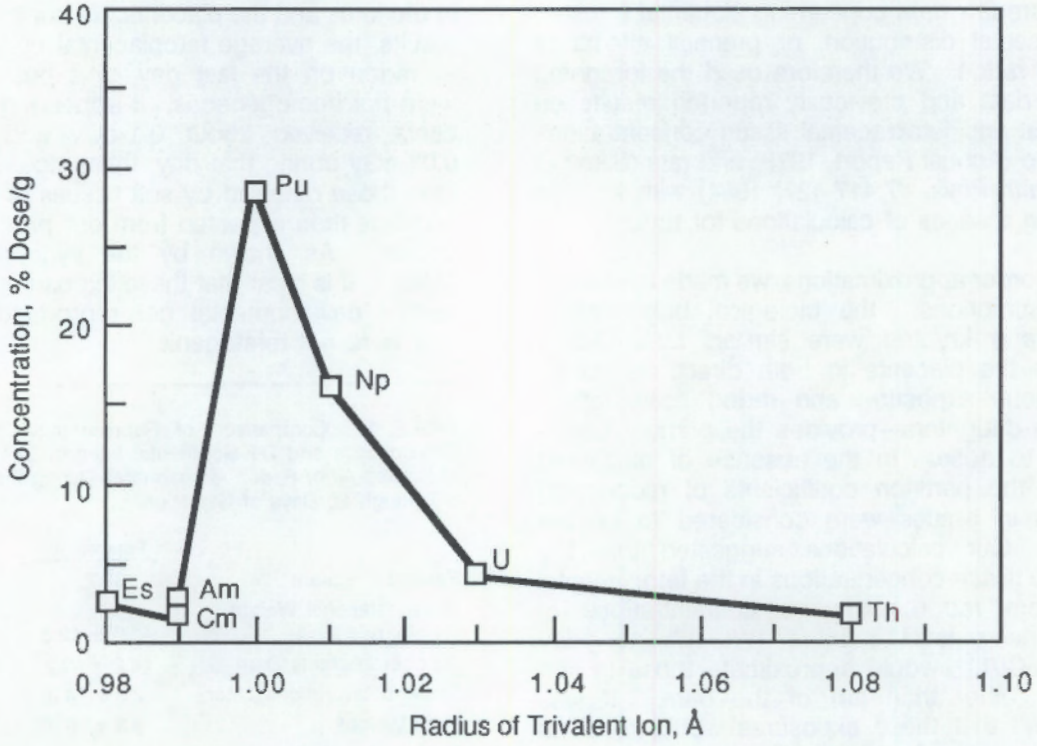

FIGURE 4. Fetal Concentration of Heavy Elements at 1 Day After Intravenous Injection in Rats at 15 Days of Gestation Relative to Their Trivalent Radii.

Molecular Markers During Development

Principal Investigator: D. L. Springer

Other Investigators: M. G. Horstman and R. C. Zangar

For this new project we have conducted multilevel studies to identify changes in cytochrome-P450-dependent reactions associated with neonatal exposures to several pharmacologically active agents and a model polycyclic aromatic hydrocarbon (PAH). The specific purpose of the project is to determine whether agents that alter cytochrome P450 expression change the animal's susceptibility to tumor development, as indicated by DNA adduct concentrations, and whether exposure to a PAH causes altered imprinting for this enzyme system. Animals were treated neonatally with potential imprinting agents and evaluated as adults, using enzyme activity measurements, DNA adduct concentrations, and the status (growth and survival) of the intact animal. Subsequent studies will employ oligonucleotide probes that are highly specific for the cytochrome P450 gene products and will use antibodies and enzyme activity measurements to identify the isozymes involved. Initial results indicate that neonatal exposure to diethylstilbestrol, a known imprinting agent, increased hepatic cytochrome P450 concentration for female rats and decreased the binding of aflatoxin B1 to hepatic DNA for males.

The presence of stimuli such as hormones during normal development determines the capability of the organism to express and regulate certain genes later in life. These processes, known as imprinting, occur during certain sensitive periods of development. Prenatal or neonatal contact with chemicals or radiation may cause altered imprinting, which results in shifts in biochemical pathways. While these shifts may be lethal, in less severe cases they may be manifested as physiological imbalances and may alter the animal's susceptibility to disease. For example, it is well-known that a portion of female offspring from women given the synthetic steroid diethylstilbestrol (DES) have developed cervical adenocarcinoma. Although the mechanism for this effect has not been fully identified, data indicate that DES exposure disturbs the normal imprinting process and has resulted in hormonal and other imbalances which may have contributed to tumor development.

Several recent reports point to the involvement of the cytochrome-P450-catalyzed monooxygenase system in altered imprinting. For example, Lamartiniere and Pardo (*J. Biochem. Toxicol.* 3:87-103, 1988) reported that neonatal exposure of rats to DES resulted in altered hepatic activation and detoxification enzyme activities, including UDP-glucuronyltransferase, epoxide hydrolase, and glutathione transferase. Several other changes in cytochrome-P450-catalyzed activities were observed when DES animals were challenged as adults with phenobarbital. Bagley and Hayes (*Biochem. Pharmacol. 34*:1007-1014, 1985) reported that neonatal exposure to phenobarbital resulted in significant elevation of total cytochrome P450, increased activities of cytochrome P450 reductase, cytochrome c reductase, ethoxycoumarin-O-deethylase, testosterone glucuronidase and glucuronosyl transferase; the magnitude of these increases ranged from 27 to 94%. In addition, when these animals were challenged with aflatoxin B1, a known hepatic carcinogen, the amount of this compound that was covalently bound to hepatic DNA increased by 1.5- to 2.3-fold over that in corresponding controls. These results were consistent with those of Faris and Campbell (*Cancer Res. 43*:2576-2583, 1983).

These observations indicate that endogenous P450-dependent enzymes are altered by xenobiotics administered during development and that these changes may play an important role in susceptibility to cancer. Altered cytochrome P450 levels may have other important consequences, since certain cytochrome-P450-dependent enzymes catalyze reactions in the biosynthesis and metabolism of steroids. In fact, several rate-limiting or key regulatory steps in these pathways are occupied by specific P450 isozymes. Thus, altered imprinting could change the isozyme patterns as well as the total levels of P450-dependent monooxygenase activities. Since these key issues have not been addressed experimentally, we have initiated studies to determine the relationships between altered imprinting, P450-dependent enzyme activities and steroid biosynthesis and metabolism.

We injected both male and female neonatal rats with three potential imprinting agents (DES; pregnenolone-16a-carbonitrile, PCN; and 7,12-dimethylbenz[a]anthracene, DMBA, dissolved in sesame seed oil) on days 1, 3 and 5 of age; control animals received sesame seed oil. Other animals were injected with phenobarbital, another potential imprinting agent that is water-soluble (PB; dissolved in 0.9% NaCl); controls received saline only. Approximately 10 animals of each sex, randomly selected at approximately 23 weeks of age, were sacrificed, and hepatic microsomes were prepared. Other randomly selected males from each treatment group (23 weeks of age) were administered radiolabeled aflatoxin B1. Hepatic DNA was isolated, and the amount of aflatoxin bound to DNA was determined.

Microsome samples were evaluated for changes in certain cytochrome-P450-catalyzed activities and related end points. Results indicate that total cytochrome P450 concentrations for males from all treatment groups were not significantly different from controls (Figure 1). For DES-treated females, total cytochrome P450 was increased by 21%. In addition, binding of aflatoxin B1 to hepatic DNA for males treated neonatally with DES was decreased by 30% relative to corresponding controls (Figure 2). Exposure to the other test materials did not result in significant changes in aflatoxin binding.

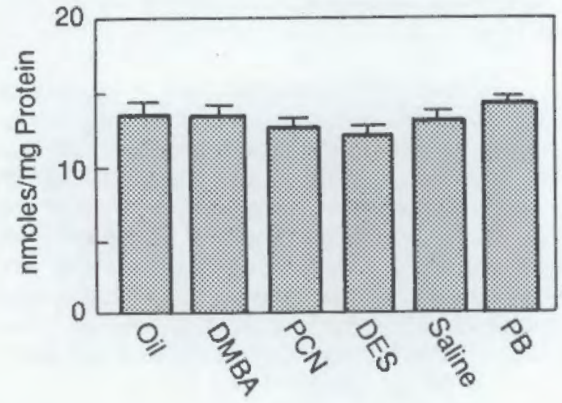

FIGURE 1. Hepatic Cytochrome P450 Concentrations for Male Rats Treated with Potential Imprinting Agents. (Mean ± SEM). DMBA = dimethylbenz[a]anthracene; PCN = pregnenolone-16a-carbonitrile; DES = diethylstilbestrol; PB = phenobarbital.

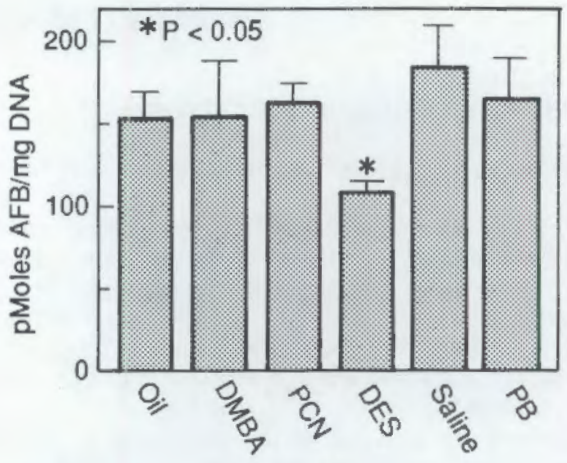

FIGURE 2. *In Vivo* Binding of Aflatoxin B1 to Hepatic DNA in Male Rats Treated with Potential Imprinting Agents (Mean ± SEM). DMBA = dimethylbenz[a]anthracene; PCN = pregnenolone-16a-carbonitrile; DES = diethylstilbestrol; PB = phenoberbital.

The primary purpose of this ongoing work is to determine the consequences of neonatal exposures on cytochrome-P450-dependent monooxygenase system at the molecular level. However, it is also important to relate these changes to the intact animal. Therefore, we evaluated the animals for survival and growth from the time of neonatal treatment until they were sacrificed as adults (at approximately 23 weeks of age). Few deaths occurred in the PCN- or phenobarbital-treated groups, or in control groups, during this period of time. Fifteen percent of the DMBA-treated males died between 20 and 23 weeks of age, whereas about 12% of the females died during the similar period; these deaths were mainly due to tumors at the injection site or to mammary tumors. Deaths also occurred in the DES-treated group beginning at about 7 weeks of age; by the time of final sacrifice, 35% of the animals in this group had died; the cause of these deaths was not identified. Body weights for treated females were not significantly different from those of controls (Table 1). These data were consistent with those of Lamartiniere and Pardo (*J. Biochem. Toxicol. 3*: 87-103, 1988).

TABLE 1. Body Weight for Male Rats After Neonatal Treatment with Potential Imprinting Agents (Mean ± SEM; N = 8 or 9). One-way analysis of variance indicated that body weight means for treated animals were not significantly different from controls.

Weeks of Age	Oil Control	DMBA[a]	PCN[b]	DES[c]	Saline Control	PB[d]
3	61.40 ± 1.36	58.61 ± 1.74	64.07 ± 2.94	55.19 ± 2.06	66.38 ± 3.42	62.99 ± 2.08
12	448.81 ± 6.11	433.67 ± 9.41	461.85 ± 15.64	418.19 ± 5.69	461.11 ± 16.25	463.96 ± 11.30
23	605.2 ± 13.7	561.2 ± 36.0	615.5 ± 26.1	552.4 ± 21.1	613.8 ± 19.4	650.2 ± 23.1

[a] Dimethylbenz[a]anthracene
[b] Pregnenolone-16a-carbonitrile
[c] Diethylstilbestrol
[d] Phenobarbital

These data indicate that neonatal exposure to DES may alter the susceptibility of animals to tumor development (and, possibly, other diseases) and that cytochrome-P450-dependent pathways may be involved. In addition, these changes demonstrate the need for further evaluation of these animals, with particular emphasis on the cytochrome P450 isozymes involved in aflatoxin binding for DES-treated females, since their total cytochrome P450 concentrations were 21% higher than those of controls. Future work will be concentrated on methods to identify the isozymes involved by analyzing with a combination of oligonucleotide probes (for mRNA) and with antibodies to specific P450 activities.

Molecular Control of Lung Development

Principal Investigators: T. J. Mast and F. C. Leung

Other Investigators: J. R. Coleman and R. L. Rommereim

Coal-derived liquids have previously been shown to be teratogenic when pregnant rats or mice were exposed to these complex mixtures (CM) by either inhalation, oral, or dermal routes. Pulmonary hypoplasia is a major abnormality induced in the offspring of pregnant rats exposed to this CM. (When compared to those of controls, hypoplastic lungs are not only much smaller but had less organization in the interstitial tissue and also had increased septal thickness.) This study concerns the expression of growth factors which regulate cellular differentiation and maturation in development of CM-induced hypoplastic fetal lungs in rats. Epidermal growth factors and transforming growth factor alpha were altered both in intensity and temporal sequence in hypoplastic fetal lungs. Results of this study will be used as a basis for future work intended to elucidate the molecular mechanisms regulating lung maturation and differentiation.

Coal-derived liquids have previously been shown to be teratogenic when pregnant rats or mice were exposed to these complex mixtures (CM) by either inhalation, oral, or dermal routes (Hackett, Annual Report for 1985, 1986). Subsequent studies on the chemical class fractions of this mixture, obtained by liquid chromatography, showed that the teratogenic activity resided almost entirely in the polynuclear aromatic hydrocarbon fraction (Mast, Annual Report for 1986). Although a variety of major malformations result from exposure to these materials, the most prevalent is pulmonary hypoplasia. Ultrastructural examination of the hypoplastic lungs over the course of development and comparison with electron micrographs of untreated fetal lungs showed that gestational exposure to CM resulted in precocious differentiation and maturation of the fetal lung tissue in the absence of adequate pulmonary growth (Mast, Annual Report for 1987). The precocious differentiation in the treated lungs was followed by continued growth of the mesenchymal tissue, which resulted in very thick and disorganized septal walls at the time of birth.

In light of the precocious differentiation of the hypoplastic lungs and the continued proliferation of the mesenchymal tissue, we hypothesized that gestational exposure to CM may have caused altered expression of the growth factors which regulate cellular differentiation and maturation. In order to determine if this was the case, the expression of three growth factors and one growth factor receptor in the lungs of rat fetuses from control and treated dams were evaluated over the course of development. Because the administration of triamcinolone (TAC), a synthetic glucocorticoid, during pregnancy has also been shown to cause fetal pulmonary hypoplasia, another group of dams was treated with this compound, and the lungs of their fetuses were evaluated for growth factor expression.

Timed-pregnant (2-hour matings) Sprague-Dawley rats were dermally exposed to CM in acetone or to a vehicle control (acetone) on days 11 to 15 of gestation (dg). Another group of animals were injected intramuscularly with TAC. Groups of dams were sacrificed daily from 15 to 22 dg, and the fetal lungs were perfused *in situ* with 10% neutral-buffered formalin, and fixed in paraffin blocks. Paraffin sections were then evaluated for expression of epidermal growth factor (EGF), EGF receptor (EGF-R), bombesin, and transforming growth factor alpha (TGF-α), using immunocytochemical techniques. The results are presented as the mean "stain intensity." The intensity of the stain for each lung was graded qualitatively and assigned a number between 0 and 4. The responses were averaged for each litter, and the average response per litter was averaged for each experimental group. The number of litters per data point, 1 to 3, was too small to permit statistical analyses.

Epidermal growth factor expression was observed in mesenchymal cells but not in columnar epithelial cells in both treated and control lungs (Figures 1A and 1B). Expression in control fetal lungs was maximal on 15 dg and a minimal level of expression was also observed on 21 dg. Gestational exposure to either TAC or CM appeared to alter both the intensity and the temporal sequence of EGF expression in the fetal lung. Epidermal growth factor expression following gestational exposure to CM was much lower than that of controls on 15 dg but appeared to be nearly equivalent to that of controls on 16 dg

and exceeded that of controls by 20 dg. Beginning on 19 dg, there was a continual rise in expression through the end of gestation at 22 dg. In the case of TAC, the 16-dg expression of EGF was depressed with respect to the control lungs, but a significant level was observed on 19 dg. The late expression on 21 dg was similar to EGF expression in the control lungs.

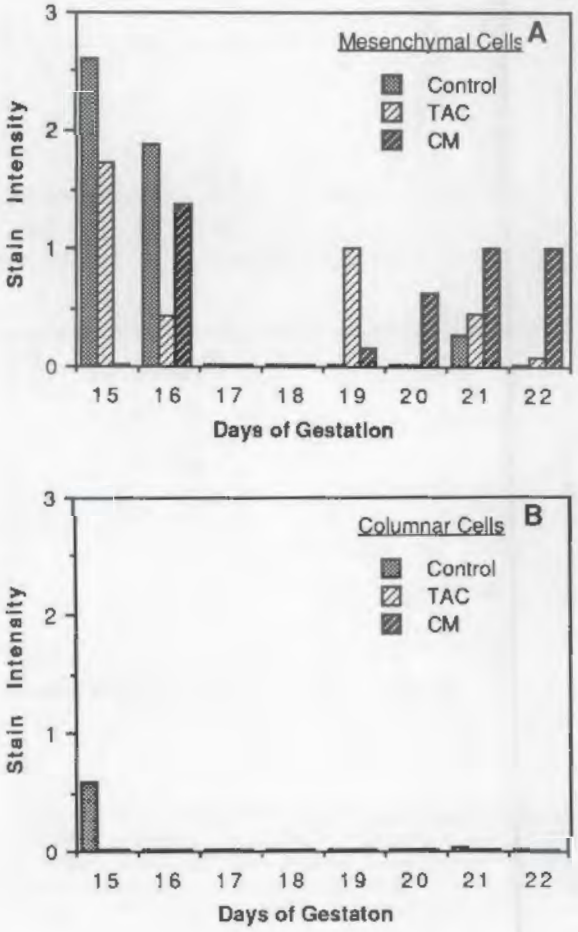

FIGURE 1. Expression of Epidermal Growth Factor in Fetal Lung Mesenchymal Cells (A) and Columnar Epithelial Cells (B) in Untreated Fetuses or Following Gestational Exposure to Complex Mixture (CM) or Triamcinolone (TAC). The degree of expression is directly proportional to the intensity of the immunocytochemical stain.

Preliminary evaluation of fetal pulmonary EGF-R expression indicated that the level of expression was not severely altered following gestational exposure to CM or TAC (Figure 2). Further evaluation of these slides will enable us to localize expression to either the mesenchymal or epithelial tissue.

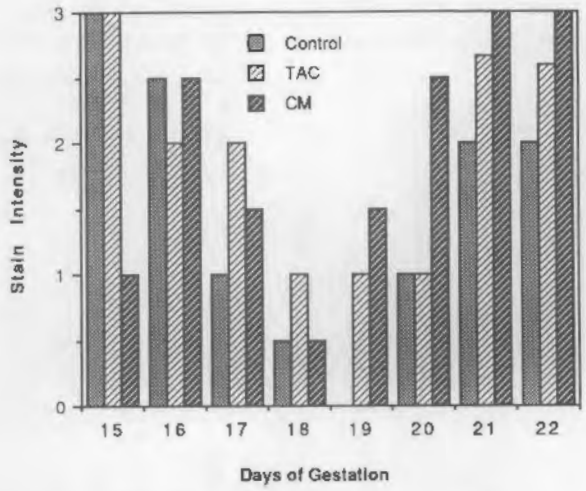

FIGURE 2. Expression of Epidermal Growth Factor Receptor (EGF-R) in Fetal Lung Tissue from Untreated Fetuses or Following Gestational Exposure to Complex Mixture (CM) or Triamcinolone (TAC). The degree of expression is directly proportional to the intensity of the immunocytochemical stain.

Bombesin, the nonmammalian peptide hormone homologous to gastrin-releasing peptide (GRP), was expressed in mesenchymal cells from 15 to 18 dg and in columnar cells on 15 and 16 dg (Figure 3A and 3B). Expression of this peptide in fetal lungs, although relatively intense, was variable, and definitive statements as to treatment-related effects are not possible. However, it appears that expression in mesenchymal cells on 17 and 18 dg may have been reduced following exposure to CM.

Expression of the TGF-α was maximal in control fetal lungs on 15 and 16 dg and was found primarily in mesenchymal cells (Figure 4A and 4B). Gestational exposure of the fetuses to either CM or TAC considerably altered both the temporal sequence and the magnitude of TGF-α expression. Although it has been reported that EGF and TGF-α have substantial structural homology and bind to the same receptor (Nexo et al., *Proc. Natl. Acad. Sci. (USA)* 77:2782-2785, 1980; Twardzik et al., *Cancer Res.* 42:590-593, 1982), results from our study indicate that their expression during development differs. In summary, it appears that the fetal pulmonary hypoplasia following gestational exposure to either CM or TAC results from, or is closely correlated to, alterations in growth factor expression. Furthermore, since the altered growth factor expression which followed exposure to CM differed from the alterations in expression following gestational exposure to TAC, it may be

conjectured that the mechanisms of action of these two toxicants are dissimilar. The results of this study will be used as the basis for further inquiry into the molecular mechanisms regulating fetal pulmonary development during normal and abnormal development.

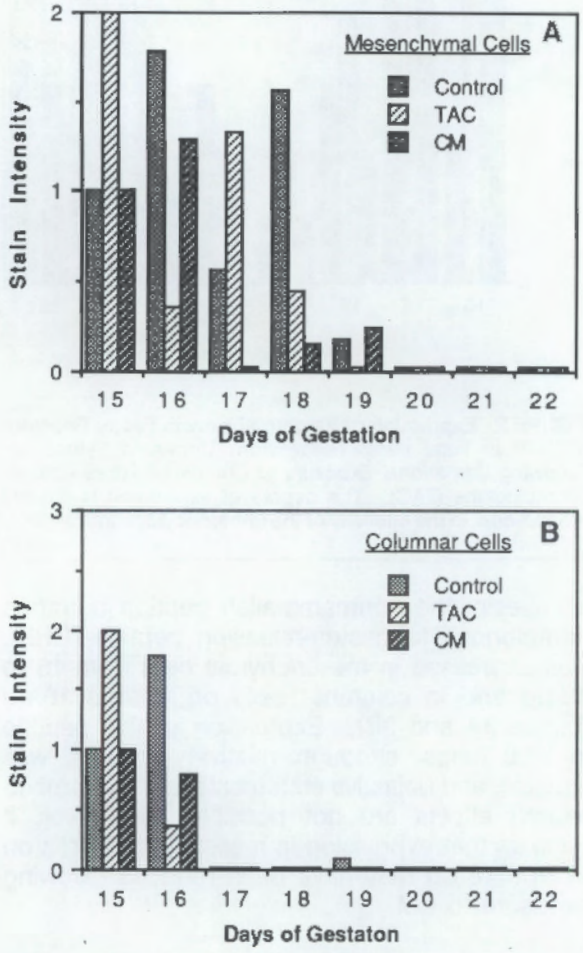

FIGURE 3. Expression of Bombesin in Fetal Lung Mesenchymal Cells (A) and Columnar Epithelial Cells (B) in Untreated Fetuses or Following Gestational Exposure to Complex Mixture (CM) or Triamcinolone (TAC). The degree of expression is directly proportional to the intensity of the immunocytochemical stain.

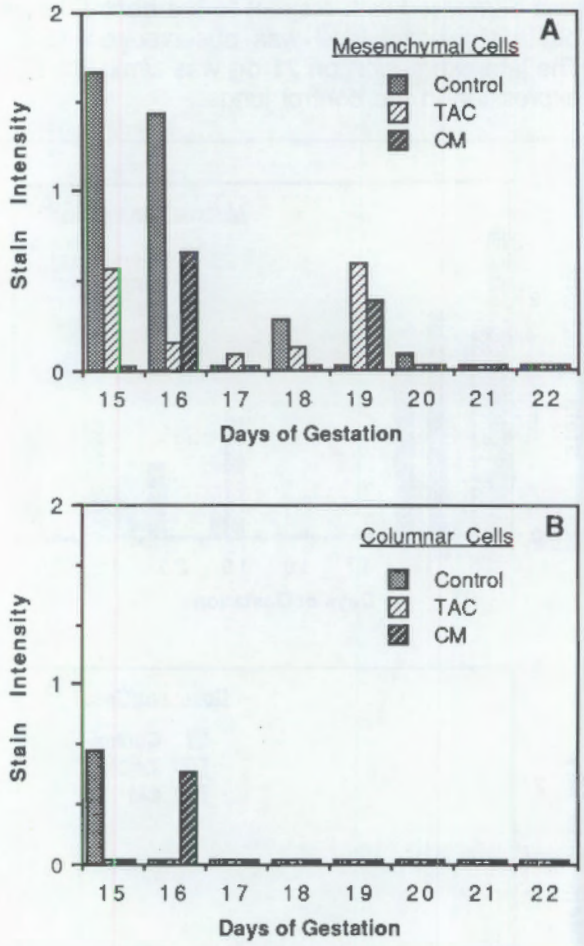

FIGURE 4. Expression of Transforming Growth Factor-Alpha in Fetal Lung Mesenchymal Cells (A) and Columnar Epithelial Cells (B) in Untreated Fetuses or Following Gestational Exposure to Complex Mixture (CM) or Triamcinolone (TAC). The degree of expression is directly proportional to the intensity of the immunocytochemical stain.

Mutation of DNA Targets

Principal Investigator: R. A. Pelroy

Other Investigator: L. K. Fritz

Oligonucleotide-length DNA-targets specifying frameshift mutations were synthesized and inserted into a plasmid-borne structural gene (*lac* Z) to yield a selectable marker for mutagenesis studies. Plasmids containing DNA-targets were then transformed into *Salmonella typhimurium* to provide a defined genetic background for mutagen exposure experiments. DNA-targets with "core" sequences enriched in repeated sequences of guanine (G)/cytosine (C) appeared to be sensitive to reverse mutations induced by the promutagens 6-aminochrysene, 2-aminoanthracene and benzo[a]pyrene. Clones of bacteria from the mutagen exposure experiments with the phenotype expected for restored *lac* Z function were used to produce plasmids for molecular and biochemical analysis. A double-insert DNA-target with alternating GC cores appeared to undergo high frequencies of deletions. A single insert of the same oligonucleotide that was much less active as a DNA-target did not appear to be deleted. A single oligonucleotide insert with a core consising of a run of Gs was the only DNA-target that showed activity with all three of the polycyclic hydrocarbons used in this study.

Construction of the System

Synthetic deoxyribonucleic acid oligonucleotides (DNA-targets) specifying (+1) or (+2) frameshift mutations were cloned into a *Bam* H1 restriction site near the extreme N-terminal end of the *lac* Z (β-galactosidase) gene in the *Escherichia coli* lactose (*lac*) operon. The sequences of three DNA-targets are shown in Figure 1. The *Bam* H1 sites were placed at the extreme 5-prime and 3-prime ends, respectively, of each DNA-target.

A 6-base pair (bp) "core" sequence of alternating guanine (G)/cytosine (C), or a repeated run of Gs was placed near the middle of the DNA targets. The cores were bounded by two Cs on the 5-prime side and three Cs on the 3-prime end, so that cores plus immediate boundaries consisted of 11 consecutive G/C bp on one of the two DNA strands. Directly repeated DNA sequences rich in G/C bp are commonly found in the genetic hotspots for polycyclic chemical mutagens, in both bacterial and mammalian cells.

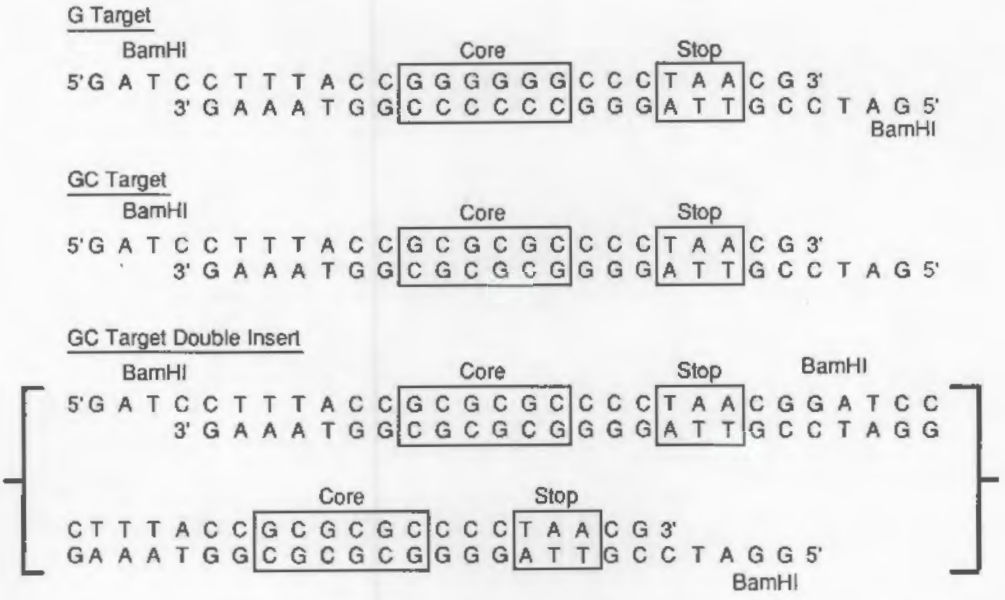

FIGURE 1. Synthetic DNA-Targets for Mutagenesis Studies. Core regions and stop condons shown by the boxed DNA base pair; *Bam* HI restriction sites for cloning shown at the ends of the oligonucleotide targets.

Frameshift mutations can be reversed by second-site frameshifts some distance along the DNA of the gene from the original mutation. To confine the reversing mutations to the DNA-targets, translational stop codons in the reading frame of *lac* Z were placed 3-prime to each of the core sequences (Figure 1). The stop codons were designed to restrict detectable mutational events between the translational stop codon and the N-terminal boundary of *lac* Z.

Detection of mutational events was accomplished by two means: (1) Putative mutations within DNA-targets were screened by selecting for growth on lactose as sole carbon source by strains of *Salmonella typhimurium* that are otherwise incapable of growth on this substrate. (2) *Lac* Z function, indicative of reversal of the frameshift mutations carried by the DNA-targets, was scored by observing chromogenic blue dye formation (X gal) catalyzed by the *lac* Z gene product, β-galactosidase.

To insure sufficient expression of *lac* Z by the revertants so that growth on lactose could be used as a selectable marker for mutagenesis (see below), it was necessary to place the *lac* operon under the control of a high expression synthetic promoter (LPP), or a lower expression promoter (DM) derived by mutation of LPP. The DNA-targets shown in Figure 1 were cloned into the transformable plasmids pDM or pLPP. Plasmid pLPP is distinguished by having LPP as its promoter for the *lac* operon. The plasmid pDM was derived from pLPP by selecting a "down" mutation near the translational start codon of the synthetic promoter that lowered expression of the *lac* Z gene. The scheme for construction of the pDM plasmids is shown in Figure 2.

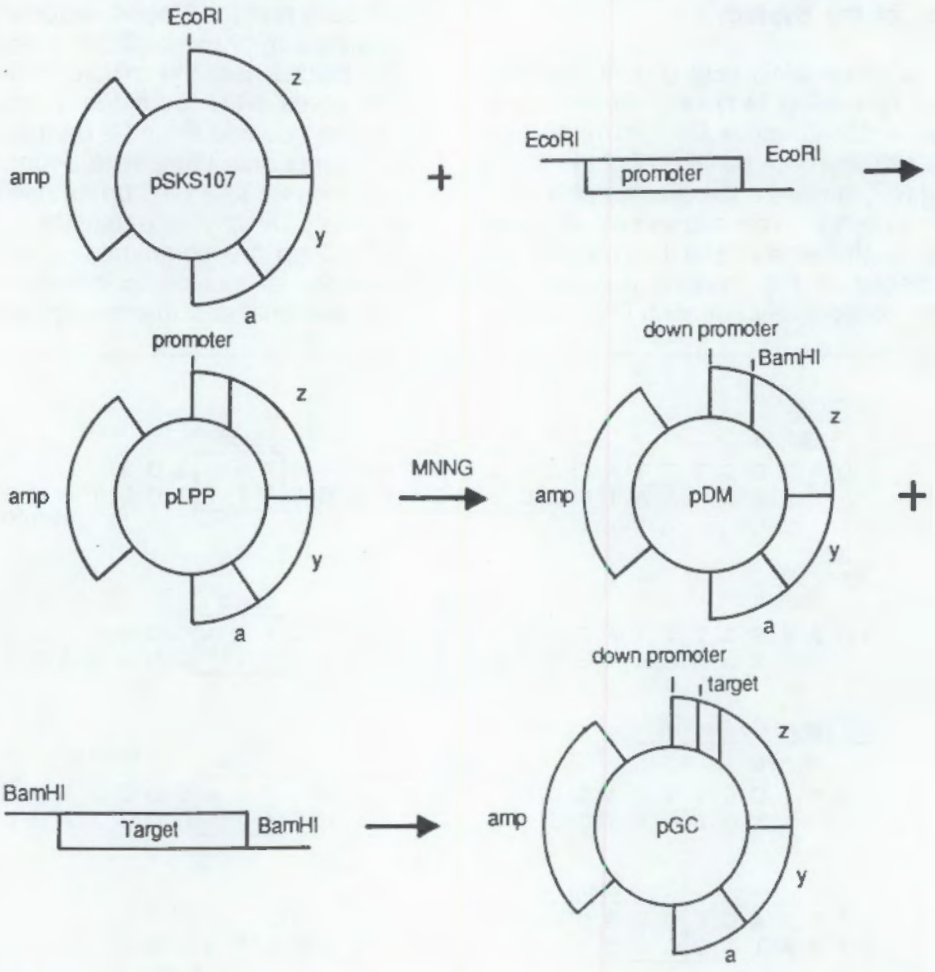

FIGURE 2. System Construction. Main experimental steps in placing the *lac* operon under the control of a synthetic promoter, introduction of a "down" mutation to lower *lac* Z expression, and insertion of DNA-targets for cloning indicated by the flow diagram.

Verification of the System Function

As shown by the data in Table 1, transformation of S. *typhimurium* with plasmid pDM conferred the ability for growth on lactose as a carbon source to this bacterium. As stated, the *lac* operon in pDM and pLPP are under constitutive promoters based on the *E. coli* LPP promoter. Clones of *S. typhimurium* that contain pDM grow much more rapidly on lactose than bacteria containing pLPP, even though pLPP caused much higher levels of *lac* Z expression (Table 1). Evidently, the high levels of *lac* Z expression by pLPP inhibit growth of *S. typhimurium* on lactose mineral-base medium. However, DNA-target-pLPP constructions can be used in *S. typhimurium* to detect reverse mutations in *lac* Z. This is because reversion mutations of DNA-targets in pLPP occur as "one-or-none" events under the conditions of the mutagen exposure experiments. Because the copy number, or number of plasmids per cell, is about 10, pLPP revertants in *S. typhimurium* are expected to contain about 1 revertant plasmid per cell. This was confirmed indirectly by transformation experiments, in which the revertant/total plasmid ratio was estimated at roughly 6% of the total plasmid population from revertant clones of *S. typhimurium*. The lower levels of *lac* Z expression by 1/10 of the DNA-target-pLPP constructions evidently allow growth of *S. typhimurium* on lactose, whereas when the same bacterium contains 10 copies of pLPP that are functional with respect to *lac* Z expression, it is apparently inhibited for growth on this substrate. Growth inhibition by high expression of *lac* Z by pLPP is not linked to lactose metabolism. It is expressed on any mineral-base medium and is therefore probably a generalized response to overproduction of β-galactosidase by cells on a mineral-base medium.

TABLE 1. Characteristics of Target Strains and Lactose Revertants for Three DNA Targets in Plasmid pDM.

Target/ Mutagen[a]	Units of β-galactosidase on:		Division Time (hr) on:			Probe for Target/ Promoter[d]
	Glucose[b]	LB[c]	Lactose	Glucose	LB	
pGC21 target	13	75.3	>42.0	1.4	0.8	+/+
pGC21 cont. 1	6809	2681	18.0	2.1	0.8	Δ/+
pGC21 cont. 2	1527	5904	>42.0	2.0	0.6	Δ/+
pGC21 6AC 9	408	1152	6.9	2.9	0.8	Δ/+
pGC21 6AC 11	5789	4661	8.0	5.0	0.7	Δ/+
pGC21 6AC 24	2146	551	9.6	1.1	0.7	+/+
pGC1 target	33	553	>42.0	2.2	0.6	+/+
pGC1 6AC 11	330	821	19.0	1.4	0.4	+/+
pGC1 6AC 29	263	416	16.0	3.0	0.7	+/+
pGC1 2AA 31	240	421	24.0	2.4	0.8	+/+
pGC1 cont. 1	529	588	24.0	3.1	0.8	+/+
pGC1 cont. 2	250	589	7.0	3.0	0.7	+/+
pGC6 target	54	255	>42.0	1.3	0.5	+/+
pGC6 6AC 24	3628	3850	24.0	No Data		+/+
pGC6 6AC 18	2876	1101	9.2	1.7	0.7	+/+
pGC6 6AC 14	640	301	12.0	No Data	0.7	+/+
pLPP	>6000	848	>20.0	2.3		–/–
pDM	5786	1289	7.5	2.3	0.6	–/–

(a) 6AC = 6-aminochrysene, 2AA = 2-aminoanthracene, BaP = benzo[a]pyrene, cont = unexposed control. pIPP = contains up promoter of *lac* Z, pDM = contains down promoter of *lac* Z.
(b) Glucose-rich mineral-base medium.
(c) Luria broth (organicaly rich medium).
(d) + = target/promoter detected by oligonucleotide probe, - = target/promoter not detectable, Δ = deletion of DNA-target confirmed by sequencing of revertant.

Insertion of the DNA-targets into pDM (i.e., in pGC21, pGC1, and pGC6) prevented the growth of *S. typhimurium* SL4213 on lactose mineral-base medium (Table 1). As expected, *lac* Z function was nearly abolished by the insertion of the DNA-targets into the *lac* Z of pDM, as shown by the low levels of β-galactosidase activity for bacteria containing these plasmid constructs (Table 1). Likewise, insertion of DNA-targets into the *lac* Z gene in pLPP nearly abolished the activity of this structural gene in the strong promoter plasmid construction (data not shown).

Mutagenesis of the Target Sequence

The DNA-targets in Figure 1 were tested in the Ames-*Salmonella*/mutagen bioassay for response to chemical polycyclic promutagens after metabolic activation. The aromatic amines 6-aminochrysene (6AC) and 2-aminoanthracene (2AA) appeared to induce reverse mutations in plasmids carrying the alternating GC DNA-targets (Figures 3A to 3C). The plasmid with a double oligonucleotide insert (pGC21) produced greater numbers of lactose revertants than the target consisting of a single insert (pGC6; Figure 3A versus Figure 3B). Response to benzo[a]pyrene (BaP) was minimal by both of the alternating GC targets contained on pGC21 and pGC6.

In terms of net response, pGC21 was comparable in sensitivity to the histidine frameshift mutation (D3052) carried on the chromosome of the host, *S. typhimurium* TA1538. However, this estimate of mutagenic response for this DNA-target is probably inflated, because there are roughly 5 to 10 times more copies of the DNA-target plasmid per cell than of the D3052 on the host chromosome. The net probability of mutations in the DNA-target should therefore be increased proportionately. The single-insert pGC6 was less active than D3052 on the host chromosome in net response and probably much less active in absolute terms because of the copy number.

A DNA-target with a single oligonucleotide, 6-bp G core sequence, was inserted into pLPP to yield plasmid pLG6 (Figure 3B). This DNA-target showed a high spontaneous rate of mutagenesis, as shown by the data for the controls (labeled low S9 and high S9). It also appeared to be sensitive to mutations induced by all three promutagens, 6AC, 2AA and BaP. Mutability of this DNA-target was dependent on the use of the strong synthetic promoter; when placed in the less active pDM, the same DNA-target was not active in detecting these promutagens (data not shown).

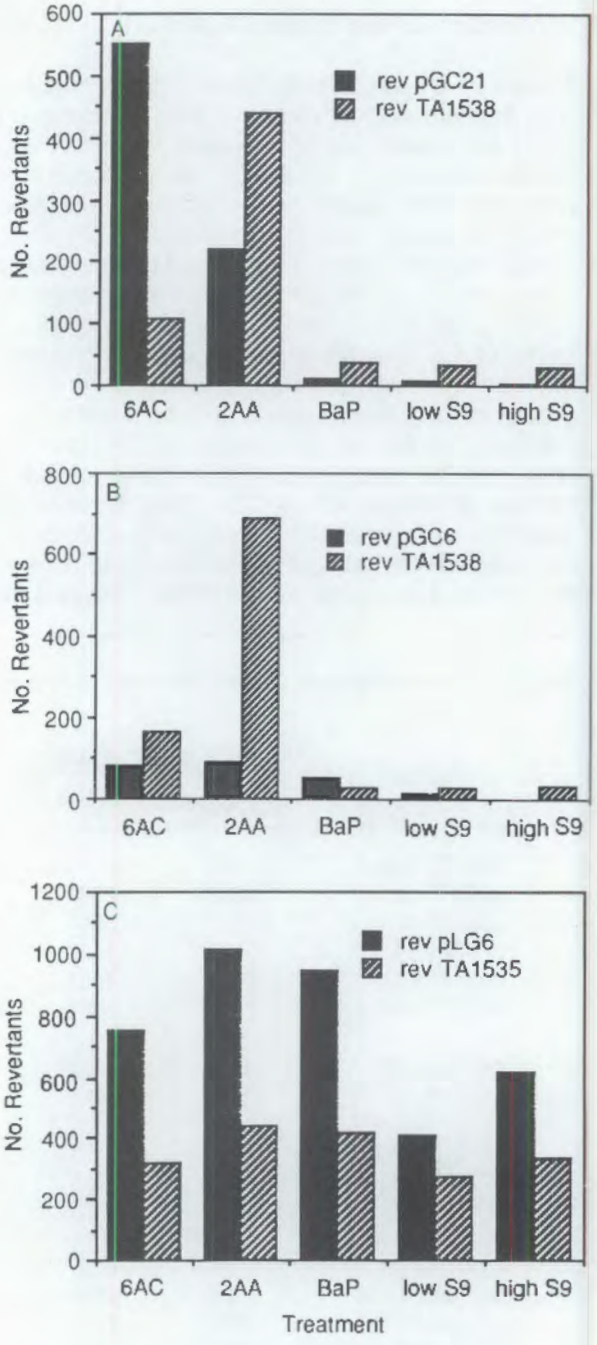

FIGURE 3. Reversion to Lactose Catabolism in Target Plasmids and Histidine Reversion in TA1538. Low S9 and high S9 refer to negative controls exposed to low and high concentrations of S9 activating enzymes (no promutagen). Concentrations (μg/plate) of promutagens were: 6-aminochrysene (6AC), 0.01; 2-aminoanthracene (2AA), 0.05; benzo[a]pyrene (BaP), 5.0. A, lactose reversion in pGC21 versus histidine reversion in TA1538; B, lactose reversion in pGC6 versus histidine reversion in TA1538; C, lactose reversion in pLG6 versus histidine reversion in TA1538.

Several other DNA-targets containing adenine (A) and thymine (T) cores, or the G6 core under the weak promoter (pDM), were inactive as DNA-targets or showed unacceptably high rates of spontaneous mutation (data not shown). Revertant bacterial clones containing pGF21 or pGC6 were subcultured on lactose medium for molecular and enzymatic analysis of changes in DNA-targets accompanying lactose reversion (Table 1, see below). Plasmid pGC6 is a copy of pGC1, independently isolated from transformants of *S. typhimurium* SL4213 during the construction of the pDM DNA-targets.

Table 1 contains a summary of molecular data on the types of mutations induced in the DNA-target-containing strains in the pDM-derived plasmids. Revertant plasmids were isolated from randomly selected lactose-utilizing clones formed after exposure to the chemical mutagens discussed, or from lactose-utilizing clones formed by spontaneous mutation on the S9 control plates. Plasmids were purified from independent clones of lactose-utilizing *S. typhimurium* SL4213 for molecular and biochemical analyses. The transformation step was necessary because all the lactose-positive clones produced on mutagen exposure plates, or from S9 control plates, contained multiple copies of the nonmutated plasmid-DNA-target. Revertant plasmids were purified from the nonrevertant plasmids by the transformation step. Under the conditions of the transformation experiment, only single plasmids were taken up by competent cells of *S. typhimurium* SL4213. The chromogenic assay for β-galactosidase was then used to detect those transformants carrying plasmids with restored *lac* Z function. Estimates of the ratios of revertant to nonrevertant plasmids averaged roughly 1 revertant to about 10 nonrevertant plasmids. The copy number of PDM and pLPP is roughly 10.

In all cases, the plasmids extracted from the lactose-positive Ames-*Salmonella* strains had restored *lac* Z function when transformed into *S. typhimurium* SL4213. Most of the transformed clones of 4213 also acquired the ability to grow on lactose mineral-base medium, although it appeared that the doubling time for these revertant cultures on lactose was slower than for glucose (a carbon source commonly shared by all *S. typhimurium* strains).

In order to gain information on molecular events occuring in the DNA-targets from the revertant, lactose positive Ames-*Salmonella* strains, plasmid DNA from the reverant clones was isolated and hybridized with radioactivity-labeled probes for the DNA-targets and promoter sequences. The promoter is a positive control because it was required in all plasmids capable of expressing the *lac* operon and *lac* Z. The DNA-targets probed for similar sequences that might be expected for frameshift mutations that would have left most of the original DNA-target intact.

As can be seen in Table 1, four of the six double-insert DNA-targets in pGC21 reverted to lactose utilization by complete deletion of the DNA-target. This was suggested by the dot-blot probing experiments with synthetic oligonucleotides complementary to the promoter and DNA-target sequences and was confirmed by direct DNA-sequencing data. The deletion occurred between the directly repeated *Bam* H1 sites situated at the ends and in the middle of the DNA-target in pGC21. It appears that complete deletion of this DNA-target is a common, if not preferred, molecular event accompanying mutagenesis. Deletions were detected in the DNA-targets from the spontaneous and induced lactose revertants.

The lactose revertant plasmids with single-insert DNA-target (pGC1 and pGC) all probed strongly for the DNA-targets, indicating that target sequences remained after reversion of the frameshift mutations. Four of the DNA-targets from the revertant plasmids were sequenced and showed that the inserted DNA-targets were intact. Evidently, the reversing frameshift mutations were not confined to the DNA-target sequence by the stop codons.

Detection of polycyclic mutagens appears to be possible using DNA-targets that contain alternating G/C or repeated runs of G as core sequences. Levels of sensitivity are comparable to those obtained with conventional mutagen/genotoxin bioassays. We hope that DNA-targets can be used for mechanistic studies by correlating the activity and selectivity of primary sequence with changes in DNA-sequence that accompany induced mutations. These plasmid constructions have features advantageous for mechanistic work in molecular genetics. First, it is possible to control the sequence of both the DNA-target and the surrounding flanking regions in a way that is not easily available in other molecular systems based on forward mutations (e.g., *lac* I, or tetracycline gene). Secondly, the data presented suggest that stop codons can be used to confine mutational events to the selected sequences of the DNA-targets. This is an important consideration in trying to relate the genetic activity of frameshift mutations to designated DNA

sequences, since reversing mutations can occur at a second site some distance from the initial frameshift. It is noteworthy that pGC21 is a doubly inserted, alternating GC DNA-target; therefore it contains two stop codons as opposed to a single stop codon for the single-insert, alternating-GC targets of pGC1 and pGC6. Plasmid pGC21 also specifies a (+2) rather than a (+1) frameshift mutation like all the other DNA-targets in this study. Until further work is done, it is not clear whether the reading frame is important in determining the type of event, e.g., deletion versus point mutation.

Initial DNA sequencing data suggest that single-insert, alternating-GC targets (pGC1 and pGC2) are unchanged in the revertant clones (Table 1). The explanation for this may lie in the occurrence of both direct repeats and palindromic sequences that could promote secondary stem/loop structures in mRNA. Such secondary structures may allow synthesis of *lac* Z past the stop codons that are masked within secondary structures of the mRNA. To minimize the possibilities for secondary structure in mRNA, we are designing the next generation of DNA-targets without the extensive palindromic and/or directly repeated sequences found in the DNA-targets reported in this study.

Another advantage of this sequencing of mutations is that it is simpler than the procedures used for molecular analysis of mutations in the *lac* I repressor gene of *E. coli* or the structural tetracycline gene of pBR322, or for comparable molecular studies of the *his* D gene in *S. typhimurium*.

The results obtained in this study show that the sensitivity of the DNA-targets is affected both by their primary DNA-sequences (as expected) and by the strength of the promoter for expression of the lactose operon.

Synthesis of Human Genome Information

Principal Investigator: J. E. Schmaltz

This project is investigating existing data bases that contain information on the human genome, analytical tools for relating experimental data from mapping and sequencing efforts to known information, and methods for researchers to gain access to data bases and tools via networks. The goal is to develop a prototype and expand an information system for the use of archival information in investigations associated with the DOE Human Genome Initiative.

The DOE has launched its Human Genome Initiative in a major effort to improve understanding of human genetic structure and function. This initiative has been approached in two phases: first, development of resources and technology for mapping and sequencing the human genome; second, application of these developments to intensively mapping and sequencing the human genome. Computer-based information resources will play a major role in accomplishing these goals and making results available to researchers in biology and medicine. This project will work toward integrating and expanding existing analytical tools and data bases that contain information on the human genome as well as developing a prototype of an information system that will encompass the results of the Human Genome Initiative.

To initiate this work, the Principal Investigator of this project has been detailed to the Office of Health and Environmental Research at DOE in Germantown, Maryland. Nationwide and worldwide networking resources available to the human genome scientific community have been investigated. Plans are being implemented to become involved with efforts relevant to the computational aspects of the DOE Human Genome Initiative, to integrate these efforts, and to make results readily available and useful to program participants.

Genome Graphics Interface

Principal Investigator: R. J. Douthart

Other Investigator: V. Lortz

The purpose of this project is to develop a graphics-oriented computer workstation to process the vast amounts of information produced by the human genome initiative. The workstation will present information in a graphics format tightly integrated with pictorial representations of chromosomes, various genetic and physical maps, and DNA sequences. The system will access data bases and information resources such as the New Haven genome mapping library and GenBank.

An examination of any compendium of genetic maps or modern genetics and molecular biology textbooks and journals attests to the fact that the preferred method for presenting genomic information is pictorial. Chromosomes, physical maps, and regions related to DNA sequence are drawn as boxes, shaded regions, etc., or a linear map. Objects are identified as labels to drawings. If the objects are too numerous, then location is defined by some metric, such as chromosome band or base number, and they are listed in a table.

Although the amount of information that will be generated by the genome initiative is enormous, concepts such as data, progressive disclosure, and descriptive information that can be furnished on demand can successfully provide overviews as well as specific information about large genomes. These techniques have been used in the CAGE/GEM™ system, developed by PNL, to represent sequenced genomes up to 5×10^5 bases in size. Descriptive information and general features have been constructed graphically for lambda bacteriophage (48,000 bases) and Epstein-Barr virus (172,000 bases).

From these representations, the features most noticeable at low magnification are:

(1) Color-coding graphic representations of known objects, such as coding regions, repeated sequences, and promoters that give important insights into genome topology.

(2) Representing, by the use of color, derived data, such as base sequence distribution, location of consensus sequences and restriction enzyme sites, gives insights into organization and structure.

Using similar graphics representation, insights can be gained at all levels of the human genome hierarchy.

Genome Graphics Structure

The architecture for the human genome graphics has been planned in some detail. The network base management system db VISTA has been chosen for the system. Programming is in the C language, using the UNIX operating system on a SUN workstation. The X-windowing system, which is being used extensively, will be an integral part of the software.

Queries initiated by the user will determine the nature of objects presented graphically, either as color-coded drawings, such as boxes, colored regions, or arrows with appropriate labels, or as color-coded histograms. Histograms represent the number of objects of a given type found in a particular region. At higher levels of magnification or at different levels in the hierarchy, objects represented by histograms revert to drawings on the map. For example, the object gene may appear as a histogram at the karyotype or chromosome level and revert to boxed regions at the restriction map or sequence level. A search query would generate successive layered representations of the locations of all genes, oncogenes, and oncogenes called *ras*, appropriately color-coded. Progressive disclosure guides the user from chromosome to restriction map, to actual nucleotide sequences for objects found as a result of the query. Descriptive information appears in "priority" windows by simply pointing to the labels of a particular object with a "mouse." The mouse is also used to access different levels in the hierarchy, which the user perceives as a simple magnification process.

Figure 1 shows computer-generated representations of various chromosomes of the human genome. The entire human karyotype of 23 metaphase chromosomes at the 400 band level, with "zoom" capability to higher-resolution mapping is nearing completion. At the left of the

chromosome is a "metric" of average size, represented in micrometers, as viewed under a light microscope. Also shown are accepted nomenclature and positions of chromosomal banding patterns. A query on the left side of the chromosome representation identifies a particular band label or selected region. Information about the band or region appears in a window as alphanumeric output. Searches can be limited by the user to specific objects. Detailed descriptive text, references, and other alphanumerical information can be part of the user-selected output.

The right side of the chromosome is reserved primarily for graphic display of information. Currently, this display is limited to known information, however, as the system develops, derived information will also be displayed. The display is a color-coded histogram for numerous objects, or boxed regions for less numerous objects.

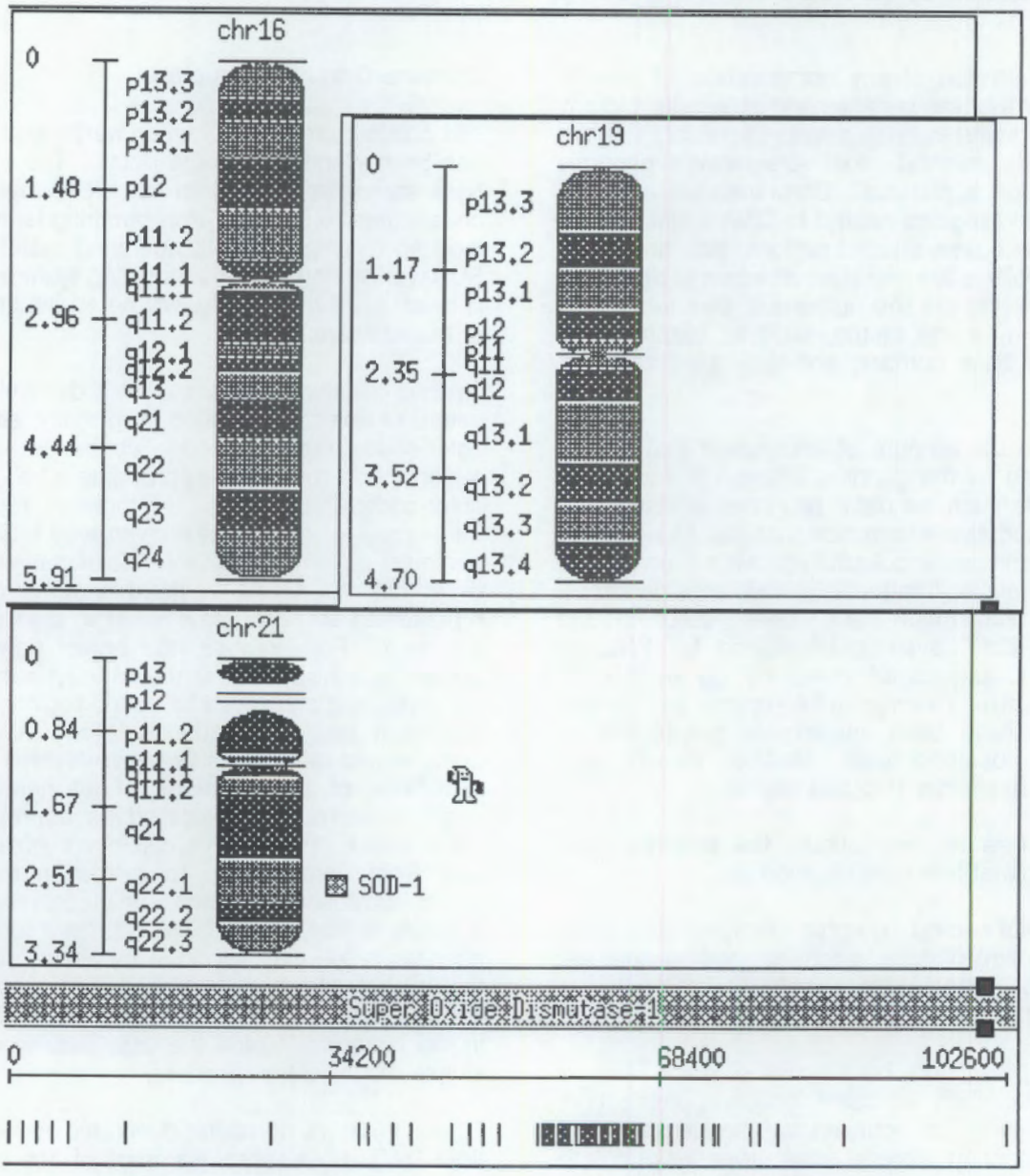

FIGURE 1. Graphics Representations of Chromosomes 16, 19, and 21. The superoxide dismutase (SOD-1) region has been located at the q22.1 band of chromosome 21. A zoom is shown to a 102-kb fragment that has been restriction enzyme mapped. Specific sites are represented as color-coded bars. The dense region near the center of the map represents the intron-exon junctions of the SOD-1 gene.

Information is displayed about the extent of mapped information, from chromosome to restriction map to sequence, with respect to any object or region. Immediate access to different levels is available by pointing and/or keyboard entry.

Work has begun on the representation of physical mapping, which is the second level in the hierarchy. Restriction enzyme mapping will be represented by a linear map, with sites as objects in the data base. An enzyme site will be represented by a location (base number), a restriction enzyme name, and a cut recognition sequence. Recognition sequence will allow flexibility in rearranging and manipulating a given map.

Ideally, the information hierarchy will relate restriction maps to chromosome regions. Specific gene loci and other landmarks on the physical map will refer to specific enzyme cut locations. Entry to the physical map representation, or any other representation, can be gained without reference to higher levels in the hierarchy. This is especially important for regions that are restriction enzyme mapped and may occur on specific ordered cosmids or other ordered libraries that have not yet been mapped back to specific regions on chromosomes. Where a connected hierarchy exists, the chromosome can be displayed horizontally, with a capability for "zooming" to the mapped region of interest, so that user orientation is maintained. For specific gene loci, information about restriction fragment length polymorphisms (RFLP) and specific maps and comparisons will be available on demand. Graphic representations of gel banding patterns for RFLP are also planned.

To demonstrate: The hierarchy of the superoxide dismutase (SOD) loci located on chromosome 21, band location of q21.1, is being developed. A 100-kb region has been restriction-mapped, and the SOD genomic loci are putatively located within it. Information about sequence, intron-exon junctions and analytically determined restriction enzyme sites has been structured into one file, utilizing the GenBank sequence data base and the file structure and analytical capabilities of the CAGE/GEM system. This information is entered in the architecture of the genome graphics system for SOD at the sequence level.

Medical Applications Of Nuclear Technology

Radioisotope Customer List

Principal Investigator: D. A. Lamar

Other Investigators: R. A. Peloquin and N. C. Van Houten

This project has continued to provide technical assistance to the DOE Office of Energy Research, Office of Health and Environmental Research by preparing the annual DOE radioisotope customer list. The report decribes radioisotope distribution from DOE facilities to private firms, both domestic and foreign, and to other DOE facilities.

Information summarizing the FY 1987 commercial radioisotope production and distribution activities at DOE facilities was compiled using a computer database management system to aid in tracking the quantities and subsequent revenues generated from the sale of radioisotopes produced at DOE facilities. A total of 1264 shipments of radioisotopes was distributed from DOE facilities during FY 1987, with a value of $10 M. This information was summarized in the document entitled *List of DOE Radioisotope Customers with Summary of Radioactive Shipments, FY 1987*. The document contains information on isotope suppliers, customers (domestic and foreign private firms), as well as other DOE facilities, geographic locations of customers, isotopes purchased, sold and transferred. DOE facilities included in the report are Argonne National Laboratory, Brookhaven National Laboratory, Idaho National Engineering Laboratory, Los Alamos National Laboratory, Oak Ridge National Laboratory, Pacific Northwest Laboratory, Savannah River Operations Office, and Westinghouse Hanford Company.

Appendix

DOSE-EFFECT STUDIES WITH INHALED PU-239 OXIDE IN BEAGLES

DOSE GROUP	DOG IDENT	INITIAL ALVEOLAR DEPOSITION NCI	NCI/G LUNG	NCI/ KG	INHALATION EXPOSURE WEIGHT (KG)	AGE* (MO)	DATE	DATE OF DEATH	MONTHS SINCE INHALATION 9/30/88	DEATH	COMMENTS ON DEAD DOGS
CONTROL	738 F	0	0.00	0.00				08/11/83		171.5*	Hemangiosarcoma, Heart
CONTROL	740 F	0	0.00	0.00				06/18/83		169.8*	Malignant Lymphoma
CONTROL	749 F	0	0.00	0.00				09/14/84		183.4*	Adrenalitis
CONTROL	755 M	0	0.00	0.00				12/10/82		162.2*	Status Epilepti, Nephrosclero
CONTROL	766 M	0	0.00	0.00				06/26/84		180.3*	Lung Tumor
CONTROL	775 F	0	0.00	0.00				10/05/81		147.3*	Pulmonary Thromboembolism
CONTROL	785 M	0	0.00	0.00				09/02/87		217.6*	Luxated Vertebral Disc
CONTROL	789 M	0	0.00	0.00				07/25/83		167.9*	Malignant Lymphoma
CONTROL	792 M	0	0.00	0.00				04/28/78		79.6*	Oral Tumor
CONTROL	800 F	0	0.00	0.00				11/17/86		204.9*	Malignant Pheochromocytoma
CONTROL	801 M	0	0.00	0.00				02/23/82		148.1*	Lung Tumor
CONTROL	811 F	0	0.00	0.00				02/24/85		183.1*	Oral cav.: Malignant Melanoma
CONTROL	848 M	0	0.00	0.00				04/08/83		159.8*	Nephrosclerosis
CONTROL	861 M	0	0.00	0.00				11/18/86		202.6*	Cushing's,Intestinal Carcinom
CONTROL	868 F	0	0.00	0.00				03/24/87		205.4*	Chronic Nephropathy
CONTROL	872 F	0	0.00	0.00				11/05/82		152.8*	Lung Tumor
CONTROL	878 M	0	0.00	0.00				01/22/85		177.4*	Chronic Nephropathy
CONTROL	882 M	0	0.00	0.00				11/06/81		138.7*	Hemangiosarcoma, Liver
CONTROL	885 F	0	0.00	0.00				02/18/83		153.6*	Lung Tumor
CONTROL	903 F	0	0.00	0.00				01/30/85		174.6*	Malignant Lymphoma
CONTROL SACRIFICE	701 F	0	0.00	0.00				04/18/79		121.0*	Sacrificed
CONTROL SACRIFICE	703 M	0	0.00	0.00				03/24/77		96.2*	Sacrificed
CONTROL SACRIFICE	724 M	0	0.00	0.00				03/30/78		107.9*	Sacrificed
D-1 LOWEST	756 M	0	0.00	0.00	13.0	19.5	01/19/71	04/21/83		147.0	Epilepsy
D-1 LOWEST	782 M	0	0.00	0.00	11.5	19.3	01/19/71	01/24/77		72.2	Sacrificed
D-1 LOWEST	847 M	0	0.00	0.00	13.0	18.5	07/06/71	01/23/85		162.6	Kidney Failure
D-1 LOWEST	858 M	0	0.00	0.00	13.5	18.2	07/06/71	10/01/86		182.9	Lymphocytic Leukemia
D-1 LOWEST	865 F	0	0.00	0.00	9.0	17.4	07/06/71	09/16/86		182.4	Acute Pneumonia, Lung Tumor
D-1 LOWEST	879 M	0	0.00	0.00	14.5	17.9	10/07/71	07/27/84		153.7	Hemangiosarcoma, Liver,Spleen
D-1 LOWEST	886 F	0	0.00	0.00	10.5	18.2	11/10/71	04/04/84		148.8	Meningioma, Malignant
D-1 LOWEST	907 F	0	0.00	0.00	11.5	16.9	11/10/71	05/10/88		174.0	Pneumonia
D-1 LOWEST	825 F	1	0.01	0.12	11.5	18.1	06/06/71	11/17/82		137.3	Hemangiosarcoma, Spleen
D-1 LOWEST	849 F	1	0.01	0.10	10.0	21.3	10/07/71	10/26/72		12.8	Sacrificed
D-1 LOWEST	904 F	1	0.01	0.07	9.5	15.9	11/10/71	12/19/83		145.3	Chondrosarcoma, Nasal
D-1 LOWEST	832 F	2	0.02	0.22	9.0	16.5	04/26/71	03/03/86		178.2	Malignant Lymphoma
D-1 LOWEST	900 M	3	0.02	0.22	13.0	16.0	11/10/71	05/21/82		126.3	Round Cell Sarcoma
D-1 LOWEST	870 F	4	0.03	0.32	12.0	16.9	07/06/71	05/04/84		154.0	Pneumonia
D-1 LOWEST	899 F	4	0.03	0.31	11.5	16.0	11/10/71	03/29/81		112.6	Hemangiosarcoma, Heart
D-1 LOWEST	867 M	5	0.04	0.41	11.5	17.4	07/06/71	02/07/86		175.1	Malignant Lymphoma
D-1 LOWEST	891 M	6	0.04	0.41	14.0	16.0	11/10/71	06/26/81		115.5	Septicemia
D-1 LOWEST	853 M	8	0.05	0.51	15.0	21.3	10/07/71	12/12/84		158.2	Bronchopneumonia
D-1 LOWEST	875 M	8	0.06	0.54	14.0	16.8	07/06/71	05/21/78		82.5	Kidney: Malignant Lymphoma
D-1 LOWEST	770 F	8	0.06	0.63	9.5	19.1	01/19/71	11/29/84		166.3	Glomerulosclerosis

* Indicates age in months since birth, all other ages are in months since exposure.

DOSE-EFFECT STUDIES WITH INHALED PU-239 OXIDE IN BEAGLES

DOSE GROUP	DOG IDENT	INITIAL ALVEOLAR DEPOSITION NCI	NCI/G LUNG	NCI/ KG	INHALATION EXPOSURE WEIGHT (KG)	AGE* (MO)	DATE	DATE OF DEATH	MONTHS SINCE INHALATION 9/30/88	DEATH	COMMENTS ON DEAD DOGS
D-1 LOWEST	788 M	8	0.06	0.62	13.0	18.8	02/10/71	04/13/84		158.1	Chronic Nephropathy
D-1 LOWEST	850 F	5	0.08	0.63	8.0	21.3	10/07/71	06/06/83		140.0	Bone Tmr, Chronic Nephropathy
D-1 LOWEST	893 M	9	0.06	0.61	14.0	14.9	10/07/71	07/01/86		176.8	Pneumonia
D-1 LOWEST	807 F	8	0.07	0.73	11.0	14.6	02/10/71	07/24/81		125.4	Pituitary Tumor, Cushing's
D-1 LOWEST	841 F	8	0.07	0.75	8.0	17.7	06/08/71	04/01/86		177.8	Malignant Lymphoma
D-1 LOWEST	908 M	9	0.07	0.77	11.0	15.9	11/10/71	04/01/80		100.7	Unknown, Pulmon. Hyalinosis
D-2 LOW	778 M	10	0.07	0.74	13.5	20.2	03/04/71	09/19/84		162.6	Bronchopneumonia
D-2 LOW	842 M	10	0.07	0.77	13.5	18.6	07/06/71	05/01/85		165.8	Lung Tmr, Chronic Nephropathy
D-2 LOW	787 M	10	0.08	0.83	12.0	18.2	12/21/70	12/09/85		179.6	Valvular Endocardiopathy
D-2 LOW	920 M	11	0.08	0.92	12.0	16.0	06/08/72	07/07/72		1.0	Sacrificed
D-2 LOW	862 M	13	0.09	1.00	13.0	17.3	06/08/71	06/25/83		144.6	Peritonitis
D-2 LOW	871 M	13	0.09	0.96	13.5	16.9	07/06/71	07/24/86		180.6	Malignant Melanoma, Oral
D-2 LOW	874 M	16	0.11	1.24	13.0	16.8	07/08/71	04/09/85		165.1	Chronic Nephropathy
D-2 LOW	754 M	22	0.15	1.69	13.0	19.5	01/19/71	01/10/78		83.7	Epilepsy
D-2 LOW	845 F	19	0.15	1.63	11.5	17.6	06/08/71	08/09/84		158.1	Urinary Bladder Tumor
D-2 LOW	748 F	14	0.16	1.75	8.0	19.5	01/19/71	08/19/81		127.0	Unknown Cause
D-2 LOW	798 F	18	0.16	1.78	9.0	15.7	02/10/71	08/29/74		42.6	Sacrificed
D-2 LOW	826 F	19	0.17	1.90	10.0	19.1	07/06/71	04/17/84		153.4	Hemangioma, Spleen
D-2 LOW	831 F	21	0.18	2.00	10.5	17.9	06/08/71	05/14/84		155.2	Pneumonia
D-2 LOW	881 F	19	0.19	2.09	9.0	17.7	10/07/71	12/20/86		182.4	Acute Pneumonia
D-2 LOW	780 F	24	0.22	2.40	10.0	18.2	01/19/71	04/08/82		134.6	Pheochromocytoma
D-2 LOW	859 M	35	0.22	2.41	14.5	18.2	07/08/71	04/22/84		153.6	Urinary Bladder Tumor
D-2 LOW	757 M	38	0.23	2.57	14.0	18.5	12/21/70	11/26/86		191.2	Leiomyosarcoma,Kidney,Lung Tm
D-2 LOW	876 F	19	0.24	2.69	7.0	17.9	10/07/71	05/05/86		174.9	Nephropathy,Lung Tumor
D-2 LOW	808 F	26	0.25	2.74	9.5	15.3	03/04/71	10/29/82		139.9	Palate: Malignant Melanoma
D-2 LOW	813 F	32	0.29	3.20	10.0	15.1	03/04/71	12/15/83		153.4	Multilobular Sarcoma, Skull
D-2 LOW	877 F	34	0.29	3.24	10.5	17.9	10/07/71	05/06/86		174.9	Lung Tumor
D-2 LOW	769 F	28	0.32	3.50	8.0	18.2	12/21/70	06/23/78		90.1	Ovarian Tumor
D-2 LOW	802 M	40	0.33	3.64	11.0	18.1	04/28/71	12/28/84		164.1	Pneumonia
D-3 MED-LOW	781 F	48	0.38	4.17	11.5	17.3	12/21/70	02/20/81		122.0	Kidney Tumor, Lung Tumor
D-3 MED-LOW	771 F	44	0.40	4.40	10.0	19.2	01/20/71	11/02/83		153.4	Lung Tumor
D-3 MED-LOW	782 M	62	0.42	4.59	13.5	19.0	02/10/71	05/27/83		147.5	Neurofibrosarcoma,Brach.Pl.
D-3 MED-LOW	786 M	62	0.42	4.59	13.5	19.5	03/04/71	05/29/86		182.8	Adrenocortical Carc, Lung Tmr
D-3 MED-LOW	752 M	62	0.43	4.77	13.0	18.8	12/21/70	02/22/79		98.1	Lung Tumor, Adrenal Tumor
D-3 MED-LOW	823 M	65	0.44	4.81	13.5	16.8	04/28/71	05/24/84		156.9	Urinary Bladder Tumor
D-3 MED-LOW	883 M	63	0.44	4.86	13.0	17.7	10/07/71	01/25/88		195.6	Chronic Nephropathy
D-3 MED-LOW	778 M	74	0.48	5.10	14.5	20.2	03/04/71	08/26/79		101.7	Pulmonary Thromboembolism
D-3 MED-LOW	838 M	56	0.48	5.09	11.0	17.8	06/08/71	07/20/84		157.4	Malignant Lymphoma, Lung Tmr
D-3 MED-LOW	795 F	54	0.49	5.40	10.0	15.0	01/20/71	09/06/83		151.5	Lung Tumor
D-3 MED-LOW	816 M	68	0.52	5.67	12.0	16.8	04/28/71	05/22/73		24.9	Sacrificed
D-3 MED-LOW	851 F	53	0.54	5.89	9.0	21.3	10/07/71	12/07/88		182.0	Thyroid Carc, Hypothyroidism
D-3 MED-LOW	918 M	74	0.58	6.43	11.5	16.0	06/08/72	07/06/72		0.9	Sacrificed
D-3 MED-LOW	834 F	67	0.68	7.44	9.0	17.8	06/08/71	07/05/79		98.9	Pyometra

* Indicates age in months since birth, all other ages are in months since exposure.

DOSE-EFFECT STUDIES WITH INHALED PU-239 OXIDE IN BEAGLES

DOSE GROUP	DOG IDENT	INITIAL ALVEOLAR DEPOSITION NCI	NCI/G LUNG	NCI/ KG	INHALATION EXPOSURE WEIGHT (KG)	AGE* (MO)	DATE	DATE OF DEATH	MONTHS SINCE INHALATION 9/30/88	DEATH	COMMENTS ON DEAD DOGS
D-3 MED-LOW	797 F	85	0.70	7.73	11.0	16.4	03/04/71	06/16/86		182.4	Lung Tumor
D-3 MED-LOW	848 F	75	0.72	7.94	9.5	21.3	10/07/71	10/02/86		179.8	Acute Pneumonia
D-3 MED-LOW	827 F	89	0.74	8.09	11.0	16.7	04/26/71	01/06/85		164.4	Acute Pneumonitis
D-3 MED-LOW	697 M	140	0.85	9.33	15.0	19.5	10/30/70	05/08/80		114.3	Cardiac Valve Insufficiency
D-3 MED-LOW	750 M	118	0.93	10.26	11.5	19.8	01/20/71	08/28/84		161.2	Lung Tmr, Malignant Lymphoma
D-3 MED-LOW	884 M	123	1.12	12.30	10.0	17.8	10/08/71	09/12/84		155.2	Lung Tumor
D-3 MED-LOW	844 F	135	1.17	12.86	10.5	17.6	06/08/71	08/08/85		170.0	Nephropathy,Lung Tumor
D-3 MED-LOW	905 F	127	1.38	14.94	8.5	15.9	11/10/71	02/07/83		134.9	Malignant Lymphoma
D-4 MEDIUM	866 M	200	1.35	14.81	13.5	17.4	07/06/71	06/27/84		155.7	Lung Tumor
D-4 MEDIUM	809 F	157	1.36	14.95	10.5	15.3	03/04/71	05/28/81		122.8	Liver Cirr,Thy Tm,Addison's
D-4 MEDIUM	784 F	158	1.37	15.05	10.5	16.2	12/21/70	07/07/82		138.5	Lung Tumor
D-4 MEDIUM	835 F	163	1.48	16.30	10.0	16.4	04/26/71	06/25/78		86.0	Reticulum Cell Sarcoma
D-4 MEDIUM	839 F	189	1.49	16.43	11.5	16.3	04/26/71	02/03/86		177.3	Lung Tumor,Bile Duct Carcinom
D-4 MEDIUM	814 F	140	1.50	16.47	8.5	15.1	03/04/71	10/17/79		103.5	Lung Tumor, Thyroid Adenoma
D-4 MEDIUM	836 M	256	1.66	18.29	14.0	17.8	08/08/71	03/16/81		117.3	Lung Tumor
D-4 MEDIUM	819 F	163	1.74	19.18	8.5	16.2	06/08/71	08/20/85		170.4	Nephropathy,Lung Tumor
D-4 MEDIUM	888 M	274	1.76	19.57	14.0	17.1	10/08/71	07/02/79		92.8	Lung Tumor
D-4 MEDIUM	824 F	227	1.79	19.74	11.5	18.1	06/08/71	01/26/81		115.6	Bronchopneumonia
D-4 MEDIUM	860 M	254	1.85	20.32	12.5	17.3	08/08/71	06/24/82		132.5	Lung Tumor
D-4 MEDIUM	833 F	248	2.37	26.11	9.5	16.5	04/26/71	04/04/83		143.3	Metritis,Adrenal & Thyr Tumr
D-4 MEDIUM	810 F	302	2.39	26.26	11.5	15.3	03/04/71	09/09/81		126.2	Lung Tumor
D-4 MEDIUM	794 M	444	2.60	28.65	15.5	17.7	03/04/71	02/17/81		119.5	Pituitary Tumor, Cushing's
D-4 MEDIUM	854 M	485	2.64	29.06	18.0	21.3	10/08/71	01/25/82		123.8	Lung Tumor
D-4 MEDIUM	478 M	298	2.71	29.80	10.0	84.0	10/09/70	10/16/70		0.2	Sacrificed
D-4 MEDIUM	808 F	270	2.89	31.76	8.5	14.6	02/10/71	09/09/82		138.9	Lung Tumor
D-4 MEDIUM	805 F	257	3.12	34.27	7.5	18.5	06/08/71	07/22/82		133.5	Esophageal & Lung Tumor
D-4 MEDIUM	812 M	438	3.19	35.04	12.5	17.1	04/26/71	11/12/79		102.8	Lung Tumor
D-4 MEDIUM	857 M	486	3.40	37.38	13.0	17.3	08/08/71	07/01/80		108.8	Lung Tumor
D-4 MEDIUM	892 M	494	3.59	39.52	12.5	16.0	11/10/71	10/26/81		119.5	Lung Tumor
D-4 MEDIUM	816 M	398	3.62	39.80	10.0	16.8	04/26/71	05/11/71		0.5	Sacrificed
D-4 MEDIUM	777 M	546	3.97	43.68	12.5	20.2	03/04/71	03/26/80		108.7	Lung Tumor
D-4 MEDIUM	803 M	547	4.32	47.57	11.5	18.1	04/28/71	11/10/77		78.5	Interstitial Pneumonitis
D-5 MED-HIGH	787 M	651	4.73	52.08	12.5	19.5	03/04/71	02/08/79		95.2	Lung Tumor, Intestinal Tumor
D-5 MED-HIGH	840 F	703	4.92	54.08	13.0	17.7	06/08/71	04/29/80		106.7	Lung Tumor
D-5 MED-HIGH	727 M	733	5.33	58.64	12.5	18.8	10/26/70	11/10/76		72.5	Lung Tumor
D-5 MED-HIGH	898 F	711	5.39	59.25	12.0	16.0	11/10/71	02/03/81		110.8	Uri Bladr & Lung & Adr Tumor
D-5 MED-HIGH	858 F	818	5.72	62.92	13.0	18.2	07/07/71	06/02/79		93.8	Lung Tumor
D-5 MED-HIGH	759 M	809	6.13	67.42	12.0	18.3	12/21/70	08/02/75		53.4	Lung Tumor
D-5 MED-HIGH	864 F	801	6.62	72.82	11.0	17.4	07/07/71	11/02/79		99.9	Lung Tumor
D-5 MED-HIGH	909 M	737	6.70	73.70	10.0	15.9	11/10/71	06/04/81		114.8	Lung Tumor
D-5 MED-HIGH	734 M	914	6.92	76.17	12.0	19.2	11/10/70	04/01/71		4.7	Sacrificed
D-5 MED-HIGH	837 M	1263	8.04	88.48	14.5	18.8	07/07/71	07/21/77		72.5	Lung Tumor
D-5 MED-HIGH	863 F	980	8.48	93.33	10.5	17.4	07/07/71	10/21/77		75.5	Lung Tumor

* Indicates age in months since birth, all other ages are in months since exposure.

DOSE-EFFECT STUDIES WITH INHALED PU-239 DXIDE IN BEAGLES

DOSE GROUP	DOG IDENT	INITIAL ALVEOLAR DEPOSITION NCI	NCI/G LUNG	NCI/ KG	INHALATION EXPOSURE WEIGHT (KG)	AGE* (MO)	DATE	DATE OF DEATH	MONTHS SINCE INHALATION 9/30/88	DEATH	COMMENTS ON DEAD DOGS
D-5 MED-HIGH	820 F	847	8.58	94.11	9.0	18.2	06/08/71	06/01/79		95.8	Lung Tumor
D-5 MED-HIGH	852 F	1187	9.38	103.22	11.5	21.3	10/08/71	02/22/78		76.5	Lung Tumor
D-5 MED-HIGH	880 F	840	9.55	105.00	8.0	17.8	10/08/71	12/04/78		85.9	Lung Tumor
D-5 MED-HIGH	889 F	1089	9.90	108.90	10.0	16.0	11/10/71	09/20/79		94.3	Lung Tumor, Osteoarthropathy
D-5 MED-HIGH	783 M	1394	10.14	111.52	12.5	19.0	02/10/71	12/03/75		57.7	Lung Tumor
D-5 MED-HIGH	804 M	1344	10.18	112.00	12.0	20.5	07/07/71	08/18/74		37.4	Lung Tumor, Rad. Pneumonitis
D-5 MED-HIGH	873 M	1787	10.71	117.80	15.0	16.8	07/07/71	09/03/76		61.9	Lung Tumor
D-5 MED-HIGH	760 M	1378	10.89	119.83	11.5	19.3	01/20/71	08/15/73		30.8	Radiation Pneumonitis
D-5 MED-HIGH	796 F	1318	11.41	125.52	10.5	15.7	02/10/71	09/17/75		55.2	Lung Tumor, Osteoarthropathy
D-5 MED-HIGH	761 M	1460	12.07	132.73	11.0	19.3	01/20/71	11/02/76		69.4	Lung Tumor
D-5 MED-HIGH	709 M	1726	12.55	138.08	12.5	19.6	11/10/70	03/31/71		4.6	Sacrificed
D-5 MED-HIGH	772 M	1896	14.99	164.87	11.5	19.8	02/10/71	06/26/75		52.5	Lung Tumor, Osteoarthropathy
D-5 MED-HIGH	702 F	1682	15.29	168.20	10.0	19.8	11/10/70	03/31/71		4.6	Sacrificed
D-5 MED-HIGH	739 F	1511	17.17	188.88	8.0	18.5	11/10/70	04/01/71		4.7	Sacrificed
D-6 HIGH	753 F	2448	23.43	257.88	9.5	18.5	12/21/70	10/02/78		89.4	Lung Tumor
D-6 HIGH	817 M	3164	23.97	263.67	12.0	19.2	07/07/71	03/26/73		20.6	Radiation Pneumonitis
D-6 HIGH	829 M	3515	24.58	270.38	13.0	19.1	07/07/71	09/13/73		26.3	Radiation Pneumonitis
D-6 HIGH	890 F	3101	31.32	344.50	9.0	16.0	11/10/71	06/13/74		31.1	Radiation Pneumonitis
D-6 HIGH	435 F	3840	33.25	365.71	10.5	75.5	11/05/70	11/12/70		0.2	Sacrificed
D-6 HIGH	913 M	4900	35.84	392.00	12.5	17.4	07/19/72	08/18/72		1.0	Sacrificed
D-6 HIGH	908 F	6632	63.46	698.11	9.5	15.9	11/09/71	11/22/72		12.5	Radiation Pneumonitis
D-6 HIGH	896 F	5515	66.85	735.33	7.5	16.0	11/10/71	02/12/73		15.1	Radiation Pneumonitis
D-6 HIGH	747 F	7476	97.09	1068.00	7.0	19.6	01/20/71	01/13/72		11.8	Radiation Pneumonitis
D-6 HIGH	910 M	14267	103.76	1141.38	12.5	15.9	11/10/71	10/12/72		11.1	Radiation Pneumonitis

* Indicates age in months since birth, all other ages are in months since exposure.

DOSE-EFFECT STUDIES WITH INHALED PU-238 OXIDE IN BEAGLES

DOSE GROUP	DOG IDENT	INITIAL ALVEOLAR DEPOSITION NCI	NCI/G LUNG	NCI/ KG	INHALATION EXPOSURE WEIGHT (KG)	AGE* (MO)	DATE	DATE OF DEATH	MONTHS SINCE INHALATION 9/30/88	DEATH	COMMENTS ON DEAD DOGS
CONTROL	939 M	0	0.00	0.00				10/01/82		136.9*	Urinary Bladder Tumor
CONTROL	949 F	0	0.00	0.00				10/30/84		181.7*	Malignant Lymphoma
CONTROL	978 M	0	0.00	0.00				04/07/88		202.8*	Processing
CONTROL	990 F	0	0.00	0.00				07/08/79		97.4*	Pyometra
CONTROL	996 F	0	0.00	0.00				07/06/84		157.2*	Malignant Lymphoma
CONTROL	1005 M	0	0.00	0.00				02/24/87		188.8*	Processing
CONTROL	1007 F	0	0.00	0.00				03/29/88		201.9*	Processing
CONTROL	1024 M	0	0.00	0.00				07/13/87		192.9*	Processing
CONTROL	1038 M	0	0.00	0.00				12/16/86		183.9*	Hemangiosarcoma, Spleen
CONTROL	1045 M	0	0.00	0.00				06/08/86		177.6*	Renal Amyloid,Spl Hemangioma
CONTROL	1054 F	0	0.00	0.00					205.1*		
CONTROL	1061 F	0	0.00	0.00				07/07/81		118.2*	Malignant Lymphoma
CONTROL	1093 M	0	0.00	0.00				11/04/83		142.4*	Pituitary Tumor, Cushing's
CONTROL	1097 F	0	0.00	0.00				09/15/88		200.1*	Processing
CONTROL	1112 M	0	0.00	0.00				12/02/86		178.4*	Malignant Lymphoma
CONTROL	1116 F	0	0.00	0.00					200.1*		
CONTROL	1186 F	0	0.00	0.00				07/26/85		155.3*	Urinary Bladder Tumor
CONTROL	1197 M	0	0.00	0.00					193.0*		
CONTROL	1209 M	0	0.00	0.00					192.7*		
CONTROL	1225 F	0	0.00	0.00				10/10/87		180.2*	Pituitary Adenoma
CONTROL SACRIFICE	968 M	0	0.00	0.00				04/30/77		71.6*	Sacrificed
CONTROL SACRIFICE	1011 F	0	0.00	0.00				06/01/78		83.9*	Sacrificed
CONTROL SACRIFICE	1013 F	0	0.00	0.00				05/29/79		95.8*	Sacrificed
CONTROL SACRIFICE	1087 M	0	0.00	0.00				12/14/76		60.0*	Sacrificed
CONTROL SACRIFICE	1118 M	0	0.00	0.00				01/13/76		47.5*	Sacrificed
CONTROL SACRIFICE	1223 M	0	0.00	0.00				05/15/75		31.9*	Sacrificed
CONTROL SACRIFICE	1227 M	0	0.00	0.00				12/01/76		49.9*	Sacrificed
CONTROL SACRIFICE	1228 M	0	0.00	0.00				10/31/78		72.9*	Sacrificed
D-1 LOWEST	998 M	0	0.00	0.00	10.5	19.6	01/18/73	04/11/86		158.7	Lung Tumor
D-1 LOWEST	1003 M	0	0.00	0.00	14.0	19.6	01/18/73	04/01/87		170.4	Processing
D-1 LOWEST	1023 F	0	0.00	0.00	12.5	19.2	01/18/73	03/27/88		182.2	Processing
D-1 LOWEST	1039 M	0	0.00	0.00	11.0	17.0	01/18/73	07/04/86		161.5	Heart Failure
D-1 LOWEST	1044 F	0	0.00	0.00	11.5	17.0	01/18/73	08/31/88		187.4	Processing
D-1 LOWEST	1055 M	0	0.00	0.00	13.0	16.8	01/18/73	06/04/87		172.5	Processing
D-1 LOWEST	1063 M	0	0.00	0.00	14.5	16.7	01/18/73	11/11/80		93.8	Brain Tumor, Heart Tumor
D-1 LOWEST	1105 F	0	0.00	0.00	10.0	16.4	05/31/73	02/08/85		140.3	Malignant Lymphoma
D-1 LOWEST	1194 F	0	0.00	0.00	10.5	19.8	04/18/74	12/03/85		139.5	Malignant Lymphoma
D-1 LOWEST	1215 M	0	0.00	0.00	15.5	19.3	04/18/74	04/26/77		36.3	Sacrificed
D-1 LOWEST	1230 M	0	0.00	0.00	12.5	18.4	04/18/74	09/30/86		149.4	Hemangiosarcoma, Liver
D-1 LOWEST	951 M	2	0.01	0.14	14.0	19.3	12/19/72	02/14/83		121.9	Anesthetic Death
D-1 LOWEST	1008 M	2	0.01	0.15	13.5	19.8	01/18/73	10/24/85		153.2	Fibrosarcoma, Spleen
D-1 LOWEST	1193 F	2	0.01	0.16	12.5	19.8	04/18/74	01/22/86		141.2	Immune Hemolytic Anemia
D-1 LOWEST	959 M	3	0.02	0.22	13.5	19.2	12/19/72	08/22/84		138.1	Liver Abcess

* Indicates age in months since birth, all other ages are in months since exposure.

DOSE-EFFECT STUDIES WITH INHALED PU-238 OXIDE IN BEAGLES

DOSE GROUP	DOG IDENT	INITIAL ALVEOLAR DEPOSITION NCI	NCI/G LUNG	NCI/ KG	INHALATION EXPOSURE WEIGHT (KG)	AGE* (MO)	DATE	DATE OF DEATH	MONTHS SINCE INHALATION 9/30/88	DEATH	COMMENTS ON DEAD DOGS
D-1 LOWEST	1069 F	2	0.02	0.24	8.5	18.1	05/31/73	06/24/83		120.8	Malignant Lymphoma
D-1 LOWEST	1095 F	2	0.02	0.19	10.5	16.6	05/31/73	08/12/87		170.4	Processing
D-1 LOWEST	921 F	3	0.03	0.31	10.0	19.5	11/30/72	12/27/72		0.9	Sacrificed
D-1 LOWEST	923 F	3	0.03	0.35	8.5	19.5	11/30/72	01/26/73		1.9	Sacrificed
D-1 LOWEST	989 F	3	0.03	0.32	9.5	18.8	12/19/72	03/05/81		98.5	Bone Tumor, Fibrosarcoma
D-1 LOWEST	925 M	5	0.04	0.40	12.5	19.5	11/30/72	02/27/73		2.9	Sacrificed
D-1 LOWEST	1204 M	6	0.04	0.43	14.0	17.7	02/26/74		175.1		
D-1 LOWEST	970 F	6	0.05	0.55	11.0	19.2	12/19/72	01/04/77		48.5	Sacrificed
D-1 LOWEST	993 F	6	0.05	0.60	12.0	18.6	12/19/72	07/01/86		162.4	Malignant Lymphoma
D-1 LOWEST	1108 F	5	0.05	0.50	10.0	16.4	05/31/73	03/14/83		117.4	Adrenal Tmr,Osteoarthropathy
D-2 LOW	1065 F	6	0.05	0.60	10.0	18.3	05/31/73	04/10/86		154.3	Malignant Lymphoma, Lung Tmr
D-2 LOW	1082 M	11	0.06	0.69	16.0	18.0	05/31/73	12/04/79		78.1	Paralysis, Spinal Cord Degen.
D-2 LOW	1188 M	11	0.06	0.71	15.5	18.4	02/26/74	01/15/84		118.6	Metastatic Lng Tmr, Prim. Unk
D-2 LOW	1084 M	13	0.07	0.76	17.0	17.5	05/31/73		184.0		
D-2 LOW	1090 F	10	0.08	0.83	12.0	17.3	05/31/73	05/10/87		167.3	Heart Failure
D-2 LOW	1222 M	15	0.10	1.07	14.0	19.0	04/18/74	03/19/86		143.0	Malign (mediast) Mesothelioma
D-2 LOW	971 F	13	0.11	1.24	10.5	19.2	12/19/72	05/04/83		124.5	Hemangiosarcoma, Spleen
D-2 LOW	999 F	11	0.11	1.16	9.5	18.7	12/19/72	01/31/86		157.4	Nasal Sarcoma, Lung Tumor
D-2 LOW	1229 M	16	0.11	1.19	13.5	16.8	02/26/74	05/25/84		122.9	Pneumonia, Thyroid Tumor
D-2 LOW	1070 M	22	0.12	1.33	16.5	18.1	05/31/73	12/13/83		126.4	Round Cell Sarcoma: Kidney
D-2 LOW	1214 M	17	0.12	1.36	12.5	19.3	04/18/74	05/12/75		12.8	Sacrificed
D-2 LOW	956 M	17	0.14	1.55	11.0	19.2	12/19/72	01/27/87		169.3	Processing
D-2 LOW	1033 M	17	0.14	1.55	11.0	19.1	02/22/73	12/17/85		153.8	Lung Tumor
D-2 LOW	1036 F	16	0.14	1.52	10.5	18.2	02/22/73	05/06/87		170.4	Processing
D-2 LOW	1216 M	23	0.16	1.77	13.0	19.3	04/18/74	04/22/87		156.1	Malignant Lymphoma
D-2 LOW	1060 F	22	0.18	2.00	11.0	17.6	02/22/73	12/21/84		141.9	Pneumonia
D-2 LOW	981 M	30	0.21	2.31	13.0	19.0	12/19/72		189.4		
D-2 LOW	1046 M	27	0.22	2.45	11.0	18.1	02/22/73	12/15/87		177.7	Processing
D-2 LOW	1050 F	22	0.22	2.44	9.0	18.1	02/22/73	05/14/86		158.7	Lung Tumor
D-2 LOW	1078 F	29	0.22	2.42	12.0	18.0	05/31/73	11/09/83		125.3	Meningioma, Malignant
D-2 LOW	1207 F	22	0.24	2.59	8.5	17.6	02/26/74	08/11/88		173.5	Processing
D-2 LOW	1196 F	28	0.25	2.80	10.0	17.9	02/26/74		175.1		
D-2 LOW	1189 M	38	0.26	2.81	13.5	20.0	04/18/74	04/25/79		60.2	Sacrificed
D-2 LOW	930 M	38	0.27	2.92	13.0	19.2	11/30/72	12/28/72		0.9	Sacrificed
D-3 MED-LOW	1066 M	54	0.31	3.38	16.0	18.3	05/31/73	06/21/83		120.7	Malignant Lymphoma
D-3 MED-LOW	972 F	40	0.33	3.64	11.0	19.2	12/19/72	03/04/86		158.5	Allergic Bronchitis
D-3 MED-LOW	1089 F	41	0.34	3.73	11.0	17.3	05/31/73	08/21/88		182.7	Processing
D-3 MED-LOW	1310 M	54	0.34	3.72	14.5	18.5	03/04/75	04/01/77		24.9	Sacrificed
D-3 MED-LOW	1312 M	58	0.34	3.74	15.5	18.5	03/04/75	03/26/79		48.7	Sacrificed
D-3 MED-LOW	1311 M	54	0.36	4.00	13.5	18.5	03/04/75	04/03/78		37.0	Sacrificed
D-3 MED-LOW	1219 F	48	0.40	4.38	10.5	19.0	04/18/74	12/05/86		151.6	Chronic Nephropathy
D-3 MED-LOW	1317 M	72	0.41	4.50	16.0	18.1	03/04/75	04/01/77		24.9	Sacrificed
D-3 MED-LOW	1158 M	73	0.43	4.71	15.5	17.7	11/06/73	08/16/88		175.3	Processing

* Indicates age in months since birth, all other ages are in months since exposure.

DOSE-EFFECT STUDIES WITH INHALED PU-238 DXIDE IN BEAGLES

DOSE GROUP	DOG IDENT	INITIAL ALVEOLAR DEPOSITION NCI	NCI/G LUNG	NCI/ KG	INHALATION EXPOSURE WEIGHT (KG)	AGE* (MO)	DATE	DATE OF DEATH	MONTHS SINCE INHALATION 9/30/88	DEATH	COMMENTS ON DEAD DOGS
D-3 MED-LOW	1165 M	76	0.43	4.75	16.0	17.3	11/06/73	07/21/86		152.4	Acute Pneumonia
D-3 MED-LOW	1309 M	60	0.44	4.80	12.5	18.5	03/04/75	04/22/87		145.6	Hemangiosarcoma, Liver
D-3 MED-LOW	1318 M	67	0.46	4.98	13.5	18.1	03/04/75	03/08/76		12.2	Sacrificed
D-3 MED-LOW	929 F	41	0.50	5.47	7.5	19.2	11/30/72	01/25/73		1.8	Sacrificed
D-3 MED-LOW	1316 M	84	0.53	5.79	14.5	18.1	03/04/75		162.9		
D-3 MED-LOW	960 M	68	0.54	5.91	11.5	19.2	12/19/72	11/07/80		94.6	Malignant Lymphoma
D-3 MED-LOW	1072 M	98	0.54	5.94	16.5	18.1	05/31/73	09/22/83		123.7	Delayed Radiation Pneumonitis
D-3 MED-LOW	1190 F	71	0.54	5.92	12.0	18.1	02/26/74	05/09/85		134.4	Lung Tumor
D-3 MED-LOW	926 M	75	0.55	6.00	12.5	19.5	11/30/72	02/28/73		3.0	Sacrificed
D-3 MED-LOW	1315 M	90	0.55	6.00	15.0	18.1	03/04/75	03/31/77		24.9	Sacrificed
D-3 MED-LOW	982 M	76	0.58	6.33	12.0	19.0	12/19/72	01/29/86		157.3	Pneumonia, Thyroid Carcinoma
D-3 MED-LOW	1040 M	84	0.61	6.72	12.5	18.2	02/22/73	03/04/81		96.3	Parathyroid Adenoma
D-3 MED-LOW	1059 F	71	0.65	7.10	10.0	17.8	02/22/73	08/08/83		125.5	Malignant Lymphoma
D-3 MED-LOW	1319 M	89	0.67	7.33	13.5	18.1	03/04/75	03/09/76		12.2	Sacrificed
D-3 MED-LOW	1108 F	84	0.69	7.84	11.0	16.4	05/31/73	01/14/87		163.5	Posterior Paralysis
D-3 MED-LOW	1000 F	70	0.71	7.78	9.0	18.7	12/19/72	12/02/87		179.4	Processing
D-3 MED-LOW	1056 M	97	0.71	7.76	12.5	17.9	02/22/73	08/17/86		159.8	Pneumonia, Thyroid Carcinoma
D-3 MED-LOW	1004 M	116	0.73	8.00	14.5	19.6	01/18/73	04/30/87		171.3	Processing
D-3 MED-LOW	1026 M	116	0.78	8.59	13.5	19.2	01/18/73	11/13/85		153.8	Hepatic Displasia
D-3 MED-LOW	1043 F	98	0.89	9.80	10.0	18.1	02/22/73	09/21/81		102.9	Empyema, Pituit.T., Cushing's
D-3 MED-LOW	1031 F	76	0.92	10.13	7.5	19.1	02/22/73	05/04/84		134.3	Pneumonia
D-3 MED-LOW	1212 F	111	1.12	12.33	9.0	17.6	02/26/74	06/24/88		171.9	Processing
D-4 MEDIUM	1176 M	129	0.87	9.56	13.5	16.6	11/06/73	12/12/85		145.2	Hemangioma, Spleen
D-4 MEDIUM	1221 F	124	1.13	12.40	10.0	19.0	04/18/74	09/30/88		173.4	Processing
D-4 MEDIUM	1195 M	228	1.38	15.20	15.0	18.1	02/26/74	07/29/87		161.0	Chron Nephr,Bile Duct Adenoma
D-4 MEDIUM	1032 M	182	1.40	15.43	10.5	16.3	11/30/72	12/08/72		0.3	Sacrificed
D-4 MEDIUM	1053 F	148	1.42	15.58	9.5	17.9	02/22/73	02/02/85		143.3	Cushing's Disease
D-4 MEDIUM	997 M	203	1.60	17.65	11.5	19.6	01/18/73	05/08/86		159.6	Lung Tumor
D-4 MEDIUM	991 F	194	1.76	19.40	10.0	18.8	12/19/72	06/20/83		126.0	Urinary Bladder & Ovarian Tmr
D-4 MEDIUM	1177 M	262	1.76	19.41	13.5	16.6	11/06/73	03/12/85		136.1	Bone Tumor
D-4 MEDIUM	932 F	216	1.79	19.64	11.0	19.1	11/30/72	01/25/73		1.8	Sacrificed
D-4 MEDIUM	1103 F	260	1.89	20.80	12.5	16.5	05/31/73	04/08/83		118.2	Bone Tumor, Lung Tumor
D-4 MEDIUM	973 F	271	2.24	24.64	11.0	19.2	12/19/72	10/08/84		141.6	Bone Tumor
D-4 MEDIUM	931 F	289	2.39	26.27	11.0	19.1	11/30/72	12/28/72		0.9	Sacrificed
D-4 MEDIUM	1091 F	243	2.80	28.59	8.5	17.3	05/31/73	11/10/86		161.3	Thyroid Carcinoma
D-4 MEDIUM	1114 M	430	2.70	29.66	14.5	16.4	05/31/73	04/23/85		142.8	Bone Tumor,Bile Duct Carcinom
D-4 MEDIUM	1062 M	435	2.93	32.22	13.5	17.8	02/22/73	05/30/84		135.2	Bone Tumor, Lung Tumor
D-4 MEDIUM	934 M	454	3.08	33.63	13.5	19.1	11/30/72	03/01/73		3.0	Sacrificed
D-4 MEDIUM	1081 M	541	3.07	33.81	16.0	18.0	05/31/73	01/18/80		79.6	Hemangiosarcoma, Heart
D-4 MEDIUM	1030 F	340	3.25	35.79	9.5	19.1	02/22/73	04/14/83		121.7	Pneumonia, Rad. Pneumonitis
D-4 MEDIUM	1198 M	539	3.50	38.50	14.0	17.9	02/26/74	09/14/86		150.6	Acute Pneumonia, Lung Tumor
D-4 MEDIUM	952 F	365	3.69	40.58	9.0	19.2	12/19/72	06/03/83		125.4	Bone Tumor
D-4 MEDIUM	1166 M	673	4.08	44.87	15.0	17.3	11/06/73	06/23/84		127.5	Malignant Lymphoma
D-4 MEDIUM	1220 F	518	4.28	47.09	11.0	19.0	04/18/74	12/09/86		151.7	Malignant Lymphoma, Addison's
D-4 MEDIUM	992 F	555	4.39	48.28	11.5	18.8	12/19/72	07/26/84		139.2	Bone Tumor
D-4 MEDIUM	983 M	617	4.67	51.42	12.0	19.0	12/19/72	12/29/83		132.3	Adrenal & Pituitary Tumor

* Indicates age in months since birth, all other ages are in months since exposure.

DOSE-EFFECT STUDIES WITH INHALED PU-238 OXIDE IN BEAGLES

DOSE GROUP	OOG IDENT		INITIAL ALVEOLAR DEPOSITION NCI	NCI/G LUNG	NCI/ KG	INHALATION EXPOSURE WEIGHT (KG)	AGE* (MO)	DATE	DATE OF DEATH	MONTHS SINCE INHALATION 9/30/88	DEATH	COMMENTS ON DEAD DOGS
D-5 MED-HIGH	1191	F	591	4.48	49.25	12.0	19.8	04/18/74	03/21/77		35.1	Interstitial Pneumonitis
D-5 MED-HIGH	1157	M	700	4.71	51.85	13.5	17.7	11/06/73	03/02/84		123.8	Bone Tumor
D-5 MED-HIGH	1035	F	571	5.46	60.11	9.5	18.2	02/22/73	03/04/84		132.3	Bone Tumor, Cushing's Disease
D-5 MED-HIGH	1192	F	764	6.53	71.81	10.5	18.1	02/26/74	03/29/83		109.0	Bone Tumor
D-5 MED-HIGH	1140	M	1014	6.58	72.43	14.0	18.2	11/06/73	12/14/81		97.2	Bone Tumor
D-5 MED-HIGH	1071	M	1289	6.79	74.65	17.0	18.1	05/31/73	01/09/81		91.3	Bone Tumor, Lung Tumor
D-5 MED-HIGH	1173	M	1023	7.75	85.25	12.0	17.3	11/06/73	02/09/82		99.1	Bone Tumor
D-5 MED-HIGH	1178	M	1125	8.52	93.75	12.0	16.6	11/06/73	01/06/83		110.0	Bone Tumor, Lung Tumor
D-5 MED-HIGH	1047	M	900	8.61	94.74	9.5	18.1	02/22/73	10/05/82		115.4	Vertebral Disk Herniation
D-5 MED-HIGH	1109	F	1119	8.85	97.30	11.5	16.4	05/31/73	08/06/80		86.2	Bone & Lung Tumor, Addison's
D-5 MED-HIGH	1160	F	1344	10.18	112.00	12.0	17.3	11/06/73	09/22/81		94.5	Bone Tumor, Lung Tumor
D-5 MED-HIGH	1211	M	1764	11.08	121.88	14.5	17.6	02/26/74	05/17/82		98.6	Bone Tumor
D-5 MED-HIGH	1096	F	1478	12.20	134.18	11.0	16.8	05/31/73	05/08/78		59.2	Addison's Disease
D-5 MED-HIGH	1218	F	1710	12.95	142.50	12.0	17.3	02/26/74	04/24/81		86.9	Bone Tumor
D-5 MED-HIGH	1092	M	1848	13.44	147.84	12.5	17.3	05/31/73	10/23/78		64.8	Bone Tumor
D-5 MED-HIGH	1027	M	2148	13.95	153.43	14.0	19.2	01/18/73	12/01/78		70.4	Bone Tumor, Lung Tumor
D-5 MED-HIGH	1115	F	1885	14.90	163.91	11.5	16.1	05/31/73	07/11/78		61.3	Bone Tumor
D-5 MED-HIGH	974	F	1718	15.62	171.80	10.0	20.2	01/18/73	05/24/78		64.1	Bone Tumor
D-5 MED-HIGH	1079	M	2620	15.88	174.67	15.0	18.0	05/31/73	02/12/78		56.4	Addison's Disease, G.I. Tumor
D-5 MED-HIGH	1058	F	1907	16.51	181.62	10.5	17.8	02/22/73	11/01/79		80.3	Bone Tumor, Adrenal Tumor
D-6 HIGH	1002	M	2907	18.88	207.64	14.0	19.6	01/18/73	01/21/80		84.1	Bone Tumor, Lung Tumor
D-6 HIGH	1057	M	3116	20.98	230.81	13.5	17.9	02/22/73	03/07/79		72.4	Bone Tumor
D-6 HIGH	1009	M	3630	26.40	290.40	12.5	19.6	01/18/73	04/01/78		62.4	Lung Tumor, Osteoarthropathy
D-6 HIGH	1042	F	2959	28.32	311.47	9.5	19.1	02/22/73	11/10/78		68.6	Bone Tumor, Lung Tumor
D-6 HIGH	994	F	3453	31.39	345.30	10.0	19.6	01/18/73	07/04/76		41.5	Addison's Disease
D-6 HIGH	1006	F	3810	31.49	346.38	11.0	19.6	01/18/73	01/18/79		72.0	Bone Tumor, Lung Tumor
D-6 HIGH	976	F	3968	36.07	396.80	10.0	20.2	01/18/73	07/25/78		66.2	Bone Tumor, Lung Tumor
D-6 HIGH	1037	M	4854	44.13	485.40	10.0	18.2	02/22/73	11/21/78		68.9	Bone Tumor
D-6 HIGH	1143	M	7691	53.78	591.62	13.0	18.2	11/06/73	12/05/77		49.0	Bone Tumor, Lung Tumor
D-6 HIGH	1025	M	8479	57.10	628.07	13.5	19.2	01/18/73	03/17/77		49.9	Lung Tumor
D-6 HIGH	1084	M	9453	63.66	700.22	13.5	16.7	01/18/73	04/14/77		50.8	Bone Tumor, Lung Tumor
D-6 HIGH	1162	F	6959	70.29	773.22	9.0	17.3	11/06/73	12/19/78		61.4	Bone Tumor, Addison's Disease
D-6 HIGH	1175	F	8201	75.16	826.80	7.5	16.6	11/06/73	02/24/78		51.6	Lung Tumor

* Indicates age in months since birth, all other ages are in months since exposure.

INHALED PLUTONIUM NITRATE IN DOGS

DOSE GROUP	DOG IDENT	INITIAL ALVEOLAR DEPOSITION NCI	NCI/G LUNG	NCI/ KG	INHALATION EXPOSURE WEIGHT (KG)	AGE* (MO)	DATE	DATE OF DEATH	MONTHS SINCE INHALATION 9/30/88	DEATH	COMMENTS ON DEAD DOGS
CONTROL	1356 M	0	0.00	0.00				04/07/87		154.9*	Processing
CONTROL	1365 M	0	0.00	0.00				07/16/88		170.1*	Processing
CONTROL	1378 F	0	0.00	0.00				05/11/80		70.8*	Pneumonia
CONTROL	1388 M	0	0.00	0.00				09/11/81		86.7*	Sacrificed
CONTROL	1393 M	0	0.00	0.00				06/19/87		155.9*	Processing
CONTROL	1405 M	0	0.00	0.00				08/13/84		121.3*	Sacrificed, Heart Base Tumor
CONTROL	1409 M	0	0.00	0.00					170.8*		
CONTROL	1418 M	0	0.00	0.00					170.5*		
CONTROL	1425 M	0	0.00	0.00				08/02/82		96.5*	Status Epilepticus
CONTROL	1450 F	0	0.00	0.00				11/04/81		87.4*	Sacrificed
CONTROL	1455 F	0	0.00	0.00				08/20/87		156.5*	Processing
CONTROL	1483 F	0	0.00	0.00					168.9*		
CONTROL	1509 M	0	0.00	0.00				10/30/86		145.1*	Sacrificed
CONTROL	1516 F	0	0.00	0.00					167.9*		
CONTROL	1525 M	0	0.00	0.00				11/14/87		157.1*	Processing
CONTROL	1526 M	0	0.00	0.00					167.6*		
CONTROL	1528 F	0	0.00	0.00				04/06/87		149.2*	Cerebral hemorrhage
CONTROL	1543 M	0	0.00	0.00				08/12/86		141.3*	Vertebral Disc
CONTROL	1563 F	0	0.00	0.00					156.8*		
CONTROL	1572 F	0	0.00	0.00					156.7*		
CONTROL	1577 M	0	0.00	0.00					156.7*		
CONTROL	1584 F	0	0.00	0.00					156.6*		
CONTROL	1594 F	0	0.00	0.00					156.8*		
CONTROL	1608 M	0	0.00	0.00					156.4*		
CONTROL	1633 F	0	0.00	0.00				11/10/86		126.9*	Thyroid Tumor
CONTROL	1638 F	0	0.00	0.00				09/08/87		136.5*	Processing
VEHICLE	1361 M	0	0.00	0.00	8.5	21.0	02/13/76		151.6		
VEHICLE	1381 F	0	0.00	0.00	8.5	19.8	02/13/76		151.6		
VEHICLE	1392 M	0	0.00	0.00	13.0	22.0	04/22/76		149.3		
VEHICLE	1406 M	0	0.00	0.00	13.5	21.6	04/22/76	01/21/88		141.0	Processing
VEHICLE	1412 F	0	0.00	0.00	9.0	19.0	02/13/76		151.6		
VEHICLE	1421 M	0	0.00	0.00	13.0	23.3	06/23/76	02/26/88		140.1	Processing
VEHICLE	1457 F	0	0.00	0.00	12.0	20.6	04/22/76		149.3		
VEHICLE	1491 F	0	0.00	0.00	8.0	21.6	06/23/76		147.3		
VEHICLE	1504 F	0	0.00	0.00	10.0	20.9	06/23/76		147.3		
VEHICLE	1514 M	0	0.00	0.00	14.0	20.9	06/23/76	08/06/82		73.4	Malignant Lymphoma
VEHICLE	1524 M	0	0.00	0.00	12.0	21.5	07/27/76	03/27/88		140.0	Processing
VEHICLE	1531 F	0	0.00	0.00	9.0	20.9	07/27/76		146.1		
VEHICLE	1542 M	0	0.00	0.00	12.0	20.8	07/27/76		146.1		
VEHICLE	1566 M	0	0.00	0.00	14.0	18.3	03/15/77		138.5		
VEHICLE	1578 M	0	0.00	0.00	10.5	18.2	03/15/77		138.5		
VEHICLE	1593 F	0	0.00	0.00	11.0	18.0	03/15/77		138.5		
VEHICLE	1601 F	0	0.00	0.00	8.5	18.0	03/15/77		138.5		
VEHICLE	1620 M	0	0.00	0.00	11.0	21.1	12/01/77	01/06/87		109.2	Vertebral Disc
VEHICLE	1634 F	0	0.00	0.00	10.5	19.6	12/01/77		130.0		
VEHICLE	1651 F	0	0.00	0.00	11.0	19.2	12/01/77		130.0		

* Indicates age in months since birth, all other ages are in months since exposure.

INHALED PLUTONIUM NITRATE IN DOGS

DOSE GROUP	DOG IDENT	INITIAL ALVEOLAR DEPOSITION NCI	NCI/G LUNG	NCI/ KG	INHALATION EXPOSURE WEIGHT (KG)	AGE* (MO)	DATE	DATE OF DEATH	MONTHS SINCE INHALATION 9/30/88	DEATH	COMMENTS ON DEAD DOGS
D-1 LOWEST	1418 M	0	0.00	0.00	12.0	22.1	05/20/76		148.4		
D-1 LOWEST	1458 F	0	0.00	0.00	10.5	21.5	05/20/76		148.4		
D-1 LOWEST	1489 F	0	0.00	0.00	8.0	20.5	05/20/76	08/04/84		98.5	Esophageal Tumor
D-1 LOWEST	1501 M	0	0.00	0.00	14.0	20.4	05/20/76	01/03/84		91.5	Thyroid Tumor
D-1 LOWEST	1515 M	0	0.00	0.00	13.5	19.8	05/20/76		148.4		
D-1 LOWEST	1573 M	0	0.00	0.00	11.5	19.4	04/19/77		137.4		
D-1 LOWEST	1581 M	0	0.00	0.00	16.5	19.3	04/19/77	07/31/86		111.4	Hemangiosarcoma
D-1 LOWEST	1598 M	0	0.00	0.00	14.0	19.2	04/19/77		137.4		
D-1 LOWEST	1600 F	1	0.01	0.11	11.0	19.2	04/19/77		137.4		
D-1 LOWEST	1603 M	2	0.01	0.12	14.0	19.2	04/19/77		137.4		
D-1 LOWEST	1339 F	2	0.02	0.22	9.0	17.5	10/16/75	11/13/75		0.9	Sacrificed
D-1 LOWEST	1519 M	2	0.02	0.18	12.5	19.5	05/20/76		148.4		
D-1 LOWEST	1570 F	2	0.02	0.18	10.0	19.4	04/19/77	06/19/87		122.0	Stomach tumor
D-1 LOWEST	1465 F	4	0.03	0.35	12.0	21.0	05/20/76		148.4		
D-1 LOWEST	1470 F	3	0.03	0.29	10.5	21.0	05/20/76	04/09/84		94.7	Meningioma
D-1 LOWEST	1507 M	4	0.03	0.32	14.0	19.8	05/20/76	06/07/88		144.6	Processing
D-1 LOWEST	1592 F	4	0.03	0.29	13.5	19.2	04/19/77		137.4		
D-1 LOWEST	1607 M	5	0.03	0.35	13.0	19.0	04/19/77	07/26/88		135.2	Processing
D-1 LOWEST	1335 M	5	0.04	0.42	11.5	18.0	10/16/75	11/13/75		0.9	Sacrificed
D-1 LOWEST	1487 F	6	0.04	0.46	13.0	20.5	05/20/76		148.4		
D-1 LOWEST	1583 F	4	0.04	0.40	9.5	19.2	04/19/77		137.4		
D-1 LOWEST	1351 M	7	0.08	0.61	11.0	17.2	10/16/75	11/13/75		0.9	Sacrificed
D-1 LOWEST	1565 F	8	0.06	0.67	11.5	19.4	04/19/77	09/28/85		101.3	Hemangiosarcoma
D-2 LOW	1513 M	0	0.00	0.00	11.5	19.8	05/20/76		148.4		
D-2 LOW	1520 M	1	0.01	0.12	10.5	19.5	05/20/76		148.4		
D-2 LOW	1415 M	2	0.02	0.20	11.5	22.2	05/20/76		148.4		
D-2 LOW	1575 M	3	0.02	0.19	14.0	19.4	04/19/77	12/26/87		128.3	Prostate Tumor
D-2 LOW	1466 F	5	0.03	0.37	14.0	21.0	05/20/76		148.4		
D-2 LOW	1606 F	5	0.04	0.42	12.5	19.0	04/19/77		137.4		
D-2 LOW	1579 M	8	0.05	0.59	14.0	19.3	04/19/77		137.4		
D-2 LOW	1590 F	6	0.05	0.51	12.0	19.2	04/19/77	03/16/87		118.9	Mammary Tumor
D-2 LOW	1585 F	8	0.06	0.68	12.0	19.2	04/19/77		137.4		
D-2 LOW	1580 F	9	0.07	0.82	11.0	19.3	04/19/77		137.4		
D-2 LOW	1591 M	11	0.07	0.76	15.0	19.2	04/19/77		137.4		
D-2 LOW	1417 M	11	0.08	0.89	12.0	22.1	05/20/76		148.4		
D-2 LOW	1423 M	10	0.08	0.87	11.0	22.1	05/20/76		148.4		
D-2 LOW	1567 M	10	0.08	0.83	12.0	19.4	04/19/77		137.4		
D-2 LOW	1472 F	10	0.09	1.01	10.0	21.0	05/20/76		148.4		
D-2 LOW	1503 F	9	0.09	1.03	8.5	19.8	05/20/76	12/13/84		102.8	Thyroid Tumor
D-2 LOW	1602 M	15	0.09	1.03	14.5	19.2	04/19/77	08/10/86		111.7	Epilepsy
D-2 LOW	1484 F	11	0.10	1.08	10.0	20.5	05/20/76		148.4		
D-2 LOW	1599 F	10	0.10	1.14	9.0	19.2	04/19/77	03/12/86		106.7	Adrenal Tumor
D-2 LOW	1490 F	16	0.15	1.65	9.5	20.5	05/20/76		148.4		

* Indicates age in months since birth, all other ages are in months since exposure.

INHALED PLUTONIUM NITRATE IN DOGS

DOSE GROUP	DOG IDENT	INITIAL ALVEOLAR DEPOSITION NCI	NCI/G LUNG	NCI/ KG	INHALATION EXPOSURE WEIGHT (KG)	AGE* (MO)	DATE	DATE OF DEATH	MONTHS SINCE INHALATION 9/30/88	DEATH	COMMENTS ON DEAD DOGS
D-3 MED-LOW	1336 M	21	0.14	1.52	13.5	18.0	10/16/75	11/13/75		0.9	Sacrificed
D-3 MED-LOW	1341 F	19	0.16	1.78	10.5	17.2	10/16/75	11/13/75		0.9	Sacrificed
D-3 MED-LOW	1605 F	25	0.20	2.19	11.5	17.8	03/15/77	03/24/82		60.3	Sacrificed
D-3 MED-LOW	1386 M	34	0.21	2.36	14.5	22.0	04/20/76	01/04/86		116.5	Hemangiosarcoma
D-3 MED-LOW	1389 M	27	0.23	2.54	10.5	21.9	04/20/76	06/04/76		0.5	Sacrificed
D-3 MED-LOW	1413 F	29	0.24	2.68	11.0	18.2	01/20/76	03/01/85		109.3	Malignant Lymphoma
D-3 MED-LOW	1445 F	34	0.24	2.60	13.0	21.0	04/20/76	05/05/76		0.5	Sacrificed
D-3 MED-LOW	1568 M	46	0.29	3.17	14.5	18.3	03/15/77	12/02/86		116.6	Pneumonia
D-3 MED-LOW	1595 M	50	0.29	3.23	15.5	18.0	03/15/77		138.5		
D-3 MED-LOW	1390 M	43	0.30	3.29	13.0	21.9	04/20/76	05/04/76		0.5	Sacrificed
D-3 MED-LOW	1391 M	54	0.30	3.26	16.5	21.9	04/20/76	07/22/85		111.0	Thyroid Tumor, Lung Tumor
D-3 MED-LOW	1587 M	53	0.31	3.40	15.5	18.1	03/15/77	01/14/86		108.0	Hemangiosarcoma, Lung Tumor
D-3 MED-LOW	1359 M	50	0.32	3.57	14.0	20.2	01/20/76	01/23/76		0.1	Sacrificed
D-3 MED-LOW	1540 M	54	0.32	3.51	15.5	20.7	07/22/76	11/25/86		124.1	Lung tumor
D-3 MED-LOW	1344 F	41	0.33	3.60	11.5	17.2	10/16/75	11/14/75		1.0	Sacrificed
D-3 MED-LOW	1589 F	41	0.34	3.75	11.0	18.0	03/15/77	06/08/82		62.8	Sacrificed, Lung Tumor
D-3 MED-LOW	1588 M	50	0.36	3.98	12.5	18.1	03/15/77	03/22/78		12.2	Sacrificed
D-3 MED-LOW	1529 F	43	0.37	4.08	10.5	20.8	07/22/76	10/19/76		2.9	Sacrificed
D-3 MED-LOW	1574 M	46	0.38	4.21	11.0	18.2	03/15/77		138.5		
D-3 MED-LOW	1375 F	50	0.40	4.35	11.5	19.1	01/20/76	01/23/76		0.1	Sacrificed
D-3 MED-LOW	1564 F	40	0.40	4.44	9.0	18.3	03/15/77	03/20/78		12.2	Sacrificed
D-3 MED-LOW	1444 F	49	0.41	4.50	11.0	21.0	04/20/76		149.4		
D-3 MED-LOW	1439 F	53	0.42	4.61	11.5	21.0	04/20/76	03/30/88		143.3	Processing
D-3 MED-LOW	1523 F	55	0.42	4.60	12.0	21.3	07/22/76		146.3		
D-3 MED-LOW	1539 M	65	0.45	4.99	13.0	20.7	07/22/76	10/20/76		3.0	Sacrificed
D-3 MED-LOW	1380 M	63	0.46	5.06	12.5	19.1	01/20/76	05/24/87		136.1	Processing
D-3 MED-LOW	1407 F	50	0.51	5.56	9.0	18.5	01/20/76	01/23/76		0.1	Sacrificed
D-3 MED-LOW	1569 F	58	0.53	5.82	10.0	18.2	03/15/77	09/27/87		126.4	Lung tumor
D-3 MED-LOW	1576 M	70	0.53	5.86	12.0	18.2	03/15/77	03/17/82		60.1	Sacrificed
D-3 MED-LOW	1582 F	57	0.54	5.98	9.5	18.1	03/15/77	08/12/88		136.9	Processing
D-3 MED-LOW	1571 F	68	0.57	6.22	11.0	18.2	03/15/77	03/21/78		12.2	Sacrificed
D-3 MED-LOW	1427 F	68	0.62	6.81	10.0	21.1	04/20/76		149.4		
D-3 MED-LOW	1522 F	78	0.71	7.78	10.0	21.3	07/22/76	10/18/76		2.9	Sacrificed
D-3 MED-LOW	1363 M	85	0.74	8.09	10.5	20.2	01/20/76	05/12/87		135.7	Processing
D-3 MED-LOW	1604 M	85	0.74	8.10	10.5	18.0	03/15/77		138.5		
D-3 MED-LOW	1530 F	72	0.76	8.41	8.5	20.8	07/22/76	09/17/86		121.9	Bone Tumor, Lung Tumor
D-3 MED-LOW	1458 F	61	0.79	8.68	7.0	20.5	04/20/76	04/21/87		132.0	Pneumonia
D-3 MED-LOW	1598 F	93	1.06	11.65	8.0	18.0	03/15/77	03/10/82		59.8	Sacrificed
D-3 MED-LOW	1422 F	99	1.12	12.35	8.0	18.1	01/20/76		152.3		

* Indicates age in months since birth, all other ages are in months since exposure.

INHALED PLUTONIUM NITRATE IN DOGS

DOSE GROUP	DOG IDENT	INITIAL ALVEOLAR DEPOSITION NCI	NCI/G LUNG	NCI/ KG	INHALATION EXPOSURE WEIGHT (KG)	AGE* (MO)	DATE	DATE OF DEATH	MONTHS SINCE INHALATION 9/30/88	DEATH	COMMENTS ON DEAD DOGS
D-4 MEDIUM	1637 M	192	1.45	15.99	12.0	18.9	11/07/77		130.8		
D-4 MEDIUM	1404 M	260	1.48	16.25	16.0	21.5	04/20/76	02/03/84		93.5	Pleuritis
D-4 MEDIUM	1521 F	205	1.49	16.37	12.5	21.3	07/22/76	06/07/85		106.5	Bone Tumor, Lung Tumor
D-4 MEDIUM	1656 M	211	1.54	16.90	12.5	18.4	11/07/77		130.8		
D-4 MEDIUM	1379 M	278	1.74	19.16	14.5	19.1	01/20/76	01/20/88		144.0	Processing
D-4 MEDIUM	1362 M	267	1.87	20.54	13.0	20.2	01/20/76		152.3		
D-4 MEDIUM	1639 F	248	2.05	22.57	11.0	18.5	11/07/77		130.8		
D-4 MEDIUM	1647 M	294	2.05	22.58	13.0	18.5	11/07/77		130.8		
D-4 MEDIUM	1640 M	307	2.06	22.71	13.5	18.5	11/07/77	03/20/84		76.4	Lung Tumor
D-4 MEDIUM	1645 F	267	2.13	23.39	11.0	18.5	11/07/77	08/07/86		105.0	Lung Tumor
D-4 MEDIUM	1534 M	295	2.14	23.57	12.5	20.8	07/22/76	05/26/85		106.1	Congestive Heart Failure
D-4 MEDIUM	1414 F	233	2.35	25.86	9.0	18.2	01/20/76	08/14/86		126.8	Bone, Lung, and Liver tumors
D-4 MEDIUM	1618 F	277	2.40	26.36	10.5	20.3	11/07/77		130.8		
D-4 MEDIUM	1385 M	373	2.42	26.63	14.0	19.0	01/20/76	07/12/84		101.7	Bone Tumor, Lung Tumor
D-4 MEDIUM	1408 F	331	2.62	28.77	11.5	18.5	01/20/76	10/12/83		92.7	Bone Tumor
D-4 MEDIUM	1428 F	378	3.12	34.36	11.0	21.1	04/20/76	10/28/85		114.3	Bone Tumor, Lung Tumor
D-4 MEDIUM	1535 F	345	3.13	34.48	10.0	20.7	07/22/76	10/06/86		122.5	Bone and lung tumors
D-4 MEDIUM	1446 F	354	3.22	35.40	10.0	21.0	04/20/76	08/10/86		123.7	Pyometra, Liver tumor
D-4 MEDIUM	1384 M	463	3.24	35.65	13.0	20.2	01/20/76	08/02/84		102.4	Lung Tumor
D-4 MEDIUM	1387 F	345	4.48	49.30	7.0	19.0	01/20/76	08/13/80		54.8	Bone Tumor
D-5 MED-HIGH	1329 F	363	3.30	38.27	10.0	18.0	10/16/75	11/14/75		1.0	Sacrificed
D-5 MED-HIGH	1346 M	656	4.42	48.59	13.5	17.2	10/16/75	11/14/75		1.0	Sacrificed
D-5 MED-HIGH	1648 M	811	5.90	64.90	12.5	18.5	11/07/77	07/11/85		92.1	Bone Tumor, Lung Tumor
D-5 MED-HIGH	1347 F	688	6.95	76.47	9.0	17.2	10/16/75	11/14/75		1.0	Sacrificed
D-5 MED-HIGH	1659 F	990	7.32	80.51	12.3	18.3	11/07/77	08/19/83		69.4	Bone Tumor
D-5 MED-HIGH	1638 M	1212	8.48	93.25	13.0	18.9	11/07/77	05/03/83		65.8	Bone Tumor
D-5 MED-HIGH	1621 M	1334	8.66	95.26	14.0	20.3	11/07/77	11/19/84		84.4	Bone Tumor, Lung Tumor
D-5 MED-HIGH	1646 F	1061	8.77	96.45	11.0	18.5	11/07/77	11/11/82		60.1	Bone Tumor
D-5 MED-HIGH	1429 M	1376	9.62	105.85	13.0	23.2	06/23/76	05/29/81		59.2	Bone Tumor, Lung Tumor
D-5 MED-HIGH	1641 M	1275	9.66	106.24	12.0	18.5	11/07/77	06/28/85		91.7	Lung Tumor
D-5 MED-HIGH	1660 M	1518	10.22	112.41	13.5	18.3	11/07/77	09/05/84		81.9	Bone Tumor, Lung Tumor
D-5 MED-HIGH	1508 M	1716	10.76	118.37	14.5	20.9	06/23/76	01/24/80		43.0	Bone Tumor
D-5 MED-HIGH	1655 M	1094	11.05	121.56	9.0	18.4	11/07/77	03/18/85		88.3	Bone Tumor, Lung Tumor
D-5 MED-HIGH	1652 F	1320	12.00	131.95	10.0	18.4	11/07/77	07/20/83		68.4	Bone Tumor, Lung Tumor
D-5 MED-HIGH	1619 F	1490	12.32	135.50	11.0	20.3	11/07/77	01/21/83		62.5	Bone Tumor
D-5 MED-HIGH	1512 M	2411	14.81	160.71	15.0	20.9	06/23/76	12/23/79		42.0	Bone Tumor
D-5 MED-HIGH	1419 M	1559	14.92	164.11	9.5	23.3	06/23/76	10/22/82		76.0	Bone Tumor, Lung Tumor
D-5 MED-HIGH	1498 F	2018	16.68	183.45	11.0	21.5	06/23/76	04/09/82		69.5	Bone Tumor, Lung Tumor
D-5 MED-HIGH	1502 F	3008	20.25	222.80	13.5	20.9	06/23/76	01/21/81		55.0	Bone Tumor, Lung Tumor
D-5 MED-HIGH	1485 F	2330	21.18	233.00	10.0	21.7	06/23/76	12/30/80		54.2	Bone Tumor
D-5 MED-HIGH	1471 F	2508	21.71	238.82	10.5	22.1	06/23/76	05/01/79		34.2	Radiation Pneumonitis
D-5 MED-HIGH	1492 F	2473	24.98	274.82	9.0	21.6	06/23/76	10/16/80		51.8	Bone Tumor
D-5 MED-HIGH	1459 F	2645	26.72	293.89	9.0	22.6	06/23/76	09/25/80		51.1	Rad. Pneumonitis, Lung Tumor

* Indicates age in months since birth, all other ages are in months since exposure.

INHALED PLUTONIUM NITRATE IN DOGS

DOSE GROUP	DOG IDENT	INITIAL ALVEOLAR DEPOSITION NCI	NCI/G LUNG	NCI/ KG	INHALATION EXPOSURE WEIGHT (KG)	AGE* (MO)	DATE	DATE OF DEATH	MONTHS SINCE INHALATION 9/30/80	DEATH	COMMENTS ON DEAD DOGS
D-6 HIGH	1518 M	3586	29.48	324.09	11.0	20.6	06/23/76	12/18/79		41.8	Rad. Pneumonitis, Lung Tumor
D-6 HIGH	1420 M	3840	30.36	333.91	11.5	23.3	06/23/76	07/12/78		24.8	Radiation Pneumonitis
D-6 HIGH	1617 F	5185	49.82	545.79	9.5	20.8	06/23/76	11/02/77		16.3	Radiation Pneumonitis
D-6 HIGH	1510 F	6969	55.09	606.02	11.5	20.9	06/23/76	11/09/77		16.6	Radiation Pneumonitis
D-6 HIGH	1424 M	7881	69.83	768.12	10.0	23.2	06/23/76	08/31/77		14.3	Radiation Pneumonitis

* Indicates age in months since birth, all other ages are in months since exposure.

Publications and Presentations

PUBLICATIONS

Alpen, E. L., R. O. Chester, and D. R. Fisher, eds. 1988. Population Exposure from the Nuclear Fuel Cycle. Gordon and Breach Science Publishers, New York, NY.

Bair, W. J., J. F. Park, G. E. Dagle, and A. C. James. Overview of the biological consequences of exposure to plutonium and the higher actinides. *Radiat. Protect. Dosim.* (in press).

Bean, R. M., B. L. Thomas, E. K. Chess, J. G. Pavlovich, and D. L. Springer. Quantitative determination of polycyclic aromatic hydrocarbon adducts to deoxyribonucleic acid using GC/MS techniques. In: Polynuclear Aromatic Hydrocarbons: 11th International Symposium, NBS, September 23-25, 1987, Gaithersburg, MD. Lewis Publishers, Chelsea, MI (in press).

Birchall, A. and A. C. James. A microcomputer algorithm for solving first order compartmental models involving recycling. *Health Phys.* (in press).

Burditt, A. K., Jr. and F. P. Hungate. 1988. Gamma irradiation as a quarantine treatment for cherries infested by western cherry fruit fly (diptera: tephritidae). *J. Econ. Entomol. 81*: 859-862.

Cheng, Y. S. and O. R. Moss. 1988. Inhalation exposure systems, Chapter 1. In: Concepts in Inhalation Toxicology, R. O. McClellan, and R. F. Henderson (eds.). Hemisphere Publishing Corporation, Washington, DC.

Cockerham, L. G. and B. J. Kelman. 1988. Summary of Symposium on Acute Radiation-Induced Injury. *Fundam. Appl. Toxicol. 11*: 571-579.

Cross, F. T. 1987. Health effects, pp. 215-248. In: Environmental Radon, C. R. Cothern and J. E. Smith, Jr. (eds.). Plenum Publishing Corp., New York, NY.

Cross, F. T. 1988. Effects of radon progeny on laboratory animals, pp. 430-444. In: Health Risks of Radon and Other Internally Deposited Alpha-Emitters, Appendix III, NAS/NRC BEIR-IV Report. National Academy Press, Washington, DC.

Cross, F. T. 1988. Evidence of lung cancer from animal studies, Chapter 9, pp. 373-404. In: Radon and Its Decay Products in Indoor Air, W. W. Nazaroff and A. V. Nero, Jr. (eds.). John Wiley & Sons, Inc., New York, NY.

Cross, F. T., R. A. Gies, E. F. Blanton, R. L. Buschbom, G. E. Dagle, E. S. Gilbert, H. A. Ragan, and C. O. Romsos. 1988. Inhalation hazards to uranium miners, pp. 35-37. In: Pacific Northwest Laboratory Annual Report for 1987 to the DOE Office of Energy Research, Part 1, Biomedical Sciences. NTIS, Springfield, VA.

Cross, F. T., R. A. Gies, R. L. Buschbom, W. C. Cannon, G. E. Dagle, H. S. DeFord, M. E. Frazier, R. F. Jostes, F. C. Leung, J. A. Reese, S. Marks, L. L. Scott, G. L. Stiegler, and R. B. Westerberg. 1988. Mechanisms of radon injury, pp. 39-40. In: Pacific Northwest Laboratory Annual Report for 1987 to the DOE Office of Energy Research, Part 1, Biomedical Sciences. NTIS, Springfield, VA.

Dankovic, D. A., D. L. Springer, D. B. Mann, B. L. Thomas, L. G. Smith, and R. M. Bean. 1988. Preparation of microgram quantities BAP-DNA adducts using rat hepatocytes *in vitro*. *Carcinogenesis* (in press).

Dankovic, D. A., B. L. Thomas, R. C. Zangar, D. W. Later, and D. L. Springer. Inhibition of benzo(a)pyrene-7,8-diol formation in vitro by complex organic mixtures. *Toxicology* (in press).

Dauble, D. D., D. A. Dankovic, C. S. Abernethy, and R. H. Gray. Induction of hepatic aryl hydrocarbon hydroxylase activity in rainbow trout (Salmo Gairdneri) exposed to coal liquids. *Comp. Biochem. Physiol.* (in press).

Denham, D. H., F. T. Cross, and J. K. Soldat. Health effects estimation: Methods and results for uranium mill tailings contaminated properties. In: Proceedings of the 191st National Meeting of the American Society, April 13-18, 1986, New York, NY (in press).

Douthart, R. J., J. E. Schmaltz, and J. J. Thomas. 1988. Color graphics representations of large sequences in the GEM environment. *Nucleic Acids Res. 16*: 1657-1666.

Dowla, H. A., C. L. Sanders, and M. C. Datta. 1987. Hemoglobin components in irradiated adult rats of two different strains. In: The Realities of Cancer in Minority Communities, Proceedings of the First Biennial Symposium on Minorities and Cancer. The University of Texas System Cancer Center, M. D.Anderson Hospital and Tumor Institute, Houston, TX.

Dungan, C. F. and R. A. Elston. 1987. Histological and ultrastructural characteristics of bacterial destruction of the hinge ligaments of cultured juvenile Pacific oysters, Crassostrea gigas. *Aquaculture* 72: 1-14.

Dunnick, J. K., S. L. Eustis, W. W. Piegorsch, and R. A. Miller. 1988. Respiratory tract lesions in F344/N rats and B6C3F1 mice after inhalation exposure to 1,2-epoxybutane. *Toxicology* 50: 69-82.

Elston, R. A. 1988. Bonamiasis in North America. Special Publication of the French Government Agency for the Exploration and Utilization of Marine Resources (IFREMER), Paris, France.

Elston, R. A. 1988. Mitigation of Bonamiasis Through Resistant Oyster Stocks and Stock Management. Special Publication of the French Government Agency for the Exploration and Utilization of Marine Resources (IFREMER), Paris, France.

Elston, R. A. 1988. Resistant flat oysters offer hope against bonamiasis. Parasitol. *Today. 4:* 120-121.

Frazier, M. E. 1987. Overview of the role of oncogenes in radiation induced carcinogenesis: Oncogenes or potential molecular workers of radiation damage, pp. 55-58. In: Cellular and Molecular Aspects of Radiation-Induced DNA Damage and Repair, Proceedings of the DOE Contractors' Workshop, March 10-11, 1987, Albuquerque, NM. CONF-8703182, NTIS, Springfield, VA.

Frazier, M. E., T. M. Seed, L. L. Scott, and G. L. Stiegler. 1987. Radiation-induced carcinogenesis in dogs, pp. 488-493. In: Radiation Research, Vol. 2, E. M. Fielden, J. F. Fowler, J. H. Hendry, and D. Scott, (eds.), Proceedings of the Eighth International Congress of Radiation Research, July 19-24, 1987, Edinburgh, Scotland. Taylor & Francis, London, England.

Frazier, M. E., G. L. Stiegler, L. L. Scott, S. R. Peterson, and R. J. Rausch. Oncogenes in radiation-induced lung tumors. In: Proceedings, Seventh International Congress of the International Radiation Protection Association, April 10-17, 1987, Sydney, Australia (in press).

Gilbert, E. S. 1988. The Hanford study: Issues in analyzing and interpreting data from occupational studies. In: Health Effects of Low Dose Ionising Radiation - Recent Advances and Their Implications. British Nuclear Energy Society, Thomas Telford, Ltd, London, England.

Gilbert, E. S., J. A. Mahaffey, G. R. Petersen, C. R. Strader, L. E. Sever, S. E. Dietert and B. D. Breitenstein. 1988. Human health effects studies: Hanford programs protect workers' health. In: Profile, a quarterly publication by PNL for DOE/RL.

Gilbert, E. S., Park, J. F., and R. L. Buschbom. Time-related factors in the study of risks in animals and man. *Health Phys.* (in press).

Hackett, P. L., T. J. Mast, M. G. Brown, M. L. Clark, J. J. Evanoff, S. E. Rowe, B. J. McClanahan, R. L. Buschbom, J. R. Decker, R. L. Rommereim, and R. B. Westerberg. 1988. Sperm-Head Morphology Study in B6C3F1 Mice Following Inhalation Exposure to 1,3-Butadiene, PNL-6459. Pacific Northwest Laboratory, Richland, WA.

Hackett, P. L., T. J. Mast, M. G. Brown, M. L. Clark, J. J. Evanoff, S. E. Rowe, B. J. McClanahan, R. L. Buschbom, J. R. Decker, R. L. Rommereim, and R. B. Westerberg. 1988. Dominant Lethal Study in CD-1 Mice Following Inhalation Exposure to 1,3-Butadiene, PNL-6545. Pacific Northwest Laboratory, Richland, WA.

Hackett, P. L., M. R. Sikov, T. J. Mast, M. G. Brown, R. L. Buschbom, M. L. Clark, J. R. Decker, J. J. Evanoff, R. L. Rommereim, S. E. Rowe, and R. B. Westerberg. 1987. Inhalation Developmental Toxicology Studies of 1,3-Butadiene in the Rat, PNL-6414. Pacific Northwest Laboratory, Richland, WA.

Hackett, P. L., M. R. Sikov, T. J. Mast, M. G. Brown, R. L. Buschbom, M. L. Clark, J. R. Decker, J. J. Evanoff, R. L. Rommereim, S. E. Rowe, and R. B. Westerberg. 1987. Inhalation Developmental Toxicology Studies: Teratology Study of 1,3-Butadiene in Mice, PNL-6412. Pacific Northwest Laboratory, Richland, WA.

Haugen, D. A., M. S. Swanson, F. R. Kirchner, C. A. Reilly, D. D. Mahlum, and D. L. Springer. 1987. Toxicological interactions between carcinogenic and weakly carcinogenic mixtures in the mouse-skin initiation-promotion system, pp. 379-386. In: Health and Environmental Research on Complex Organic Mixtures, R. H. Gray, E. K. Chess, P. J. Mellinger, R. G. Riley, and D. L. Springer (eds.), Proceedings of the 24th Hanford Life Sciences Symposium, October 20-24, 1985, Richland, WA. CONF-851027, NTIS, Springfield, VA.

James, A. C. 1988. Lung dosimetry, pp. 259-309. In: Radon and Its Decay Products in Indoor Air, W. W. Nazaroff and A. V. Nero (eds.). Wiley Interscience, New York, NY.

James, A. C. 1988. The physics and dosimetry of inhaled radon and daughter products, pp. 195-215. In: Proceedings of the Toxicology Forum 1988 Annual Summer Meeting, Given Institute of Pathobiology, July 18-22, 1988, Aspen CO. Toxicology Forum, Inc., Washington, DC.

James, A. C. and A. Birchall. Progress in lung modeling by the ICRP Task Group. *Radiat. Protect. Dosim.* (in press).

James, A. C., J. C. Strong, K. D. Cliff, and E. Stranden. The significance of equilibrium and attachment in radon daughter dosimetry. *Radiat. Protect. Dosim.* (in press).

Kaune, W. T. 1988. Physical interaction of 1-Hz to 100-Hz electric and magnetic fields with living organisms, pp. 129-161. In: Proceedings of the 22nd Annual Meeting of the National Council on Radiation Protection and Measurements: Nonionizing Radiation and Ultrasound, April 2-3, 1986, Washington, DC. NCRP, Bethesda, MD.

Kent, M. L., C. F. Dungan, R. A. Elston, and R. A. Holt. 1988. Cytophage sp. (Cytophagales) infection in seawater pen-reared Atlantic salmon Salmo salar. *Dis. Aquat. Org.* 4: 173-179.

Kent, M. L. and R. A. Elston. 1987. Pancreas disease in pen-reared Atlantic salmon in North America. *Bull. Eur. Assoc. Fish Pathol. 7*: 29-31.

Kent, M. L., R. A. Elston, T. A. Nerad, and T. K. Sawyer. 1987. An isonema-like flagellate (Protozoa: Mastigophora) infection in larval geoduck clams, Panope abrupta. *J. Invertebr. Pathol. 50*: 221-229.

Kent, M. L., J. W. Fournie, R. E. Snodgrass, and R. A. Elston. Goussia girellae sp. n. (eimeriorina: apicomplexa) in the opaleye Girella nigricans. *J. Protozool.* (in press).

Kent, M L., M. S. Meyers, D. E. Hinton, W. D. Eaton, and R. A. Elston. 1988. Suspected toxicopathic hepatic necrosis and megalocytosis in pen-reared Atlantic salmon, Salmo salar, in Puget Sound, Washington, USA. *Dis. Aquat. Org. 4*: 91-100.

Lamar, D. A. and N. C. Van Houten. 1988. List of DOE Radioisotope Customers with Summary of Radioisotope Shipments, FY 1987, PNL-6657. Pacific Northwest Laboratory, Richland, WA.

Leung, F. C. and L. R. Bohn. 1987. Elevated epidermal growth factor (EGF) receptor binding in dog lung tumors. In: DOE Contractor's Workshop, Albuquerque, NM.

Leung, F. C., L. R. Bohn, and G. E. Dagle. Elevated epidermal growth factor (EGF) receptor binding in dog lung tumors. In: Proceedings, Eighth International Congress of Endocrinology, Kyoto, Japan (in press).

Leung, F. C., L. R. Bohn, R. H. Towner, and N. G. Zimmermann. 1987. Sex-specific differences in circulating concentrations of growth hormone (GH) and hepatic GH receptor binding in broiler chickens. *Poultry Sci. 66* (Suppl. 1): 132.

Leung, F. C., J. R. Coleman, G. E. Dagle, and F. T. Cross. Involvement of growth factors and their receptors in radiation-induced carcinogenesis. In: Multilevel Health Effects Research: From Molecules to Man, Proceedings of the 27th Hanford Symposium on Health and the Environment, October 18-21, 1988, Richland, WA (in press).

Leung, F. C. and G. Saccomanno. Growth factors and their receptors in uranium-miner lung

tumors. In: Multilevel Health Effects Research: From Molecules to Man, Proceedings of the 27th Hanford Symposium on Health and the Environment, October 18-21, 1988, Richland, WA (in press).

Mahaffey, J. A. and J. A. Mewhinney. 1988. Modeling for scaling to man: Biology, dosimetry, and response. *Int. J. Radiat. Biol. 54*(4): 687-689.

Mahaffey, J. A. and J. A. Mewhinney (eds.) Modeling for Scaling to Man: Biology, Dosimetry, and Response, Proceedings of the 26th Hanford Life Sciences Symposium, October 20-23, 1987, Richland, WA. *Health Phys.* (Special Issue; in press).

Mann, D. B., G. L. Stiegler, and D. L. Springer. Mapping of benzo[a]pyrene adducts to the 5S rRNA gene carried on a plasmid target. In: Multilevel Health Effects Research: From Molecules to Man, Proceedings of the 27th Hanford Symposium on Health and the Environment, October 18-21, 1988, Richland, WA (in press).

Mast, T. J., H. Nau, W. Wittfoht, and A. G. Hendrickx. 1987. Teratogenicity and pharmacokinetics of valproic acid in the rhesus monkey, pp. 131-147. In: Pharmacokinetics in Teratogenesis, Vol. I, H. Nau and W. J. Scott (eds.). CRC Press, Inc., Boca Raton, FL.

Mast, T. J., R. L. Rommereim, and J. S Young. 1987. Pulmonary hypoplasia in rats prenatally exposed to coal-derived complex mixtures: Histological and subcellular development. In: DOE Contractor's Meeting on Chemical Toxicity, Office of Health and Environmental Research, U.S. Department of Energy, and Biomedical Sciences Division, Lawrence Livermore National Laboratory, June 23-26,1987, Monterey, CA. DOE/ER-0343, NTIS, Springfield, VA.

Mennear, J. H., E. E. McConnell, J. E. Huff, R. A. Renne, and E. Giddens. 1988. Inhalation toxicology and carcinogenesis studies of methylene chloride (dichloromethane) in F344/N rats and B6C3F$_1$ mice. *Ann. NY Acad. Sci. 534*: 343-352.

Mercer, B. W., W. Wakamiya, S. E. Petty, J. A. Strand, and D. D. Mahlum. Assessment of synfuel spill cleanup options. In: Proceedings of the DOE Workshop on Processing Needs and Methodology for Wastewater from the Conversion of Coal, Oil Shale and Biomass to Synfuels, July 23, 1981, Washington, DC. NTIS, Springfield, VA (in press).

Mialhe, E., V. Boulo, R. A. Elston, B. Hill, M. Hine, J. Montes, P. Van Banning, and H. Grizel. 1988. Serological analysis of bonamia in Ostrea edulis and Tiostrea lutaria using monoclonal and polyclonal antibodies. *Aquat. Living. Res.* 1: 67-69.

Miller, D. L. 1988. The influence of hematocrit on hemolysis by ultrasonically activated gas-filled micropores. *Ultrasound Med. Biol. 14*: 293-297.

Moss, O. R. and Y. S. Cheng. 1988. Generation and characterization of test atmosphere: Particles, Chapter 2. In: Concepts in Inhalation Toxicology, R. O. McClellan, and R. F. Henderson (eds.). Hemisphere Publishing Corporation, Washington, DC.

Park, J. F., C. L. Sanders, G. E. Dagle, R. E. Weller, E. Gilbert, R. Buschbom, K. E. McDonald, and K. E. Lauhala. Comparative toxicology of inhaled $^{239}PuO_2$ in dogs and rats. In: Modeling for Scaling to Man: Biology, Dosimetry, and Response, Proceedings of the 26th Hanford Life Sciences Symposium, October 20-23, 1987, Richland, WA (in press).

Poston, T. M., R. M. Bean, D. R. Kalkwarf, B. L. Thomas, M. L. Clark, and B. W. Killand. 1988. Initial characterization of photooxidation products of SGF No. 2 fog oil and toxicity to Hyallela azteca. *Environ. Toxicol. Chem. 7*: 753-762.

Pyne, J. W., Jr., D. L. Stewart, J. Fredrickson, and B. W. Wilson. 1987. Solubilization of Leonardite by an extracellular fraction from Coriolus versicolor. *Appl. Environ. Microbiol. 53*: 2844-2848.

Ragan, H. A. Comparative hematology. In Clinical Hematology, M. M. Wintrobe, G. R. Lee, and J. K. Athens (eds.). Lea and Febiger, Philadelphia, PA (in press).

Ragan, H. A. Markers of renal function and injury. In: Clinical Chemistry of Laboratory Animals, W. F. Loeb and F. W. Quinby (eds.). University Park Press, Baltimore, MD (in press).

Reilly, C. A. and R. A. Renne. 1988. Toxicological effects of coal-based synfuels. Chapter 3, pp. 57-245. In: Toxicology of Coal Conversion Processing, R. H. Gray, H. Drucker,

and M. J. Massey (eds.). John Wiley & Sons, New York, NY.

Rhoads K., J. P. Geraci, J. A. Mahaffey, B. W. Killand, and C. L. Sanders. Lung clearance and fate of inhaled transuranic oxides in combination with other radionuclides or with external neutron and gamma exposure. In: Proceedings of the Sixth International Symposium in Conjunction with the Second International Workshop on Lung Dosimetry, British Occupational Hygiene Association, September 1985, Cambridge, England (in press).

Rudolf, G., W. Stahlhofen, and A. C. James. Extrathoracic aerosol deposition for nose and mouth breathing: Intercomparison and model. *J. Aerosol Med.* (in press).

Sanders, C. L., K. E. McDonald, and J. A. Mahaffey. 1988. Lung tumor response to inhaled Pu and its implications for radiation protection. Health Phys. 55(2): 455-462.

Sanders, C. L., K. E. McDonald, and K. E. Lauhala. 1988. SEM autoradiography: Aggregation of inhaled $^{239}PuO_2$. *Int. J. Radiat. Biol. 54*: 115-121.

Sanders, C. L., K. E. McDonald, and K. E. Lauhala. Quantitative scanning electron microscopic autoradiography of inhaled $^{239}PuO_2$. *Health Phys.* (in press).

Sanders, C. L., K. E. McDonald, and J. A. Mahaffey. 1988. Lung tumor response to inhaled Pu and its implications for radiation protection. In: Radiation Protection--A Look to the Future, W. J. Bair (ed.), Proceedings of the 25th Hanford Life Sciences Symposium, October 21-23, 1986, Richland, WA. *Health Phys.* (Special Issue) *55*: 455-462.

Sasser, L. B., D. L. Lundstrom, R. C. Zangar, D. L. Springer, and D. D. Mahlum. Elevated blood pressure and heart rate in rats exposed to a coal-derived complex organic mixture. *J. Appl. Toxicol.* (in press).

Seed, T. M., L. V. Kaspar, D. J. Grdina, and M. E. Frazier. 1987. Chronic radiation-induced leukemogenesis: Elevation of hematopoietic progenitor repair functions during preclinical phases, p. 8A. In: Cellular and Molecular Aspects of Radiation-Induced DNA Damage and Repair, Proceedings of the DOE Contractors' Workshop, March 10-11, 1987, Albuquerque, NM. CONF-8703182, NTIS, Springfield, VA.

Sikov, M. R., D. R. Fisher, J. M. Selby, and J. B. Martin. 1987. Protection of the fetus from radiation: Are current standards satisfactory? *Health Phys. 52* (1): 525-526.

Solleveld, H. A., R. A. Miller, D. A. Banas, and G. A. Boorman. 1988. Primary cardiac hemangiosarcomas induced by 1,3-butadiene in B6C3F1 hybrid mice. *Toxicol. Pathol. 16*: 46-52.

Springer, D. L., D. A. Dankovic, B. E. Thomas, K. E. Hopkins, and R. M. Bean. 1987. Metabolism and DNA binding of BaP in the presence of complex organic mixtures, pp. 369-378. In: Health and Environmental Research on Complex Organic Mixtures, R. H. Gray, E. K. Chess, P. J. Mellinger, R. G. Riley, and D. L. Springer (eds.), Proceedings of the 24th Hanford Life Sciences Symposium, October 20-24, 1985, Richland, WA. CONF-851027, NTIS, Springfield, VA.

Springer, D. L., D. B. Mann, D. A. Dankovic, B. L. Thomas, C. W. Wright, and D. D. Mahlum. Influences of complex organic mixtures on tumor initiating activity, DNA binding and adducts of benzo(a)pyrene. *Carcinogenesis* (in press).

Springer, D. L. and R. C. Zangar. Influence of imprinting agents on cytochrome P450 expression. In: Multilevel Health Effects Research: From Molecules to Man, Proceedings of the 27th Hanford Symposium on Health and the Environment, October 18-21, 1988, Richland, WA (in press).

Stahlhofen, W., G. Rudolf, and A. C. James. Intercomparison of experimental regional deposition data. *J. Aerosol Sci.* (in press).

Stranden, E., K. Magnus, A. C. James, B. M. R. Green, and T. Strand. Radon and lung cancer: An epidemiological study in Norway. *Radiat. Protect. Dosim.* (in press).

Thompson, R. C. 1988. The legacy of life-span dog studies. In: Radiation Protection--A Look to the Future, W. J. Bair (ed.), Proceedings of the 25th Hanford Life Sciences Symposium, October 21-23, 1986, Richland, WA. *Health Phys.* (Special Issue) *55*: 483-485.

Turker, M. S., R. J. Monnat, K. I. Fukuchi, P. A. Johnston, C. E. Ogburn, R. E. Weller, J. F. Park, and G. M. Martin. 1988. A novel class of unstable 6-thioguanine-resistant cells from dog and human kidneys. *Cell Biol. Toxicol. 4*: 211-223.

Wehner, A. P. 1988. Indoor Air Pollution. VII. Organic Particles and Vapors. *MEDICEF Direct Information 1*: 268-299.

Wehner, A. P. and G. E. Dagle. 1988. XXXII. Experimentell induzierte Atemwegserkrankungen im Tiermodell, pp. 1-16. In: Das Gehirn und seine Erkrankungen (II). Psychosomatik-Gentechnologie-Atemwegserkrankungen-Mykosen. MEDICENALE XVIII, E. H. Graul, S. Pütter, and D. Loew (eds.). MEDICE, Iserlohn, Germany.

Weller, R. E. 1988. Paraneoplastic syndromes, pp. 819-827. In: Handbook of Small Animal Practice, R. V. Morgan (ed.). Churchill Livingstone, New York, NY.

Williams, A. R., M. McHale, M. Bowditch, D. L. Miller, and B. Reed. 1987. Effects of MHz ultrasound on electrical pain threshold perception in humans. *Ultrasound Med. Biol. 13*: 249-258.

Wilson, B. W., R. M. Bean, J. Pyne, D. L. Stewart, and J. Fredrickson. Microbial beneficiation of low rank coals. In: Proceedings, Workshop on Biological Conversion of Coal, October 1986, Electric Power Research Institute, Palo Alto, CA (in press).

Wilson, B. W. and R. A. Pelroy. Effects of catalytic hydrogenation on coal liquids which exhibit microbial mutagenic activity. *Toxicol. Environ. Chem. Rev.* (in press).

Wright, C. W., E. K. Chess, D. J. Hendren, D. L. Stewart, D. D. Mahlum, and B. W. Wilson. 1988. Chemical and biological analyses of feeds and product streams from two petroleum resid/coal coprocessing technologies. *Fuel 67*: 1283-1284.

Wright, C. W., E. K. Chess, R. B. Lucke, W. C. Weimer, D. W. Later, D. D. Mahlum, D. L. Stewart, and B. W. Wilson. 1987. Methods for separating chemical classes of coal liquefaction materials, pp. 49-61. In: Health and Environmental Research on Complex Organic Mixtures, R. H. Gray, E. K. Chess, P. J. Mellinger, R. G. Riley, and D. L. Springer (eds.), Proceedings of the 24th Hanford Life Sciences Symposium, October 20-24, 1985, Richland, WA. CONF-851027, NTIS, Springfield, VA.

Wright, C. W., E. K. Chess, R. A. Renne, and R. L. Buschbom. 1988. Effects of nitrosation on the chemical composition and epidermal carcinogenicity of the nitrogen-rich fraction of a high-boiling coal liquid. *J. Appl. Toxicol. 8*: 95-104.

Wright, C. W., D. W. Later, E. K. Chess, R. B. Lucke, D. L. Stewart, R. A. Pelroy, D. D. Mahlum, and B. W. Wilson. 1987. Comparative biology and chemistry of boiling point fractions from different coal liquefaction processes, pp. 199-210. In: Health and Environmental Research on Complex Organic Mixtures, R. H. Gray, E. K. Chess, P. J. Mellinger, R. G. Riley, and D. L. Springer (eds.), Proceedings of the 24th Hanford Life Sciences Symposium, October 20-24, 1985, Richland, WA. CONF-851027, NTIS, Springfield, VA.

Yates, R. W. and R. E. Weller. 1988. Have you seen the cardiopulmonary form of parvovirus infection? pp. 380-386, Veterinary Medicine, April. Beecham Laboratories, Bristol, TN.

Zangar, R. C., L. B. Sasser, D. D. Mahlum, R. H. Abhold, and D. L. Springer. 1987. Cardiovascular effects in rats following exposure to a high-boiling coal liquid. *Fundam. Appl. Toxicol. 9*: 659-667.

PRESENTATIONS

Carbaugh, E. H., W. A. Decker, and M. J. Swint. (Presented by A. C. James). 1988. Medical and Health Physics Management of a Plutonium Wound. Presented at the CEA/DOE/CEC Workshop on the Biological Assessment of Occupational Exposure to Actinides, May 30-June 2, 1988, Versailles, France.

Creim, J. A., R. H. Lovely, D. L. Miller, and L. E. Anderson. 1988. Effects of Magnetic Fields on Calcium Ion Related Neurological Function. Presented at the DOE/EPRI Contractors Review, October 30-November 3, 1988, Phoenix, AZ.

Cross, F. T. 1988. Evidence of Lung Cancer Risk from Animal Studies. Presented at the 24th Annual Meeting of the NCRP, April 30, 1988, Washington, DC.

Dagle, G. E., J. F. Park, E. S. Gilbert, and R. E. Weller. 1988. Risk Estimates for Lung Tumors from Inhaled $^{239}PuO_2$, $^{238}PuO_2$, and $^{239}Pu(NO_3)_4$ in Beagle Dogs. Presented at the Workshop on Biological Assessement of Occupational Exposure to Actinides, May 30-June 2, 1988, Versailles, France.

Dill, J. A., R. B. Westerberg, L. A. Pingel, and W. C. Forsythe. 1988. Automated Determination of Formic Acid Vapors Using Long Pathlength Infrared Spectroscopy. Presented at the American Chemical Society Meeting, July 1, 1988, Spokane, WA.

Douthart, R. J. 1988. Computer-Aided Design in Molecular Biology. Presented at the Synphar Laboratories, Inc. Workshop, August 14-18, 1988, Radium Hot Springs, Alberta, Canada.

Douthart, R. J. 1988. Simulated Cloning and Large Sequence Representations in the CAGE/GEM Environment. Presented at the Oncogene Symposium, October 30-31, 1988, Seattle, WA.

Douthart, R. J. 1988. Simulated Cloning and Large Sequence Representations in the CAGE/GEM Environment. Presented at the Washington Exhibition of Science and Technology, October 17, 1988, Seattle, WA.

Douthart, R. J. 1988. The Sequence Attributes Method for Determining Correlations Between Amino Acid Sequence and Protein Secondary Structure. Presented at the Department of Energy, June 10, 1988, Washington, DC.

Elston, R. A. 1988. Progression, Remission, and Transplantation of Hemic Neoplasia in the Bay Mussel, *Mytilus edulis*. Presented at the Fourth International Society for Developmental and Comparative Immunology Congress, July 24-29, 1988, Nottingham, England.

Fisher, D. R. 1988. The Dosimetry of Inhaled Plutonium. Presented at Texas A&M University, October 12, 1988, College Station, TX.

Fisher, D. R. 1988. The Microdosimetry of Monoclonal Antibodies Labeled With Alpha Emitters. Presented at Harvard University Medical School, Joint Center for Radiation Therapy, July 8, 1988, Boston, MA.

Fisher, D. R. 1988. The Microdosimetry of Radon Daughters in the Respiratory Tract. Presented at the DOE Radon Contractors Meeting, May 3-4, 1988, Berkeley, CA.

Fisher, D. R. 1988. The Microdosimetry of Alpha Emitters in Radioimmunotherapy. Presented at the 35th Annual Meeting of the Society of Nuclear Medicine, June 14-17, 1988, San Francisco, CA.

Fisher, D. R. and J. B. Martin. 1988. Internal Dosimetry and Other Health Physics Considerations in High-Dose Radioimmunotherapy. Presented at the 33rd Annual Meeting of the Health Physics Society, July 4-8, 1988, Boston, MA.

Frazier, M. E., T. M. Seed, L. L. Scott, and G. L. Stiegler. 1988. Evidence for Oncogene Activation in Radiation-Induced Carcinogenesis. Presented at the 27th Hanford Life Sciences Symposium, October 18-20, 1988, Richland, WA.

Gies, R. A., F. T. Cross, and R. F. Jostes. 1988. An *In Vitro* System for Exposing Cells to Radon Gas. Presented at the 1988 Annual Health Physics Society Meeting, July 6, 1988, Boston, MA.

Gieschen, A. W., R. J. Weigel, K. H. Stoney, and R. B. Westerberg. 1988. Determination of Chloropyrene and Related Compounds in Inhalation Chambers by Gas Chromatography. Presented at the American Chemical Society Meeting, July 1, 1988, Spokane, WA.

Gilbert, E. S. 1988. Health Effects Studies and the Hanford Site. Presentations to the Hanford Guard, Building Trades, January 1988, Richland, WA.

Gilbert, E. S. 1988. Health Effects Studies and the Hanford Site. Presented at the Benton-Franklin Medical Society, February 16, 1988, Richland, WA.

Gilbert, E. S. 1988. Radon Risk in Animals with Reference to Man. Presented at the 27th Hanford Symposium on Health and the Environment, October 18-21, 1988, Richland, WA.

Gilbert, E. S. 1988. The Hanford Mortality Study. Presented at the International Agency for Research on Cancer Meeting to consider pooled analyses of cancer risk in nuclear workers, June 7-10, 1988, Lyon, France.

Gilbert, E. S. 1988. The Hanford Mortality Study. Presented at the Physics Department Seminar, Washington State University, March 1988, Pullman, WA.

Gilbert, E. S. 1988. The Hanford Mortality Study. Presented at the Workshop on Planning a Collaborative Study of Nuclear Utility Workers, February 9, 1988, Cherry Hill, NJ.

Greenspan, B. J. and O. R. Moss. 1988. Development of a Hand-Held Metered Dose Inhaler. Presented at the Seventh International Congress on Aerosols in Medicine, September 25-29, 1988, Rochester, NY.

James, A. C. 1988. Radon Dosimetry and the Projection of Risk. Presented at the APCA '88, 81st Annual Meeting of the Air Pollution Control Association Meeting, June 19-24, 1988, Dallas, TX.

James, A. C. 1988. Task Group Progress on Lung Deposition, Clearance and Dosimetry Models. Presented at the ICRP Committee II Meeting, July 18, 1988, Seattle, WA.

James, A. C. 1988. The Physics and Dosimetry of Inhaled Radon and Daughter Products. Presented at the Summer Toxicology Forum, July 19-22, 1988, Aspen, CO.

James, A. C. and A. Birchall. 1988. Progress in Lung Modeling by the ICRP Task Group. Presented at the CEA/DOE/CEC Workshop on the Biological Assessment of Occupational Exposure to Actinides, May 30-June 2, 1988, Versailles, France.

Kelman, B. J. and M. R. Sikov. 1988. Analytical Components in Modeling Transplacental Movements of the Heaviest Metals (Z 82). Presented at the 27th Annual Meeting of the Society of Toxicology, February 16-19, 1988, Dallas, TX.

Kelman, B J. and M. R. Sikov. 1988. Evaluation of Changes in Placental Function Produced by Ultrasound Exposure. Presented at the 11th Rochester Trophoblast Conference and The European Placenta Group, October 9-12, 1988, Rochester. NY.

Lee, R. N., R. B. Westerberg, D. R. Baer, and M. H. Engelhard. 1988. The Application of Particle Induced X-Ray Emission to Inhalation Toxicology Studies. Presented at the American Chemical Society Meeting, July 1, 1988, Spokane, WA.

Mahlum, D. D. 1988. Residence Time and Tumor-Initiating Activity of Benzo(a)pyrene and a Complex Mixture. Presented at the Annual Meeting of the Society of Toxicology, February 16, 1988, Dallas, TX

Mahlum, D. D., D. L. Springer, D. B. Mann, and D. A. Dankovic. 1988. Can Carcinogenicity of BaP in Mixtures be Predicted by Chemical Analysis and DNA Binding? Presented at the 27th Hanford Life Sciences Symposium, October 18-20, 1988, Richland, WA.

Mann, D. B., G. L. Stiegler, and D. L. Springer. 1988. BaP Adduct Locations in the Xenopus 5S rRNA Gene. Presented at the 1988 Annual Meeting of the Pacific Northwest Association of Toxicologists, September 23-24, 1988, Moscow. ID.

Mann, D. B., G. L. Stiegler, and D. L. Springer. 1988. Mapping of BaP Adducts to the 5S rRNA Gene Carried on a Plasmid Target. Presented at the 27th Hanford Life Sciences Symposium. October 18-20, 1988, Richland, WA.

Masse, R. and F. T. Cross. 1987. Risk Considerations Related to Lung Modeling. Presented at the 26th Hanford Life Sciences Symposium, October 20-23, 1987, Richland, WA.

Mast, T. J., R. L. Rommereim, and J. S. Young. 1987. Pulmonary Hypoplasia in Rats Prenatally Exposed to Coal-Derived Complex Mixtures: Histological and Subcellular Development. Presented at the PANWAT Meeting, September 18-19, 1987, Port Townsend, WA.

Miller, D. 1987. The Influence of Hematocrit on Hemolysis from Ultrasonically Activated Gas-Filled Micropores. Presented at the 32nd Annual Convention of the American Institute of Ultrasound in Medicine, October 6-9, 1987, New Orleans, LA.

Miller, D. L., A. Delius, A. R. Williams, and W. Scharze. 1988. Cavitation in Flowing Media by Lithotripter Shock Waves *In Vitro* and *In Vivo*. Presented at the Acoustical Society of America Meeting, May 1988, Seattle, WA.

Miller, D. L., J. A. Reese, M. E. Frazier, and J. E. Morris. 1988. Analysis of Single Strand DNA Breaks in Human Leukocytes after Exposure to Ultrasound. Presented at the World Federation of Ultrasound in Medicine Convention, October 1988, Washington, DC.

Miller, D. L. and A. R. Williams. 1988. The Influence of Focusing, Standing Waves and Synchronous Intesity Modulation on Cavitation-Induced Hemolysis in a Rotating-Tube Ultrasound Exposure System. Presented at the World Federation of Ultrasound in Medicine Convention, October 1988, Washington, DC.

Miller, R. A., H. A. Ragan, B. J. Chou, R. L. Melnick, and J. H. Roycroft. 1988. Morphology of Neoplastic Lesions Induced by 1,3-Butadiene in B6C3F1 Mice. Presented at the Symposium on the Toxicology, Carcinogenesis and Human Health Aspects of 1,3-Butadiene in B6C3F1 Mice, April 12, 1988, Research Triangle Park, NC.

Moss, O.R. and R. Cuddihy. 1987. Dosimetry to Lung from Inhaled Pollutants. Presented at the 26th Hanford Life Sciences Symposium, October 23, 1987, Richland, WA.

Park, J. F., C. L. Sanders, G. E. Dagle, R. E. Weller, E. S. Gilbert, R. L. Buschbom, K. E. Lauhala, and K. E. McDonald. 1987. Comparative Toxicology of Inhaled $^{239}PuO_2$ in Dogs and Rats. Presented at the 26th Hanford Life Sciences Symposium, October 20-23, 1987, Richland, WA.

Sanders, C. L., K. E. McDonald, and K. E. Lauhala. 1988. Fluctuations in Bronchiolar Epithelial Proliferation Leading to Lung Tumor Formation. Presented at the XVII International Congress of the International Academy of Pathology and Eighth World Congress of Academic and Environmental Pathology, September 4-9, 1988, Dublin, Ireland.

Sanders, C. L., K. E. McDonald, and K. E. Lauhala. 1988. Relationship Between Bronchiolar Dose and Lung Carcinoma Induction Following Inhalation of $^{239}PuO_2$. Presented at the 14th L. H. Gray Conference, September 11-15, 1988, New College, Oxford, England.

Sanders, C. L., K. E. McDonald, and K. E. Lauhala. 1988. Scanning Electron Microscopic Examination of Lung Following Inhalation of $^{239}PuO_2$. Presented at the 33rd Annual Meeting of the Health Physics Society, July 4-8, 1988, Boston, MA.

Sasser, L. B. 1988. Elevated Blood Pressure in Mini Pigs Following Chronic Low Level Exposure to Cadmium. Presented at the Annual Meeting of the Pacific Northwest Association of Toxicologists, September 23-24, 1988, Moscow, ID.

Sasser, L. B., R. A. Miller, and J. A. Cushing. 1988. Subchronic Oral Toxicity Study of Sulfur Mustard in Rats. Presented at the 27th Annual Meeting of the Society of Toxicology, February 16-19, 1988, Dallas, TX.

Seed, T. M., M. E. Frazier, L. V. Kaspar, G. K. Niiro, and D. L. Lundberg. 1988. Chronic Radiation Leukemogenesis: Preclinical Responses of Hematopoietic Progenitors and Hematopoietins. Presented at the 36th Annual Meeting of the Radiation Research Society, April 16-25, 1988, Philadelphia, PA.

Sikov, M. R. 1987. Some Comparative Aspects of the Placental Transfer of the Actinides. Presented at the 26th Hanford Life Sciences Symposium, October 20-23, 1987, Richland, WA.

Sikov, M. R. 1988. Tumorigenesis Following Perinatal Radionuclide Exposure. Presented at the International Symposium on Perinatal and Multigeneration Carcinogenesis, World Health Organization, June 1, 1988, Leningrad, Russia.

Sikov, M. R. and B. J. Kelman. 1987. Development of Analytical Models for Placental Transfer of the Heaviest Metals. Presented at the Meeting of the Northwest Section of the Society for Experimental Biology and Medicine, October 10, 1987, Newport, OR.

Springer, D. L., E. R. Campbell, D. W. Later, D. A. Dankovic, and R. C. Zangar. 1988. Comparison of Capillary Supercritical Fluid Chromatography (SFC) and High Performance Liquid Chromatography (HPLC) for the Analysis of Pesticides in Biological Systems. Presented at the 27th Annual Meeting of the Society of Toxicology, February 16-18, 1988, Dallas, TX.

Springer, D. L., B. L. Thomas, D. A. Dankovic, D. B. Mann, E. K. Chess, and R. M. Bean. 1988. Characterization of Non-Classical DNA Adducts from Mouse Skin. Presented at the 27th Annual Meeting of the Society of Toxicology, February 16-19, 1988, Dallas, TX.

Springer, D. L. and R. C. Zangar. 1988. Influence of Imprinting Agents on Cytochrome P450 Expression. Presented at the 27th Hanford Life Sciences Symposium, October 18-20, 1988, Richland, WA.

Stewart, D. L., B. L. Thomas, J. K. Frederickson, and R. M. Bean. 1988. Qualitative and Quantitative Determinations of Fungal Biosolubilization of Coals. Presented at the 88th Annual Meeting of the American Society for Microbiology, May 8-13, 1988, Miami Beach, FL.

Stiegler, G. L. and M. E. Frazier. 1988. Molecular Analysis of Specific DNA Sequences Using the Polymerase Chain Reaction Method. Presented at the 27th Hanford Life Sciences Symposium, October 18-20, 1988, Richland, WA.

Tenforde, T. S. 1988. Review of Cellular and Molecular Biology. Presented at the EMF and Cancer Workshop, Electric Power Research Institute, July 13, 1988, Carmel, CA.

Tibbs, J. F., R. A. Elston, R. W. Dickey, and A. Guarino. 1988. Studies on the Accumulation of Antibiotics in Shellfish. Presented at the Aquaculture International Congress and Exposition, September 6-9, 1988, Vancouver, British Columbia, Canada.

Watson, C. R. Interlaboratory Toxicology Knowledge Base: Progress Report. Presented at the Meeting of DOE laboratory representatives conducting life-span studies in beagle dogs, January 1988, Salt Lake City, UT.

Wehner, A. P. and G. E. Dagle. 1988. Experimentell Induzierte Atemwegserkrankungen im Tiermodell. Presented at MEDICENALE XVIII, September 24-25, 1988, Iserlohn, West Germany (invited paper).

Weller, R. E. 1988. Advances in the Diagnosis and Treatment of Diseases of Laboratory Animals. Presented at the XI Panamerican Congress of Veterinary Sciences, August 14-20, 1988, Lima, Peru.

Weller, R. E. 1988. Use of Wild-Caught Versus Laboratory-Bred Monkeys: Scientific Issues. Presented at the WHO Consultation on the Role of Non-Human Primates in Malaria Vaccine Development, April 18-19, 1988, Geneva, Switzerland.

Weller, R. E., J. F. Park, G. E. Dagle, and R. F. Nachreiner. 1987. The Clinicopathological Features of Canine Testicular Neoplasms. Presented at the Seventh Annual Scientific Forum of the Veterinary Cancer Society, October 26, 1987, Madison, WI.

Westerberg, R. B., J. R. Decker, and T. J. Goehl. 1988. Analytical Chemistry Support of the Battelle Toxicology Inhalation Studies Performed at Battelle Northwest. Presented at the American Chemical Society Meeting, July 1, 1988, Spokane, WA.

Zangar, R. C. and D. L. Springer. 1988. The Effects of Four Potential Imprinting Agents on Aflatoxin Binding to DNA and on Growth and Survival Patterns. Presented at the Annual Meeting of the Pacific Northwest Association of Toxicologists, September 23-24, 1988, Moscow, ID.

Author Index

AUTHOR INDEX

Distribution

DISTRIBUTION

OFFSITE

G. E. Adams, Director
Medical Research Council
Radiobiology Unit
Harwell, Didcot
Oxon OX11 ORD
ENGLAND

W. R. Albers
EH-12, GTN
Department of Energy
Washington, DC 20545

R. E. Albert, Professor & Chairman
Department of Environmental Health
University of Cincinnati Medical Center
3223 Eden Avenue
Cincinnati, OH 45267-0056

E. L. Alpen
University of California Study Center
21 Stratton Ground
London SW1 P2HY
ENGLAND

T. W. Ambrose
Battelle - Seattle
4000 NE 41st Street
P.O. Box 5395
Seattle, WA 98105-5428

D. Anderson
ENVIROTEST
1108 NE 200th Street
Seattle, WA 98155-1136

G. Anderson
Department of Oceanography
University of Washington
Seattle, WA 98115

M. Anderson
Library
Department of National Health & Welfare
Ottawa, Ontario
CANADA

R. K. Appleyard, Director
Biology
European Atomic Energy Community, EURATOM
Brussels
BELGIUM

V. E. Archer
Rocky Mountain Center for Occupational & Environmental Health
Building 512
University of Utah
50 North Medical Drive
Salt Lake City, UT 84112

O. Auerbach
VA Hospital
East Orange, NJ 97919

D. C. Aumann
Institut für Physikalische Chemie
Universität Bonn
Abt. Nuklearchemie
Wegelerstraβe 12
5300 Bonn 1
FEDERAL REPUBLIC OF GERMANY

J. A. Auxier
IT/Radiological Services Laboratory
1550 Bear Creek Road
P.O. Box 549
Oak Ridge, TN 37831

F. Badgley
13749 NE 41st Street
Seattle, WA 98125

R. E. Baker
8904 Roundleaf Way
Gaithersburg, MD 20879-1630

M. R. Balakrishnan, Head
Library & Information Services
Bhabha Atomic Research Centre
Central Complex
Trombay, Bombay-400 085
INDIA

R. M. Baltzo
Radiological Safety Division
University of Washington
Seattle, WA 98105

R. W. Barber
EH-131, GTN
Department of Energy
Washington, DC 20545

G. W. Barendsen
Laboratory for Radiobiology
AMC, FO 212
Meibergdreef 9
1105 AZ Amsterdam
THE NETHERLANDS

A. D. Barker
Battelle Columbus Laboratories
505 King Avenue
Columbus, OH 43201

J. R. Barker
Office of Environmental Audit and Compliance
Department of Energy
Washington, DC 20545

W. W. Barker, Chairman
Department of Biology
Central Washington University
Ellensburg, WA 98926

N. F. Barr
ER-72, GTN
Department of Energy
Washington, DC 20545

J. K. Basson, Vice-President
Raad Op Atomic
Atoomkrag Energy Board
Privaatsk X 256
Pretoria 0001
REPUBLIC OF SOUTH AFRICA

J. W. Baum
Brookhaven National Laboratory
Building 703-M
Upton, Long Island, NY 11973

J. R. Beall
ER-72, GTN
Department of Energy
Washington, DC 20545

A. M. Beau, Librarian
Département de Protection Sanitaire
Commissariat à l'énergie Atomique
BP No. 6
F-92265 Fontenay-aux-Roses
FRANCE

G. Bengtsson, Director-General
Statens Stralskyddsinstitut
Box 60204
S-104 01 Stockholm
SWEDEN

D. J. Beninson
Gerencía de Protección Radiológica y Seguridad
Comisión Nacional de Energía Atómica
Avenida del Libertador 8250
2° Piso Of. 2330
1429 Buenos Aires
ARGENTINA

G. L. Bennett
Code RP
National Aeronautics & Space Administration
Washington, DC 20545

S. O. W. Bergstrom
Health and Safety Section
Aktiebolaget Atomienergi
Studsvik Energiteknik AB
S-611 82 Nykoping
SWEDEN

R. P. Berube
EH-151, GTN
Department of Energy
Germantown, MD 20545

M. H. Bhattacharyya
BIM Div., Bldg. 202
Argonne National Laboratory
9700 South Cass Avenue
Argonne, IL 60439

A. Bianco
International Atomic Energy Agency
V.I.C.
P.O. Box 200
A-1400 Vienna
AUSTRIA

W. R. Bibb
Energy Programs and Support Division
Department of Energy
P.O. Box B
Oak Ridge, TN 38731

R. W. Bistline
Rockwell International
Rocky Flats Plant
P.O. Box 464
Golden, C0 80401

B. B. Boecker
Inhalation Toxicology Research Institute
The Lovelace Foundation for Medical Education & Research
P.O. Box 5890
Albuquerque, NM 87108

V. P. Bond
Life Sciences, Chemistry and Safety
Brookhaven National Laboratory
Building 460
Upton, Long Island, NY 11973

J. Booz
KFA Jülich Institut für Medezin
Kernsforschungsanlage Jülich
Postfach 1913
D-5170 Jülich
FEDERAL REPUBLIC OF GERMANY

C. M. Borgstrom
Acting Director, NEPA
EH-25, Room 3E080
Department of Energy
1000 Independence Avenue, SW
Washington, DC 20585

J. D. Brain
Professor of Physiology
Director, Harvard Pulmonary Specialized Center of Research Harvard University School of Public Health
665 Huntington Avenue
Boston, MA 02115

L. C. Brazley, Jr.
NE-22, GTN
Department of Energy
Washington, DC 20545

A. Brink
SASOL-One Limited
P.O. Box 1
Sasolburg 9570
REPUBLIC OF SOUTH AFRICA

A. Brodsky
16412 Kipling Road
Derwood, MD 20855

F. W. Bruenger
Division of Radiobiology
Building 586
University of Utah
Salt Lake City, UT 84112

P. Buhl
FE-232, GTN
Department of Energy
Washington, DC 20545

D. R. Buhler, Chairman
Toxicology Program
Oregon State University
Corvallis, OR 97331

R. J. Bull
Associate Professor of Pharmacology/Toxicology
College of Pharmacy
Pullman, WA 99164-6510

M. J. Bulman, Librarian
Medical Research Council
Radiobiology Unit
Harwell, Didcot
Oxon OX11 ORD
ENGLAND

G. Burley
Office of Radiation Programs, ANR-458
Environmental Protection Agency
Washington, DC 20460

W. W. Burr, Chairman
Medical & Health Sciences Division
Oak Ridge Associated Universities
P.O. Box 117
Oak Ridge, TN 37830

L. K. Bustad
College of Veterinary Medicine
Washington State University
Pullman, WA 99164-7010

M. Calamosia
ENEA-LAB Fisica E Tossicologia Aerosol
Via Mazzini 2
I-40138 Bologna
ITALY

Cao Shu-Yuan, Deputy Head
Laboratory of Radiation Medicine
North China Institute of Radiation Protection
P.O. Box 120
Tai-yuan, Shan-Xi
THE PEOPLE'S REPUBLIC OF CHINA

M. Carpentier
Commission of the European Communities
200 rue de la Loi
J-70 6/16
B-1049 Brussels
BELGIUM

C. E. Carter
National Institute of Environmental Health Sciences
P.O. Box 12233
Research Triangle Park, NC 27709

G. W. Casarett
Biophysics Department
University of Rochester Medical Center
Rochester, NY 14642

H. W. Casey, Chairman
Department of Veterinary Pathology
School of Veterinary Medicine
Louisiana State University
Baton Rouge, LA 70803

R. J. Catlin
Electric Power Research Institute
3412 Hillview Avenue
P.O. Box 10412
Palo Alto, CA 94303

M. W. Charles
Central Electricity Generating Board
Berkeley Nuclear Laboratories
Berkeley
Gloucestershire GL 13 9PB
ENGLAND

Chen Xing-An
Laboratory of Industrial Hygiene
Ministry of Public Health
2 Xinkang Street
Deshengmenwai, Beijing
THE PEOPLE'S REPUBLIC OF CHINA

R. Clarke
National Radiological Protection Board
Harwell, Didcot
Oxon OX11 ORQ
ENGLAND

G. F. Clemente, Director
Radiation Toxicology Laboratory
National Committee of Nuclear Energy (CNEN)
Casaccia Centre for Nuclear Studies (CSN)
Casella Postale 2400
I-00100 Roma
ITALY

H. Coffigny
Institut de Protection et de Sûreté Nucléaire
Département de Protection Sanitaire
Service de Pathologie Expérimentale
BP No. 6
F-92265 Fontenay-aux-Roses
FRANCE

N. Cohen
New York University Medical Center
P.O. Box 817
Tuxedo, NY 10987

D. W. Cole, Jr.
ER-73, GTN
Department of Energy
Washington, DC 20545

J. A. Coleman
NE-24, GTN
Department of Energy
Washington, DC 20545

Commission of the European Communities
DG XII - Library SDM8 R1
200 rue de la Loi
B-1049 Brussels
BELGIUM

W. Cool
Nuclear Regulatory Commission
Washington, DC 20545

Council on Environmental Quality
722 Jackson Place, NW
Washington, DC 20503

K. E. Cowser
The Maxima Corporation
107 Union Valley Road
Oak Ridge, TN 37830

D. K. Craig
Battelle Columbus Laboratory
505 King Avenue
Columbus, Ohio 43201-2693

E. P. Cronkite
Medical Department
Brookhaven National Laboratory
Upton, Long Island, NY 11973

J. Crowell
The Maxima Corporation
107 Union Valley Road
Oak Ridge, TN 37830

F. G. Dawson
Battelle Memorial Institute
505 King Avenue
Columbus, OH 43201

J. F. Decker
ER-1, FORS
Department of Energy
Washington, DC 20585

B. de la Cruz, Head
Biomedical Department
Republic of the Philippines
National Science Development Board
Philippine Atomic Energy Commission
P.O. Box 932
Manila
THE PHILIPPINES

Deng Zhicheng
North China Institute of Radiation Protection
Tai-yuan, Shan-Xi
THE PEOPLE'S REPUBLIC OF CHINA

Department of Energy
Environment & Health Division
P.O. Box 5400
Albuquerque, NM 87115

G. DePlanque, Director
Department of Energy-EMEL
375 Hudson Street
New York, NY 10014

M. Di Paola
ENEA, PAS/VALEPID
C.R.E. Casaccia
Casella Postale 2400
I-00100 Roma
ITALY

Director
Commissariat à l'énergie Atomique
Centre d'Etudes Nucléaires
Fontenay-aux-Roses (Seine)
FRANCE

Director
Commonwealth Scientific and Industrial Research Organization
Aspendal, Victoria
AUSTRALIA

Director
Laboratorio di Radiobiologia Animale
Centro di Studi Nucleari Della Casaccia
Comitate Nazionale per l'Energia Nucleare
Casella Postale 2400
I-00100 Roma
ITALY

G. P. Dix
26619 Haney Avenue
Damascus, MD 20750

D. Djuric
Institute of Occupational and Radiological Health
11000 Beograd
Deligradoka 29
YUGOSLAVIA

T. J. Dobry, Jr.
DP-226.3, GTN
Department of Energy
Washington, DC 20545

DOE/Office of Scientific & Technical Information (10)

DOE - Savannah River Operations Office
Environmental Division
P.O. Box A
Aiken, SC 29801

M. Dousset
Département de la Protection Sanitaire
Commissariat à l'énergie Atomique
BP No. 6
F-92260 Fontenay-aux-Roses
FRANCE

B. Drozdowicz
Air Products & Chemicals, Inc.
P.O. Box 538
Allentown, PA 18105

H. Drucker
Argonne National Laboratory
9700 South Cass Avenue
Argonne, IL 60439

R. Ducousso
Section de Pathologie et de Toxicologie Expérimentale
Département de la Protection Sanitaire
Commissariat à l'énergie Atomique
BP No. 6
F-92260 Fontenay-aux-Roses
FRANCE

G. D. Duda
ER-72, GTN
Department of Energy
Washington, DC 20545

A. P. Duhamel
ER-74, GTN
Department of Energy
Washington, DC 20545

D. Dungworth
Associate Dean of Research and Professor & Chairman
Department of Veterinary Pathology
School of Veterinary Medicine
University of California
Davis, CA 95616

H. J. Dunster
National Radiological Protection Board
Chilton, Didcot
Oxon OX11 ORO
ENGLAND

J. Eapen
Biochemistry Division
Bhabha Atomic Research Centre
Bombay-400 085
INDIA

K. F. Eckerman
Health Studies Section
Health and Safety Research Division
Oak Ridge National Laboratory
P.O. Box 2008
Oak Ridge, TN 37831-6383

C. W. Edington, Director
Board on Radiation Effects Research
National Research Council
2101 Constitution Avenue, NW
Washington, DC 20418

G. R. Eisele
Medical Division
Oak Ridge Associated Universities
P.O. Box 117
Oak Ridge, TN 37830

M. Eisenbud
711 Bayberry Drive
Chapel Hill, NC 27514

W. H. Ellett
BRER—National Research Council, MH-370
2101 Constitution Avenue, NW
Washington, DC 20418

Employment Medical Advisory Service
Deputy Director, Medical Services (Scientific Policy)
Health and Safety Executive
25 Chapel Street
London NW1 5DT
ENGLAND

R. J. Engelmann
11701 Karen
Potomac, MD 20854

B. M. Erickson
DOE - Schenectady Naval Reactors Office
P.O. Box 1069
Schenectady, NY 12301

Estação Agronómica Nacional
Biblioteca
2780 Oeiras
PORTUGAL

N. B. Everett
Department of Biological Structure
University of Washington
School of Medicine
Seattle, WA 98105

L. Feinendegen, Director
Institut für Medezin
Kernsforschungsanlage Jülich
Postfach 1913
D-5170 Jülich
FEDERAL REPUBLIC OF GERMANY

B. H. Fimiani
Battelle, Pacific Northwest Laboratories
Washington Operations
370 L'Enfant Promenade, Suite 900
901 D Street, SW
Washington, DC 20024

T. M. Fliedner
Institut für Arbeits- u. Sozialmedizin
Universität Ulm
Oberer Eselsberg M 24, 309
D-7900 Ulm
FEDERAL REPUBLIC OF GERMANY

L. Friberg
The Karolinska Institute
Stockholm
SWEDEN

H. L. Friedell
School of Medicine, WA77
Case-Western Reserve University
2109 Abington Road
Cleveland, OH 44106

R. M. Fry, Head
Office of the Supervising Scientist for the Alligator Rivers Region
P.O. Box 387
Bondi Junction NSW 2022
AUSTRALIA

D. E. Gardner
Northrop Services, Inc.
P.O. Box 12313
Research Triangle Park, NC 27709

G. B. Gerber
Radiobiology Department
Commission of the European Communities
200 rue de la Loi
B-1049 Brussels
BELGIUM

T. F. Gesell
Idaho Operations Office
Department of Energy
785 DOE Place
Idaho Falls, ID 83402-4149

R. D. Gilmore, President
Environmental Health Sciences, Inc.
Nine Lake Bellevue Building
Suite 104
Bellevue, WA 98005

T. Giuseppe
ENEA-PAS-FIBI-AEROSOL
Via Mazzini 2
I-40138 Bologna
ITALY

H. L. Gjørup, Head
Health Physics Department
Atomic Energy Commission
Research Establishment
Risø, Roskilde
DENMARK

M. Goldman
Department of Radiological Sciences (VM)
University of California
Davis, CA 95616

R. Goldsmith
ER-73, GTN
Department of Energy
Washington, DC 20545

G. Goldstein
ER-74, GTN
Department of Energy
Washington, DC 20545

A. R. Gopal-Ayengar
73-Mysore Colony
Mahul Road, Chembur
Bombay-400 074
INDIA

J. A. Graham
ECAO, Mail Drop 52
Environmental Protection Agency
Research Triangle Park, NC 27711

R. A. Griesemer, Director
National Toxicology Program
National Institutes of Health
P.O. Box 12233
Research Triangle Park, NC 27709

R. V. Griffith
International Atomic Energy Agency
Wagramerstraβe 5
P.O. Box 200
A-1400 Vienna
AUSTRIA

G. H. Gronhovd
Grand Forks Energy Research Center
Department of Energy
Box 8213, University Station
Grand Forks, ND 58202

J. G. Hadley
Owens Corning Fiberglas Corporation
Technical Center
P.O. Box 415
Granville, OH 42023

F. F. Hahn
Lovelace Inhalation Toxicology Research Institute
P.O. Box 5890
Albuquerque, NM 87115

E. J. Hall
Radiological Research Laboratory
Columbia University
630 West 168th Street
New York, NY 10032

R. Hamlin
Dept. of Veterinary Physiology
The Ohio State University
1900 Coffey Road
Columbus, OH 43201

Y. Hamnerius
Applied Electron Physics
Chalmers University of Technology
S-412 96 Göteborg
SWEDEN

J. W. Healy
51 Grand Canyon Drive
White Rock, NM 87544

C. H. Hobbs
Inhalation Toxicology Research Institute
The Lovelace Foundation for Medical Education & Research
P.O. Box 5890
Albuquerque, NM 87185

L. M. Holland
Los Alamos National Laboratory
P.O. Box 1663
Los Alamos, NM 87545

A. P. Hull
Safety and Environmental Protection Division
Brookhaven National Laboratory
Building 535-A
Upton, Long Island, NY 11973

F. Hutchinson
Department of Molecular Biophysics & Biochemistry
Yale University
260 Whitney Avenue
P.O. Box 6666
New Haven, CT 06511

D. S. Ingle
Dayton Area Office
DOE - Albuquerque Operations Office
P.O. Box 66
Miamisburg, OH 45342

International Atomic Energy Agency
Documents Library
Attn: Mrs. Javor
Kaerntnerring 11
A-1010 Vienna 1
AUSTRIA

E. Iranzo
Jefe, División Protección Radiológica
Centro Investigaciones Energéticas, Mediambientales y Tecnológicas (CIEMAT)
Avenida Complutense 22
2804 Madrid
SPAIN

H. Ishikawa, General Manager
Nuclear Safety Research Association
P.O. Box 1307
Falls Church, VA 22041

K. L. Jackson, Chairman
Radiological Sciences Group SB-75
University of Washington
Seattle, WA 98195

W. Jacobi
Institut für Strahlenschutz
Ingolstadter Landstraβe 1
D-8042 Neuherberg
FEDERAL REPUBLIC OF GERMANY

K. E. Lennart Johansson
National Defense Research Institute
FOA 45 1
S-901-82 Umeå
SWEDEN

A. W. Johnson
Vice President for Academic Affairs
San Diego State University
San Diego, CA 92182

J. F. Johnson
Kenworth Truck Co.
P.O. Box 1000
Kirkland, WA 98033

R. K. Jones
The Lovelace Foundation for Medical Education & Research
Building 9200, Area Y
Sandia Base
Albuquerque, NM 87108

G. Y. Jordy, Director
ER-30, GTN
Department of Energy
Washington, DC 20545

E. Karbe
c/o Centre d'Elevage et de Recherche
Avetonou, B.P. 27
Agou Gare, Togo
REPUBLIC OF SOUTH AFRICA

M. Kashima
National Institute of Radiological Sciences
Division of Radiation Hazards
9-1, Anagawa-4-chome
Chiba-shi 260
JAPAN

A. M. Kellerer
Institut für Medezin Strahlenkunde
Universität Würzburg
Versbacher Straβe 5
D-8700 Würzburg
FEDERAL REPUBLIC OF GERMANY

C. M. Kelly
Air Products and Chemicals, Inc.
Corporate Research and Development
P.O. Box 538
Allentown, PA 18105

A. R. Kennedy
Department of Physiology
Harvard School of Public Health
665 Huntington Avenue
Boston, MA 02115

H.-J. Klimisch
BASF Aktiengesellschaft
Abteilung Toxikologie, Z470
D-6700 Ludwigshafen
FEDERAL REPUBLIC OF GERMANY

H. E. Knoell
Battelle-Institut e.V.
Am Römerhof 35
Postfach 900160
D-6000 Frankfurt am Main 90
FEDERAL REPUBLIC OF GERMANY

R. T. Kratzke
EH-131, GTN
Department of Energy
Germantown, MD 20545

H. Kraybill
National Cancer Institute
Landau Building, Room C-337
Bethesda, MD 20014

T. Kumatori, Director
National Institute of Radiological Sciences
9-1, Anagawa-4-chome
Chiba-shi 260
JAPAN

J. Lafuma, Head
Département de Protection Sanitaire
Commissariat à l'énergie Atomique/IPSN
BP No. 6
F-92265 Fontenay-aux-Roses
FRANCE

J. R. A. Lakey, Director
Department of Nuclear Sciences & Technology
Royal Naval College, Greenwich
London SE10 9NN
ENGLAND

W. Lauder
Office of Health and Environmental Research
Office of Energy Research
Department of Energy
Germantown, MD 20545

W. M. Leach
Food & Drug Administration
5600 Fishers Lane, HFZ-100
Rockville, MD 20857

Li De-Ping
Professor and Director of North China Institute of Radiation Protection, NMI
Tai-yuan, Shan-Xi
THE PEOPLE'S REPUBLIC OF CHINA

Librarian
Alberta Environmental Center
Bag 4000
Vegreuille, Alberta TOB 4LO
CANADA

Librarian
Brookhaven National Laboratory
Research Library, Reference
Upton, Long Island, NY 11973

Librarian
Centre d'Etudes Nucléaires de Saclay
P.O. Box 2, Saclay
Fig-sur-Yvette (S&O)
FRANCE

Librarian
Colorado State University
Documents Department—The Libraries
Ft. Collins, CO 80523

Librarian
CSIRO
314 Albert Street
P.O. Box 89
East Melbourne, Victoria
AUSTRALIA

Librarian
CSIRO
Rangelands Research Centre
Private Mail Bag, P.O.
Deniliquin, NSW 2710
AUSTRALIA

Librarian
Electric Power Research Institute
3412 Hillview Avenue
P.O. Box 10412
Palo Alto, CA 94303

Librarian
HCS/EHE
World Health Organization
CH-1211 Geneva 27
SWITZERLAND

Librarian
Health Sciences Library, SB-55
University of Washington
Seattle, WA 98195

Librarian
Kernforschungzentrum Karlsruhe
Institut für Strahlenbiologie
Postfach 3640
D-75 Karlsruhe 1
FEDERAL REPUBLIC OF GERMANY

Librarian
Lawrence Livermore National Laboratory
University of California
Technical Information Dept., L-3
P.O. Box 808
Livermore, CA 94550

Librarian
Los Alamos National Laboratory
Report Library, MS P364
P.O. Box 1663
Los Alamos, NM 87545

Librarian
Max-Planck-Institut für Biophysics
Forstkasstraβe
D-6000 Frankfurt/Main
FEDERAL REPUBLIC OF GERMANY

Librarian
Medical Research Council
Radiobiology Unit
Chilton
Oxon OX11 ORD
ENGLAND

Librarian
Ministry of Agriculture, Fisheries & Food
Fisheries Laboratory
Lowestoft, Suffolk NR33 OHT
ENGLAND

Librarian
National Institute of Radiological Sciences
9-1, Anagawa-4-chome
Chiba-shi 260
JAPAN

Librarian
OECD - NEA
38, Blvd. Suchet
75016, Paris
FRANCE

Librarian
Oregon Regional Primate Research Center
505 NW 185th Avenue
Beaverton, OR 97006

Librarian
Supervising Scientist for the Alligator Rivers Region
Level 23, Bondi Junction Plaza
P.O. Box 387
Bondi Junction NSW 2022
AUSTRALIA

Librarian
Washington State University
Pullman, WA 99164-6510

Library
Atomic Energy Commission of Canada, Ltd.
Whiteshell Nuclear Research Establishment
Pinawa, Manitoba ROE 1L0
CANADA

Library
Department of Meteorology
University of Stockholm
Arrhenius Laboratory
S-106 91 Stockholm
SWEDEN

Library
Risø National Laboratory
DK-4000 Roskilde
DENMARK

Library
Serials Department (#80-170187)
University of Chicago
1100 East 57th Street
Chicago, IL 60637

B. Lindell
National Institute of Radiation Protection
Fack S-104 01
Stockholm 60
SWEDEN

J. B. Little
Department of Physiology
Harvard School of Public Health
665 Huntington Avenue
Boston, MA 02115

Liu Shu-Zheng
Department of Radiation Biology
Norman Bethune University of Medical Sciences
6 Xinmin Street
Changchun 130021
THE PEOPLE'S REPUBLIC OF CHINA

A. B. Lovins
Rocky Mountain Institute
1739 Snowmass Creek Road
Snowmass, CO 81654-9199

O. R. Lunt
Laboratory of Biomedical & Environmental Sciences
University of California
900 Veteran Avenue
Los Angeles, CA 90024-1786

C. C. Lushbaugh
Medical Division
Oak Ridge Associated Universities
P.O. Box 117
Oak Ridge, TN 37830

J. N. Maddox
ER-73, GTN
Department of Energy
Washington, DC 20545

J. R. Maher
ER-65, GTN
Department of Energy
Washington, DC 20545

T. D. Mahony
750 Swift Boulevard
Richland, WA 99352

J. R. Maisin
Radiobiology Department
C.E.N. - S.C.K.
Mol
BELGIUM

C. R. Mandelbaum
ER-32, GTN
Department of Energy
Washington, DC 20545

A. M. Marko, Director
Atomic Energy Commission of Canada, Ltd.
Biology and Health Physics Division
Chalk River Nuclear Laboratories
P.O. Box 62
Chalk River, Ontario KOJ 1JO
CANADA

S. Marks
c/o U.S. Marine Corps Air Station
ABCC/RERF
FPO
Seattle, WA 98764-5000

R. Martin
Environmental Protection Branch
Mail Stop G-108
Department of Energy
P.O. Box E
Oak Ridge, TN 37830

D. R. Mason
Nuclear Safety Branch
Department of Energy
P.O. Box A
Aiken, SC 29801

R. Masse
Institut de Protection et de Sûreté Nucléaire
Département de Protection Sanitaire
Service d'Etudes Appliquées de Protection Sanitaire
BP No. 6
F-92260 Fontenay-aux-Roses
FRANCE

W. H. Matchett
Graduate School
New Mexico State University
Box 3G
Las Cruces, NM 88003-0001

O. Matsuoka, Deputy Director-General
Division of Comparative Radiotoxicology
National Institute of Radiological Sciences
9-1, Anagawa-4-chome
Chiba-shi 260
JAPAN

N. Matsusaka
Department of Veterinary Medicine
Faculty of Agriculture
Iwate University
Ueda, Morioka
Iwate 020
JAPAN

C. W. Mays
Radiation Epidemiology Branch
Executive Plaza North 408
Bethesda, MD 20892

H. M. McCammon
ER-75, GTN
Department of Energy
Washington, DC 20545

R. O. McClellan, President
Chemical Industry Institute of Toxicology
P.O. Box 12137
Research Triangle Park, NC 27709

R. G. C. McElroy
Atomic Energy Commission of Canada, Ltd.
Dosimetric Research Branch
Chalk River, Ontario KOJ 1JO
CANADA

J. F. McInroy
Los Alamos National Laboratory
Mail Stop K484
P.O. Box 1663
Los Alamos, NM 87545

F.-I. S. Medina
Cytogenetics Laboratory
Biomedical Research Division
A.R.C.
Philippine Atomic Energy Commission
P.O. Box 932
Manila
THE PHILIPPINES

C. B. Meinhold
Radiological Sciences Division
Building 703M
Brookhaven National Laboratory
Upton, Long Lsland, NY 11973

M. L. Mendelsohn
Biomedical and Environmental Research Program
Lawrence Livermore National Laboratory, L-452
University of California
P.O. Box 5507
Livermore, CA 94550

H. Menkes
Assistant Professor of Medicine & Environmental Medicine
The John Hopkins University
Baltimore, MD 21205

D. B. Menzel
Associate Professor of Medicine and Pharmacology
Division of Environmental Medicine
Duke University Medical Center
Durham, NC 27706

P. Metalli
ENEA-PAS
CRE Casaccia
Casella Postale 2400
I-00100 Roma
ITALY

H. J. Metivier
Chef de la Section de Toxicologie et Cancérologie Expérimentale
Institut de Protection et de Sûreté Nucléaire
Département de Protection Sanitaire
Service de Pathologie Expérimentale
BP No. 12
91680 Bruyères-le-Châtel
FRANCE

S. Michaelson
University of Rochester Medical Center
Rochester, NY 14642

C. Miller
P.O. Box 180
Watermill, NY 11976

W. A. Mills
Committee on Interagency Radiation Research & Policy Coordination (CIRRPC)
Oak Ridge Associated Universities
1019 19th Street, NW
Suite 700
Washington, DC 20036

A. Morgan
Inhalation Toxicology Group
Envirommental and Medical Sciences Division
Atomic Energy Research Establishment, Building 551
Harwell, Didcot
Oxon OX11 ORA
ENGLAND

K. Z. Morgan
1984 Castleway Drive
Atlanta, GA 30345

P. E. Morrow
University of Rochester
Rochester, NY 14642

Y. I. Moskalev
Institute of Biophysics
Ministry of Public Health
Givopisnaya 46
Moscow
USSR

W. F. Mueller
New Mexico State University
Box 4500
Las Cruces, NM 88003-4500

J. Muller
Special Studies and Services Branch
8th Floor
400 University Avenue
Toronto, Ontario M7A 1T7
CANADA

D. K. Myers, Head
Radiation Biology Branch
Atomic Energy Commission of Canada, Ltd.
Chalk River, Ontario
CANADA

D. S. Nachtwey
NASA-Johnson Space Center
Mail Code SD-5
Houston, TX 77058

D. B. Nash, Editorial Assistant
Department of Radiation Biology and Biophysics
University of Rochester
School of Medicine and Dentistry
260 Crittenden Boulevard
Rochester, NY 14620

R. Nathan
Battelle Project Management Division
505 King Avenue
Columbus, Ohio 43201

National Library of Medicine
TSD-Serials
8600 Rockville Pike
Bethesda, MD 20014

S. M. Nealey
Battelle - Seattle
4000 NE 41st Street
Seattle, WA 98105

N. S. Nelson
Office of Radiation Programs (ANR-461)
Environmental Protection Agency
401 M Street, SW
Washington, DC 20460

J. C. Nénot, Deputy Director
Département de Protection
Centre d' Etudes Nucléaires
BP No. 6
F-92260 Fontenay-aux-Roses
FRANCE

P. Nettesheim
National Institutes of Environmental Health Sciences
Research Triangle Park, NC 27711

W. R. Ney, Executive Director
National Council on Radiation Protection and Measurements
7910 Woodmont Avenue
Suite 1016
Washington, DC 20014

S. W. Nielsen
Department of Pathology
New York State Veterinary College
Cornell University
Ithaca, NY 14850

R. A. Nilan
Division of Sciences
Washington State University
Pullman, WA 99164

M. Nolan
10958 Rum Cay Court
Columbia, MD 21044

Nuclear Regulatory Commission
Advisory Committee on Reactor Safeguards
Washington, DC 20555

D. E. Olesen
Battelle Memorial Institute
505 King Avenue
Columbus, OH 43201

T. B. Owen, Project Officer
Smoking and Health Program
National Cancer Institute
Bethesda, MD 20014

J. Pacha
Silesian University
Department of Microbiology
Ul. Jagiellonska 28
40-032 Katowice
POLAND

J. L. Palotay
Oregon Regional Primate Center
505 NW 185th Avenue
Beaverton, OR 97005

H. G. Paretzke
GSF Institut für Strahlenschutz
Ingolstadter Landstraβe 1
D-8042 Neuherberg
FEDERAL REPUBLIC OF GERMANY

N. Parmentier
Département de Protection Sanitaire
Centre d'Etudes Nucléaires
BP No. 6
F-92260 Fontenay-aux-Roses
FRANCE

G. Patrick
Medical Research Council
Radiobiology Unit
Harwell, Didcot
Oxon OX11 ORD
ENGLAND

O. Pavlovski
Institute of Biophysics
Ministry of Public Health
Givopisnaya 46
Moscow D-182
USSR

A. F. Perge
RW-43, FORS
Department of Energy
Washington, DC 20545

R. Perraud
Commissariat à l'énergie Atomique
BP No. 1
87640 Razes
FRANCE

D. F. Petersen
Los Alamos National Laboratory
P.O. Box 1663
Los Alamos, NM 87545

H. Pfuderer
Oak Ridge National Laboratory
P.O. Box X
Oak Ridge, TN 37830

E. Pochin
National Radiological Protection Board
Chilton, Didcot
Oxon OX11 ORQ
ENGLAND

G. Premazzi
Commission of the European Communities
Joint Research Centre
Ispra Establishment
I-21020 Ispra
ITALY

V. Prodi
Department of Physics
University of Bologna
Via Irnerio 46
I-40126 Bologna
ITALY

O. G. Raabe
Laboratory for Energy-Related Health Research
University of California
Davis, CA 95616

R. Rabson
Division of Biological Energy Research
ER-17, GTN
Department of Energy
Washington, DC 20545

D. P. Rall, Director
National Institutes of Environmental Health Sciences
P.O. Box 12233
Research Triangle Park, NC 27709

J. Rasey
Division of Radiation Oncology
University of Washington
Medical School
Seattle, WA 98195

O. Ravera
Commission of the European Communities, C.C.R.
I-21020 Ispra (Varese)
ITALY

E. J. Reagan
Monsanto Research Corp.
Mound Laboratory
P.O. Box 32
Miamisburg, OH 45342

D. V. Rebollo
Junta de Energia Nuclear
Sección de Isotopos
Calle de Serrano, 121
6 Madrid
SPAIN

R. D. Reed, Chief
Rocky Flats Area Office
Albuquerque Operations Office
Department of Energy
P.O. Box 928
Golden, CO 80402-0928

C. A. Reilly, Jr.
Argonne National Laboratory
Building 203
9700 South Cass Avenue
Argonne, IL 60439

REP Institutes TNO
TNO Division of Health
Research Library
P.O. Box 5815
151 Lange Kleiweg
2280 HV Rijswijk
THE NETHERLANDS

Reports Librarian
Harwell Laboratory, Bldg. 465
UKAEA
Harwell, Didcot
Oxon OX11 ORB
ENGLAND

C. R. Richmond
Oak Ridge National Laboratory
4500N, MS-62523
P.O. Box 2008
Oak Ridge, TN 37831-6253

J. S. Robertson
ER-73, GTN
Department of Energy
Washington, DC 20545

B. Robinson
Monsanto Research Corp.
Mound Laboratory
P.O. Box 32
Miamisburg, OH 45342

J. R. Roeder
Environment, Safety & Health Division
P.O. Box 5400
Albuquerque, NM 87115

P. J. A. Rombout
Inhalation Toxicology Department
National Institute of Public Health and Environmental Protection
P.O. Box 1
NL-3720 BA Bilthoven
THE NETHERLANDS

S. L. Rose
ER-73, GTN
Department of Energy
Washington, DC 20545

G. J. Rotariu
4609 Woodfield Road
Bethesda, MD 20814

M. Roy
Institut de Protection et de Sûreté Nucléaire
Département de Protection Sanitaire
Service d'Etudes Appliqués de Protection Sanitaire
BP No. 6
F-92260 Fontenay-aux-Roses
FRANCE

G. Runkle, Chief
Department of Energy, AL
HPB/EHD
P.O. Box 5400
Albuquerque, NM 87115

M. Rzekiecki
Commissariat à l'énergie Atomique
Centre d'Etudes Nucléaires de Cadarache
BP No. 13-St. Paul
Les Durance
FRANCE

G. Saccomanno
Pathologist and Director of Laboratories
St. Marys and V. A. Hospitals
Grand Junction, CO 81501

F. A. Sacherer
Battelle-Institut e.V.
Am Römerhof 35
Postfach 900160
D-6000 Frankfurt am Main 90
FEDERAL REPUBLIC OF GERMANY

U. Saffiotti
Laboratory of Experimental Pathology, DCCP
National Cancer Institute
Bldg. 560, Rm. 32-60
Frederick, MD 21701

L. Sagan
Electric Power Research Institute
3412 Hillview Avenue
P.O. Box 10412
Palo Alto, CA 94304

R. A. Scarano
Mill Licensing Section
Nuclear Regulatory Commission
Washington, DC 20545

R. A. Schlenker
Center for Human Radiobiology
Argonne National Laboratory
9700 South Cass Avenue
Argonne, IL 60439

E. Schmetz
FE-34, GTN
Department of Energy
Washington, DC 20545

E. Schreiber
Department of Geology
Queens College
Flushing, NY 11367

C. R. Schuller
Battelle - Seattle
4000 NE 41st Street
Seattle, WA 98105

M. Schulman
ER-70, GTN
Department of Energy
Washington, DC 20545

J. D. Seamans
CRI Ventures, Inc.
4815 Seton Drive
Baltimore, MD 21215-3211

T. M. Seed
BIM 202
Argonne National Laboratory
9700 South Cass Avenue
Argonne, IL 60439

W. Seelentag, Chief Medical Officer
Radiation Health Unit
World Health Organization
CH-1211 Geneva 27
SWITZERLAND

R. B. Setlow
Brookhaven National Laboratory
Upton, Long Island, NY 11973

R. Shikiar
Battelle - Seattle
4000 NE 41st Street
Seattle, WA 98105

T. Sibley
Department of Fisheries, WH-10
University of Washington
Seattle, WA 98195

P. H. Silverman
Lawrence Berkeley Laboratory
Donner Laboratory, Room 466
University of California
Berkeley, CA 94720

C. S. Sims
Oak Ridge National Laboratory
X-10, Building 7710, Room 101
P.O. Box 2008
Oak Ridge, TN 37831-6379

W. K. Sinclair, President
National Council on Radiation Protection
7910 Woodmont Avenue
Suite 1016
Bethesda, MD 20814

D. H. Slade
ER-74, GTN
Department of Energy
Washington, DC 20545

D. A. Smith
ER-72, GTN
Department of Energy
Washington, DC 20545

G. S. Smith
New Mexico State University
Box 3-I
Las Cruces, NM 88003-0001

H. Smith
International Commission on Radiological Protection
P.O. Box 35
Didcot
Oxon OX11 ORJ
ENGLAND

J. M. Smith
NIOSH
4676 Columbia Parkway
Cincinnati, OH 45226

J. N. Stannard
University of California
17441 Plaza Animado #132
San Diego, CA 92128

G. E. Stapleton
ER-72, GTN
Department of Energy
Washington, DC 20545

J. Stara
Environmental Protection Agency
Health Effects Research Laboratory
26 West St. Clair
Cincinnati, OH 45268

R. W. Starostecki
NE-40, GTN
Department of Energy
Washington, DC 20545

J. W. Stather
National Radiological Protection Board
Building 383
Chilton, Didcot
Oxon OX11 ORQ
ENGLAND

R. J. Stern
EH-10, FORS
Department of Energy
Washington, DC 20585

A. M. Stewart
Cancer Epidemiology Research Unit
University of Birmingham
Edgbaston
Birmingham B15 2TT
ENGLAND

C. G. Stewart
Chalk River Nuclear Laboratories
P.O. Box 62
Chalk River, Ontario KOJ 1JO
CANADA

K. G. Steyer
Nuclear Regulatory Commission
Washington, DC 20555

E. T. Still
Kerr-McGee Corporation
P.O. Box 25861
Oklahoma City, OK 73125

J. B. Storer
Biology Division
Oak Ridge National Laboratory
P.O. Box 2009
Oak Ridge, TN 37831-8077

B. Stover
Department of Pharmacology
1106A FLOB 231H
University of North Carolina
Chapel Hill, NC 27514

M. J. Suess
Regional Officer for Environmental Hazards
World Health Organization
8, Scherfigsvej
DK-2100 Copenhagen
DENMARK

Sun Shi-quan, Head
Radiation-Medicine Department
North China Institute of Radiation Protection, MNI
P.O. Box 120
Tai-yuan, Shan-Xi
THE PEOPLE'S REPUBLIC OF CHINA

F. Swanberg
Nuclear Regulatory Commission
Washington, DC 20545

D. Swanger
Biology Department
Eastern Oregon State College
La Grande, OR 97850

J. Swinebroad
PE-24, GTN
Department of Energy
Washington, DC 20545

G. Tarroni
ENEA-PAS-FIBI-AEROSOL
Laboratorio Fisica Sanitaria
Via Ercolani 8
I-40138 Bologna
ITALY

D. M. Taylor
Kernforschungzentrum Karlsruhe
Institut für Strahlenbiologie
Postfach 3640
D-75 Karlsruhe 1
FEDERAL REPUBLIC OF GERMANY

G. N. Taylor
Division of Radiobiology
Building 351
University of Utah
Salt Lake City, UT 84112

Technical Information Service
Savannah River Laboratory
Room 773A
E. I. duPont de Nemours & Company
Aiken, SC 29801

K. H. Tempel
Institut für Pharmakologie, Toxikologie und Pharmazie
Fachbereich Tiermedizin der Universität München
Veterinärstraße 13
D-8000 München 22
FEDERAL REPUBLIC OF GERMANY

J. W. Thiessen
Radiation Effects Research Foundation
5-2 Hijiyama Park
Minami-Ku
Hiroshima 732
JAPAN

R. G. Thomas
ER-72, GTN
Department of Energy
Washington, DC 20545

P. W. Todd
Center for Chemical Engineering
National Bureau of Standards (773.10)
325 Broadway
Boulder, CO 80303

P. T'so
Division of Biophysics, Room 3102
School of Hygiene & Public Health
The Johns Hopkins University
615 North Wolfe Street
Baltimore, MD 21205

United Nations Scientific Committee on the Effects of Atomic Radiation
Vienna International Center
P.O. Box 500
A-1400 Vienna
AUSTRIA

A. C. Upton
New York University Medical Center
Institute of Environmenal Medicine
A. J. Lanza Laboratory
Long Meadow Road
Tuxedo, NY 10987

E. J. Vallario
15228 Red Clover Drive
Rockville, MD 20853

D. Van As
Atomic Energy Board
Private Bag X 256
Pretoria 0001
REPUBLIC OF SOUTH AFRICA

R. L. Van Citters, Dean
Research and Graduate Programs
University of Washington
Seattle, WA 98105

L. M. Van Putten
Radiobiological Institute TNO
P.O. Box 5815
151 Lange Kleiweg
2280 HV Rijswijk
THE NETHERLANDS

J. Vaughan
1 Fairlawn End
First Turn
Wolvercote
Oxon OX2 8AR
ENGLAND

J. Vennart
Bardon, Ickleton Road, Wantage
Oxon OX12 9OA
ENGLAND

C. R. Vest
Battelle, Pacific Northwest Laboratories
Washington Operations
370 L'Enfant Promenade, Suite 900
901 D Street, SW
Washington, DC 20024

Vienna International Centre Library
Gifts and Exchange
P.O. Box 100
A-1400 Vienna
AUSTRIA

G. J. Vodapivc
DOE - Schenectady Naval Reactors Office
P.O. Box 1069
Schenectady, NY 12301

G. L. Voelz
Los Alamos National Laboratory
MS-K404
P.O. Box 1663
Los Alamos, NM 87545

V. Volf
Kernforschungzentrum Karlsruhe
Institut für Genetik und Toxikologie von Spaltstoffen
Postfach 3640
D-7500 Karlsruhe 1
FEDERAL REPUBLIC OF GERMANY

B. W. Wachholz
Radiation Effects Branch
National Cancer Institute
EPN, Room 530
8000 Rockville Pike
Bethesda, MD 20892

N. Wald
School of Public Health
University of Pittsburgh
Pittsburgh, PA 15213

G. Walinder
Unit of Radiological Oncology
University of Agricultural Sciences
P.O. Box 7031
S-750 07 Uppsala
SWEDEN

M. L. Walker
EH-1, FORS
Department of Energy
Washington, DC 20585

R. A. Walters
Assistant to the Associate Director
Los Alamos National Laboratory
MS-A114
P.O. Box 1663
Los Alamos, NM 87545

Wang Hengde
North China Institute of Radiation Protection
P.O. Box 120
Tai-yuan, Shan-Xi
THE PEOPLE'S REPUBLIC OF CHINA

Wang Renzhi
Institute of Radiation Medicine
11# Tai Ping Road
Beijing
THE PEOPLE'S REPUBLIC OF CHINA

Wang Ruifa, Associate Director
Laboratory of Industrial Hygiene
Ministry of Public Health
2 Xinkang Street
P.O. Box 8018
Deshengmenwai, Beijing 100088
THE PEOPLE'S REPUBLIC OF CHINA

Wang Yibing
North China Institute of Radiation Protection
P.O. Box 120
Tai-yuan, Shan-Xi
THE PEOPLE'S REPUBLIC OF CHINA

M. E. Weaver
Professor of Anatomy
University of Oregon Health Science Center
School of Dentistry
Portland, OR 97201

M. H. Weeks
U.S. AEHA, Bldg. 2100
Edgewood Arsenal
Aberdeen Proving Ground, MD 21014

Wei Lü-Xin
Laboratory of Industrial Hygiene
Ministry of Public Health
2 Xinkang Street
Deshengmenwai, Beijing 100088
THE PEOPLE'S REPUBLIC OF CHINA

J. Wells
Radiobiology Laboratory
Health Physics Research
Central Electricity Generating Board
Berkeley Nuclear Laboratories
Berkeley, Gloucestershire GL 13 9PB
ENGLAND

C. G. Welty, Jr.
EH-123, GTN
Department of Energy
Washington, DC 20545

I. Wender
Department of Chemical Engineering
1249 Benedum Hall
University of Pittsburgh
Pittsburgh, PA 15261

W. W. Weyzen
Electric Power Research Institute
3412 Hillview Avenue
P.O. Box 10412
Palo Alto, CA 94303

D. L. Willis
Department of General Science
Oregon State University
Corvallis, OR 97331

K. Wilzbach
Argonne National Laboratory
9700 South Cass Avenue
Argonne, IL 60439

B. C. Winkler, Director
Licensing
Raad Op Atomic
Atoomkrag Energy Board
Privaatsk X 256
Pretoria 0001
REPUBLIC OF SOUTH AFRICA

F. J. Wobber
Department of Energy
14 Goshen Court
Gaithersburg, MD 20879-4403

R. W. Wood
PTRD, OHER
ER-74, GTN
Department of Energy
Washington, DC 20545

M. E. Wrenn
Environmental Radiation & Toxicology Laboratory
956 West Levoy, Suite 100
Salt Lake City, UT 84123

Wu De-Chang
Institute of Radiation Medicine
27# Tai Ping Road
Beijing
THE PEOPLE'S REPUBLIC OF CHINA

Yao Jiaxiang
Laboratory of Industrial Hygiene
2 Xinkang Street
Deshengmenwai, Beijing 100088
THE PEOPLE'S REPUBLIC OF CHINA

R. E. Yoder
Rockwell International
P.O. Box 464
Golden, CO 80401

K. Yokoro, Director
Research Institute for Nuclear Medicine & Biology
Hiroshima University
Kasumi 1-2-3, Minami-ku
Hiroshima 734
JAPAN

Zhu Zhixian
Laboratory for Energy-Related Health Research
University of California
Davis, CA 95616

ONSITE

DOE Richland Operations Office (3)

K. R. Absher
E. L. Nilson
E. C. Norman/D. L. Hoff

Tri-Cities University Center (2)

J. Cooper, Librarian
B. Valett

Hanford Environmental Health (5)

S. E. Dietert
R. L. Kathren
L. J. Maas
W. C. Milroy
M. J. Swint

U. S. Testing

V. H. Pettey

Westinghouse Hanford Co. (2)

R. O. Budd
D. E. Simpson

Pacific Northwest Laboratory

R. R. Adee
D. K. Anderson
L. E. Anderson
G. A. Apley
R. W. Baalman (5)
J. F. Bagley
W. J. Bair (15)
L. A. Braby
M. G. Brown
R. L. Buschbom
W. C. Cannon
T. D. Chikalla
B. J. Chou
M. L. Clark
J. R. Coleman
P. E. Conselman
J. A. Creim
F. T. Cross
E. M. Crow
J. A. Cushing
G. E. Dagle
J. R. Decker
H. S. DeFord
J. A. Dill
R. D. DuBois
F. N. Eichner
C. E. Elderkin
J. J. Evanoff
D. Felton
D. R. Fisher
L. G. Florek
W. C. Forsythe
M. E. Frazier
L. K. Fritz
R. A. Gelman
K. M. Gideon
R. A. Gies
A. W. Gieschen
E. S. Gilbert
M. F. Gillis
W. A. Glass
L. S. Gorham
B. J. Greenspan
D. K. Hammerberg
L. A. Hargrow
B. K. Hayden
K. Heid
M. G. Horstman
V. G. Horstman
A. C. James
A. E. Jarrell
J. R. Johnson
R. F. Jostes
D. R. Kalkwarf
M. T. Karagianes
B. J. Kelman
E. G. Kuffel
K. E. Lauhala
C. L. Leach
F. C. Leung
M. K. Lien
V. L. Madden
J. A. Mahaffey
D. D. Mahlum
D. B. Mann
T. J. Mast
K. M. McCarty
K. E. McDonald
P. W. Mellick
M. E. Mericka
H.. K. Meznarich
D. L. Miller
J. H. Miller
M. C. Miller
R. A. Miller
J. E. Minor
J. E. Morris
D. A. Mueller
D. A. Nelson
J. M. Nelson
J. M. Nielsen
R. P. O'Donnell
J. F. Park (100)
R. A. Pelroy
C. E. Peraino
R. W. Perkins
J. T. Pierce
C. A. Poindexter
G. J. Powers
H. A. Ragan
R. A. Renne
P. Roberson
D. N. Rommereim
R. L. Rommereim
C. O. Romsos
E. J. Rossignol
S. E. Rowe
P. S. Ruemmler
J. L. Ryan
C. L. Sanders
L. B. Sasser
G. F. Schiefelbein
L. C. Schmid
R. P. Schneider
L. L. Scott
M. R. Sikov
C. L. Simpson
J. C. Simpson
L. G. Smith
D. L. Springer
E. G. Stephan
R. G. Stevens
D. L. Stewart
G. L. Stiegler
K. H. Stoney
R. D. Swannack
K. L. Swinth
W. L. Templeton
T. S. Tenforde (2)
R. M. Thomas
R. C. Thompson
L. H. Toburen
R. J. Traub
V. D. Tyler
B. E. Vaughan
C. R. Watson
A. P. Wehner
R. J. Weigel
R. E. Weller
R. B. Westerberg
T. J. Whitaker
L. S.Whiting
E. L. Wierman (2)
R. E. Wildung
W. E. Wilson
R. M. Wistisco
Health Physics Department
Library
Life Sciences Library (2)
Publishing Coordination (2)
Technical Report Files (5)